Contributions to the Asymmetric Synthesis of Octahedral Ruthenium(II) Complexes and to Bioactive Hexacoordinate Silicon Complexes

A DISSERTATION

In

Chemistry

Presented to the Faculties of Philipps-Universität Marburg in Partial Fulfillment
of the Requirements for the Degree of Doctor of Science
(Dr. rer. nat.)

Chen Fu

Fuzhou, Jiangxi, P. R. China

Marburg/Lahn 2014

Department of Chemistry of Philipps-Universität Marburg, accepted as a

dissertation on

Supervisor: Prof. Dr. Eric Meggers

Defence committee: Prof. Dr. Jörg Sundermeyer

                     Prof. Dr. Bernard Roling

Date of defence: May 14th, 2014

This thesis is dedicated to my beloved family...

Acknowledgements

Foremost, I would like to gratefully and sincerely thank Prof. Eric Meggers for for the continuous support of my Ph.D. study and research. His great passion and inspiration for science are indeed impressive, and his diligence and conscientious scholarly attitude are respectable. With his patient guidance and encouragement, I have learned how to analyze and approach scientific problems in a comprehensive but efficient way. I am deeply grateful for the opportunity he offered to me to work on diverse exciting projects, and all the experiences working with him is a valuable fortune for me which will no doubt be very helpful for my future career. I wish him continuing and more success in the future.

Another person who deserves a great amount of my sincere gratitude is Prof. Lilu Zhang, I am really very grateful for her kind concern, understanding and help in my work and life, I wish her all the best in the future. I would also like to thank Prof. Tingbin Wen, who led me into the fascinating world of organometallic chemistry, I wish him more achievement in heterocycle chemistry. And the thank also goes to Prof. Xumin He who introduced me to Prof. Meggers, without her warmhearted help, I would not have the great opportunity to work in this group.

I would also like to thank all of the other members of Meggers group. First of all, our secretary lab technician Katjia Kräling and Ina Pinnschmidt, they are always very helpful with great patience and kindness. Lei Gong, Yonggang Xiang and Zhijie Lin, they helped me a lot in work and life, and I will miss the good times we had in and out of lab. And I also need to thank Nathan Kilah, Pijus Sasmal, Gabriella Benedek, Alexander Wilbuer, Sandra Dieckmann, Sebastian Blanck, Stefan Mollin, Matthias Bischof, Tom Breiding, Peter Göbel, Manuel Streib, Anja Kastl, Marianne Wenzel, Kathrin Wähler, Jens Henker, Melanie Helms, Elisabeth Martin, Rajathees Rajaratnam, Cornelia Ritter, Markus Dörr, Xiaodong Shen, Haohua Huo, Wei Zuo, Chuanyong Wang for their kind cooperation and friendliness, which made my working in a German lab easy. I also would like to thank the facilities directors in chemistry department, Dr. Xiulan Xie of the NMR facility, Dr. Uwe Linne of MS

Part of this work has been already published:

1) "Asymmetric Catalysis with Substitutionally Labile yet Stereochemically Stable Chiral-at-Metal Iridium(III) Complex" Huo, H. H.; **Fu, C.**; Harms, K.; Meggers E. *J. Am. Chem. Soc.*, **2014**, *136* (8), 2990–2993.

2) "Proline as Chiral Auxiliary for the Economical Asymmetric Synthesis of Ruthenium(II) Polypyridyl Complexes" **Fu, C.**; Wenzel, M.; Treutlein, E.; Harms, K.; Meggers E. *Inorg. Chem.* **2012**, *51*, 10004−10011.

3) **"**Hydrolytically stable octahedral silicon complexes as bioactive scaffolds: application to the design of DNA intercalators.**"** Xiang, Y. G.; **Fu, C.**; Breiding, T.; Sasmal, P. K.; Liu, H. D.; Shen, Q.; Harms, K.; Zhang, L. L.; Meggers, E. *Chem. Commun.* **2012**, *48*, 7131-7133.

4) "*N*-Sulfinylcarboximidates as a Novel Class of Chiral Bidentate Ligands: Application to Asymmetric Coordination Chemistry" Lin, Z.; Celik, M. A.; **Fu, C.**; Harms, K.; Frenking, G.; Meggers, E. *Chem. Eur. J.* **2011**, *17*, 12602-12605.

Abstract

This thesis mainly includes two parts: one is about the asymmetric synthesis of octahedral ruthenium complexes, and the other one is about the synthesis and investigation of the biological activities of octahedral silicon complexes.

In the first part of this thesis, we started with a straightforward and economical method for the asymmetric synthesis of mononuclear ruthenium(II) complexes [Ru(pp)(pp')(pp'')](PF$_6$)$_2$ (pp = polypyridyl ligands) by using the readily available racemic starting material [Ru(pp)(pp')Cl$_2$] together with the natural amino acid L-proline (Scheme I). Next, we initially studied the asymmetric synthesis of dinuclear octahedral ruthenium(II) complexes, and synthesized an enantiomerically enriched dinuclear ruthenium complex for the first time.
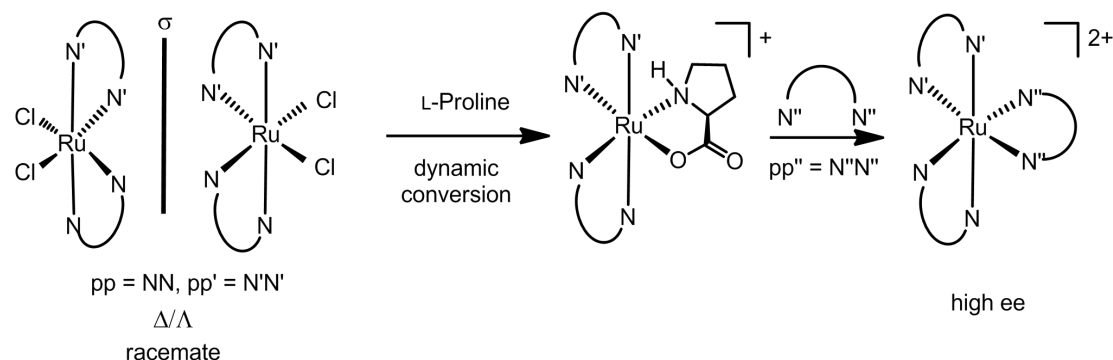
Scheme I. Asymmetric synthesis of octahedral mononuclear ruthenium(II) complexes [Ru(pp)(pp')(pp'')](PF$_6$)$_2$ with high enantiomeric excess mediated by L-proline.

In the second part of this thesis, we developed the syntheses of hydrolytically stable octahedral silicon complexes, such as silicon arenediolate complexes, silicon arenediaminate complexes, enantiopure silicon BINOLate complexes, and silicon-ruthenium sandwich complexes (Scheme II). Furthermore, we investigated the biological activities of the octahedral silicon complexes and found that the silicon arenediolate complexes could be used as efficient DNA intercalators, while the bulky silicon-ruthenium sandwich complexes could detect mismatched DNA and serve as insertors.

O,O = *ortho*-arenediolate
N,N = bipyridines, phenanthrolines
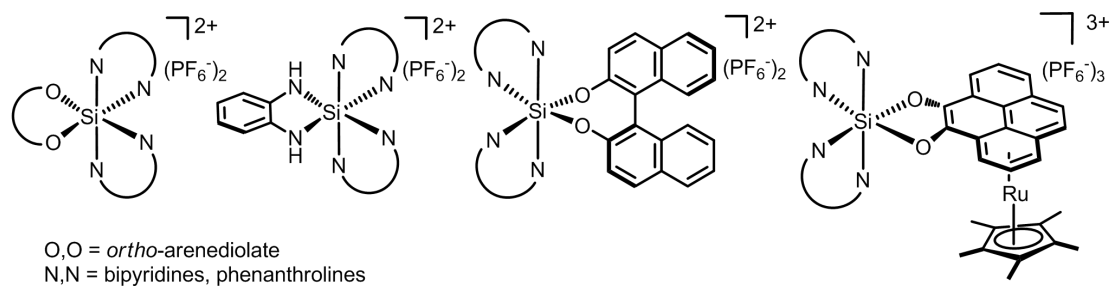
Scheme II. Structures of synthesized octahedral silicon complexes.

Abstract auf Deutsch

Diese Doktorarbeit ist aus zwei Teilen zusammengesetzt. Bei dem ersten Teil handelt sich um die asymmetrische Synthese oktaedrischer Rutheniumkomplexe und in dem zweiten Teil wurden die Synthese sowie die biologische Aktivität oktaedrischer Siliciumkomplexe erforscht.

Ausgehend von leicht herstellbarem racemischem Material [Ru(pp)(pp')Cl$_2$] (pp = Polypyridylliganden) wurden in dem ersten Teil dieser Arbeit die einkernigen Ruthenium(II)komplexe [Ru(pp)(pp')(pp'')](PF$_6$)$_2$ mit dem kommerziell verfügbarem Naturstoff L-Prolin bei einer einfachen und kostengünstigen asymmetrischen Synthese hergestellt (Schema I). Bei der ersten Untersuchung von doppelkernigen Ruthenium(II)komplexe wurde zum ersten Mal ein enantiomerenreiner doppelkerniger Ru-Komplex synthetisiert.
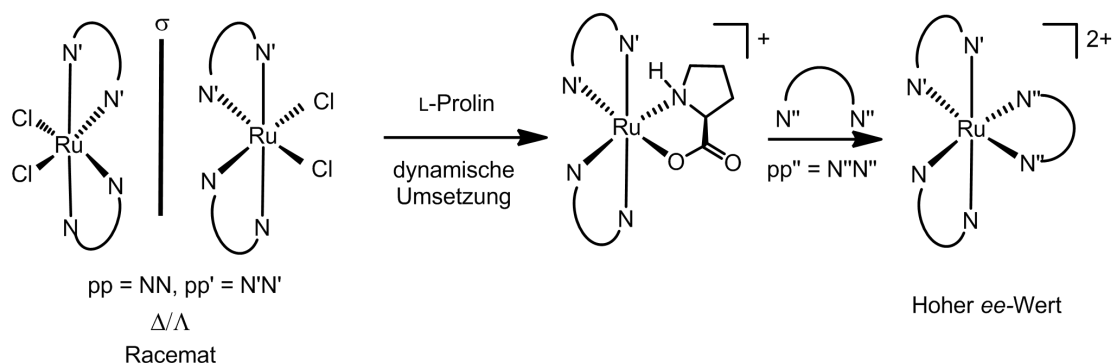
Schema I. L-Prolin-vermittelete asymmetrische Synthese oktaedrischer einkerniger Ruthenium(II)komplexe [Ru(pp)(pp')(pp'')](PF$_6$)$_2$ mit hohem Enantiomerenüberschuss.

In dem zweiten Teil dieser Arbeit wurden oktaedrische hydrolysestabile Siliciumkomplexe z.B. Siliciumkomplexe mit Arendiolat- und Arendiaminatliganden, enantiomerenreine Silicium-BINOLat-Komplexe und Silicium-Ruthenium-Sandwichkomplexe, erfolgreich synthetisiert (Schema II). Weiterhin wurde die biologische Aktivität oktaedrischer Siliciumkomplexe erforscht. Dabei wurde herausgefunden, dass die Siliciumkomplexe mit Arendiolatliganden als effiziente DNA-Interkalatoren dienen konnten. Außerdem konnten

Silicium-Ruthenium-Sandwichkomplexe Basenfehlpaarungen in Duplex DNA stabilisieren.

O,O = *ortho*-Arendiolate
N,N = Bipyridin-, Phenanthrolinliganden
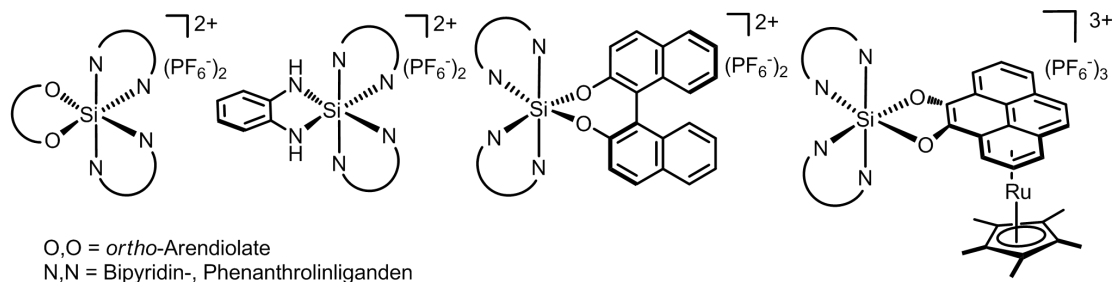
Schema II. Strukturen erfolgreich synthetisierter oktaedrischer Siliciumkomplexe.

Table of Contents

Chapter 1 Theoretical Part

1.1 Introduction

Chiral metal complexes are an important research object in current organometallic chemistry.[1-3] The almost unique strategy developed so far for the preparation of chiral metal complexes is based on the association of a chiral ligand with a metal ion, however, the chirality of the complex may also be located at the metal center itself and not at the ligands (Figure 1).
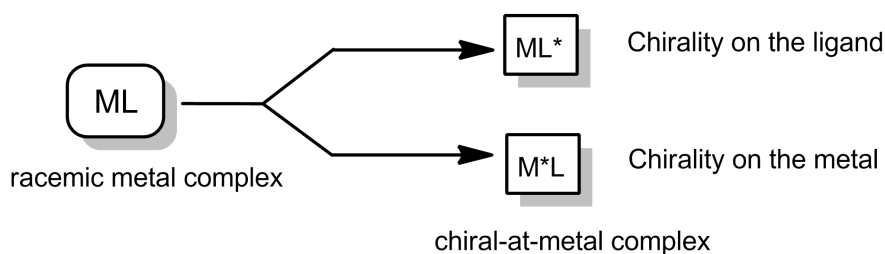
Figure 1. Chiral metal complexes in two different classification.

By and large, chiral-at-metal complexes can be divided into two groups, chiral half-sandwich and chiral octahedral complexes. In half-sandwich complexes, the aromatic ring system, mainly benzene or cyclopentadienyl (η^5-C_5H_5, Cp) and their derivatives, can be viewed as one of the four monodentate ligands.[2] Similar to an asymmetric carbon atom in an organic molecule, the coordination of centered metal by four different monodentate ligands in a tetrahedral configuration generates a chiral complex with two possible enantiomers, *R* and *S*. Such a chiral manganese half-sandwich complex (**1a**, **1b**) of tetrahedral configuration is shown in Figure 2.[4] However, the chirality of the metal center in chiral octahedral complexes results from the coordination of polydentate ligands, and the prototype complex is the octahedral tris-diimine ruthenium complex [Ru(diimine)₃]²⁺ (**2**), with diimine = bipyridines or phenanthrolines. As shown in Figure 2, such a chiral octahedral complex exists in two enantiomeric forms named Λ and Δ.
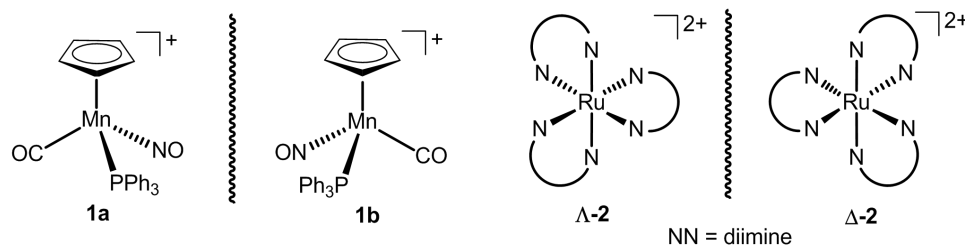
Figure 2. Two major groups of chiral-at-metal complexes.

Actually, the concept of metal-centered octahedral chirality can date back to over a century ago. In 1893, Alfred Werner applied van't Hoff and Le Bel's stereochemical theories of the carbon atom's tetrahedral nature to the octahedral configuration of metal, and ingeniously proposed that octahedral coordination complexes are capable of possessing metal-centered optical activity.[5] This prediction was later verified by a resolution of the two enantiomers from octahedral coordination complexes $[Co(en)_2(NH_3)X]^{2+}$ (**3**), X = Cl or Br, en = ethylene diamine, as shown in Figure 3.[6]
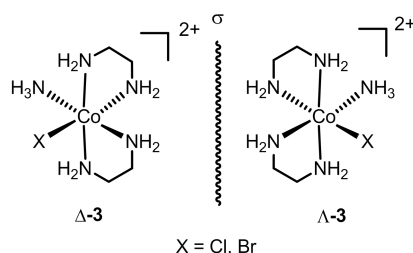
Figure 3. Werner's discovery of optically active enantiomers resolved from the cationic complexes of $[Co(en)_2(NH3)X]^{2+}$ (X = Cl or Br).

For an octahedral coordination complex with six different monodentate ligands, the number of its stereoisomers can reach up to 30, including 15 pairs of enantiomers.[7] As a result, the elaborate stereochemistry of hexacoordinate octahedral coordination geometries is nowadays a key feature for many applications in different areas of chemical research, ranging from catalysis to the life sciences.[8-10]

In the applications to the life sciences, the chirality-at-metal plays an important role in molecular recognition of chiral biomacromolecules. Interestingly, more than six decades ago, Dwyer already reported a significant stereodifferentiation in the binding of the enantiomers of $[Ru(bpy)_3](ClO_4)_2$, bpy = 2,2'-bipyridine, to the enzyme acetylcholine esterase—the Δ-enantiomer with 90% inhibition vs the Λ-enantiomer

with 20% inhibition.[11] Meggers group also reported that the two enantiomers of octahedral ruthenium complex **4** exhibiting totally different biological activities. As shown in Figure 4, compared to the almost inactive Δ-**4**, the mirror-image complex Λ-**4** served as a highly potent and selective inhibitor for the protein kinase GSK3.[12]
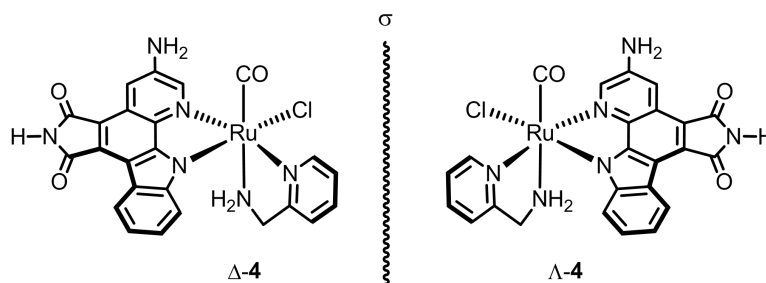
Figure 4. The ruthenium complex Λ-**4** with a highly selective inhibition for the protein kinase GSK3 in contrast to the almost inactive mirror-image complex Δ-**4**.

Octahedral chiral-at-metal complexes with carefully tailored ligands also can be applied to the field of asymmetric catalysis. For instance, Meggers group recently reported an inert chiral-at-metal iridium(III) complex Λ-**5** as a highly efficient catalyst for asymmetric transfer hydrogenation of β,β′-disubstituted nitroalkenes (Scheme 1), which exceeded the performance of most organocatalysts for extraordinary enantiomeric excess (up to 99%) and catalyst loading (down to 0.1 mol %).[13]
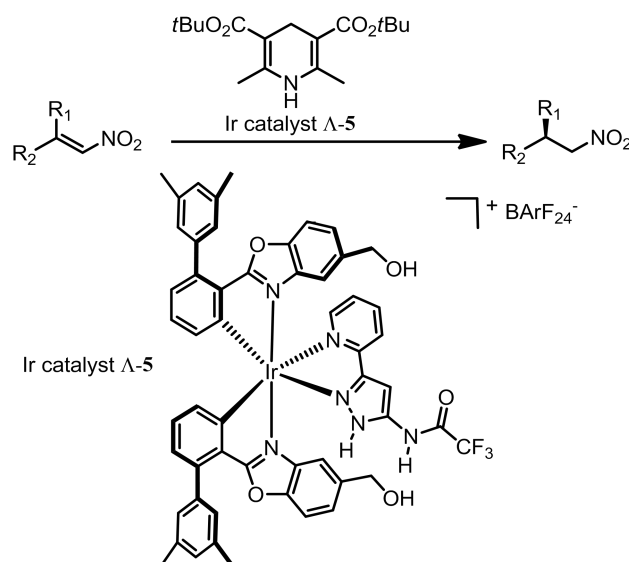
Scheme 1. An efficient asymmetric catalyst with octahedral chirality-at-metal.

Although chiral octahedral metal complexes have shown remarkable properties

in asymmetric catalysis and life sciences, in contrast to numerous sophisticated synthetic methodologies can be adopted to control the configuration at the tetrahedral carbon atoms for organic compounds, the stereochemical control of octahedral coordination compounds is still in its infancy. Therefore, developing general synthetic methods to control the chirality-at-metal is our foremost concern in this thesis.

1.2 Methods to Obtain Enantiopure Octahedral Metal Complexes

The methods to obtain enantiopure octahedral metal complexes can be classified in four ways: resolution of chiral cations, chiral-anion-induced asymmetric synthesis, diastereoselective coordination with chiral ligands, and chiral-auxiliary-mediated asymmetric synthesis.

1.2.1 Resolution of Chiral Cations

The largest number of resolutions are performed *via* the conversion of a racemate into a mixture of diastereomers mediated by chiral anions.[14] In this type of reaction, the cations to be resolved are treated with one enantiomer of a chiral anion (the resolving agent). The resulting diastereomeric pairs can be ionic and the vast majority of the resolutions are based on solubility differences of solids. For instance, Leveque reported that racemic cation $[Ru(bpy)_2(py)_2]^{2+}$ (py = pyridine) **8** can be selectively resolved by *O,O'*-dibenzoyl-L-tartrate **6**, while antimonyl L-/D-tartrate **7** allowed the resolution of $[Ru(bpy)_2(CO)_2]^{2+}$ **9** and $[Ru-(phen)_2(CO)_2]^{2+}$ **10** (Figure 5).[15]
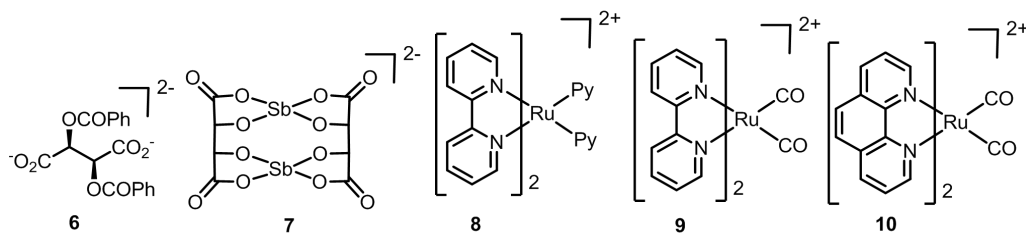
Figure 5. Resolution of racemic ruthenium(II) cations (**8~10**) with chiral anions (**6, 7**).

Compared to the resolution based on solubility differences of solids, chromatographic resolution is a more direct method, which is carried out through ionic diastereomer mixtures with the addition of non-racemic counterions into the mobile phase.[16] For example, Sauvage and Keene have reported the resolution of double helical iron(II) dinuclear complex **11** by chromatography (Figure 6), a racemic mixture of the sulfate salt of **11** was absorbed onto a column of SP Sephadex C-25 cation exchanger and eluted with the aqueous sodium salt of chiral *O,O'*-di-4-toluyl-L-tartrate **6**.[17,18]
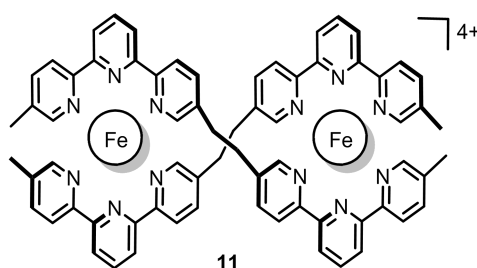
Figure 6. The structure of double helical iron(II) dinuclear complex **11**.

The resolution can also be achieved by selective asymmetric extraction. As an example, Lacour reported an excellent resolution of the racemic [Ru(dmp)$_3$]Cl$_2$ {[**12**]Cl$_2$} in an aqueous solution, by combination with an organic phase containing the enantiopure TRISPHAT salt [Bu$_3$NH][Λ-**13**].[19] Upon vigorous stirring of the biphasic mixture, selective transfer of one enantiomeric cation [Λ-**12**] from water to the organic layer occurred, affording [Δ-**12**][Cl]$_2$ in the water layer with a enantiomeric ratio (e.r.) up to 35 : 1 and [Λ-**12**][Λ-**13**] in the CHCl$_3$ layer with a diastereomeric ratio (d.r.) up to 49 : 1, as the schematic shown in Figure 7.
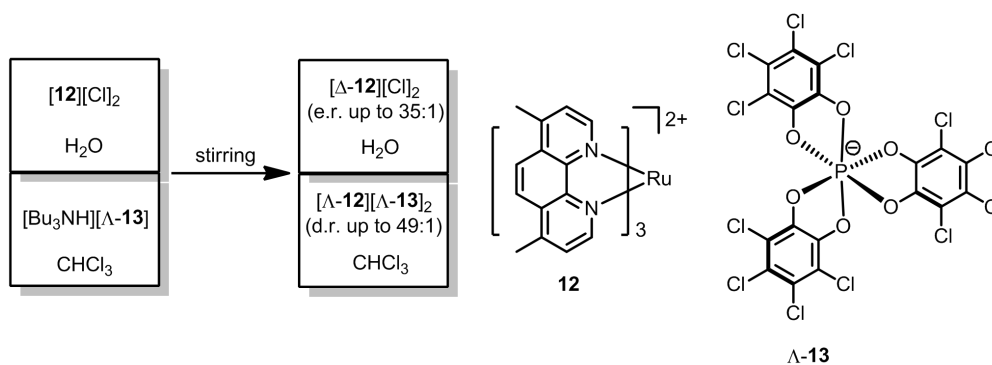
Figure 7. Schematic representation of the asymmetric extraction of [**12**]Cl$_2$.

1.2.2 Chiral-Anion-Induced Asymmetric Synthesis

As mentioned before, chiral anion such as enantiopure TRISPHAT worked nicely in discriminating between the two enantiomers of chiral metal complexes. Moreover, it also can be exploited as chiral-inducing agent for the control of the configuration at the metal center. As an example, Lacour and coworkers reported that Δ-TRISPHAT (Δ-**13**) shifted the equilibrium between the configurationally labile iron(II)–tris(diimine) enantiomers Λ-**14** and Δ-**14** to reach a diastereomeric ratio greater than 50:1.[20]
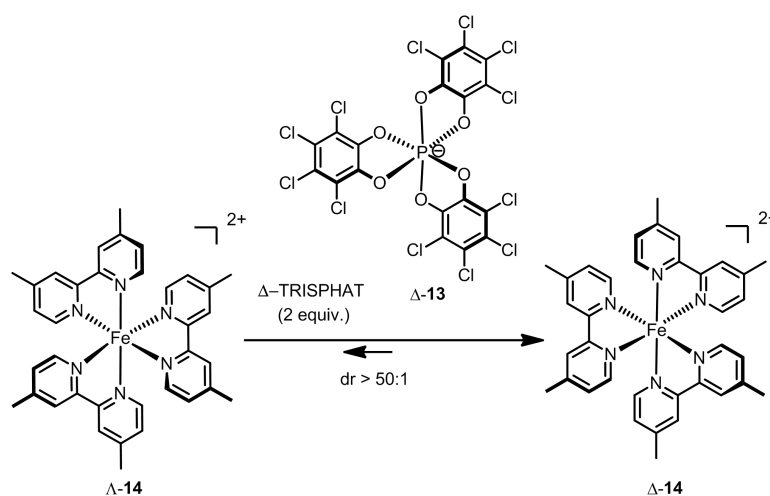
Scheme 2. The equilibrium between the Λ- and Δ-configurations of a labile iron complex **14** shifted by the Δ-TRISPHAT.

Under certain conditions, TRISPHAT is even able to influence the metal-centered chirality in configurationally more stable coordination compounds. Scheme 3 depicts a remarkable reaction reported by Lacour group, the octahedral iron(II) complex [Fe(Me$_2$bpy)$_3$]$^{2+}$ **15** reacted with tetradentate ligand **16** in the presence of 2 equiv of Δ-TRISPHAT (Δ-**13**) in DCM under reflux, affording the configurationally more stable iron(II) complex Δ-**17** with a high diastereomeric ratio greater than 20:1.[21]
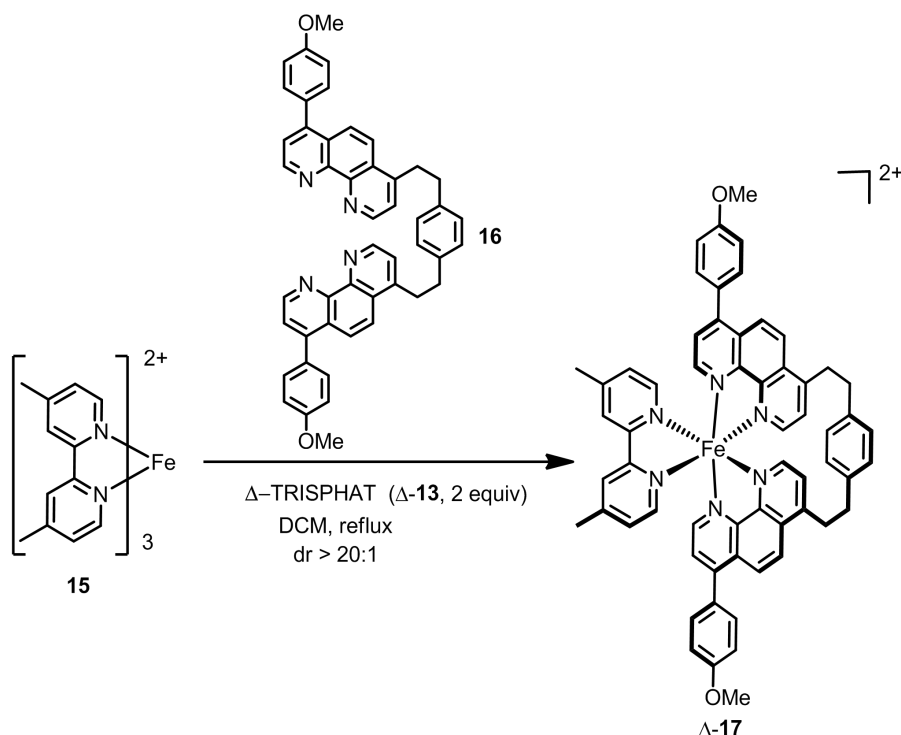
Scheme 3. Chiral-anion-induced asymmetric synthesis of a configurationally stable tris(diimine) iron(II) complex Δ-**17** in the presence of Δ-TRISPHAT (Δ-**13**).

1.2.3 Diastereoselective Coordination with Chiral Ligands

Over the past decades, chemists made a better understanding to stereochemical control of chirality transfer from chiral coordinating ligands to transition metal centers, *via* employing chiral ligands or carefully tailored chiral multidentate ligands to provide high diastereoselectivities in the course of coordination chemistry.[22-24]

The first asymmetric synthesis of a chiral coordination complex can trace back to the work reported by Smirnoff, he found that enantiopure propane-1,2-diamine (pn) reacted with H_2PtCl_6 to provide octahedral complexes with optical activity, and he concluded that the reaction occurred diastereoselectively.[25] 85 years later, von Zelewsky carefully restudied this work, which further verified Smirnoff's conclusion, and the *mer*-Λ-[Pt{(*S*)-pn}$_3$]$^{4+}$ (**18**) was determined to be the most preferred product by precipitation and crystallization steps (Scheme 4).[23]
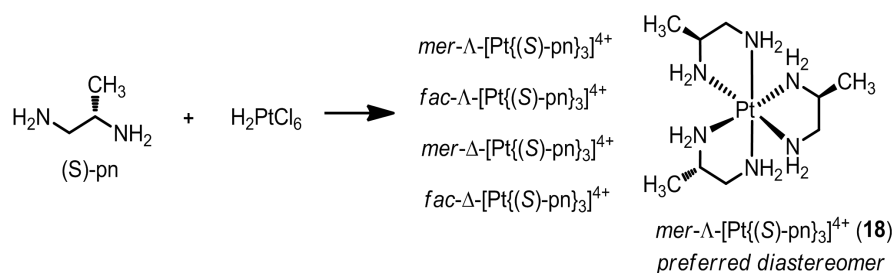
Scheme 4. The first asymmetric synthesis of a chiral coordination complex **18** reported by Smirnoff and restudied by Zelewsky 85 years later.

Inspired by nature's strategy to control metal-centered configuration, synthetic chemists have designed and developed various mimicked chiral multidentate ligands for asymmetric synthesis of chiral metal complexes.[26] Von Zelewsky developed CHIRAGENs (from CHIRAlity GENerator), terpene-derived chiral tetradentate bis(2,2'-bipyridine)s, to stereospecifically generate one exclusive chirality at the metal centers. As an example shown in Scheme 5, the (+)-chiragen[6] first reacted with [Ru(DMSO)$_4$Cl$_2$], followed by Me$_2$bpy (4,4'-dimethyl-2,2'-bipyridine), yielding the cationic complex Δ-[Ru{(+)-chiragen[6]}(Me$_2$bpy)] (Δ-**19**) as a single diastereomer in a yield of 25%.[27]
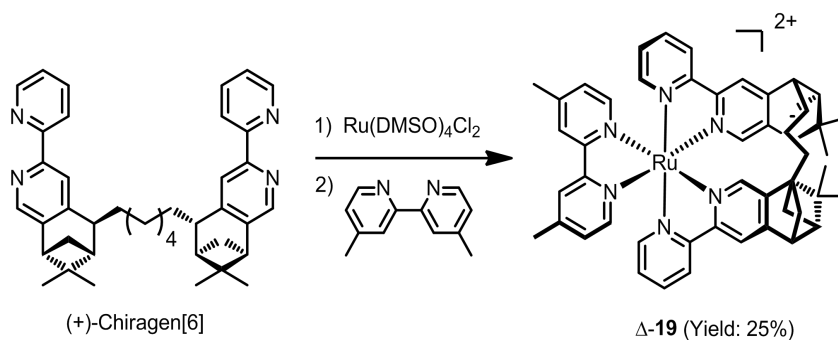
Scheme 5. The asymmetric synthesis of cationic complex (Δ-**19**) as a single diastereomer by using the (+)-Chiragen[6] ligand.

Besides the highly predesigned geometries of multidentate ligands, aromatic face-to-face π-stacking also can be exploited for the control of absolute metal-centered configuration.[28] As shown in Scheme 6, the reaction of chiral iminopyridines **20** with Fe(ClO$_4$)$_2$·6H$_2$O in MeCN afforded the single diastereomer *fac*-Δ-[Fe{(*R*)-**20**}$_3$](ClO$_4$)$_2$ (*fac*-Δ-**21**), and each of the three pyridine units formed a

face-to-face π-interaction with a phenyl unit on a neighboring ligand, leading to the impressive stereospecificity.[29]
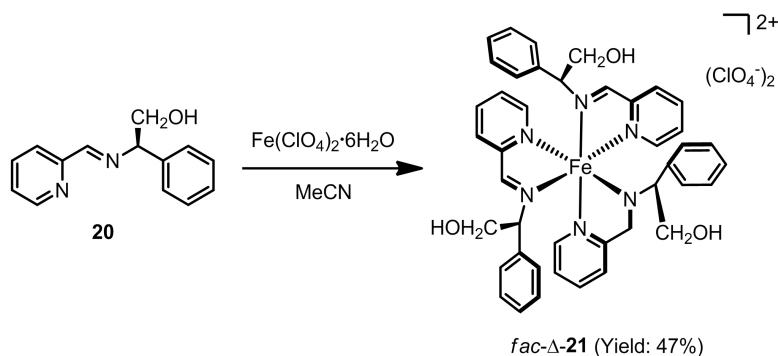
Scheme 6. The asymmetric synthesis of cationic complex (*fac*-Δ-**21**) directed by aromatic face-to-face π-stacking.

These tailored chiral multidentate ligands are capable of efficiently and stereospecifically ruling the metal-centered configuration, however, they are always irremovable or removable with a total loss of chiral information in the metal center.[30,31] Therefore, developing the chiral ligands that can be further cleaved with the retention of metal-centered configuration is extremely desired.

1.2.4 Chiral-Auxiliary-Mediated Asymmetric Synthesis

Chiral auxiliaries are utilized extensively in organic chemistry for the synthesis of enantiopure compounds in a predictable and efficient way.[32,33] In this strategy, the chiral auxiliary is firstly temporarily linked to a substrate to direct the stereochemical course of a diastereoselective reaction, and subsequently the auxiliary is detached. Applied to metal complexes, a chiral auxiliary may constitute a transiently metal-coordinating chiral ligand which directs the stereochemical course of ligand substitutions, and it is removed afterwards, leaving an enantiomerically enriched metal complex behind.

The first example of chiral-auxiliary-mediated asymmetric synthesis was introduced by Baila and co-workers. In 1948, Bailar Jr. reported that (*R*,*R*)-(+)-tartrate can be employed as a chiral auxiliary for the synthesis of (+)-[Co(en)₃]³⁺, en =

1,2-ethylenediamine, in dynamic kinetic resolutions.[11] Namely, racemic $[Co(en)_2CO_3]^+$ (en = 1,2-ethylene diamine) firstly reacted with the (R,R)-(+)-tartrate to generate two diastereomers, (+)-$[Co(en)_2\{(R,R)$-(+)-tartrate$\}]^+$ and (−)-$[Co(en)_2\{(R,R)$-(+)-tartrate$\}]^+$, as shown in Scheme 7. Subsequently, the two diastereomers reacted with en at different rate based on their own different stability, the less stable diastereomer (+)-$[Co(en)_2\{(R,R)$-(+)-tartrate$\}]^+$ reacted faster with en to afford the major complex (+)-$[Co(en)_3]^{3+}$ **22** (the Λ-enantiomer) in a yield of 70% and with an enantiomeric purity of up to 90%.

On the basis of the same strategy, Bailar group also reported the first auxiliary-mediated asymmetric synthsis of enantiomerically enriched cationic complex $[Ru(bpy)_3]^{2+}$ **23** from the reaction of K_2RuCl_5 hydrate with the (R,R)-(+)-tartrate, followed by excess bpy. However, in comparison to the enantiomeric purity of the cobalt complex (up to 90%), the ruthenium complex achieved a much lower enantiomeric ratio (63: 37). Analogously, enantiomerically enriched complexes $[Ru(phen)_3]^{2+}$ **24** was also obtained (Scheme 7).[34]
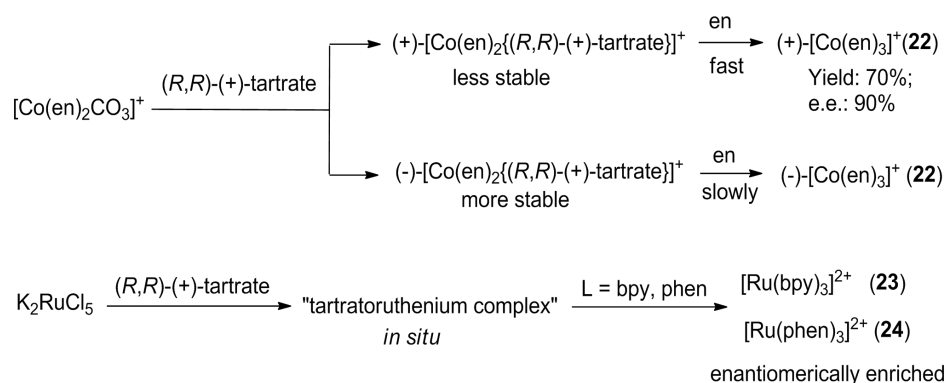
Scheme 7. (R,R)-(+)-tartrate as a chiral auxiliary for asymmetric synthesis of cobalt complex **22** and ruthenium complexes **23** and **24**.

The chiral auxiliary can also be a transient, cleavable linker between two or more multidentate ligands. For example, Wild and co-workers developed a chiral hexadentate linker, (R,R)-**25**, in which two tridentate pyridine-2-aldehyde-2'-pyridyl-hydrazones are connected by a chiral (R,R)-tartrate unit. When the hexadentate ligand **25** was reacted with $[Fe(H_2O)_6](PhSO_3)_2$,

octahedral metal complex **26** was obtained with completely diastereomeric selectivity. Unfortunately, the resulting metal complex **27** got partially racemized during the next cleavage step, yielding only an enantiomeric ratio of 85 : 15 (Scheme 8).[35]

Scheme 8. Asymmetric synthesis of iron octahedral complex **27** by using a chiral linker as an auxiliary.

Based on the similar strategy, Fletcher and co-workers reported a chair tripodal linker to control the metal-centered configuration.[36] As shown in the Scheme 9, the reaction of enantiopure tripodal hexadentate ligand (*R,R,R*)-**28** with [Ru(DMSO)$_4$Cl$_2$] in the presence of AgNO$_3$ under reflux in EtOH and high dilution, afforded the ruthenium complex Δ-(*R,R,R*)-**29** as the main diastereomer (>95:5 d.r.) albeit in a low yield of 10%. The subsequent cleavage of the ester bonds with aqueous KOH provided the final product *fac*-Δ-**30**. However, the low yield of the coordination step and the subsequent purification problem make this method rather unattractive.

Scheme 9. Asymmetric synthesis of a *fac*-Δ-ruthenium polypyridyl complex **30** with a cleavable linker (*R,R,R*)-**28**.

Inoue and co-workers reported the first use of a monodentate chiral sulfoxide—(*R*)-(+)-methyl *p*-tolyl sulfoxide **31** as a chiral auxiliary to the asymmetric synthesis of polypyridyl ruthenium complex **33**, which was further optimized by Aït-Haddou and co-workers.[37] As shown in scheme 10, the reaction of racemic *cis*-[Ru(bpy)$_2$Cl$_2$] with sulfoxide **31** afforded the configurational preferred Δ-**32** with a diastereomeric excess (de) of 74% and a high yield of 99%. Inoue et al. proposed that the preferred diastereomer was stabilized by a combination of face-to-face π-stacking of the tolyl group with a bidentate ligand and a hydrogen bond between the sulfoxide oxygen and a pyridyl *ortho*-proton, which were supported by NMR experiments and X-ray crystallographic analysis.[38]
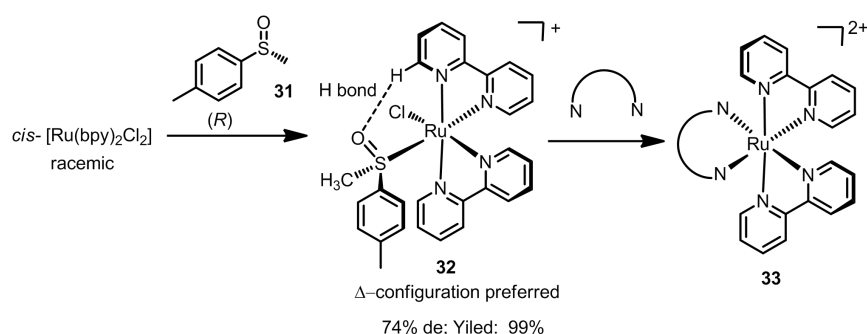
Scheme 10. Monodentate methyl *p*-tolyl sulfoxide *R*-**31** as a chiral auxiliary for the asymmetric synthesis of polypyridyl ruthenium complex **33**.

Although this monodentate chiral sulfoxide just resulted in moderate ee values of the final compounds, it was still attractive to related synthetic chemists until 2009, when Meggers group reported a general method to efficiently synthesize octahedral

polypyridyl ruthenium complexes with remarkable enantiopurity mediated by a chiral bidentate salicyloxazoline (**Salox**) ligand.[39] As shown in Scheme 11, the asymmetric synthsis of polypyridyl complex Λ-[Ru(pp)(pp')(pp'')]$^{2+}$ **36** (pp, pp', pp'' = achiral 2,2'-bipyridines) was carried out in 3 steps starting from the precursor (*S*)-**34**, which has four labile ligands. (*S*)-**34** first reacted with one equivalent of 4,4'-di-*tert*-butyl-2,2'-bipyridine (dbb) in chlorobenzene at 70 ^{o}C, subsequently with one equivalent of 5,5'-dimethyl-2,2' -bipyridine (dmb) again in chlorobenzene at 70 ^{o}C, affording only one diastereomer Λ-(*S*)-**35** under thermodynamic control in a moderate yield of 64%. For the last step, the chiral-auxiliary-mediated complex Λ-(*S*)-**35** reacted with the excess bipyridine (bpy, 15 equiv) in the presence of TFA (trifluoroacetic acid, 5 equiv), yielding the polypyridyl ruthenium complex **36** with total retention of centered-metal configuration.
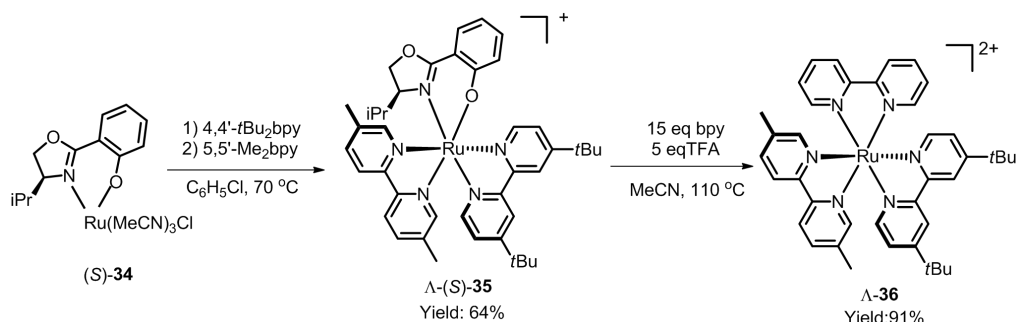
Scheme 11. Salicyloxazoline as a chiral auxiliary for the asymmetric synthesis of polypyridyl ruthenium complexes.

In an analogous fashion, Meggers group found that (*R*)-**HO**-**MOP**, (*R*)-2'-(diphenylphosphino)-1,1'-binaphthyl-2-ol, could serve as an effective chiral auxiliary starting from the commercially available half-sandwich ruthenium dimer [Ru(η^6-C$_6$H$_6$)Cl$_2$]$_2$.[40] Accordingly, [Ru(η^6-C$_6$H$_6$)Cl$_2$]$_2$ reacted with 1.25 equiv of (*R*)-**HO**-**MOP** and 2 equiv of bpy in dry ethanol and in the presence of Et$_3$N at 95 $^{\circ}$C in a sealed vial, affording the complex Λ-{Ru(bpy)$_2$[(*R*)-HO-MOP]}Cl (Λ-(*R*)-**37**) in one step with a satisfactory diastereoselectivity of 34 : 1 and a yield of 84%. Then the coordinating auxiliary (*R*)-**HO**-**MOP** in the Λ-(*R*)-**37** also can be replaced by the new added ligand (bpy) *via* TFA acidification, and the resulting Λ-[Ru(bpy)$_3$]$^{2+}$ (Λ-**23**) formed with high enantiopurity (Scheme 12).
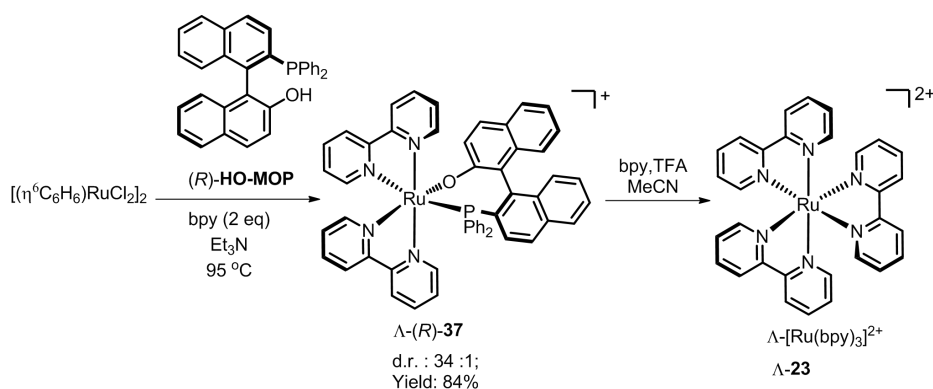
Scheme 12. Transfer of axial chirality of (*R*)-**HO-MOP** to metal-centered chirality in a chiral-auxiliary-mediated asymmetric synthesis.

Chiral sulfoxides are especially attractive ligands as components of chiral auxiliaries, because sulfoxides place their center of asymmetry—the coordinating sulfur, in direct proximity to the metal, thus promoting an especially facile transfer of chirality from the auxiliary to the metal. As described before, chiral monodentate sulfoxide **31** has shown to be a moderate chiral auxiliary for the asymmetric synthesis of polypyridyl ruthenium complexes. However, chiral bidentate chelates usually direct the asymmetric coordination chemistry more effectively than monodentate ligands, due to a restricted rotation around the M-L coordinative bonds that fixes the direction of the hindrance from the directing ligand. Indeed, Meggers group recently reported the bidentate sulfoxide (*R*)-**SO** {2-(isopropylsulfinyl)phenol}, which can be used as an effective auxiliary for the thermodynamically-controlled asymmetric synthesis of polypyridyl ruthenium complex Λ-**23**, starting from the complex *cis*-[Ru(bpy)$_2$Cl$_2$] (Scheme 13).[41] This method was successfully applied to other readily available racemic ruthenium complexes *cis*-[Ru(pp)$_2$Cl$_2$] as well, pp = 1,10-phenanthroline (phen) or 5,5'-dimethyl-2,2'-bipyridine (dmb).[42]
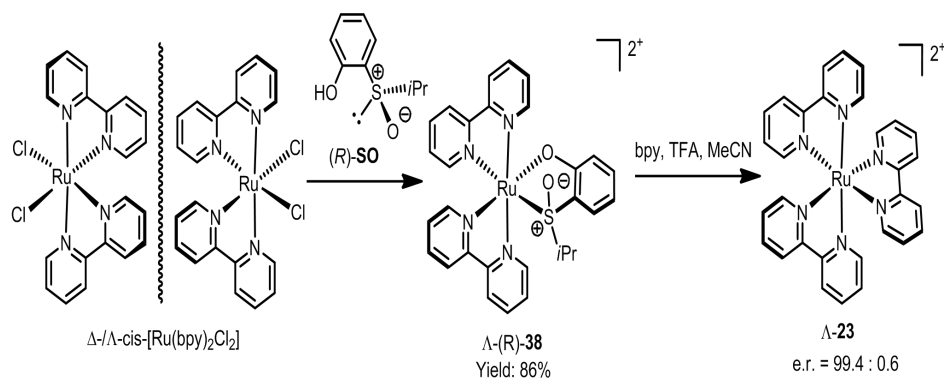
Scheme 13. (*R*)-**SO** as an efficient auxiliary for the thermodynamically-controlled asymmetric synthesis of ruthenium polypyridyl complex from the racemic starting complex *cis*-[Ru(bpy)$_2$Cl$_2$].

1.3 Metal Complexes as DNA Binders

Over the past few decades, small molecules that bind to DNA have shown significant applications as diagnostic probes, reactive agents and therapeutics.[43] The design of substitutionally inert, octahedral transition metal complexes for DNA binding agents has attracted more and more interest.[44] Compared to organic molecules, transitional metal complexes possess two advantages as DNA binding agents. First and foremost, coordination complexes offer a uniquely modular system. The centered metal substantially acts as a structural center, holding a rigid, three-dimensional scaffold of ligands. The DNA-binding and recognition properties thereby could be easily varied by changing the ligands. Secondly, transition metal complexes bear rich photophysical and electrochemical properties, and these properties have led to a wide applications, such as fluorescent markers, DNA footprinting agents and electrochemical probes etc.[45]

1.3.1 Structural Features of DNA

Before our discussion of DNA binding and recognition, some structural features of DNA should be briefly reviewed. DNA consists of two complementary, antiparallel poly-deoxyribonucleotide strands associated by specific hydrogen bonding

interactions between nucleotide bases.[46] Each base forms hydrogen bonds with its complementary base on the opposite anti-parallel strand, A (adenine) with T (thymine) and C (cytosine) with G (guanine), as shown in Figure 8a. The base pairs collectively form a central, hydrogen-bonded π-stack that runs parallel to the helical axis between the two strands of the sugar-phosphate backbone. In addition, the rise per base is 3.4 Å, and there are ten base pairs per helical turn.

DNA exists in mainly three possible conformations: A-DNA, B-DNA and Z-DNA forms.[45] The anti-parallel right-handed double helix B-DNA is the most common form found in living cells. The sugar-phosphate backbone of paired strands forms two different helical grooves, major groove and minor groove. As shown in Figure 8b, the biologically relevant B-form DNA double helix is characterized by a shallow, wide major groove and a deep, narrow minor groove.
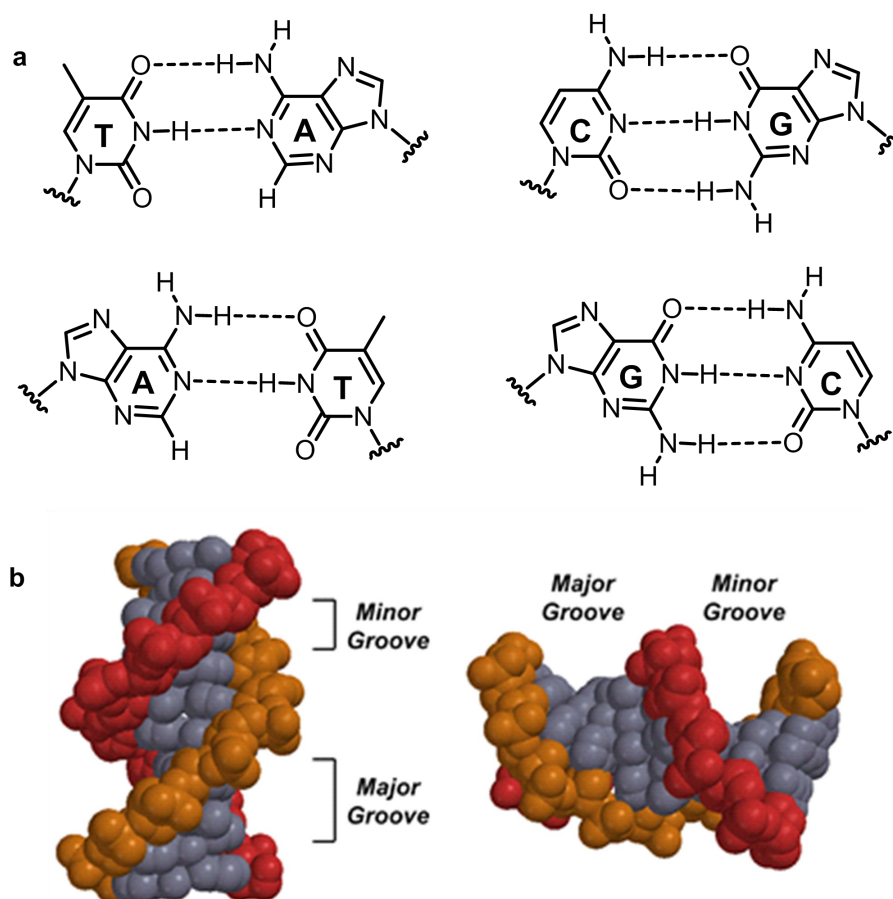
Figure 8. Structural features of the DNA double helix. (a) Chemical features of Watson-Crick base pairings. (b) Molecular rendering of B-form DNA double helix.

1.3.2 Binding Modes of Metal Complexes with DNA

Non-covalent metal complexes can bind DNA in three different modes: groove binding, intercalation, and insertion, as shown in the Figure 9. Groove binding means that the metal complexes bind to DNA *via* the minor or major grooves due to van der waals contact, while the intercalation involves the insertion of a planar-fused aromatic ring between the DNA base pairs, and metallo-insertors bearing the aromatic ligands that perform like replacements of the DNA base stack can eject a single base pair.[45]

Figure 9. The three binding modes of metal complexes with B-DNA: (A) groove binding (B) intercalation (C) insertion (ref. 45)

1.3.2.1 Groove Binding

The earliest work involving the interaction of coordinatively saturated octahedral transition-metal complexes with DNA focused on the tris(phenanthroline) metal complexes,[47] such as [Co(phen)$_3$]$^{3+}$ **39**, [Ru(phen)$_3$]$^{2+}$ **40** and [Ru(DIP)$_3$]$^{2+}$ **41** (DIP = 4,7-diphenyl-1,10-phenanthroline) (Figure 10). Based on extensive photophysical and NMR experiments, it was proposed that these complexes bind to DNA *via* two distinct modes: (i) hydrophobic interactions in the minor groove; (ii) partial intercalation of a phenanthroline ligand into the helix in the major groove.[48] More importantly, the early experiments revealed the chiral selectivity in DNA-binding. For instance, the Δ-enantiomer of [Ru(phen)$_3$]$^{2+}$ **40** is preferred in the intercalative binding mode, while the Λ-**40** is favored in the minor groove binding mode.[49] The ruthenium complex [Ru(DIP)$_3$]$^{2+}$ **41** (DIP = 4,7-diphenyl-1,10-phenanthroline) bearing more sterically

demanding phenanthroline ligand derivatives, displayed more dramatic chiral discrimination—the Δ-enantiomer bound stereospecifically to right-handed B-DNA while the Λ-enantiomer bound only to left-handed Z-DNA.[17] Furthermore, this trend of chiral selectivity in DNA-binding has always been observed for other non-covalent metal complexes.[50]
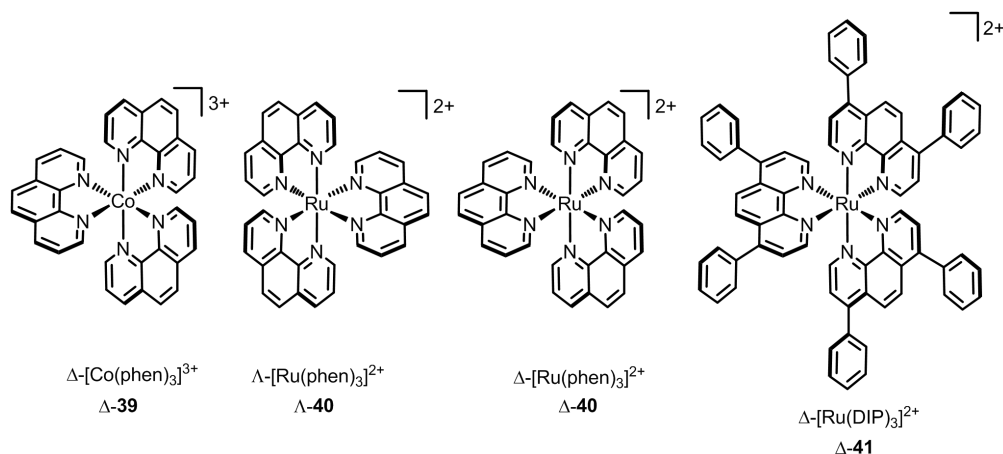
Figure 10. Some exemplified early octahedral DNA probes.

1.3.2.2 Intercalation

Metallo-intercalators bear at least one intercalating ligand, an extended aromatic system outward from the metal center that can π-stack between two base pairs. The intercalating ligand of these complexes behaves as a stable anchor in the major groove, oriented parallel to the base pairs, and directs the orientation of the ancillary ligands with respect to the DNA duplex (Figure 11). Two well-known examples of intercalating ligands are phi (phenanthrene-9,10-diimine) and dppz (dipyridophenazine), and the related octahedral complexes Δ-[Rh(phen)$_2$(phi)]$^{3+}$ (Δ-**42**) and Δ-[Rh(bpy)$_2$(dppz)]$^{2+}$ (Δ-**43**) are also shown in Figure 11.[51,52]

Δ-[Rh(phen)₂(phi)]³⁺ (Δ-**42**)   Δ-[Ru(bpy)₂(dppz)]²⁺ (Δ-**43**)
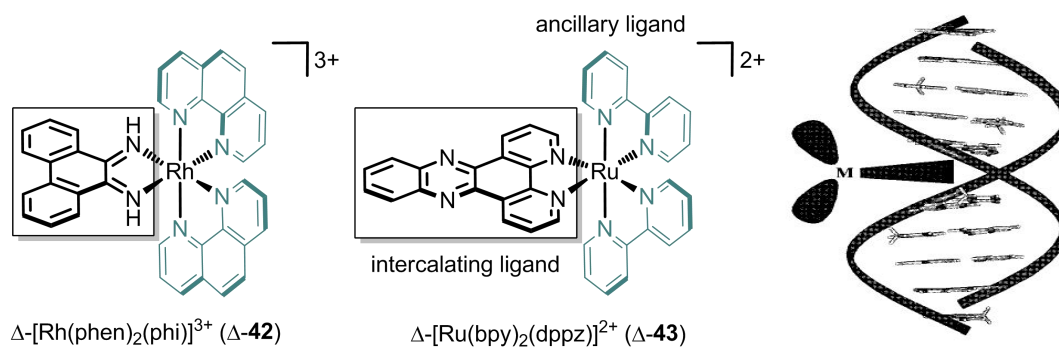
Figure 11. Structure of two representative octahedral metallo-intercalators: Δ-[Rh(phen)₂(phi)]³⁺ and Δ-[Rh(bpy)₂(dppz)]²⁺ and an illustration of the intercalating complex oriented with respect to the DNA double helix. (The intercalating ligands are framed, and the ancillary ligands are highlighted in gray.)

As described before, the earliest work shows that the Δ-enantiomer of the octahedral metal complex preferentially binds to right-handed B-DNA. Actually, this enantioselective discrimination is primarily steric in nature and depends on the size of the ancillary ligands relative to that of the DNA groove.[10,53] For instance, poor enantioselectivity is observed with metallo-intercalators bearing small ancillary ligands such as phen and bpy, whereas complete enantiospecificity is achieved with bulkier ancillary ligands such as DPB (4,4'-diphenyl-2,2'-bipyridine).[45] As shown in Figure 12, the Δ-enantiomer of [Rh(DPB)₂(phi)]³⁺ (Δ-**44**) readily cleaves the sequence 5'-CTCTAGAG-3' upon photoactivation, but no intercalation or cleavage is observed with the Λ-enantiomer, even with a thousand-fold excess of metal complex.

Δ-[Rh(bpy)₂(phi)]³⁺ (Δ-**42**)   Δ-[Rh(DPB)₂(phi)]³⁺ (Δ-**44**)
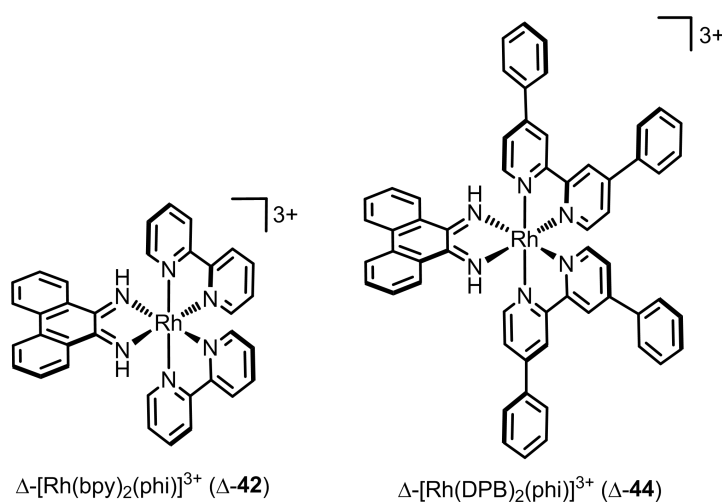
Figure 12. Metallo-intercalators of [Rh(bpy)₂(phi)]³⁺ and [Rh(DPB)₂(phi)]³⁺.

Besides octahedral metal complexes, inert and coordinatively saturated

square-planar Pt(II) complexes with aromatic ligands also have intercalative interactions with DNA. Lippard and coworkers reported that square-planar platinum(II) complexes containing heterocyclic aromatic ligands, such as terpy, phen, bipy and phi, bound to DNA duplexes through intercalating between the base pairs (Figure 13).[54] The crystal structure of [Pt(terpy)(HET)]$^+$ **45** (terpy = 2,2':6',2''-terpyridine, HET = 2-hydroxyethanethiolate) bound to (dCpG)$_2$ reveals that the flat metal cation intercalates symmetrically between two GC base pairs.[54]

[Pt(terpy)(HET)]$^+$ **45**   [Pt(phen)(en)]$^{2+}$ **46**   [Pt(bpy)(en)]$^{2+}$ **47**   [Pt(phi)(en)]$^{2+}$ **48**
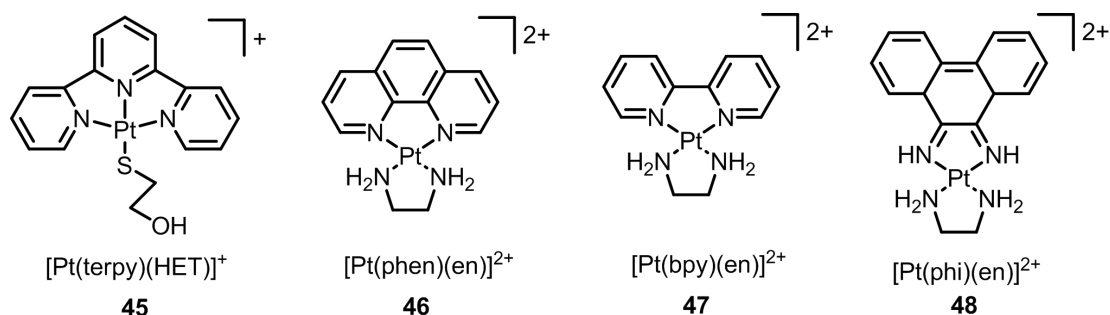
Figure 13. Square-planar platinum intercalators: terpy = 2,2':6',2''-terpyridine; HET = 2-hydroxyethanethiolate; phen = 1,10-phenanthroline; bpy = 2,2′-bipyridine; phi = phenanthrene-9,10-diimine; en = ethylenediamine.

1.3.2.3 Insertion

The third non-covalent binding mode—insertion was first proposed by Lerman, he speculated that organic moieties may bind ''a DNA helix with separation and displacement of a base-pair''.[55] Metallo-insertors, similar to metallo-intercalators, contain a planar aromatic ligand that extends into the base-stack upon DNA-binding. However, while metallo-intercalators unwind the DNA and insert their planar ligand between two intact base-pairs, metallo-insertors eject the bases of a single base-pair, with their planar ligand acting as a π-stacking replacement in the DNA base stack.

Barton and co-workers have contributed a lot to the understanding of insertion mode, and a series of rhodium complexes as mismatch-specific DNA-binding agents have been developed by them.[56] The first generation complex Δ-[Rh(bpy)$_2$(chrysi)]$^{3+}$ (chrysi = 5,6-chrysenediimine), has proved to be remarkably selective—mismatches are bound at least 1000 times tighter than matched base-pairs (Figure 14a). Moreover,

it promotes direct strand cleavage of the DNA backbone adjacent to the mismatch site upon photoactivation with UV-light.[57] More recently, higher mismatch binding affinities were obtained by the second generation complex [Rh(bpy)$_2$(phzi)]$^{3+}$ {phzi = benzo[*a*]phenazine-5,6-quinone diimine}, bearing a similar expansive intercalating ligand phzi (Figure 14b). Subsequently, a crystal structure of Δ-[Rh(bpy)$_2$(chrysi)]$^{3+}$ bound with a self-complementary oligonucleotide containing two AC mismatches (5′-CGG*A*AATT*C*CCG-3′) confirmed that the complex bound mismatched DNA *via* the mode of insertion.[53]
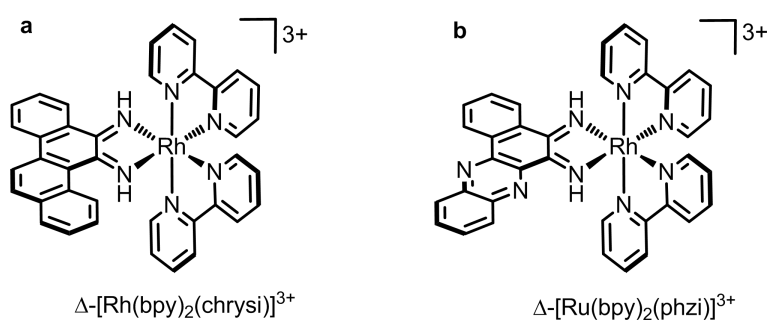
Figure 14. Chemical structures of two mismatch-specific metallo-insertors.

1.3.3 Hexacoordinate Silicon Complexes

For many of these metallo-intercalators or insertors, centered metal is just employed as a structural octahedral center. However, metal-based toxicities somewhat retard wider application of octahedral transition metal complexes for biological research and medical therapy. Compared to metal, silicon also can form octahedral compounds because of the availability of empty 3d orbitals, and more importantly, it lacks toxic concerns.[58] Accordingly, we expect to replace octahedral metal complexes by related octahedral silicon complexes under some circumstances. Hence, we here present a brief review of the preparative methods of hexacoordinate silicon complexes.

Due to the widespread use of organosilicon compounds as intermediates in the application of nucleophilic activation and catalysis, the distinctive hypervalent silicon complexes has attracted great interest in the last decades.[59,60] Hexacoordinate silicon

complexes are mainly prepared by two methods: (1) Coordination to a tetracoordinate silicon compound. (2) Substitution in a tetrafunctional silane by a bidentate ligand.

$$RSiCl_3 \xrightarrow[\text{H}_2\text{O, 0 °C}]{\text{KF (excess)}} [RSiF_5]^-K^+$$
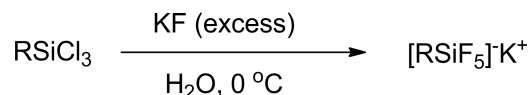
Scheme 14. Synthesis of $[RSiF_5]^-K^+$ by fluoride donation to a halogenosilane.

Müller and co-workers firstly prepared $[RSiF_5]^-$ by coordination of fluoride anion to trifluorosilanes.[61] They also reported that organopentafluorosilicates can be prepared by addition of fluoride ion to other tetracoordinate organosilanes $RSiX_3$ (X = Cl, Br, I, OR). Subsequently, Kumada et al. developed a practical preparation of these organopentafluorosilicates,[62] by the reaction of excessive KF in H_2O with $RSiCl_3$, as shown in Scheme 14.
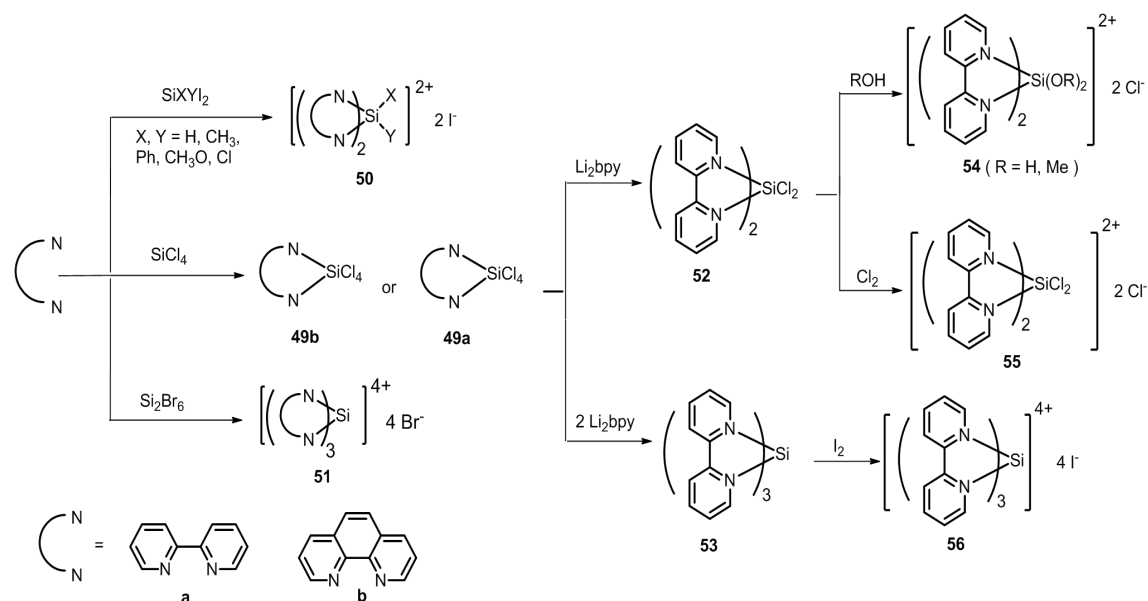
Scheme 15. Hexacoordinate silicon complexes (**49~51**) from the reaction of diimine with halogenosilanes and the silicon complexes (**54~56**) prepared from **49a**.

Organosilanes with at least two electronegative groups on silicon could further coordinate to nitrogen donors to give hexacoordinate complexes. For example, diimines NN {NN = bpy (a) or phen (b)} react with halogenosilane $SiCl_4$ to efficiently afford the hexacoordinate complexes $[Si(bpy)Cl_4]$ **49a** and $[Si(phen)Cl_4]$ **49b**

respectively.[63] Analogously, [Si(NN)$_2$XY]I$_2$ **50** and [Si(NN)$_3$]Br$_4$] **51**, with X, Y = H, CH$_3$, Ph, CH$_3$O or Cl, can also be obtained. The hexacoordinate silicon complex **49a** can serve as the starting material to prepare other hexacoordinate complexes: substitution of chlorine by dilithiobipyridyl gives neutral complexes **52** or **53**, formally Si^{II} and Si^0 respectively, depending on the stoichiometry of the reaction.[63] Subsequently, cationic complexes **54** and **55** can be prepared from **52**, while reaction of **53** with iodine gives the four positive charged complex **56** (Scheme 15).[64,65]
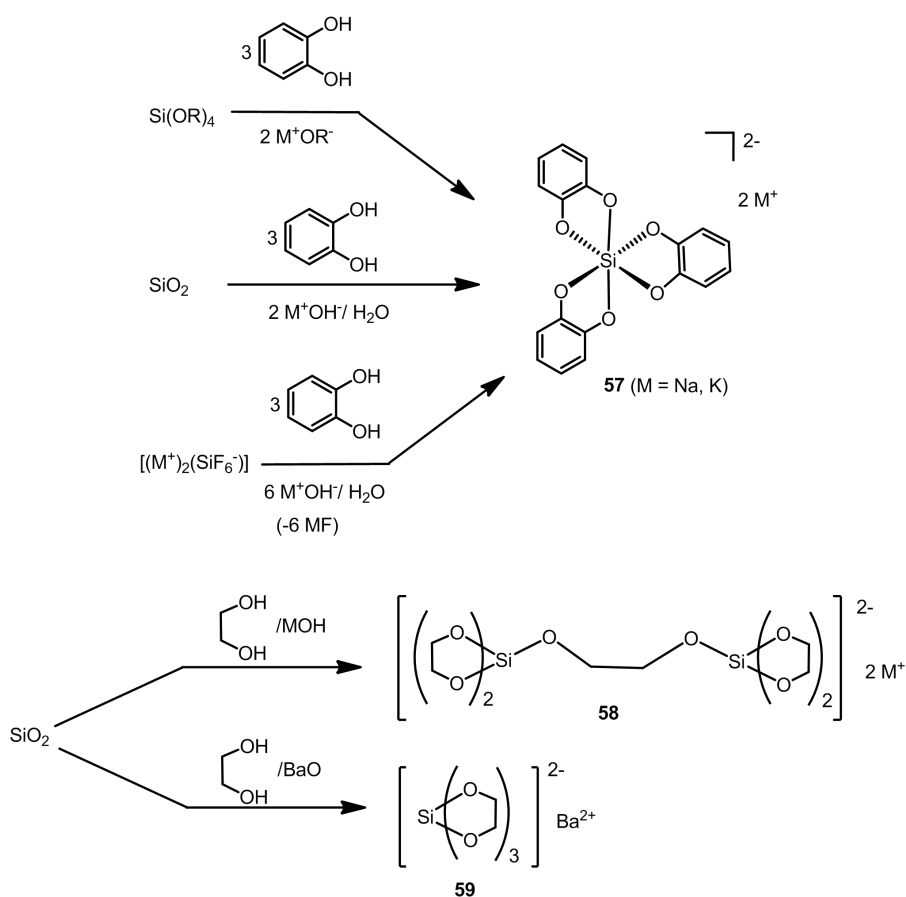
Scheme 16. Anionic hypercoordinate silicon complexes prepared *via* substitution in a tetrafunctional silane by a bidentate ligand.

As mentioned before, hexacoordinate silicon complex can be obtained *via* substitution in a tetrafunctional silane by a bidentate ligand as well. Accordingly, Frye and Corriu reported that, the anionic complex **57** was easily prepared by the reaction of catechol with tetramethoxy (or tetraethoxy)-silane in basic conditions (Scheme 16).[66] Catechol is such an effective ligand for the preparation of hypervalent silicon species that complex **57** can also be prepared from SiO$_2$ and even [(M$^+$)$_2$(SiF$_6^{2-}$)] (M =

Na, K), which is a byproduct of the fertilizer industry.[67,68] Interestingly, when aliphatic 1,2-diol reacted with SiO_2 in the presence of MOH (M = Li, Na, K, or Cs), complex **58** with two pentacoordinate silicon atoms exclusively formed, as shown in Scheme 16. However, if the reaction was performed with BaO, the product turned out to be hexacoordinate complex **59**.[69,70]

Chapter 2 Aim of Work

My research work can be divided into the following two main parts:

I. Asymmetric Synthesis of Octahedral Ruthenium Complexes

1) To develop a straightforward method for the asymmetric synthesis of octahedral mononuclear ruthenium complexes $[Ru(pp)(pp')(pp'')]^{2+}$ (pp, pp', pp''= achiral 2,2'-bipyridines or 1,10-phenanthrolines). Our group has already developed a series of efficient chiral auxiliaries for the asymmetric synthesis (Figure 15),[39-42] and the preparations of these disclosed auxiliaries are either complicated or somewhat inconvenient, we aim to expand the auxiliary list and further simplify the asymmetric synthesis. We exploit the amino acids as chiral auxiliary (shown in Figure 15).
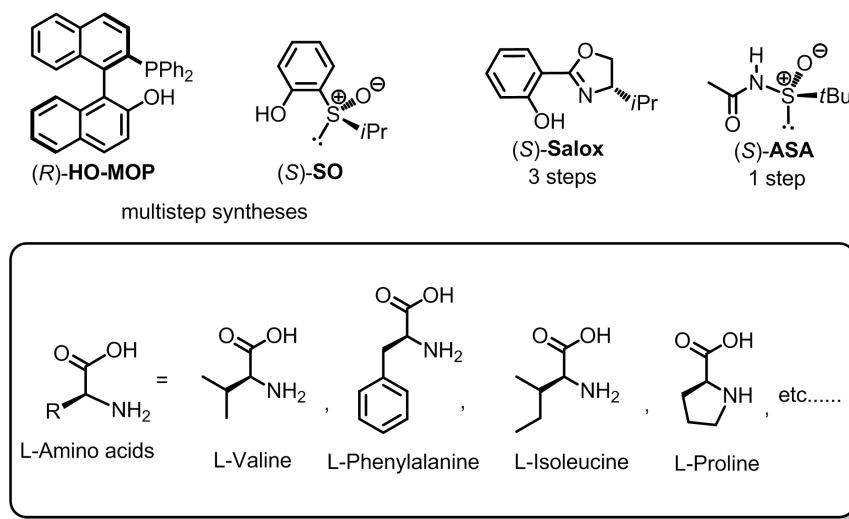
Figure 15. Reported chiral auxiliaries for the asymmetric synthesis of octahedral mononuclear ruthenium complexes and some examples of natural amino acids.

2) To investigate the asymmetric synthesis of enantiopure dinuclear ruthenium complexes. We intend to apply the currently chiral-auxiliary mediated method for asymmetric synthesis of mononuclear ruthenium complexes to the dinuclear ruthenium complexes. Our strategy is transferring chirality from one metal center to

the other through a bridging ligand, which means one chiral metal complex acting as an auxiliary to direct the configuration of the other metal center *via* steric repulsion between the ligands on both metal centers (Scheme 17).
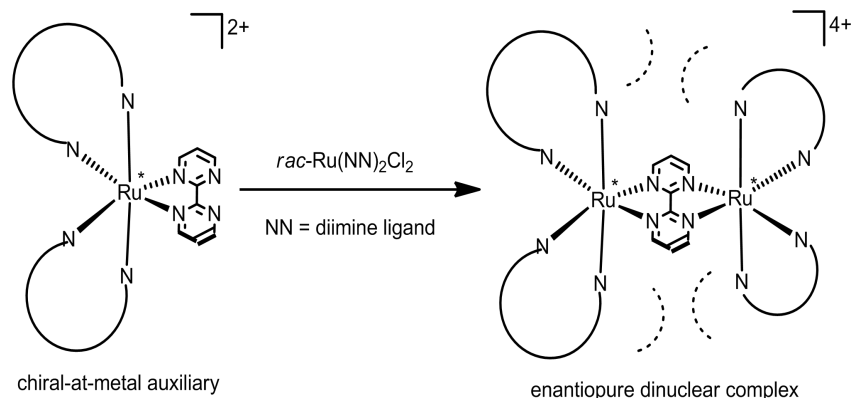
Scheme 17. Strategy for asymmetric synthesis of dinuclear ruthenium complexes.

II. Synthesis and Biological Activities of Octahedral Silicon Complexes

Octahedral transition metal complexes have shown tremendous applications in different areas of chemical research.[2,12,37] However, metal-based toxicities currently has retarded a wider application of octahedral transition metal complexes in biological systems. We have noticed that for a variety of inert octahedral transition metal complexes which are used in biological areas, the metal center actually acts as a scaffold-center holding ligands in a three-dimensional fashion. Nevertheless, silicon also can form octahedral compounds and lacks of toxic concerns. We wish octahedral silicon complexes also can be used to replace the metal complexes in some biological studies.

Hence, we plan to synthesize hydrolytically stable octahedral silicon complexes with various ligands and electric charges, the possible structures of which are shown in Figure 16, furthermore, we would like to explore some methods for asymmetric synthesis of octahedral silicon complexes. Subsequently, we will investigate biological activities of the octahedral silicon complexes, such as the interaction between silicon complexes and DNA duplexes.
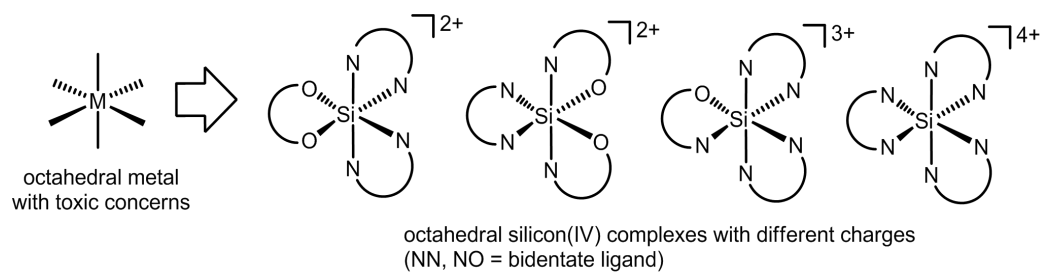
Figure 16. Possible structures of octahedral silicon complexes.

Chapter 3 Results and Discussion

3.1 Asymmetric Synthesis of Octahedral Ruthenium Complexes

As described in the theoretical part, octahedral metal complexes play an important role for the design of nucleic acid probes and enzyme inhibitors, and single enantiomers are typically desired for such applications.[1,15,71] However, compared to the highly sophisticated and tremendous methods for the asymmetric synthesis of organic molecules, synthesis of chiral metal complexes is still in its infancy. Therefore, it is very important to develop methods for efficient syntheses of enantiopure chiral-at-metal complexes.

3.1.1 Mononuclear Ruthenium Complexes

The most extensively used strategy to obtain optically pure chiral-at-metal complexes with achiral ligands involves an initial racemic synthesis, adopting standard methods of coordination chemistry, followed by a chiral resolution procedure. This method was time-consuming and inefficient, we focus on asymmetric synthesis of metal complexes by using chiral auxiliary. Recently, Meggers group has successfully developed a series of chiral auxiliaries for the asymmetric synthesis of chiral octahedral mononuclear ruthenium complexes.[39-42] However, the practical use of these chiral auxiliaries is somewhat limited, such as the syntheses of enantiomerically pure 2-diphenylphosphino-2'-hydroxy-1,1'-binaphthyl (**HO-MOP**) and 2-sulfinylphenols (**SO**) are lengthy, while for chiral salicyloxazolines (**Salox**), the asymmetric coordination chemistry of which needs specialized photochemical equipment, and for the chiral N-acetyl-tert-butanesulfinamide (**ASA**), the scaling-up procedure of which needs a careful adjustment of the reaction parameters (Figure 15).

Hence we were searching for other chiral auxiliaries that could be readily prepared or commercially available. We turned our attention to the natural amino acids, because they have been demonstrated to be highly versatile catalysts for

asymmetric organic transformations, and we assumed that they may also serve as inexpensive and readily available chiral auxiliaries for asymmetric synthesis of polypyridyl ruthenium(II) complexes.[72,73] We tried four amino acids (shown in Figure 17) and found that L-proline could be the most promising auxiliary from all the candidates. In this thesis, we just focus on the discussion about L-proline.

L-Valine   L-Phenylalanine   L-Isoleucine   L-Proline
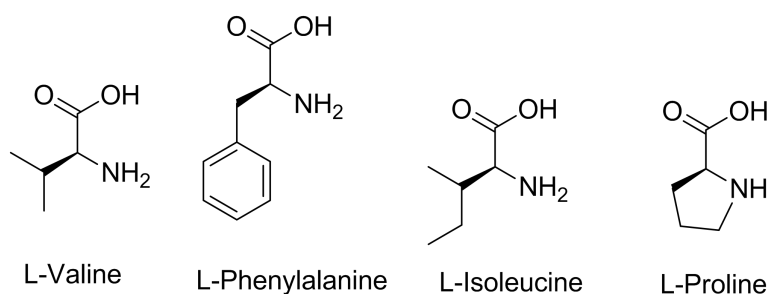
Figure 17. The four natural amino acids that have been tried.

Our new synthetic strategy is inspired by investigations of Vagg and Williams, who reported that for the (S)-aminoacidate complexes of Δ, Λ-[Ru(pp)$_2${(S)-aminoacidate}]$^+$, pp = bidentate polypyridyl ligand, the Λ-diastereoisomer is typically thermodynamically more stable.[74,75] The authors explained that an inter-ligand repulsion between the α-pyridyl proton of one polypyridyl ligand and the α-side chain of the aminoacidate ligand results in the less favored Δ-propeller, which could be clearly observed in the structural models (Figure 18). We speculated that this thermodynamic difference between the Δ, Λ-diastereomer should be pronounced in the related ruthenium-prolinate complexes which might enable us to develop an asymmetric synthesis of ruthenium polypyridyl complexes.

Λ Δ
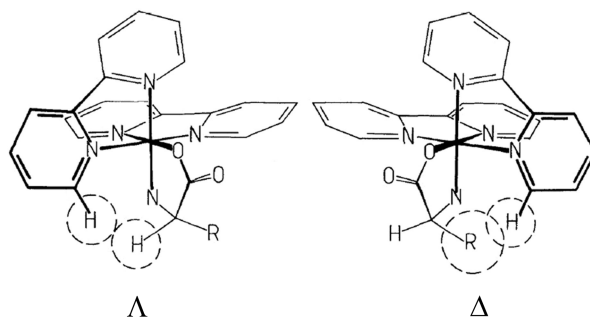
Figure 18. Structural models of diastereoisomers Δ-/Λ-[Ru(pp)$_2${(S)-aminoacidate}]$^+$.

29

Following the general experimental procedures for the synthesis of Δ-/Λ-[Ru(pp)$_2${(S)-aminoacidate}]$^+$, the racemic *cis*-[Ru(bpy)$_2$Cl$_2$] (bpy = 2,2'-bipyridine) (**60**) reacted with 1.2 equiv of L-proline in EtOH and in the presence of 2.0 equiv of K$_2$CO$_3$ at 100 °C for 2h, Λ-[Ru(bpy)$_2$(L-prolinate)]PF$_6$ {Λ-(S)-**61**}, and Δ-[Ru(bpy)$_2$(L-prolinate)]PF$_6$ {Δ-(S)-**61**} formed as the main products with a crude diastereoselectivity between the Λ- and Δ-diastereomer of proximate 1 : 1 {42% (Λ-), 40% (Δ-)} as shown in Scheme 18. These two isomers can be easily purified and separated by silicon-gel column chromatography. According to ^{1}H-NMR, the d.r. values of the two chromatographic separated isomers were larger than 100 : 1. The characteristic proton signals of these two diastereomers can be easily distinguished in high field (4.0~5.0 ppm) and low field (8.8~9.3 ppm) (Figure 19).
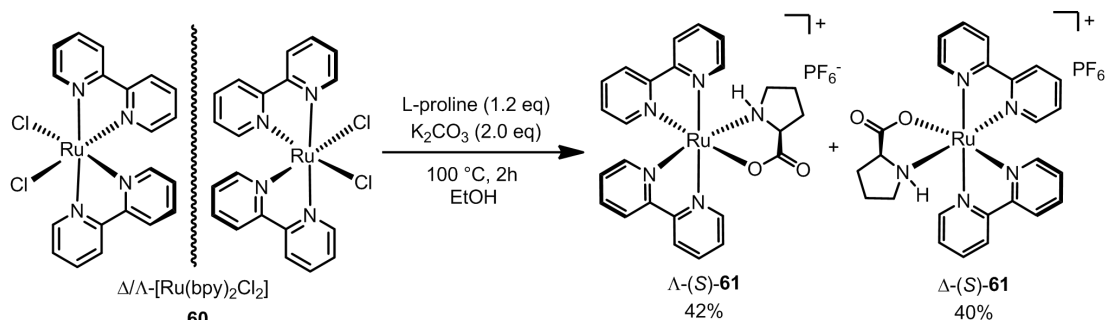
Scheme 18. Synthesis of Δ-/Λ-[Ru(bpy)$_2$(L-prolinate)]PF$_6$ (**61**).

a) the mixture of Λ-/Δ-(S)-**61**

b) pure Λ-(S)-**61**

c) pure Δ-(*S*)-**61**
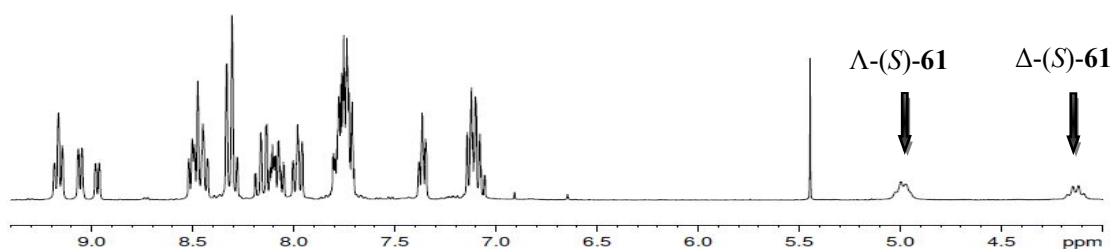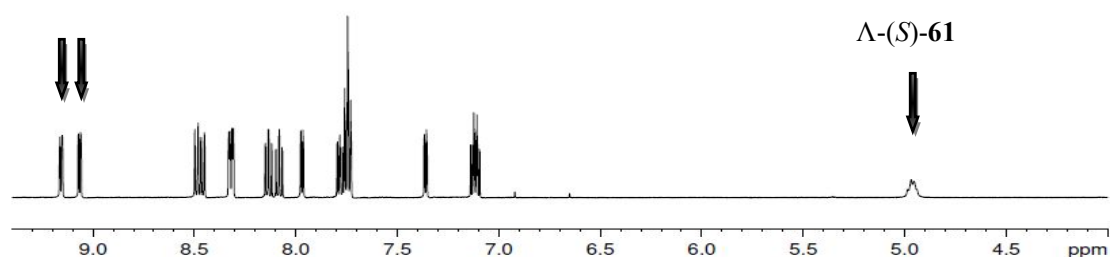
Δ-(*S*)-**61**
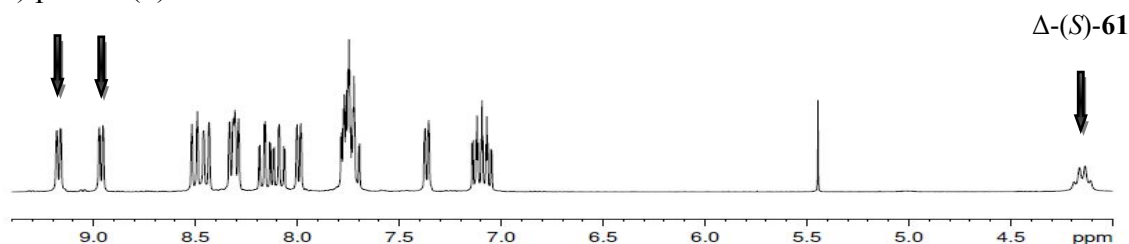
Figure 19. ^{1}H-NMR spectra of [Ru(bpy)$_2$(L-prolinate)]PF$_6$. a) the mixture of two diastereomers. b) pure Λ-(*S*)-**61**. c) pure Δ-(*S*)-**61**.

Single crystals of complex Λ-(*S*)-**61** suitable for X-ray diffraction was obtained by diffusion of Et$_2$O in DCM solution, and the crystal structure shown in Figure 20 confirms the absolute configuration of the ruthenium scaffold. The central atom in complex Λ-(*S*)-**61** is ligated by one oxygen atom and five nitrogen atoms in a slightly distorted octahedral coordination geometry. N1 and O31 occupy two sites of axis (the angle of N3-Si1-O1 is 171.2(3)°), whereas N20, N13, N25 and N8 occupy equatorial positions forming a nearly planar quadrilateral geometry around the ruthenium center {∠N8-Ru1-N20 = 94.0(4)°, ∠N20-Ru1-N13 = 77.7(4)°, ∠N8-Ru1-N25 = 93.3(3)°, ∠N13-Ru1-N25 = 95.1(4)°; Σ = 360.2(5)°}, which indicates that there is no pronounced intramolecular repulsion among the ligands in this complex.
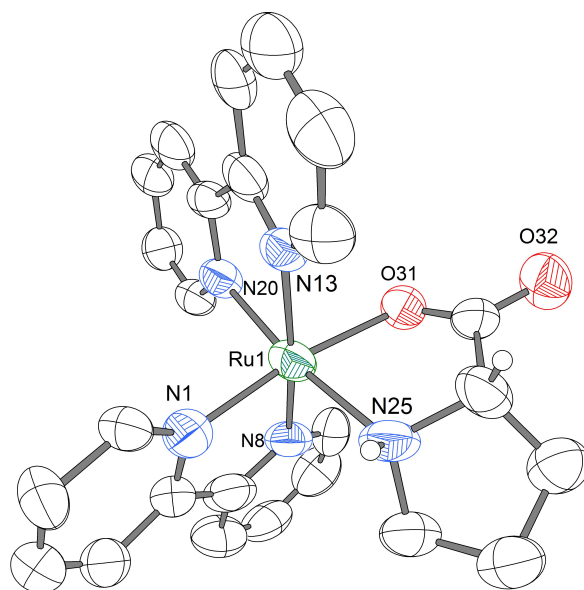
Figure 20. Crystal structure of the diastereomer Λ-(*S*)-**61**. ORTEP drawing with 50% probability thermal ellipsoids. Only one of two independent ruthenium complexes shown. A nitrate

counterion and water molecules are omitted for clarity. Hydrogens are shown at the stereogenic carbon (*S*) and nitrogen (*S*). Selected bond distances (Å) and angles (°): N1-Ru1 1.993(7), N8-Ru1 2.014(9), N13-Ru1 2.084(8), N20-Ru1 2.060(10), N25-Ru1 2.131(9), O31-Ru1 2.090(6); N1-Ru1-O31 171.2(3), N1-Ru1-N20 92.9(3), N20-Ru1-O31 94.4(3), N1-Ru1-N25 93.5(3), O31-Ru1-N25 79.8(3), N8-Ru1-N20 94.0(4), N20-Ru1-N13 77.7(4), N8-Ru1-N25 93.3(3), N13-Ru1-N25 95.1(4).

The CD spectra of the two resolved diastereomers, Λ-(*S*)-**61** and Δ-(*S*)-**61**, are displayed in Figure 21. From the CD spectra, we can see that the two curves of Λ-(*S*)-**61** and Δ-(*S*)-**61** are opposite. Based on the crystal structure of Λ-(*S*)-**61** and the CD spectra of both diastereomers, the metal-centered configuration of the other diastereomer Δ-(*S*)-**61** was able to be assigned.
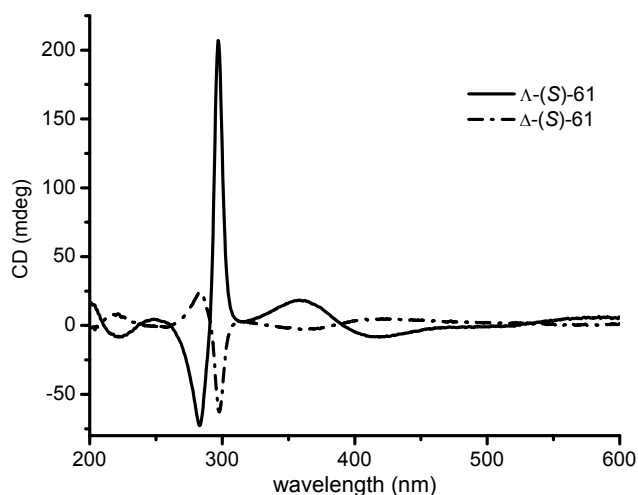
Figure 21. CD spectra of compounds Λ-(*S*)-**61** and Δ-(*S*)-**61** in CH$_3$CN (0.1 mM).

We thought that the diastereoselectivity of this reaction could be improved by changing the reaction conditions, such as reaction temperature or the ratio of reactants. Indeed, when the racemic *cis*-[Ru(bpy)$_2$Cl$_2$] (**60**) (50 mM) reacted with 2 equiv of L-proline in ethylene glycol and in the presence of 0.5 equiv of K$_2$CO$_3$ at 170 °C for around 3 minutes, Λ-[Ru(bpy)$_2$(L-prolinate)]PF$_6$ {Λ-(*S*)-**61**} formed as the main product with a crude diastereoselectivity between the Λ- and Δ-diastereomer of ≥ 10 :1 (determined by ^{1}H-NMR before purification) (Scheme 19). We found that small amounts of unidentified side products were formed with 1 equiv of L-proline and 0.5 equiv of K$_2$CO$_3$, whereas with 10 equiv of L-proline and no K$_2$CO$_3$, the reaction was slower (completed in 10 min) and the yield was also lower (around 60%, more

byproducts). Since it is not easy to remove the excess of L-proline during the purification process, larger excess of L-proline should be avoided.
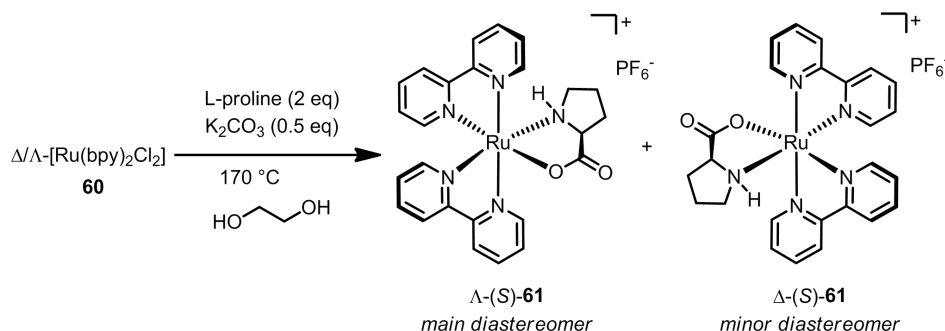
Scheme 19. Asymmetric synthesis of Λ-[Ru(bpy)$_2$(L-prolinate)]PF$_6$ {Λ-(*S*)-**61**}.

We also screened different temperatures and concentrations in order to further improve the diastereoselectivity based on the optimized reactant ratio. The best reaction conditions were shown in Table 1: the racemic *cis*-[Ru(bpy)$_2$Cl$_2$] (**60**) (200 mM) reacted with 2 equiv of L-proline and 0.5 equiv of K$_2$CO$_3$ at 190 °C (oil bath temperature) for 3~4 minutes.

Table 1. Influence of reaction temperature and concentration on the diastereoselective formation of Λ-(*S*)-**61**.

entry	concentration[a]	temperature	crude d.r.[b]	yield[c]
1	50mM	170 °C	≥10:1	65%
2	100mM	180 °C	≥15:1	67%
3	100mM	190 °C	≥20:1	67%
4	200mM	180 °C	≥18:1	70%
5	200mM	190 °C	≥20:1	74%

[a] General reaction conditions: The racemic *cis*-[Ru(bpy)$_2$Cl$_2$] (**60**) with L-proline (2.0 equiv) and K$_2$CO$_3$ (0.5 equiv) was heated in ethylene glycol under argon for 3~5 min at the indicated oil bath temperature. [b] Determined from the crude product by ^{1}H-NMR before silica-gel column chromatography. [c] Isolated yield of the hexafluorophosphate salt of the Λ-(*S*)-diastereomer after silica-gel column chromatography with high purity (final d.r. ≥ 100 : 1).

We also applied to other racemic starting complexes *cis*-[Ru(pp)₂Cl₂], pp = 5,5'-dimethyl-2,2'-bipyridine (dmb, **62**), 1,10-phenanthroline (phen, **63**), and 2'2-biquinoline (biq, **64**). Through similar procedures, single diastereomers Λ-(*S*)-**66** (70%), Λ-(*S*)-**67** (67%), and Λ-(*S*)-**68** (72%) could be obtained as the major diastereomers as the result shown in Table 2.

Table 2. Synthesis of the L-prolinate complexes Λ-(*S*)-**61**, Λ-(*S*)-**66~69**.

entry	*rac*-[Ru(pp)(pp')Cl₂]	temperature[a]	main product	crude d.r.[b]	yield[c]
1	pp = pp' = bpy (**60**)	190 °C	Λ-(*S*)-**61**	≥20:1	74%
2	pp = pp' = dmb (**62**)	190 °C	Λ-(*S*)-**66**	≥35:1	70%
3	pp = pp' = phen (**63**)	190 °C	Λ-(*S*)-**67**	≥25:1	67%
4	pp = pp' = biq (**64**)	180 °C	Λ-(*S*)-**68**	≥30:1	72%
5	pp = bpy, pp' = dmb (**65**)	190 °C	Λ-(*S*)-**69**	>40:1[d]	75%

[a] General reaction conditions: The mixture of racemic ruthenium complexes (200 mM) with L-proline (400 mM), and K₂CO₃ (100 mM) was heated in ethylene glycol under argon for several min at the indicated oil bath temperature. See experimental part for more details. [b] Determined from the crude product by ¹H-NMR before silica-gel column chromatography. [c] Isolated yield of the hexafluorophosphate salt of the Λ-(*S*)-diastereomer(s) after silica-gel column chromatography with high purity (final d.r. ≥ 100 : 1). [d] Ratio Λ-(*S*)/Δ-(*S*). The two Λ-(*S*)-diastereomers formed in a ratio of 5 : 2 determined by ¹H-NMR.

Single crystals of the two diastereomers, Λ-(*S*)-**68** and Δ-(*S*)-**68**, suitable for X-ray diffraction were obtained by slow diffusion of Et₂O in DCM solution. The crystal structures shown in Figure 22 present the difference between the two coordination modes around ruthenium centers, and indicate the thermodynamic preference for the Λ-diastereomer since the Δ-diastereomer contains a steric repulsion between the CH₂-group next to the coordinated nitrogen of L-prolinate and one of the coordinated bipyridyl ligands. This is consistent with the thermodynamic preference

of the Λ-diastereomer in ruthenium(II) (*S*)-aminoacidate complexes Δ, Λ-[Ru(pp)$_2${(*S*)-aminoacidate}]$^+$ that we mentioned before.

Λ-(*S*)-**68**   Δ-(*S*)-**68**
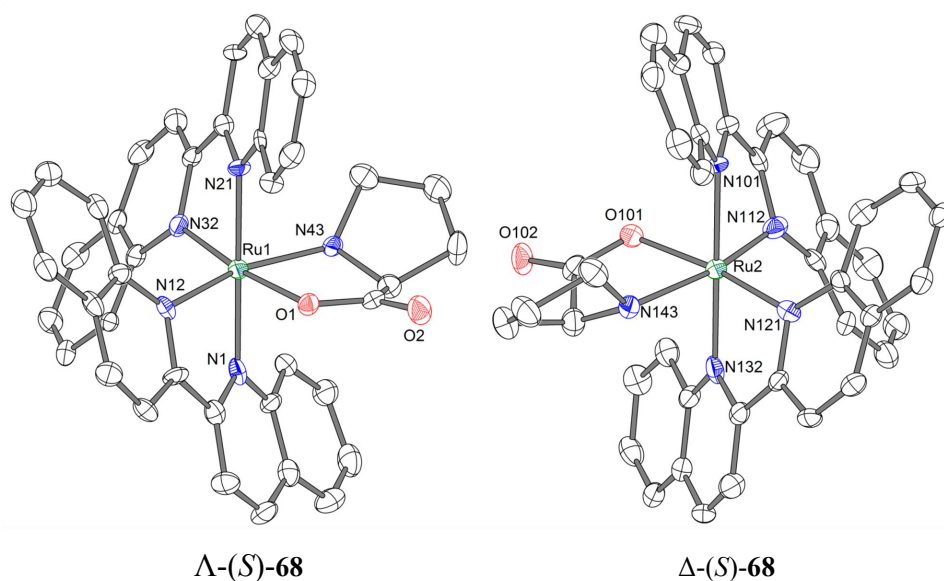
Figure 22. Structures of the two diastereomers Λ-(*S*)-**68** (favored) and Δ-(*S*)-**68** (disfavored), which co-crystallized from the mixture of two diastereomers. ORTEP drawing with 50% probability thermal ellipsoids. A hexafluorophosphate counterion is omitted for clarity. Selected bond distances (Å) and angles (°): N1-Ru1 2.064(5), N12-Ru1 2.043(5), N21-Ru1 2.064(5), N32-Ru1 2.040(6), N43-Ru1 2.157(5), O1-Ru1 2.055(5); N32-Ru1-O1 172.31(17), N12-Ru1-N1 78.70(19), N12-Ru1-N21 100.3(2), N1-Ru1-N21 178.4(2), N12-Ru1-N43 164.5(2), O1-Ru1-N43 79.74(18), N1-Ru1-N43 94.56(18), N21-Ru1-N43 86.07(19).

Based on the crystal structure analysis, taking the diastereoselective synthesis of Λ-(*S*)-**61** as an example, we assumed the mechanism of this kind of reaction as follows (Scheme 20): Initially, the L-proline auxiliary reacts with racemic *cis*-[Ru(bpy)$_2$Cl$_2$] (**60**) to form two diastereomers, Λ-(*S*)-**61** and Δ-(*S*)-**61**, but that under the optimized high temperature reaction conditions, the diastereomer Δ-(*S*)-**61** is unstable and reversibly releases the proline ligand due to the intramolecular hindrance. Since under these high temperature reaction conditions, the two enantiomers of the starting material **60** must be in an equilibrium with each other through the dissociation of one or two chlorides and the formation of coordinatively unsaturated intermediates **60***, the unstable and reversibly formed Δ-(*S*)-**61** can convert to the thermodynamically more stable diastereomer Λ-(*S*)-**61**. This would

35

constitute a dynamic resolution under thermodynamic control, similar to related conversions with the chiral auxiliaries **SO** and **ASA**.[32]
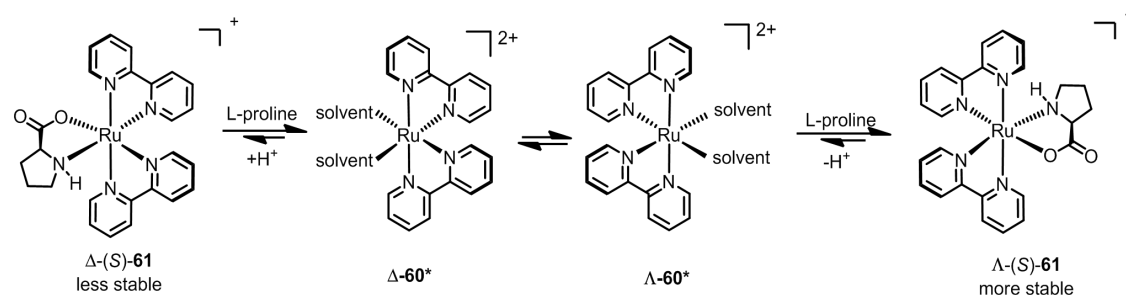
Scheme 20. Proposed mechanism of the diastereoselective synthesis of complex Δ-(*S*)-**61** and Λ-(*S*)-**61** *via* dynamic conversion under thermodynamic control.

This proposed mechanism is supported by an experiment. We heated the minor diastereomer Δ-(*S*)-**61** in ethylene glycol at 190 °C under argon for 10 min and found it converted to the major diastereomer Λ-(*S*)-**61** with a crude d.r. of ≥ 20 : 1 and an isolated yield of 60% (d.r. > 100 :1) (Scheme 22). This thermally-induced Δ to Λ conversion most likely involves the dissociation or at least labilization of the L-prolinate ligand, because the yield for this isomerization increased to 82% if the Δ to Λ conversion was performed in the presence of additional L-proline (10 equiv) at 190 °C for 20 min, thereby most likely suppressing side reactions of coordinatively unsaturated ruthenium intermediates after the dissociation of proline from Δ-(*S*)-**61**. These conversions were traced by ^1H-NMR spectrum (Figure 23).
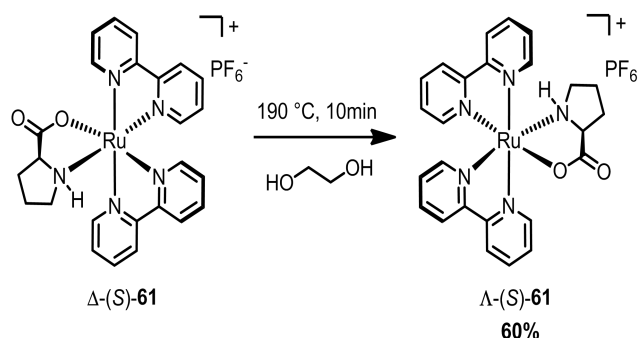
Scheme 21. A conversion of complex Δ-(*S*)-**61** to complex Λ-(*S*)-**61** by heating.
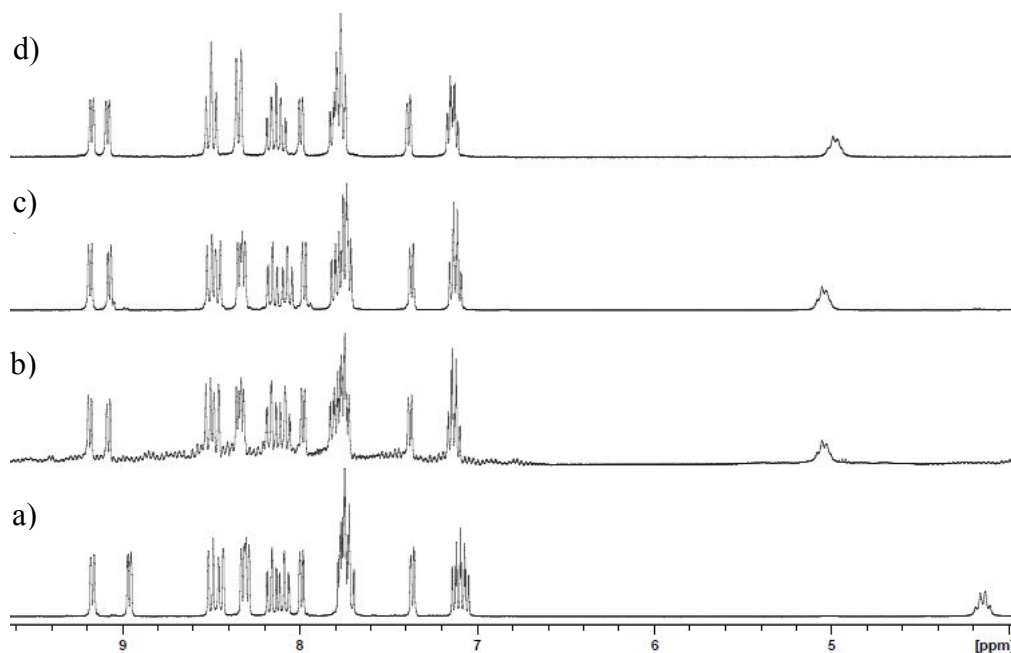
Figure 23. ^{1}H-NMR spectra of conversions Δ-(*S*)-**61** to Λ-(*S*)-**61**. a) Pure Δ-(*S*)-**61** in CD$_3$CN; b) Δ-(*S*)-**61** heated at 190 °C for 10 min; c) Δ-(*S*)-**61** heated at 190 °C in the presence of 10 equiv L-proline for 20 min; d) Pure Λ-(*S*)-**61** in CD$_3$CN.

The key issue for a good chiral auxiliary: Can it be removed under retention of configuration or not? We therefore next investigated the removal of the coordinated L-prolinate auxiliary and we expected an acid-lability of the N,O-coordinated prolinate through a protonation of the coordinated carboxylate group. Indeed, just similar to the published methods,[39] the auxiliary can be easily replaced by other polypyridyl ligands in the presence of excess trifluoroacetic acid (TFA) in MeCN at high temperature (110 °C). When Λ-(*S*)-**61** was treated with TFA (8 equiv) in the presence of an excess of bpy (15 equiv) in MeCN at 110 °C for 2.5 hours, Λ-[Ru(bpy)$_3$](PF$_6$)$_2$ (Λ-**70**) was obtained after silica gel column chromatography, and hexafluorophosphate precipitation in a yield of 79% with 99 : 1 e.r. as determined by chiral HPLC (Figure 24).
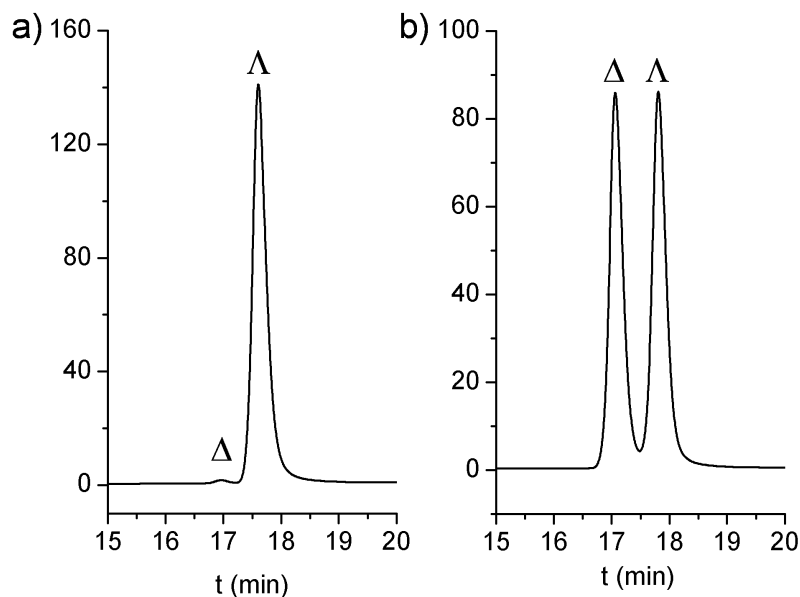
Figure 24. HPLC traces of non-racemic and racemic [Ru(bpy)$_3$](PF$_6$)$_2$ (**70**). (a) Λ-[Ru(bpy)$_3$](PF$_6$)$_2$ (Λ-**70**) with 99:1 e.r. synthesized from Λ-(*S*)-**61** (Table 2, entry 1). (b) Racemic [Ru(bpy)$_3$](PF$_6$)$_2$ as a reference. HPLC conditions: Daicel Chiralpak IA column, 250 × 4.6 mm, flow rate = 0.5 mL/min, TFA (0.1% in H$_2$O) and MeCN as eluent (15→30% in 20 min).

Starting from the other L-prolinate mediated ruthenium complexes, Λ-[Ru(dmb)$_2$(L-prolinate)]PF$_6$ {Λ-(*S*)-**66**}, Λ-[Ru(phen)$_2$(L-prolinate)]PF$_6$ {Λ-(*S*)-**67**}, the related products from ligand substitution reaction, Λ-[Ru(dmb)$_3$](PF$_6$)$_2$ (Λ-**71**) and Λ-[Ru(phen)$_3$](PF$_6$)$_2$ (Λ-**72**) (Table 3, entries 2 and 3) could also be obtained in a similar procedure with the e.r. values of 97 : 3, 99 : 1 respectively.

However, the conversion from Λ-[Ru(biq)$_2$(L-prolinate)]PF$_6$ {Λ-(*S*)-**68**} to Λ-[Ru(biq)$_2$(bpy)](PF$_6$)$_2$ (Λ-**73**) was not that successful. In a similar way, when Λ-(*S*)-**68** was treated with TFA (8 equiv) in the presence of an excess of bpy (15 equiv) in MeCN at 110 °C for 12 hours, Λ-[Ru(biq)$_2$(bpy)](PF$_6$)$_2$ (Λ-**73**) was obtained with a Λ-/Δ- ratio of only 3:2 and yield of 15%, the method by using L-proline as chiral auxiliary for the asymmetric synthesis of ruthenium polypyridyl complexes has limitation.

38

Table 3. TFA-promoted substitution of the L-proline auxiliary against achiral bidentate ligands under retention of configuration.[a]

$$\Lambda\text{-}[Ru(pp)(pp')(L\text{-}Pro)](PF_6) \xrightarrow[\text{2) }NH_4PF_6]{\text{1) TFA, pp''}} \Lambda\text{-}[Ru(pp)(pp')(pp'')](PF_6)_2$$

pp=pp'=bpy, **61**
pp=pp'=dmb, **66**
pp=pp'=phen, **67**
pp=pp'=biq, **68**
pp=bpy, pp'=dmb, **69**

pp=pp'=bpy, pp''=bpy, **70**
pp=pp'=dmb, pp''=dmb, **71**
pp=pp'=phen, pp''=phen, **72**
pp=pp'=biq, pp''=bpy, **73**
pp=bpy, pp'=dmb, pp''=phen, **74**
pp=bpy, pp'=dmb, pp''=dbb, **75**

entry	starting cpd	pp''[b]	product complex	yield	e.r.[c]
1	Λ-(S)-**61**	bpy	Λ-[Ru(bpy)$_3$](PF$_6$)$_2$ (Λ-**70**)	79%	99:1
2	Λ-(S)-**66**	dmb	Λ-[Ru(dmb)$_3$](PF$_6$)$_2$ (Λ-**71**)	83%	97:3
3	Λ-(S)-**67**	phen	Λ-[Ru(phen)$_3$](PF$_6$)$_2$ (Λ-**72**)	81%	99:1
4	Λ-(S)-**68**	biq	Λ-/Δ-[Ru(biq)$_2$(bpy)](PF$_6$)$_2$ (**73**)[d]	15%	ca. 3:2[e]
5	Λ-(S)-**69**	phen	Λ-[Ru(bpy)(dmb)(phen)](PF$_6$)$_2$ (Λ-**74**)	82%	98:2
6	Λ-(S)-**69**	dbb	Λ-[Ru(bpy)(dmb)(dbb)](PF$_6$)$_2$ (Λ-**75**)	85%	98:2

[a] General reaction conditions: Λ-(S)-**61**, **66**~**69** (100 mM) in MeCN with TFA (8 equiv) and bipyridyl ligand (15 equiv) in a closed brown glass vial under argon atmosphere at 110 °C for several hours. [b] bpy = 2,2'-bipyridine, dmb = 5,5'-dimethyl-2,2'-bipyridine, phen = 1,10-phenanthroline, biq = 2,2'-biquinoline, dbb = 4,4'-di-tertbutyl-2,2'-bipyridine. [c] Determined by chiral HPLC with a Chiralpak IA or IB column and a gradient of MeCN : TFA (0.1% in H$_2$O). [d] Complex is very light-sensitive. [e] Only partial resolution of Λ- and Δ-enantiomers by chiral HPLC.

This new and economical method also can be applied to the asymmetric synthesis of octahedral tris-heteroleptic ruthenium(II) polypyridyl complexes. Accordingly, racemic [Ru(bpy)(dmb)Cl$_2$] (**65**) was reacted with L-proline (2.0 equiv) and K$_2$CO$_3$ (0.5 equiv) in ethylene glycol at 190 °C under argon for several minutes, after silica-gel column chromatography, affording Λ-(S)-**69** in a yield of 75% as a mixture of two diastereomers with the same Λ-configuration at the metal center (Table 2, entry 5). The following reaction of Λ-(S)-**69** with phen (15 equiv) or 4,4'-di-tert-butyl-2,2'-bipyridine (dbb) (15 equiv) in the presence of TFA (8 equiv) in

MeCN at 110 °C for 2.5 hours afforded the tris-heteroleptic complexes Λ-[Ru(bpy)(dmb)(phen)](PF$_6$)$_2$ (Λ-**74**) (82% yield) and Λ-[Ru(bpy)(dmb)(dbb)](PF$_6$)$_2$ (Λ-**75**) (85% yield), respectively, both with 98:2 e.r. (Table 3, entries 5 and 6).

In conclusion, we have developed a straightforward and economical method for the asymmetric synthesis of non-racemic ruthenium(II) polypyridyl complexes [Ru(pp)(pp')(pp'')](PF$_6$)$_2$ based on using the readily available racemic starting material [Ru(pp)(pp')Cl$_2$] together with the natural amino acid L-proline. According to our experience, this method is superior to the previously disclosed auxiliaries and can be applied to a large-scale (gram level) synthesis of enantiomerically pure ruthenium(II) polypyridyl complexes.

3.1.2 Dinuclear Ruthenium Complexes

There has been an increasing interest in multinuclear ruthenium(II) polypyridyl complexes as building blocks in supramolecular devices due to their favourable excited state and redox properties as well as structural probes for DNA, in addition, dinuclear polypyridyl ruthenium(II) complexes have shown promising biological activities in targeting various of cancers and anti-tumor therapies.[76,77] For instance, Thomas and co-workers reported a eye-catching tpphz-bridging dinuclear ruthenium complex, as shown in Figure 25, which has been applied as a multifunctional biological imaging agent staining the DNA of eukaryotic and prokaryotic cells for both luminescence and transition electron microscopy.[71]
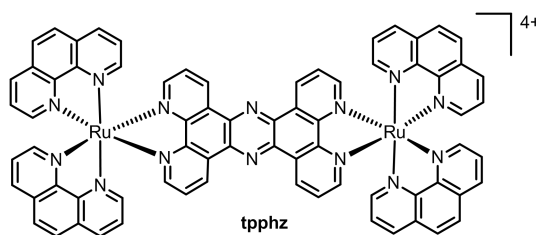
Figure 25. The structure of tpphz-bridging dinuclear ruthenium complex.

The abundant biological and optical activities of the dinuclear polypyridyl ruthenium(II) complexes encouraged us to develop the methods for asymmetric synthesis of dinuclear polypyridyl Ru(II) complexes. We therefore wondered that whether the currently chiral-auxiliary mediated method could be also applied to dinuclear polypyridyl ruthenium(II) complexes. Our strategy is transferring chirality from one metal center to the other.

This strategy can be demonstrated as follows: Firstly the enantiomerically enriched mononuclear ruthenium complex **77** with bulky ligands (2,2'-biquinoline) and small bridging ligand (bipyrimidine, **76**) might be synthesized by using the method we developed before. Secondly, the mononuclear ruthenium complex **77** that contains bridging ligand further reacts with the racemic [Ru(bpy)$_2$Cl$_2$] (**60**) stereoselectively affording a enantiomerically pure dinuclear product **78**. The reason we choose such big ligand is: final dinuclear complex might form in high diastereoselectivity due to the steric repulsion between the biq ligands on one metal and the bpy ligands on the other (Scheme 22).
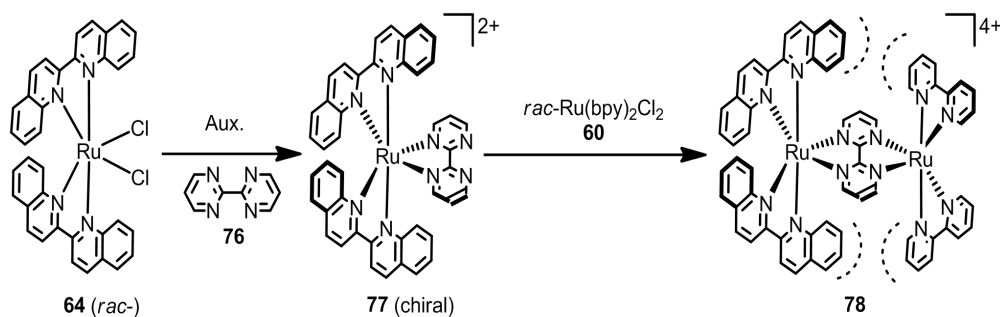
Scheme 22. The strategy for asymmetric synthesis of dinuclear ruthenium complex **78** by using enantiopure mononuclear ruthenium complex **77** as a chiral auxiliary.

We synthesized the bridging ligand bipyrimidine **76** by following the reported procedure,[78] in the presence of 0.25 equiv of NiCl$_2$(H$_2$O)$_6$, 0.50 equiv of zinc powder and 1.0 equiv of PPh$_3$, the coupling reaction of 2-chloropyrimidine in DMF at 50 °C for 60 h afforded **76** in a yield of 60% (Scheme 23).
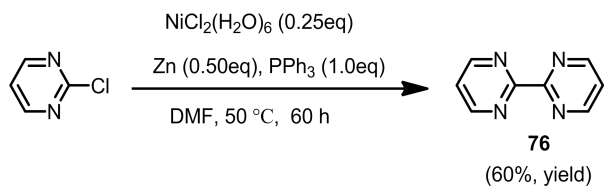
Scheme 23. The synthesis of bipyrimidine **76**.

To test our strategy proposed in Scheme 23, we first started with the racemic [Ru(biq)$_2$(bipyrimidine)]$^{2+}$ (**77**), which could be easily prepared by standard method. Racemic [Ru(biq)$_2$Cl$_2$] (**60**) was heated with 1.2 equiv of bipyrimidine in ethylene glycol at 150 °C for 1 h, after purification, affording the racemic complex **77** in a yield of 78%. Then the racemic complex **77** reacted with the excess of racemic [Ru(bpy)$_2$Cl$_2$] (2.5 equiv) in ethylene glycol at 150 °C for 3 h to give the dinuclear ruthenium complex **78** in a yield of 53% (Scheme 24).
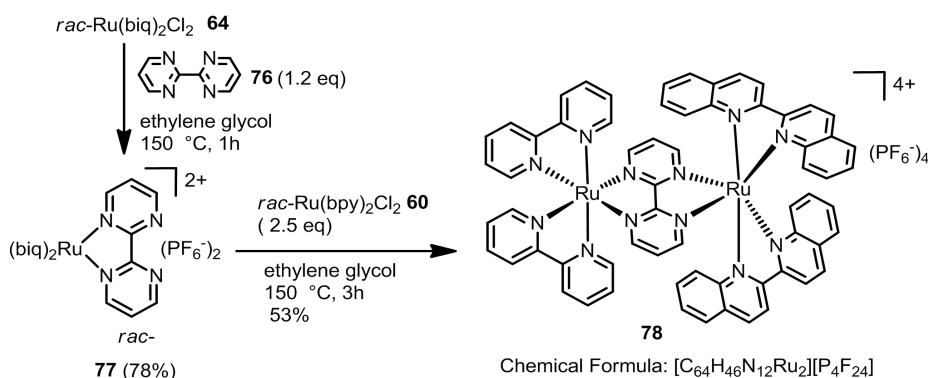
Scheme 24. The achiral synthesis of racemic dinuclear ruthenium complex **78**.

Based on the symmetry of the complex **78**, we thought that if the product we got was diastereomerically pure, only 23 different protons (a molecular **78** contains 46 protons) can be seen in the ^{1}H-NMR spectrum. However, there were 46 different protons according to the ^{1}H-NMR assignment, which means that two diastereomers (four stereoisomers) existed in the product (Figure 26) in a ratio of 1 : 1, thereby we assumed that the steric repulsion between the biq and bpy ligands maybe not strong enough to influence the stereoselectivity.
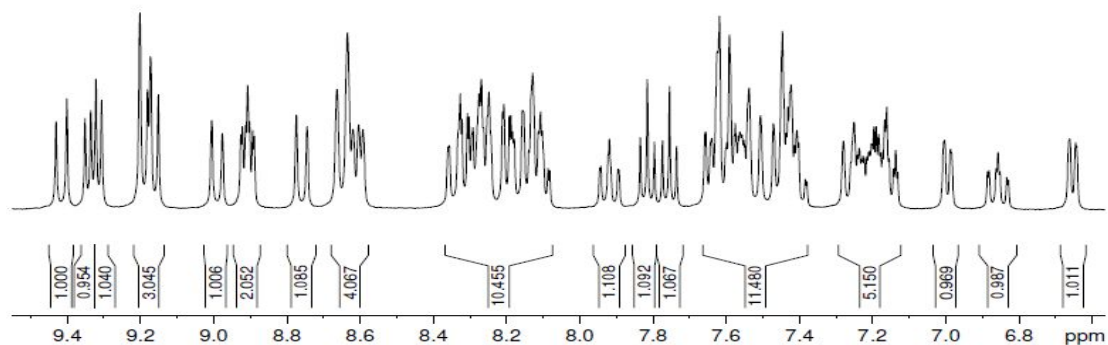
Figure 26. Integration in ^{1}H-NMR of the dinuclear ruthenium complex **78** (two diastereomers in near equal numbers) in d$_6$-acetone.

X-ray diffraction analysis of the complex **78** is basically consistent with the ^{1}H-NMR assignment. As shown in Figure 27, there are three independent cations in one cell, stereoisomer (Λ, Δ), (Λ, Λ), (Δ, Δ) respectively. We assumed that the missing stereoisomer (Δ, Λ)-**78** maybe have been decomposed or still exist in the solution or even exist in the crystals we didn't pick out.

(Λ, Δ)   (Λ, Λ)   (Δ, Δ)
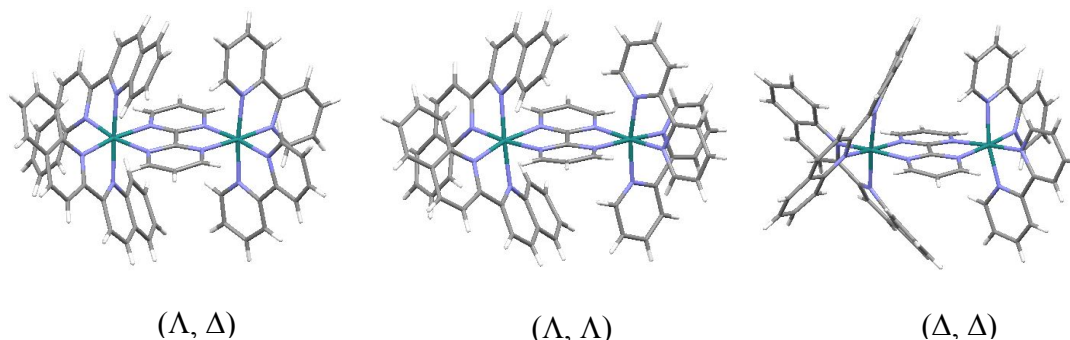
Figure 27. Structures of the three stereoisomers of dinuclear ruthenium(II) complex **78** with configuration definition.
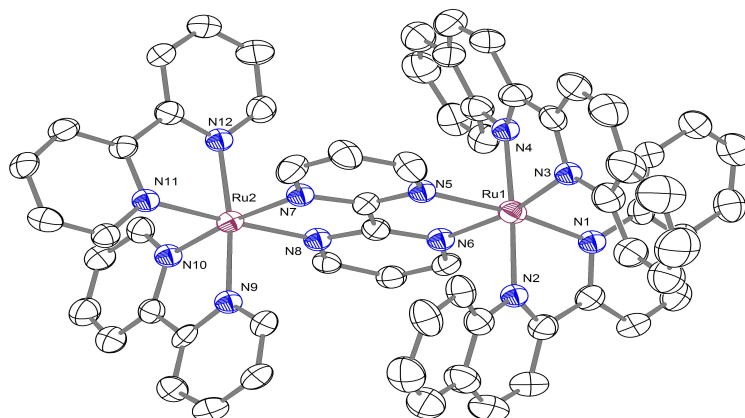
Figure 28. Structure of one stereoisomer of complex **78**, which was crystallized by slowly

43

evaporation from the mixture solution acetone and water. ORTEP drawing with 50% probability thermal ellipsoids. Four hexafluorophosphate counterions are omitted for clarity. Selected bond distances (Å) and angles (°): N1-Ru1 2.079(7), N2-Ru1 2.100(7), N3-Ru1 2.065(7), N4-Ru1 2.076(7), N5-Ru1 2.102(7), N6-Ru1 2.080(7), N7-Ru2 2.043(7), N8-Ru2 2.037(7), N9-Ru2 2.048(6), N10-Ru2 2.041(7), N11-Ru2 2.042(7), N12-Ru2 2.065(7); N4-Ru1-N1 103.3(3), N1-Ru1-N2 77.9(3), N4-Ru1-N5 81.1(3), N2-Ru1-N5 97.2(3), N3-Ru1-N6 168.4(3), N10-Ru2-N9 79.7(3), N7-Ru2-N9 96.2(3), N10-Ru2-N12 98.0(3), N7-Ru2-N12 86.8(3).

Then we studied the stability of dinuclear complex **78** by measuring ^{1}H-NMR of the complex in d_6-acetone at room temperature. This compound is not very stable in solution and some decomposed species can be detected in hours. Even in solid state, the complex slowly got racemized in air. Figure 29 shows the ^{1}H-NMR spectra of the fresh sample and the solid sample exposed in air for one week.
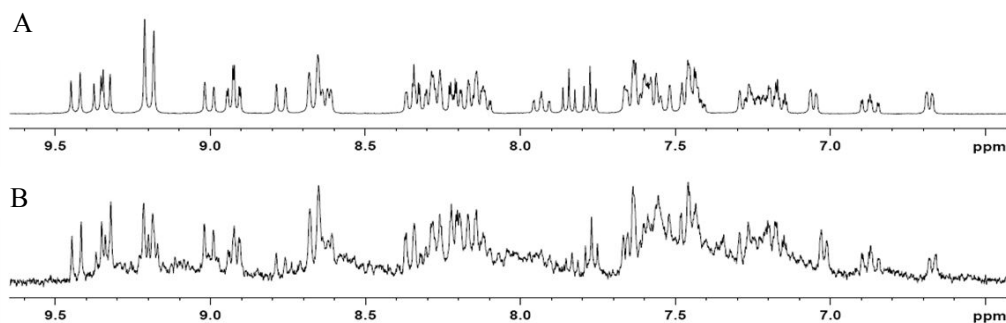
Figure 29. The ^{1}H-NMR spectra comparison between (A) fresh sample of complex **78** and (B) one-week stored sample of complex **78**.

These results were further verified by computational chemistry. Dr. Mali from Frenking group calculated the Gibbs free energy for the both diastereomers. The result shows that there is no pronounced difference stereoisomers, of (Λ, Λ), (Δ, Δ) and the stereoisomer (Λ, Δ) in Gibbs free energy. The Gibbs energies and ZPE corrected energies (in parentheses) of Ru-diastereomers at BP86/def2-SVP, (Λ, Λ) and (Δ, Δ) is (0.0, 0.0) whereas (Λ, Δ) is (0.6, -0.2). He suggested us to choose different ligands in order to enlarge the difference between the diastereomers in Gibbs energy, for example, switching from the bipyridine to 5,5'-dimethyl-2,2'-bipyridine.
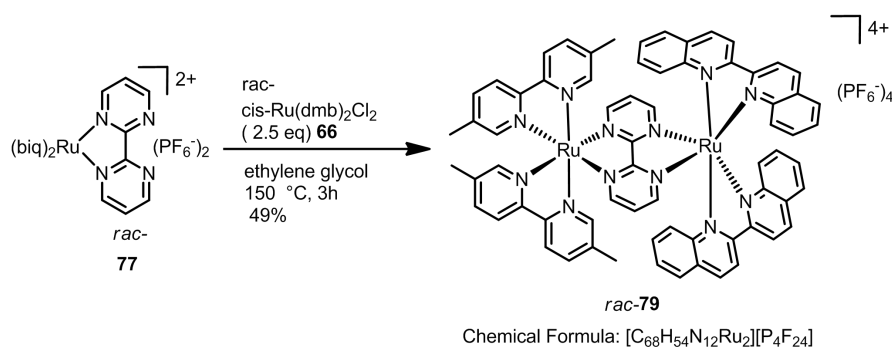
Scheme 25. The achiral synthesis of racemic dinuclear ruthenium(II) complex **79**.

The racemic dinuclear ruthenium(II) complex **79** was obtained by following the analogous synthetic route for compound **78** (Scheme 25). The racemic [Ru(biq)$_2$(bipyrimidine)]$^{2+}$ (**77**) reacted with an excess of racemic [cis-Ru(dmb)$_2$Cl$_2$] (**62**) (2.5 equiv) in ethylene glycol at 150 °C for 3 h to give the dinuclear complex **79** in a yield of 49%. Compared to complex **78**, complex **79** is much more stable, and the ^{1}H-NMR spectrum of complex **79** in d$_6$-acetone did not show any change in one week. Most importantly, there were 27 different protons in ^{1}H-NMR spectrum of complex **79** (a molecular **79** contains 54 protons), which means that only one diastereomer (two enantiomers) existed in the product and the steric repulsion between the biq and dmb ligands should be strong enough to efficiently control the stereoselectivity, as shown in Figure 30.
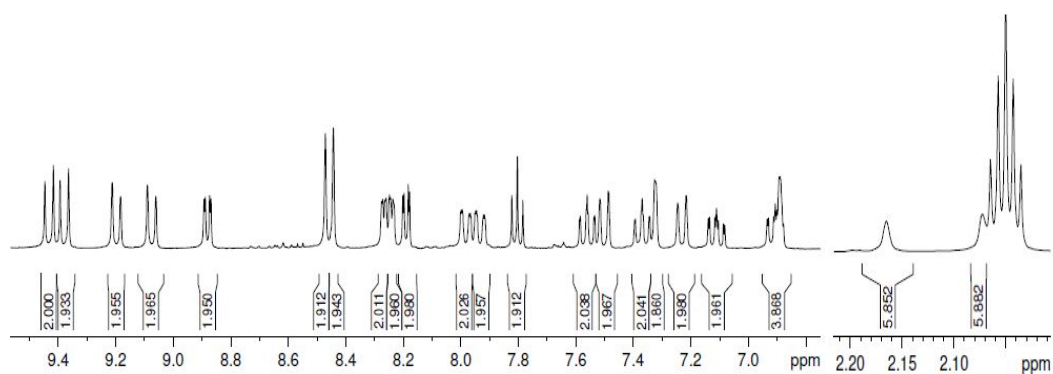
Figure 30. Integration in ^{1}H-NMR of the racemic dinuclear compound **79**.

The crystal structure of the dinuclear complex **79** further demonstrates the high diastereoselectivity. One stereoisomer (Δ, Δ) of the complex **79** shows that the

stereoisomers (Δ, Δ) or (Λ, Λ) should be less sterically strained than the other two stereoisomers (Λ, Δ) or (Δ, Λ), because of the existence of an inter-ligand repulsion between the methyl group of one 5,5'-dimethyl-2,2'-bipyridine ligand on one ruthenium center and the bulky biquinoline ligand on the other ruthenium center (Figure 31). In combination of the stability of complex **79**, there is no doubt that the isomers (Λ, Λ) and (Δ, Δ) are more thermodynamically stable than the other two isomers (Λ, Δ) and (Δ, Λ).

Figure 31. Crystal structure of complex **79** (Δ, Δ), which was crystallized by slowly evaporation from the mixture solution acetone and water. ORTEP drawing with 50% probability thermal ellipsoids. Four hexafluorophosphate counterions and four acetone molecules are omitted for clarity. Selected bond distances (Å) and angles (°): N1-Ru1 2.077(6), N21-Ru1 2.103(7), N32-Ru1 2.045(7), N41-Ru1 2.068(7), N48-Ru1 2.112(7), N45-Ru1 2.053(7), N52-Ru2 2.043(7), N53-Ru2 2.037(7), N67-Ru2 2.048(6), N74-Ru2 2.041(7), N11-Ru2 2.042(7), N12-Ru2 2.065(7); N4-Ru1-N1 103.3(3), N1-Ru1-N2 77.9(3), N4-Ru1-N5 81.1(3), N2-Ru1-N5 97.2(3), N3-Ru1-N6 168.4(3), N10-Ru2-N9 79.7(3), N7-Ru2-N9 96.2(3), N10-Ru2-N12 98.0(3), N67-Ru2-N52 86.8(3), N8-Ru2-N11 176.8(3).

Then we tried to asymmetrically synthesize dinuclear ruthenium complex **79** from the enantiomer pure starting material. However, we didn't have any efficient method for the asymmetric synthesis of enantiomeric enriched ruthenium complexes with bulky ligands, we had to switch the starting material back to Λ-[Ru(dmb)$_2$(L-prolinate)]PF$_6$ {Λ-(S)-**66**}, hopefully the chiral auxiliary can be easily replaced by the ruthenium complex **77** under total retention of metal-centered

configuration.

Scheme 26. Asymmetric synthesis of dinuclear complex **79**.

Following the synthetic route shown in Scheme 26, enantiomerically pure Λ-[Ru(dmb)$_2$(L-prolinate)]PF$_6$ {Λ-(*S*)-**66**} firstly reacted TFA (10.0 equiv) in MeCN (100 mM) at 95 °C for 3 h under an argon atmosphere, and then the solvent was removed under high vacuum, the residue reacted with 2.5 equiv of the racemic [Ru(biq)$_2$(bipyrimidine)]$^{2+}$ (**77**) in MeCN (100mM) at 100 °C for 2 h to give the enantiomerically enriched dinuclear complex **79** in a yield of 49%.
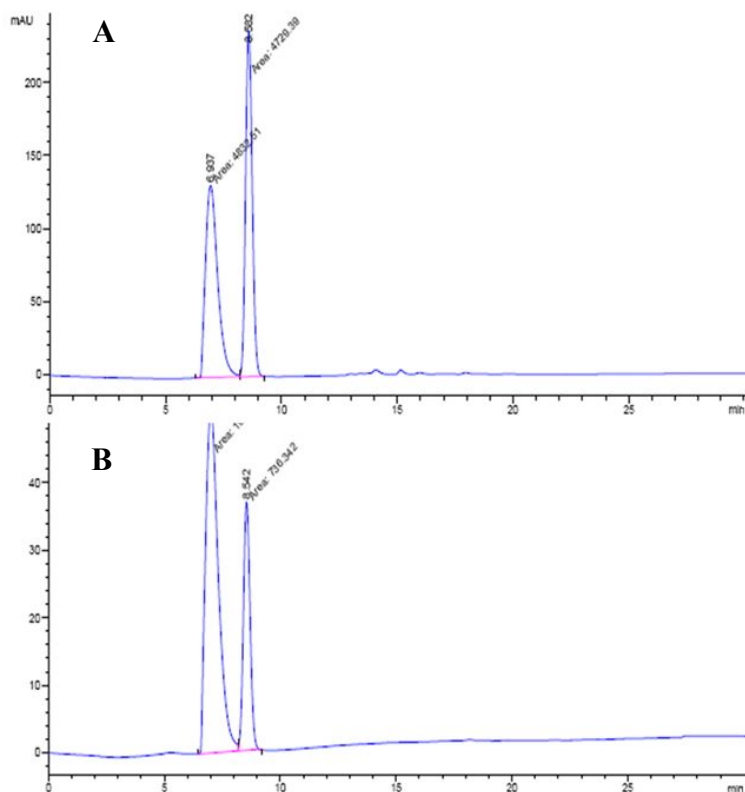
Figure 32. (A) HPLC trace for the racemic complex **79**. (B) HPLC trace for enantiomerically enriched complex **79**, integration of peak areas = 3 : 1 e.r.

The HPLC comparison between the racemic and what we got from the reaction according to scheme 26 is depicted Figure 32. Surprisingly, HPLC trace showed that one quarter of the product got racemized during the reaction process, while the e.r. value of the product didn't change in 3 days (the same sample stored in 4 $^{\circ}$C fridge). We speculated that the initially formed enantiopure dinuclear complexes partially got racemized during heating process. We tried to improve the enantiopurity of complex **79** by changing different reaction conditions, such as solvent (THF) and lower temperatures, unfortunately we didn't get the product with higher ee values.

According to the results we got, it seems that high diastereoselectivity in the step of complex formation can be achieved, however enantiopure complexes could not be easily obtained because of the racemization during reaction process.

48

3.2 Synthesis and Biological Activities of Octahedral Silicon Complexes

3.2.1 Synthesis of Octahedral Silicon Complexes

As described in the Theoretical Part, the metal center of octahedral transition metal complexes acts essentially as an anchor, holding a rigid and three-dimensional scaffold of ligands. However, a wider use of octahedral transition metal complexes is retarded because of the currently prevailing general concerns of metal-based toxicities. Since silicon can form octahedral compounds, we expect to replace octahedral metal complexes by hydrolytically stable octahedral silicon complexes.

This chapter includes two parts: the first part is the synthesis of polypyridyl octahedral silicon(IV) complexes harboring arenediolate, arenediaminate, BINOLate ligands etc., the second part is investigation of the bioactivities of silicon(IV) complexes.

3.2.1.1 Synthesis of Silicon Precursor Complexes

Almost fourty years ago, Kummer and co-workers firstly reported the synthesis of the complex cations $[Si(bpy)_3]^{4+}$ and $[Si(phen)_3]^{4+}$, with bpy = 2,2′-bipyridine and phen = 1,10-phenanthroline.[63,79] According to the reported procedures, SiI_4 (freshly prepared) reacted with 2.2 equiv of bpy or phen (purified by sublimation) in dry chloroform at room temperature to afford cis-$[Si(bpy)_2I_2]I_2$ **81** or cis-$[Si(phen)_2I_2]I_2$ **82** as shown in Scheme 27. However, we found that the desired products can only be obtained when the reaction temperature was raised to 55 °C.
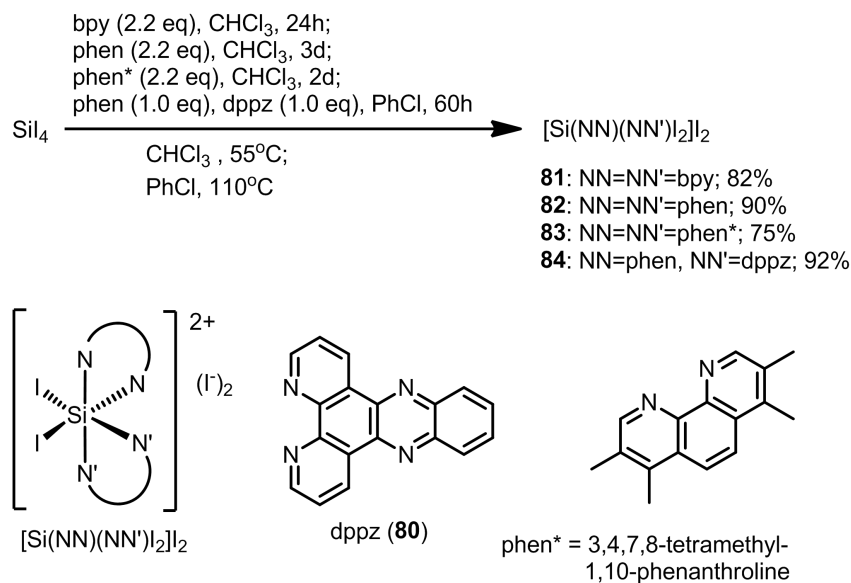
Scheme 27. Synthesis of silicon precursors (**81**~**84**).

Silicon precursor complex *cis*-[Si(phen*)$_2$I$_2$]I$_2$ **83** (phen* = 3,4,7,8-tetramethyl-1,10-phenanthroline) can also be obtained in a yield of 75% by following analogous procedures for the syntheses of precursors **81** and **82**. However, dipyridophenazine (dppz) **80** was not as reactive as bpy, phen or phen*, we can't get the desired silicon complex bearing dppz ligand under the similar condition. After a screening of different temperatures and solvents, we found that complex *cis*-[Si(phen)(dppz)I$_2$]I$_2$ **84** could be formed by the reaction of SiI$_4$ and phen (1.0 equiv), dppz (1.0 equiv) in dry chlorobenzene at 110 °C for 60 h. This reaction's yield is 92%, **84** is pale-red solid, (Scheme 27).

All the silicon precursor (**81**~**84**) are quite sensitive to moisture and unstable at room temperature, we stored them in -20 °C refrigerator under N$_2$. We could not get the NMR spectra for these silicon compounds because of their extremely poor solubilities. We could roughly judge the quality of the precursor by running a test reaction with excess catechol (detail information is in the next section).

3.2.1.2 Octahedral Silicon Complexes with Arenediolate Ligands

All the silicon precursor complexes (**81**~**84**) are not only moisture sensitive but also reactive towards alcohol. For instance, when silicon complex *cis*-[Si(phen)$_2$I$_2$]I$_2$ **82** was heated in methanol at 60 °C for 0.5 h or stirred in methanol at r.t. overnight, the methanolate compound [Si(phen)$_2$(OMe)$_2$]I$_2$ **85** formed as the main product in a yield around 55% (Scheme 28).
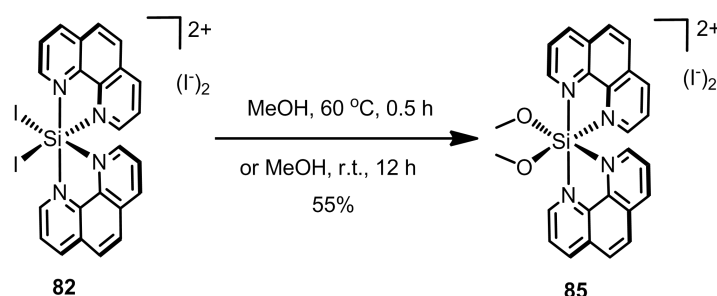
Scheme 28. The synthesis of silicon methanolate compound [Si(phen)$_2$(OMe)$_2$]I$_2$ **85**.

Crystals of compound **85** were obtained by slow diffusion from the solution of **85** in MeCN layered with Et$_2$O. The crystal structure displays that two methanolate ligands are adjacent to each other, and the hexacoordination mode on the centered-silicon is confirmed (Figure 33).
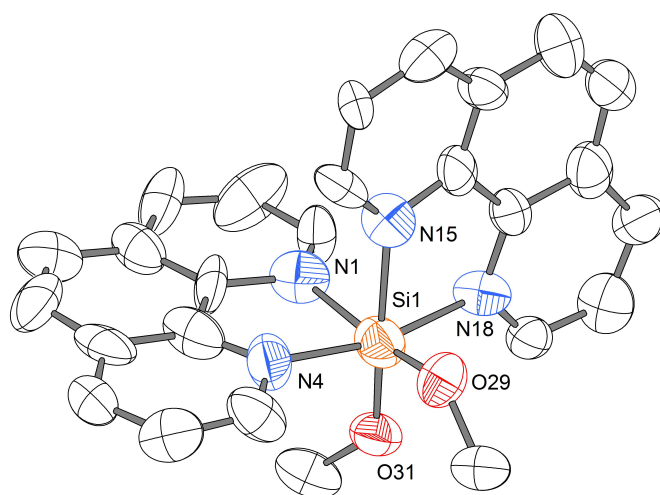
Figure 33. Crystal structure of compound **85**. ORTEP representation with 50% thermal ellipsoids. The other enantiomeric independent cation, hexafluorophosphate anions and solvent molecules (MeCN) are omitted for clarity. Selected bond distances (Å) and angles (°): N1-Si1 2.010(17), N4-Si1 1.885(16), N15-Si1 2.008(14), N18-Si1 1.950(14), O29-Si1 1.669(12), O31-Si1 1.661(11); O31-Si1-O29 100.1(6), N4-Si1-N18 166.3(8), O29-Si1-N15 86.5(6), O31-Si1-N1 90.5(6),

N15-Si1-N1 83.3(6).

Since silicon precursor reacted with methanol easily, we believed that *ortho*-dihydroxyarene can also react with these silicon complexes. The first *ortho*-dihydroxyarene we tried was catechol, it is the conjugate acid of a chelating agent widely used in coordination chemistry. Indeed, *cis*-[Si(bpy)$_2$I$_2$]I$_2$ **81** reacted with 4.0 equiv of catechol in freshly distilled CHCl$_3$ at 55 °C for 12 h, after silicon-gel column chromatography purification, [Si(bpy)$_2$(catecholate)](PF$_6$)$_2$ **86** was obtained as a pale-yellow solid in a yield of 40%.

Analogous catecholate silicon complexes silicon(IV) compound [Si(phen)$_2$(catecholate)](PF$_6$)$_2$ **87** (50%), [Si(phen*)$_2$(catecholate)](PF$_6$)$_2$ **88** (40%) could also be prepared in similar reaction condition by using *cis*-[Si(phen)$_2$I$_2$]I$_2$ **82** and *cis*-[Si(phen*)$_2$I$_2$]I$_2$ **83** as starting complexes (Scheme 29). Nevertheless, the preparation of [Si(phen)(dppz)(catecholate)](PF$_6$)$_2$ **89** needed more harsh condition and the yield was lower. Silicon precursor *cis*-[Si(phen)(dppz)I$_2$]I$_2$ **84** reacted with 4.0 equiv of catechol in dry *o*-xylene at 120 °C for 12 h, after silicon-gel column chromatography purification, the complex **89** was obtained as a yellow solid in a yield of 10%.
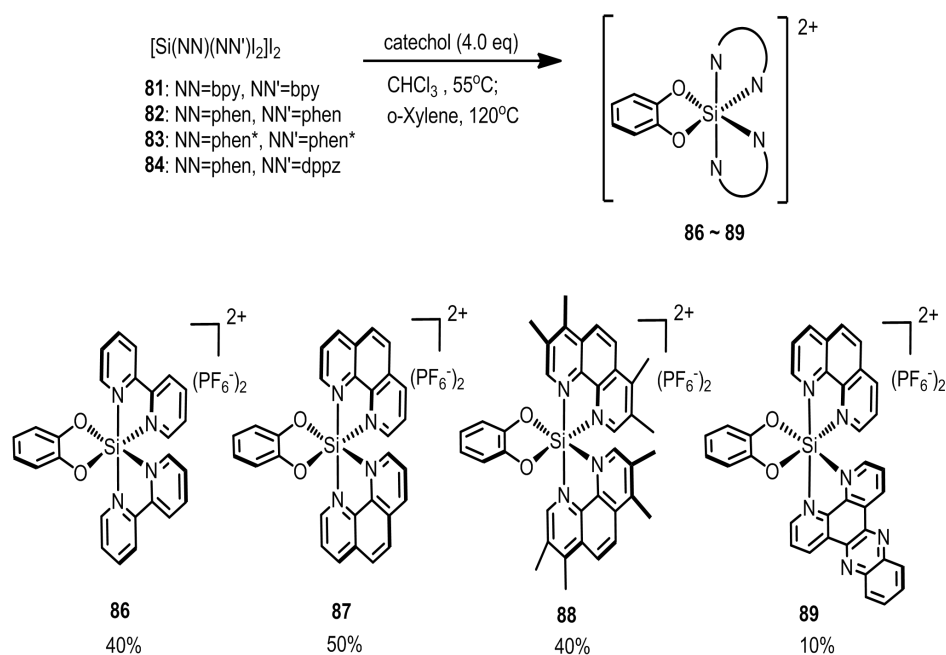
Scheme 29. Synthesis of silicon(IV) catecholate complexes (**86** ~ **89**).

Catechol is a fairly cheap and readily available compound. As referred in last section, because of the lack of suitable deuterated solvent for these silicon precursor complexes (**81~84**), we judge the quality of the precursor compounds roughly by running a test reaction with excess catechol.

We also synthesized other arenediolate compounds containing different aromatic π-systems in addition to catechol, such as *ortho*-dihydroxyarenes 4,5-pyrenediol **92** and 5,6-chrysenediol **95**. Following the reported procedures,[80] pyrene **90** was firstly oxidized to 4,5-pyrenedione **91** in the presence of $RuCl_3$ and $NaIO_4$, after silicon-gel column chromatography (flushed with DCM), the orange product **91** could be obtained in a yield 55% (Scheme 30). Compound **91** was subsequently reduced by $Na_2S_2O_4$ in the presence of n-Bu$_4$NBr, after quick workup (extraction, washing, drying and solvent removal), affording the crude compound **92** which can be used directly without further purification in a high yield of 95%. Accordingly, 5,6-chrysenedione **94** (45%) and 5,6-chrysenediol **95** (92%) were also obtained through the same route displayed in Scheme 29. Both *ortho*-dihydroxyarenes **92** and **95** are oxygen sensitive and should be stored in refrigerator at -20ºC under N_2 or used immediately after preparation.
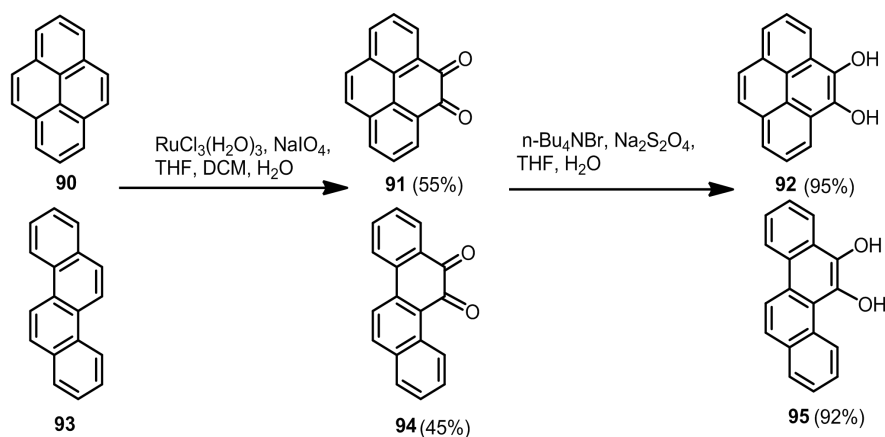
Scheme 30. Synthesis of 4,5-pyrenediol **92** and 5,6-chrysenediol **95**.
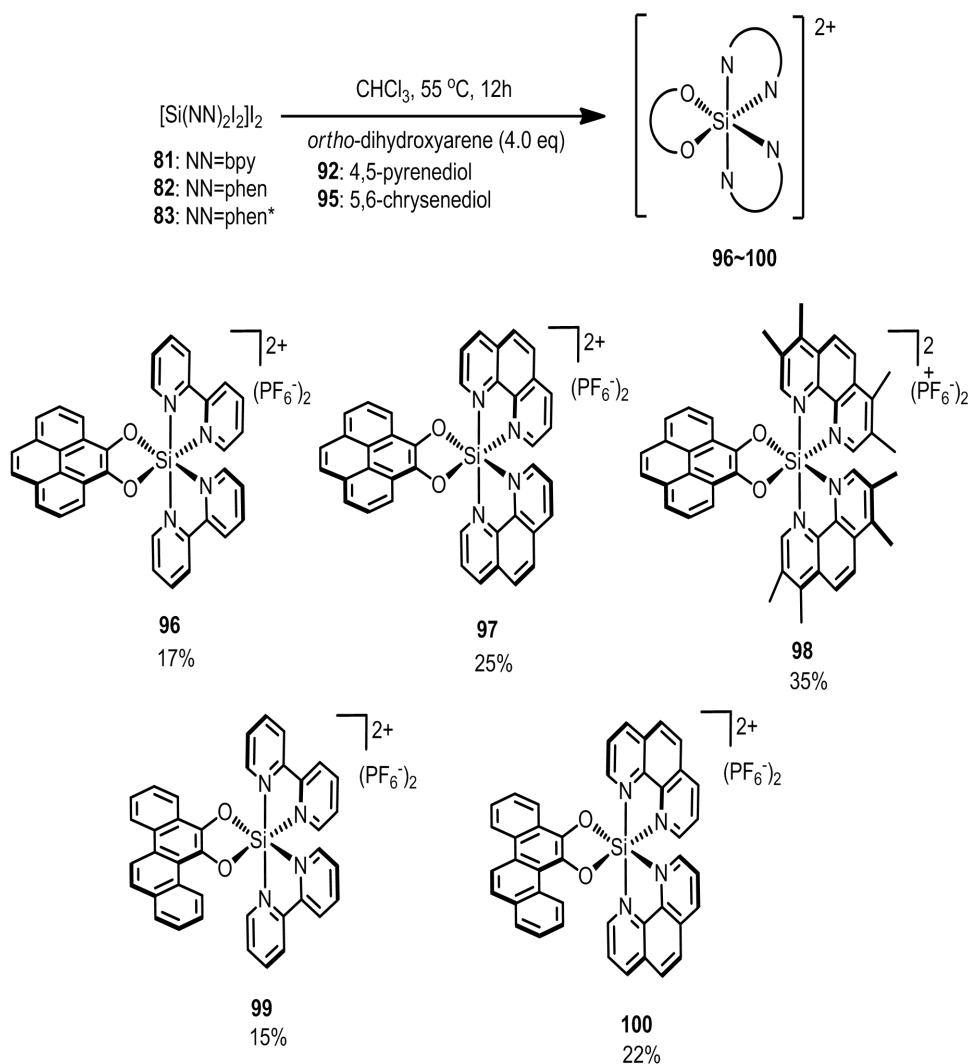
Scheme 31. Synthesis of (arenediolato)silicon(IV) complexes (**96** ~ **100**).

Silicon precursor *cis*-[Si(bpy)$_2$I$_2$]I$_2$ **81** reacted with 4.0 equiv of 4,5-pyrenediol **92** in freshly distilled CHCl$_3$ at 55 °C for 12 h, after silicon-gel column chromatography purification, [Si(bpy)$_2$(4,5-pyrenediolate)](PF$_6$)$_2$ **96** was obtained as a pale-brown solid in a yield of 17% (Scheme 31). The other four silicon(IV) arenediolate complexes [Si(phen)$_2$(4,5-pyrenediolate)](PF$_6$)$_2$ **97** (a brown-red solid, 25%), [Si(phen*)$_2$(4,5-pyrenediolate)](PF$_6$)$_2$ **98** (a yellow solid, 35%), [Si(bpy)$_2$(5,6-chrysenediolate)](PF$_6$)$_2$ **99** (a brown-red solid, 15%) and [Si(phen)$_2$(5,6-chrysenediolate)](PF$_6$)$_2$ **100** (a brown solid, 22%) were prepared respectively *via* similar reaction conditions.
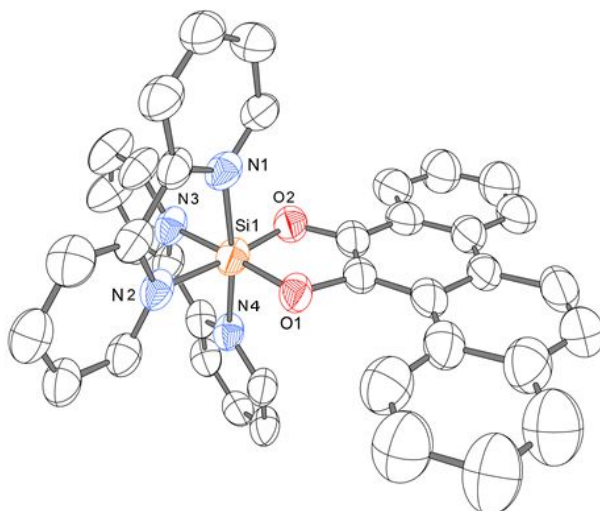
**Figure 34**. Crystal structure of the (5,6-chrysenediolato)silicon complex **99**. ORTEP representation with 50% thermal ellipsoids. The other enantiomeric independent cation, hexafluorophosphate anions and solvent molecules (MeCN) are omitted for clarity. Selected bond distances (Å) and angles (°): N1-Si1 1.914(4), N2-Si1 1.932(5), N3-Si1 1.921(4), N4-Si1 1.923(4), O1-Si1 1.719(3), O2-Si1 1.727(4); O1-Si1-N1 92.99(17), O1-Si1-N2 89.36(17), O1-Si1-N3 175.61(18), O1-Si1-N4 93.43(17), N1-Si1-N3 91.37(18)，N2-Si1-N4 93.80(19), N3-Si1-N4 = 82.26(18).

We tried to grow crystals to confirm the structures of this series of silicon(IV) arenediolate complexes, fortunately, we got the crystal structure of [Si(bpy)$_2$(5,6-chrysenediolate)](PF$_6$)$_2$ **99** (crystals obtained by slow diffusion of Et$_2$O into the solution of **99** in MeCN). In silicon complex **99**, as shown in Figure 34, the central atom is ligated by four nitrogen atoms and two oxygen atoms which constitute a slightly distorted octahedral coordination geometry. N2 and O2 occupy two sites of axis (the angle of N3-Si1-O1 is 175.61(18)°), whereas the other four atoms (O1, N1, N3 and N4) occupy equatorial positions which makes a nearly planar quadrilateral geometry around the silicon center {∠N1-Si1-O1 = 92.99(17)°, ∠N1-Si1-N3 = 91.37(18)°, ∠N3-Si1-N4 = 82.26(18)°, ∠N4-Si1-O1 = 93.43(17)°; Σ = 360.06(7)°}. Furthermore, the average Si-O bond length of 1.723 Å in **99** is longer than the average Si-O distance of 1.631 Å, and the average Si-N bond length of 1.923 Å in **99** is longer than the average Si-N distance of 1.631 Å,[81] which indicate a strong intramolecular repulsion among the ligands.

The arenediolatosilicon complexes are all be well dissolved and stable in MeCN, and no signs of any decomposition from the complexes in deuterated MeCN were

detected after one week. Moreover, the hydrolytic stability of these silicon complexes were also tested by ^{1}H-NMR, which didn't show any change in one week. Figure 27 depicts the ^{1}H-NMR trace of complex **99** in the mixture solvent CD_3CN / D_2O (3 : 1) for one week.

after one week

after three days

after one day

fresh sample
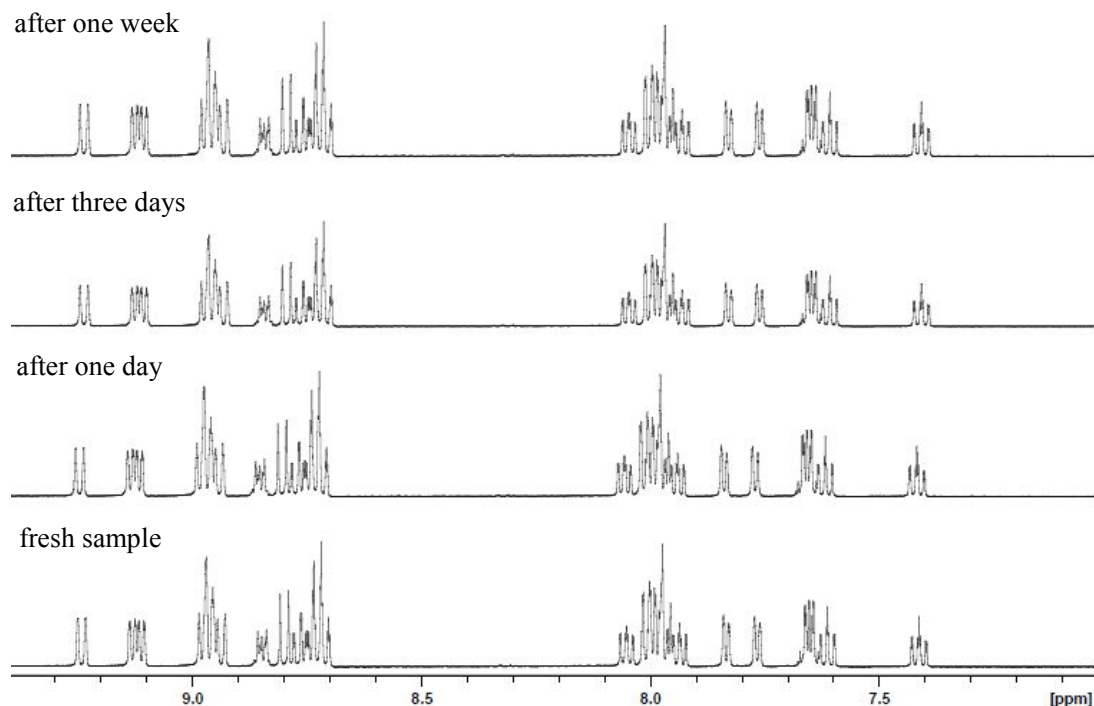
Figure 35. Hydrolytic stability of [Si(bpy)$_2$(5,6-chrysenediolate)](PF$_6$)$_2$ **99** at room temperature in CD_3CN / D_2O (3 : 1).

3.2.1.3 Octahedral Silicon Complexes with Arenediaminate Ligand

Considering *ortho*-phenylenediamine **101** has a similar structure as catechol, we therefore speculated that the reactivity of *ortho*-phenylenediamine towards silicon precursors might similar to *ortho*-arenediol. Accordingly, when the mixture of **101** (4 equiv) and silicon precursor [Si(bpy)$_2$I$_2$]I$_2$ **81** in dry CHCl$_3$ was heated at reflux for 3h under N$_2$, a dark-brown solid [Si(bpy)$_2$(*o*-phenylenediaminate)](PF$_6$)$_2$ **102** was afforded in a yield of 55% after workup (Scheme 32). Based on the similar reaction conditions, analogous complexes [Si(phen)$_2$(phenylenediaminate)](PF$_6$)$_2$ **103** (a dark-brown-red solid, 60%), [Si(phen*)$_2$(phenylenediaminate](PF$_6$)$_2$ **104** (a dark solid,

48%) could also be prepared with other starting complexes *cis*-[Si(phen)$_2$I$_2$]I$_2$ **82**, *cis*-[Si(phen*)$_2$I$_2$]I$_2$ **83** respectively.
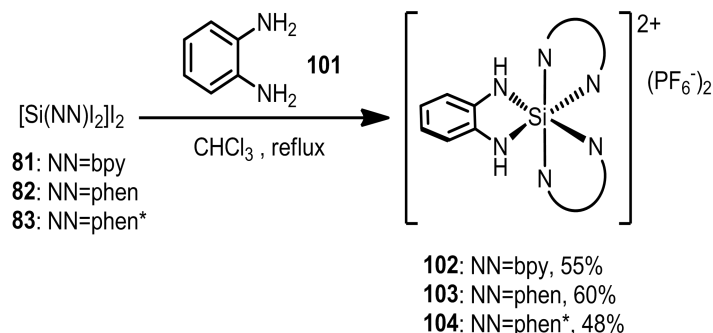
Scheme 32. The syntheses of octahedral silicon(IV) complexes (**102~104**) with *ortho*-phenylenediaminate ligand.

The *o*-phenylenediaminatosilicon complexes (**102~104**) are all well dissolved and stable in MeCN, and no signs of any decomposition from the complexes in deuterated MeCN were observed after one week. The hydrolytic stability of these silicon complexes were also tested in the mixture solvent CD$_3$CN / D$_2$O (3 : 1) by ^{1}H-NMR trace. Taking complex **102** as an example, the ^{1}H-NMR trace of it didn't show any change in one week (Figure 36).
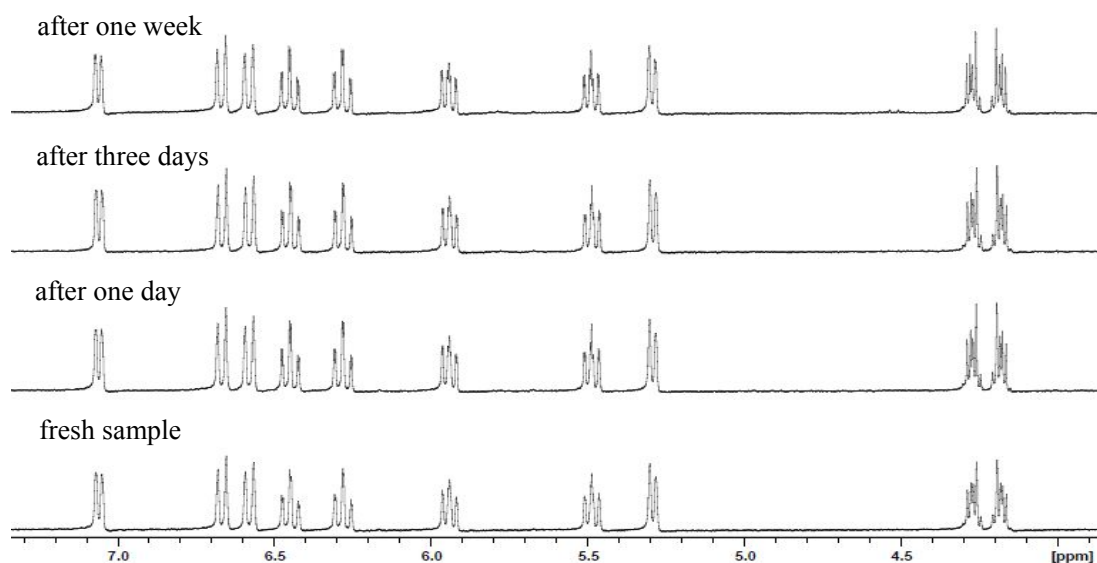
Figure 36. Hydrolytic stability of **102** at room temperature in CD$_3$CN / D$_2$O (3 : 1).

For most of our biological testing, the solvents always contain a small amount of

DMSO, so we also tested the stability of these diaminate complexes in DMSO / H_2O (1 : 1) solution. In contrast to the high stability of complex **102** in the mixture of CD_3CN / D_2O (3 : 1), the complex **102** is unstable in the mixture of DMSO / H_2O (1 : 1) determined by ^{1}H-NMR trace. As depicted in Figure 37, a set of triple signal around 7.9 ppm and two sets of multiplet signals around 6.6~6.7 ppm slowly came up within one week.
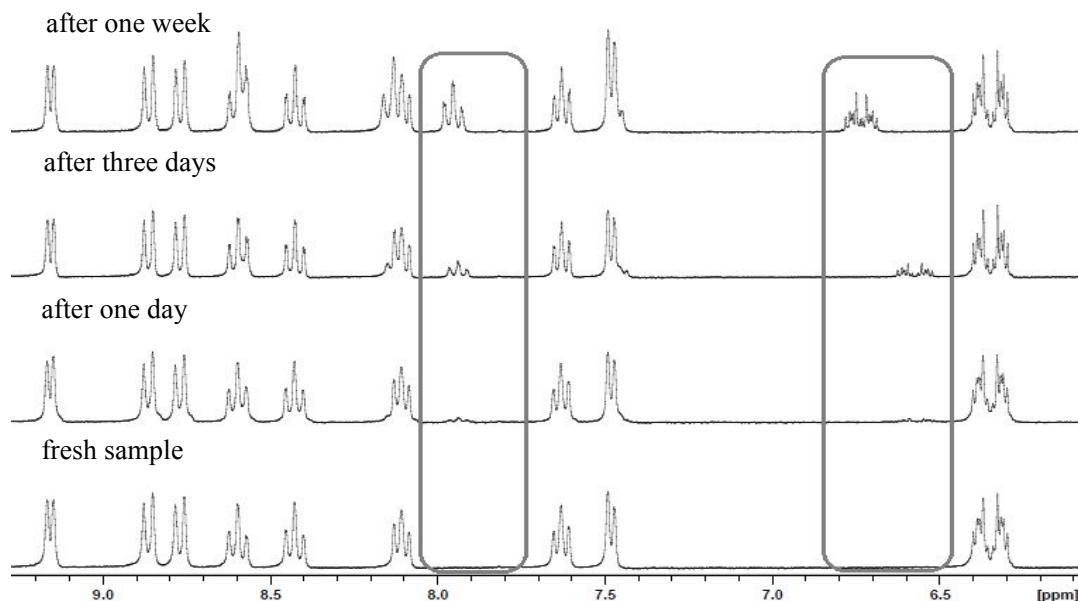
Figure 37. Hydrolytic stability of **102** at room temperature in DMSO / D_2O (1 : 1).

We speculated that the change of the silicon(IV) complex **102** in the mixture of DMSO / D_2O (1 : 1) was caused by the oxidizing property of DMSO. Since it is well-known that DMSO is frequently used as a mild oxidant in organic synthesis, we thought that DMSO could also oxidize the aminate group in the *ortho*-phenylenediaminate silicon(IV) complexes (**102~104**).

In last chapter, we introduced that the auxiliaries can be cleaved in acidic condition, thus we also wondered that whether the *ortho*-phenylenediaminate ligand of these complexes (**102~104**) can be removed or not in the presence of excess acid. To our delight, when complex **102** was treated with trifluoroacetic acid (TFA) (5.0 equiv) and in the presence of an excess of catechol (15.0 equiv) in MeCN at 110 ^{o}C for 4 h, silicon(IV) catecholate complex **86** was obtained after workup, silica-gel

column chromatography and hexafluorophosphate precipitation, in a yield of 35% (Scheme 33).
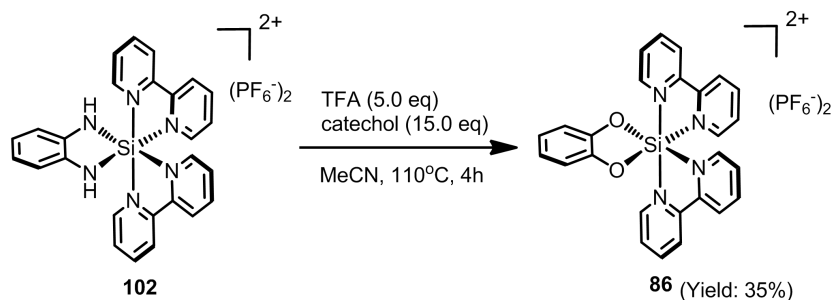
Scheme 33. The ligand substitution of complex **102** by excess catechol.

3.2.1.4 Asymmeric Synthesis of Silicon BINOLate Complexes

Recently our group has successfully developed a series of auxiliaries for asymmetric synthesis of octahedral metal complexes, we therefore intended to explore a ligand that can be used as an effective auxiliary to direct the chirality at the silicon center. Firstly we tried all the existed auxiliaries, chiral 2-sulfinylphenols (**SO**), salicyloxazolines (**Salox**), N-acetyl-tert-butanesulfinamides (**ASA**), and proline, all of which can effectively direct the chirality of the octahedral metal complexes. Unfortunately, the reactions of these auxiliaries with silicon precursors (**81~83**) all failed in the solvents like CHCl₃, PhCl, *o*-xylene, even under more harsh conditions, such as heated in a oil bath at a higher temperature for a longer time (at reflux in 1,3,5-trimethylbenzene for 24 h), no desired product can be detected by mass spectroscopy.

Then we turned our attention to the 1,1'-bi-2-naphthol (BINOL), the enantiomeric atropisomers of which have become among the most widely used ligands for both stoichiometric and catalytic asymmetric reactions.[82] In addition, BINOL is an arenediol, and it might react with silicon precursor as the *ortho*-arenediols we described before. Accordingly, when silicon precursor **81** was reacted with 4.0 equiv of *R*-BINOL in *o*-xylene at 120 °C for 20 h, Λ-[Si(bpy)₂(*R*-BINOLate)](PF₆)₂ {Λ-(*R*)-**105**} was obtained with an ee value of 90%

because of the existence of 5% minor enantiomer Δ-(*S*)-**105** (Scheme 34).

105: NN=bpy, 12% (e.e. = 90%)
106: NN=phen, 10% (e.e. = 88%)
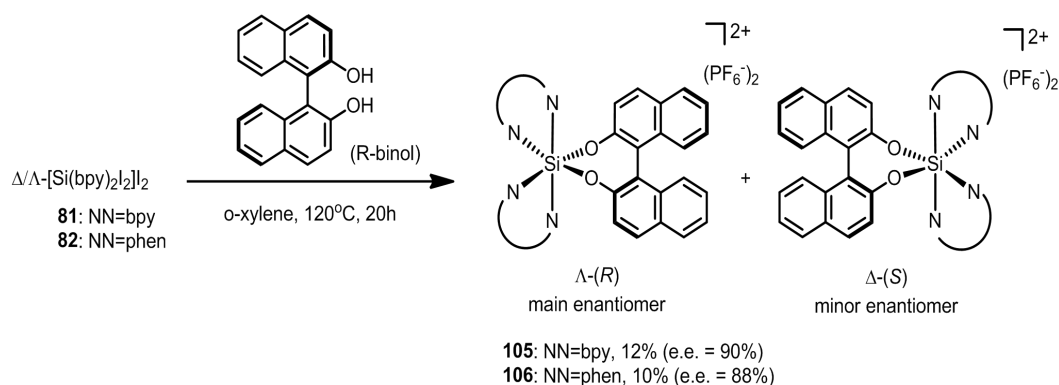
Scheme 34. Asymmetric synthesis of enantiomerically enriched octahedral silicon(IV) Λ-(*R*)-**105** and Λ-(*R*)-**106**.

It is worthy noting that HI, which formed during the reaction, is a strong acid, and it has been reported that chiral BINOL can be racemized in acidic or basic condition after a long time heating process (temperature higher than 100 $^{\circ}$C and reaction time longer than 12 h).[83] In this case, we believed that the minor enantiomer Δ-(*S*)-**105** resulted from the racemization of *R*-BINOL. Similarly, Λ-[Si(phen)$_2$(*R*-BINOLate)](PF$_6$)$_2$ {Λ-(*R*)-**106**} was also obtained through the same procedures in a yield of 10% with 94 : 6 e.r. as shown in Scheme 33.

The enantiopurity of Λ-(*R*)-**105** was determined by chiral HPLC. To make a reference, we synthesized the racemic mixture of Λ-(*R*)-**105** and Δ-(*S*)-**105** *via* the reaction of silicon complex [Si(bpy)$_2$I$_2$]I$_2$ **81** with 4 equiv racemic BINOL, and the HPLC traces are shown in Figure 38.
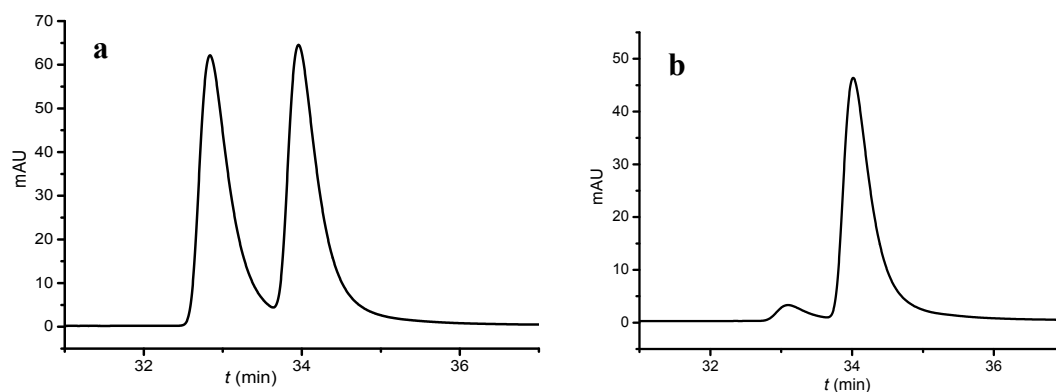
Figure 38. HPLC traces of non-racemic and racemic [Si(bpy)$_2$(R-BINOLate)](PF$_6$)$_2$ (**105**). (a) Racemic mixture of Λ-[Si(bpy)$_2$(*R*-BINOLate)](PF$_6$)$_2$ {Λ-(*R*)-**105**} and Δ-[Si(bpy)$_2$(S-BINOLate)](PF$_6$)$_2$ {Δ-(*S*)-**105**} as a reference. (b) The Λ-(*R*)-**105** with 95 : 5 e.r.

synthesized from **81** and R-BINOL (Scheme 34). HPLC conditions: Daicel Chiralpak IA column, 250 × 4.6 mm, flow rate was 0.5 mL/min, column temperature 40°C, and UV-absorption was measured at 254 nm, solvent A = 0.1% TFA, solvent B = MeCN, with a linear gradient of 15% to 24% B in 30 min.

The structure of Λ-(*R*)-**105** was confirmed by X-ray crystallography, and the single crystals were obtained slow diffusion of Et$_2$O into the solution of Λ-(*R*)-**105** in MeCN. As shown in Figure 39, the average Si-O bond length of 1.694 Å in Λ-(*R*)-**105** is shorter than the average Si-O distance of 1.723 Å in chrysenediolate complex **99**, which indicates that the new formed 7-member ring (silicon and the BINOLate ligand) does not increase but slightly decrease the tension of the octahedral configuration. Based on steric effect, the *R*-BINOLate appears to nicely fit the Λ configuration of the silicon center, which implies a high diastereoselectivity.
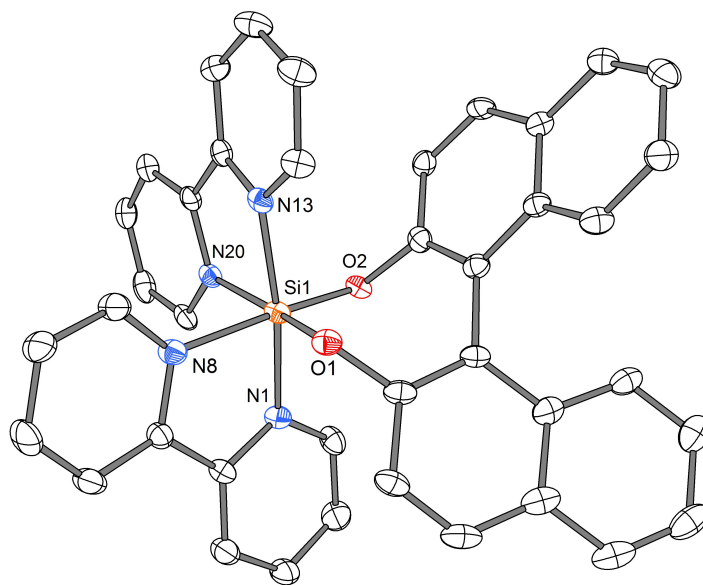
Figure 39. Crystal structure of Λ-[Si(bpy)$_2$(R-BINOLate)](PF$_6$)$_2$ {Λ-(*R*)-**105**}. ORTEP representation with 50% thermal ellipsoids. Two hexafluorophosphate anions are omitted for clarity. Selected bond distances (Å) and angles (°): N1-Si1 1.906(2), N8-Si1 1.958(2), N13-Si1 1.912(2), N20-Si1 1.965(2), O1-Si1 1.6931(17), O2-Si1 1.6941(17); O1-Si1-O2 98.43(8), O1-Si1-N1 93.82(9), O2-Si1-N1 91.73(9), O1-Si1-N8 85.94(9), N8-Si1-N20 85.77(9), O2-Si1-N20 90.41(8), N1-Si1-N13 171.56(9).

The high diastereoselectivity of the reaction can be further demonstrated by the ^{1}H-NMR spectrum of Λ-(*R*)-**105** shown in Figure 40. There was only one set of 14

different protons (a molecular **105** contains 28 protons) can be seen in the ^{1}H-NMR spectrum, which means just one diastereomer existed in the product. In addition, the silicon complex Λ-(*R*)-**105** is well dissolved and stable in MeCN, and no signs of any decomposition from the complex in MeCN were observed after one month.
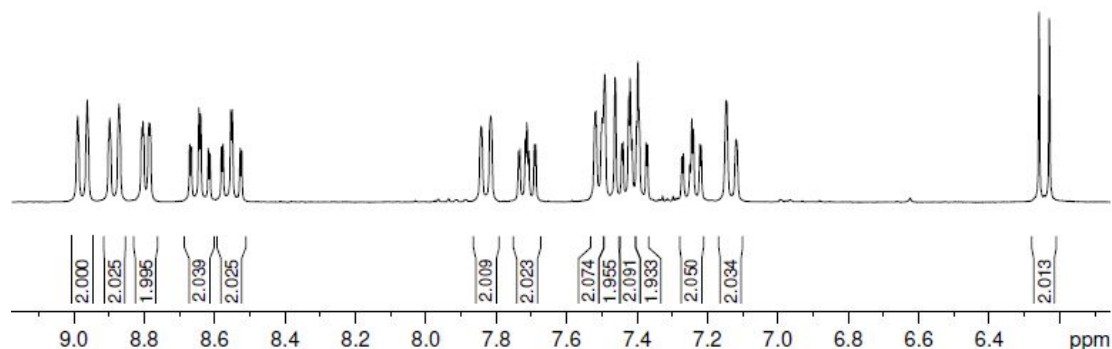
Figure 40. ^{1}H-NMR spectrum of silicon(IV) *R*-BINOLate {Λ-(*R*)-**105**} in CD$_3$CN.

The CD spectrum of Λ-(*R*)-**105** is displayed in Figure 41.
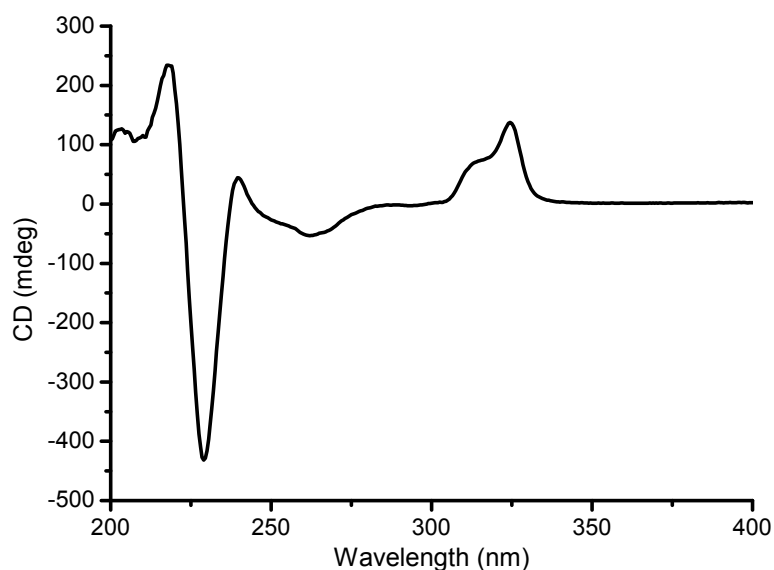
Figure 41. CD spectrum for complex Λ-(*R*)-**105** in CH$_3$CN (0.1 mM).

As mentioned at the beginning of this section, our aim was to find a ligand that can be used as an effective auxiliary for asymmetric synthesis of octahedral silicon complexes. Since the coordination chemistry of *R*-BINOL and silicon precursor complexes has presented high diastereoselectivity, the *R*-BINOLate could be considered as a good auxiliary if it can be removed under retention of configuration.

We therefore next investigated the removal of the coordinated *R*-BINOLate auxiliary. Contrast to the acid-lability of L-prolinate and other auxiliaries (**Salox**, **SO** and **ASA**), the Λ-[Si(bpy)$_2$(*R*-BINOLate)](PF$_6$)$_2$ {Λ-(*R*)-**105**} is fairly stable in acid, even heated in excess of TFA overnight. However, when the Λ-(*R*)-**105** was treated with 5 equiv K$_2$CO$_3$ in the presence of an excess of catechol (15 equiv) in MeCN at 110 °C for 5 h, the product [Si(bpy)$_2$(catecholate)](PF$_6$)$_2$ **86** can be detected by TLC and Mass spectroscopy, but yield is very low (~5%) and various unidentified byproducts are also formed (Scheme 35).
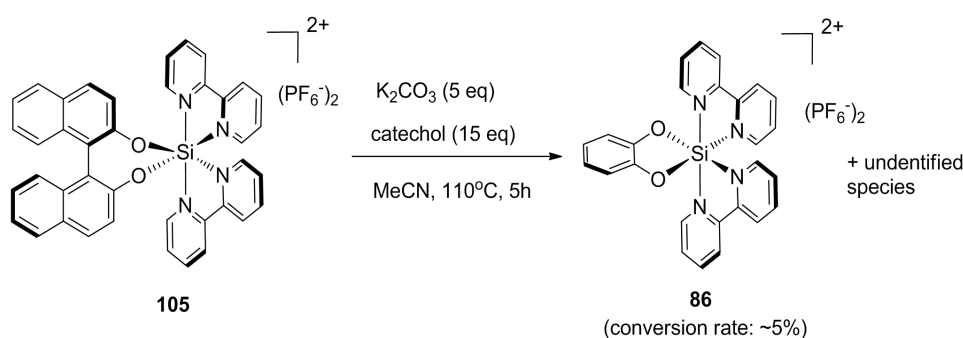
Scheme 35. Conversion of complex **105** to complex **86**.

Although the yields for the formation of the silicon(IV) BINOLate complexes {Λ-(*R*)-**105**, Λ-(*R*)-**106**} were extremely low, we still successfully synthesized the first enantiomerically enriched octahedral silicon complexes with chiral auxiliary *R*-BINOL.

3.2.1.5 Synthesis of Silicon-Ruthenium Sandwich Complexes

When we looked at the structure of these silicon arenediolate complexes {[Si(bpy)$_2$(4,5-pyrenediolate)](PF$_6$)$_2$ **96**, [Si(phen)$_2$(4,5-pyrenediolate)](PF$_6$)$_2$ **97** carefully, [Si(phen*)$_2$(4,5-pyrenediolate)](PF$_6$)$_2$ **98}**, we speculated that the fused aromatic pyrene in these complexes still could coordinate to cationic [(η^5-C$_5$R$_5$)Ru]$^+$ moiety, because the synthesis of sandwich complexes [(η^5-C$_5$R$_5$)Ru(η^6-arene)]PF$_6$ (R = Me, C$_5$R$_5$ = pentamethylcyclopentadienyl = Cp*; arene = substituted benzene) have

been reported.[84] Accordingly, when complex **96** was reacted with 0.88 equiv of {[Cp*Ru(MeCN)$_3$](PF$_6$)} **107** in 1,2-dichloroethane at 60 °C for 40 h in the dark, the silicon-ruthenium sandwich complex **108** was obtained in a yield of 45% after silica-gel column chromatography and hexafluorophosphate precipitation. Related complexes were also prepared with the similar starting complexes, [Si(phen)$_2$(4,5-pyrenediolate)]PF$_6$ (**97**) and [Si(phen*)$_2$(4,5-pyrenediolate)]PF$_6$ (**98**), providing sandwich complexes **109** (40%), **110** (42%) respectively (Scheme 36).
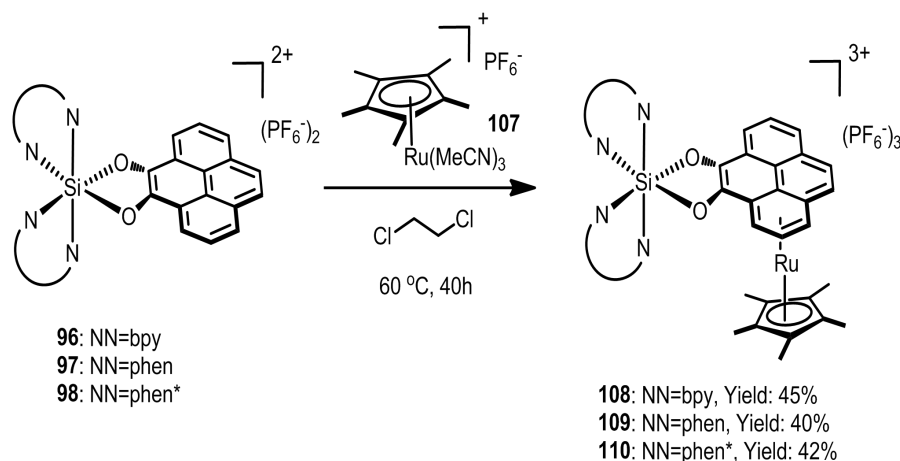
Scheme 36. Synthesis of silicon-ruthenium sandwich complexes (**108**~**110**) from the (4,5-pyrenediolato)silicon complexes (**96**~**98**).

The structures of these silicon-ruthenium sandwich complexes (**108**~**110**) can be deduced from ^{1}H-NMR spectra. Taking the ^{1}H-NMR spectrum of **109** shown in Figure 42 as an example, there are one set of 24 different protons in the low field 9.7~6.2 ppm that are assigned to all the protons from starting complex **97** (one molecular **97** contains 24 protons, but ^{1}H-NMR shows one set of 12 different protons because of symmetry), and one singlet of 15 protons around 1.0 ppm assigned to Cp*. The ^{1}H-NMR spectrum of **109** thereby indicates an asymmetric structure of **109** and a highly diastereoselective coordination chemistry. In addition, these silicon-ruthenium complexes are all stable in acetone, and no signs of any decomposition can be detected by ^{1}H-NMR trace (samples stored at 4 °C fridge under dark).
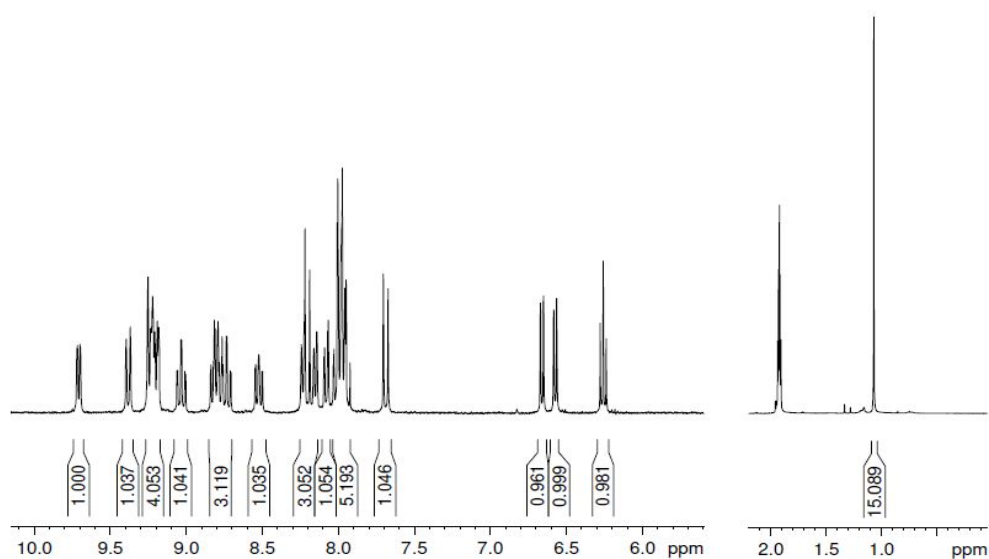
Figure 42. ^{1}H-NMR spectrum of silicon-ruthenium complex **109** in CD$_3$COCD$_3$ (10.0~5.6 ppm and 2.1~0 ppm).

The structural deduction from ^{1}H-NMR was further confirmed by X-ray crystallography, and the single crystals of silicon-ruthenium sandwich complex **109** were obtained by slow evaporation from the mixture solution acetone and water. Figure 43 (A) shows that the [Ru(Cp*)]$^{2+}$ fragment is η^6-coordinated to one terminal benzene ring (C38, C39, C40, C41, C42 and C43) in the pyrenediolate ligand and reveals the diastereomeric specificity through the steric interference, which can be more clearly observed in Figure 43 (B). Thus, we believe that the other diastereomer of complex **109**, the product of [Ru(Cp*)]$^{2+}$ fragment η^6-coordinated to the other terminal benzene ring (C31, C32, C33, C34, C35 and C44) from the same side, is totally unstable because of the existence of a strong inter-ligand repulsion between the phen ligand and the methyl group on the Cp* ligand.

A   **B**
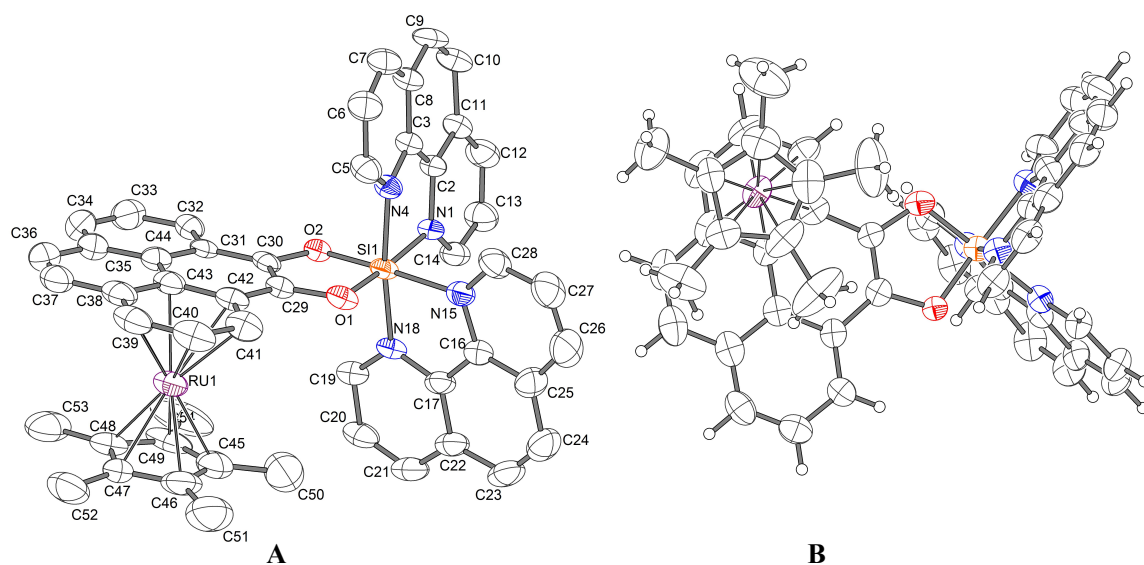
Figure 43. Crystal structure of the silicon-ruthenium complex **109** from two different perspectives (A, B: ORTEP representation with 50% thermal ellipsoids). Three hexafluorophosphate anions and solvent molecules (acetone) are omitted for clarity. Selected bond distances (Å) and angles (°): N1-Si1 1.939(4), N4-Si1 1.927(4), N15-Si1 1.933(4), N18-Si1 1.916(4), O1-Si1 1.727(4), O2-Si1 1.717(4), C38-Ru1 2.241(6), C39-Ru1 2.201(6), C40-Ru1 2.210(6), C41-Ru1 2.223(6), C42-Ru1 2.264(5), C43-Ru1 2.266(5), C45-Ru1 2.152(6), C46-Ru1 2.167(6), C47-Ru1 2.180(5), C48-Ru1 2.171(6), C49-Ru1 2.145(6); O1-Si1-O2 92.32(17), O1-Si1-N15 89.59(18), O2-Si1-N1 87.61(17), N15-Si1-N1 90.81(18), N4-Si1-N18 172.12(19).

3.2.2 Biological Activities of Octahedral Silicon Complexes

3.2.2.1 Silicon Complexes as DNA Intercalators

With the hydrolytically stable octahedral silicon(IV) complexes in hand, we firstly investigated the influence of these silicon complexes on the thermal stability of duplex DNA and we therefore monitored the melting temperature (T_m) of a mixed-sequence of 15mer duplex DNA (2 μM) in the presence of the complexes (8 μM) by temperature-dependent UV spectroscopy at 260 nm.

The 15mer oligonucleotides duplex 5′-AGTGCCAAGCTTGCA-3′ / 3′-TCACGGTTCGAACGT-5′ was chosen, and Dr. Xiang from the Zhang group did the tests for the most silicon arenediolate complexes. From his testing results (shown in his doctoral thesis), it can be observed that octahedral silicon complexes with different polyaromatic diolate ligands obviously altered the melting temperature of the DNA duplex on different levels. As the structures shown in Figure 44, catecholate complex **87** did not significantly alter the T_m of the DNA duplex, with the $\Delta T_m = 1.0$ °C, and 5,6-chrysenediolate complex **100** showed a moderate stabilization of the duplex DNA by increasing T_m for 5.6 °C, whereas 4,5-pyrenediolate complex **97** ($\Delta T_m = +19.3$ °C) led to a remarkably strong stabilization of the duplex DNA.
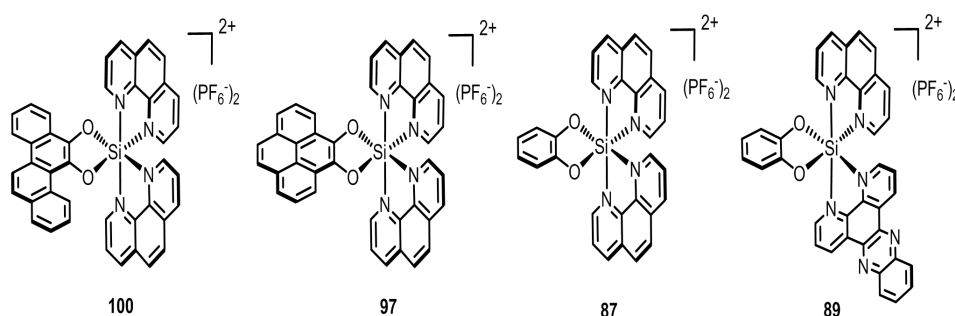
Figure 44. Some octahedral silicon(IV) arenediolate complexes for UV-melting.

We assumed that the di-imine ligands in the silicon complexes also could act as intercalators through π-stacking between two base pairs. For example, we tested the complex [Si(phen)(dppz)(catecholate)](PF$_6$)$_2$ **89** (the structure displayed in Figure 44), it indeed showed an impressive binding strength ($\Delta T_m = 11.5$ °C), compared to

[Si(phen)$_2$(catecholate)](PF$_6$)$_2$ **87** ($\Delta T_m = 1.0$ $^{\circ}$C), and the related curves are shown in Figure 45.
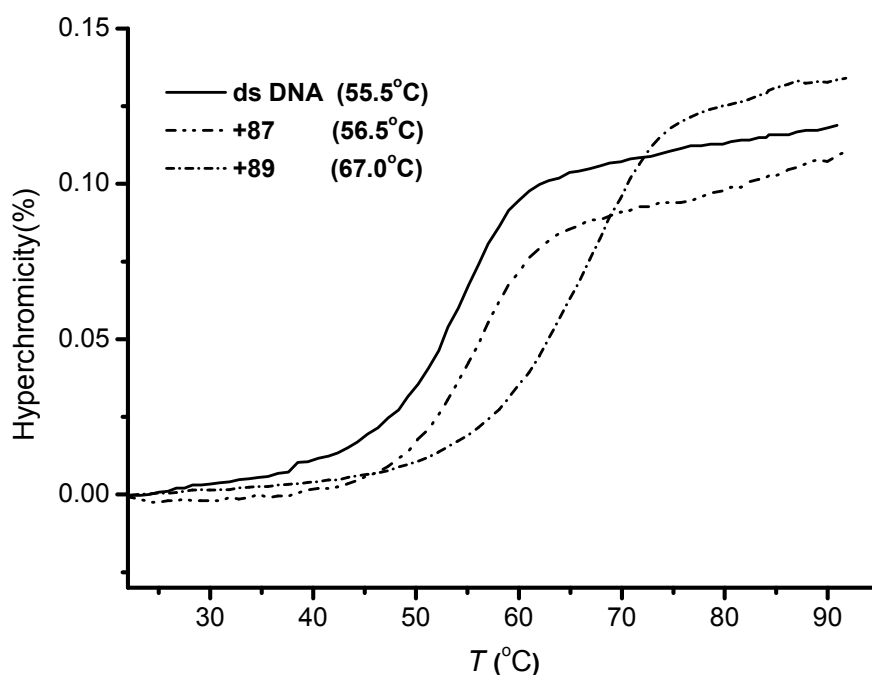
Figure 45. UV-melting curves of duplex DNA 5′-AGTGCCAAGCTTGCA-3′ / 3′-TCACGGTT CGAACGT-5′. Changes in absorbance upon heating as monitored at 260 nm. Conditions: 5 mM Tris-HCl, 50 mM NaCl, pH 7.4, and 2 μM of each strand in the presence of 8 μM silicon complexes (**87**, **89**).

To further analyze the interaction of the octahedral silicon(IV) complex [Si(phen)(dppz)(catecholate)](PF$_6$)$_2$ **89** with the duplex DNA, we also monitored CD spectroscopy of the duplex DNA and **89** in different concentrations. As shown in Figure 46, the addition of just one equiv of **89** to the duplex DNA resulted in a significant change of the Cotton effect, which was continuously intensified with the increasing amount of complex **89** until saturation was reached at a DNA : **89** ratio of around 1 : 5.
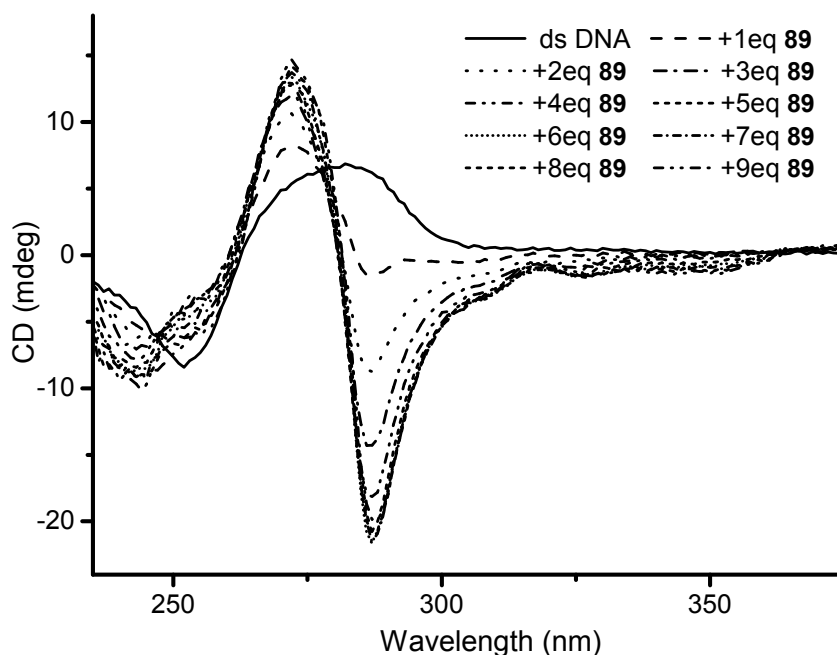
Figure 46. CD spectra of the duplex DNA 5′-AGTGCCAAGCTTGCA-3′ / 3′-TCACGGTTCGAACGT-5′ titrated with increasing amount of complex **89**. Conditions: 5 mM Tris-HCl, 50 mM NaCl, pH 7.4 and 20 μM duplex, [Si(phen)(dppz)(catecholate)](PF$_6$)$_2$ **89** (0–180 μM).

Taken together, the strong thermal stabilization of duplex DNA by the silicon complex **89**, along with the modulation of the secondary structure as observed by CD spectroscopy, are indicative of an intercalative binding with the extended π-system of the dppz ligand inserted between neighboring base pairs.

3.2.2.2 Silicon Complexes as Stabilizers of Mismatched DNA

According to Barton's work, octahedral transition metal complexes could either act as DNA intercalators by binding DNA *via* the major groove or as insertors by binding DNA *via* the minor groove, which mainly depends on the size of the aromatic ligand in metal complexes. However, there is no sharp division between intercalators and insertors in size, which means most of the metal complexes can serve as intercalators and insertors at the same time. For instance, Barton reported that Rh(bpy)$_2$(phi)]$^{3+}$ (phi = 5,6-phenanthrolinediimine) almost did not exhibit any mismatch-specificity, whereas when the phi ligand was replaced by chrysi ligand

(chrysi = 5,6-chrysenediimine), the compound [Rh(bpy)$_2$(chrysi)]$^{3+}$ turned out to be highly selective, it bounds mismatches 1000 times tighter than matched DNA base pairs.[56,57] Analogously, Dr. Xiang's thesis also showed that octahedral silicon complexes with sterically proper aromatic ligands such as [Si(bpy)$_2$(5,6-chrysenediolate)](PF$_6$)$_2$ **99** could be used as DNA mismatched base pair detectors.

To further understand the interaction between silicon complexes with duplex DNA, our investigation were focused on these silicon pyrenediolate complexes (**96~98**) and the related silicon-ruthenium sandwich complexes (**108~110**).
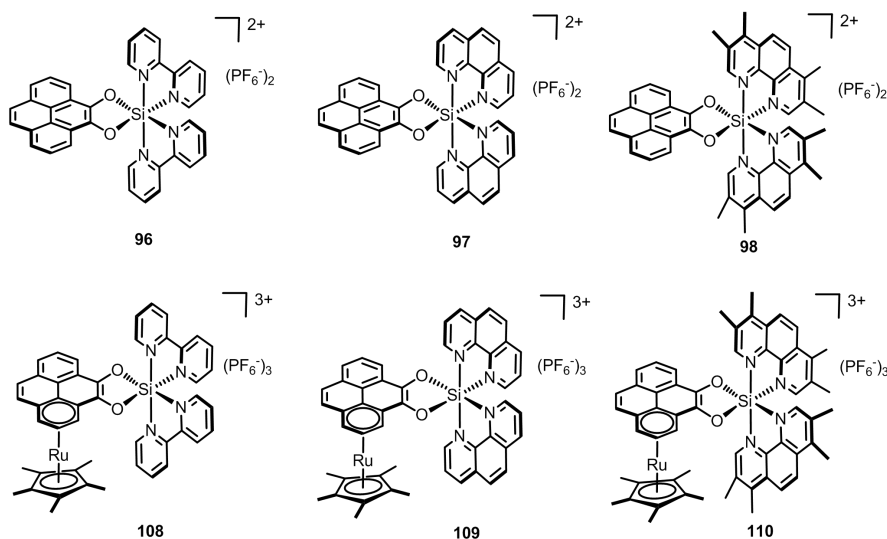
Firstly, we studied the influence of these two sets of complexes **96~98** and **108~110** on the thermal stability of matched-DNA duplex, thereby we monitored the melting temperature of a mixed-sequence of 19mer oligonucleotides (5′-GCTCGTCAT**C**GCTAGAGCA-3′ / 3′-CGAGCAGTA**G**CGATCTCGT-5′) (2μM) in the presence of equal equivalent of complexes (**96~98** and **108~110**) by temperature-dependent UV spectroscopy at 260 nm.

As the results shown in Figure 47, complexes **96~98** slightly stabilized of the duplexes, with the ΔT_m = +2.0 ^{o}C (**96**), ΔT_m = +3.0 ^{o}C (**97**) and ΔT_m = +1.1 ^{o}C (**98**), which is in line with our expectation. However, complexes **108~110** did not show any effect on the melting of matched DNA duplex, we assumed that the pyrenediolate ligand with the coordinated [Ru(Cp*)]$^{2+}$ fragment is too bulky to enter two intact base

pairs *via* the major groove.
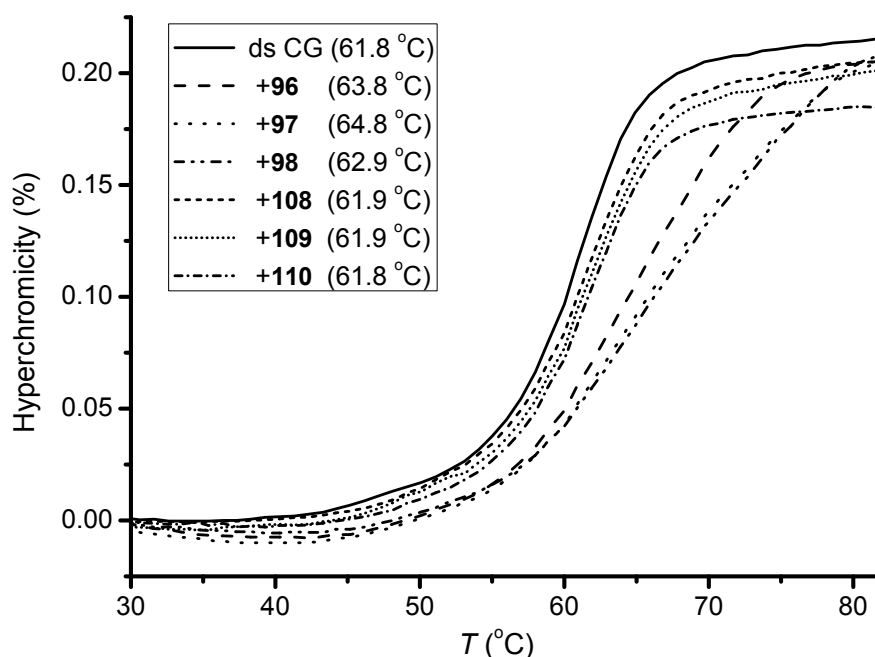
Figure 47. UV-melting curves of (λ = 260 nm) of duplex DNA 5-GCTCGTCATCGCTAGAGCA-3′ / 3-CGAGCAGTAGCGATCTCGT-5′(2μM) in Tris-HCl (5 mM, pH 7.4) with NaCl (50 mM) and in the presence of 1.0 equiv silicon complexes **96**~**98** and **108**~**110**. T_m are average values determined from three independent experiments.

Next, we also investigated the influence of these two set of complexes on the thermal stability of mismatched DNA duplexes, the same mixed-sequences of 19mer oligonucleotides with a CG base pair replaced by CC, CA and CT respectively. Complexes **96** and **97** stabilized mismatched DNA duplexes, the results are shown in Table 4. Surprisingly complexes **108** and **109** can significantly stabilize mismatched DNA duplexes that contain CC {ΔT_m = +7.3 °C (**108**), ΔT_m = +7.2 °C (**109**)} and CT {ΔT_m = +6.8 °C (**108**), ΔT_m = +7.2 °C (**109**)} mismatch, the melting curves of mismatched DNA in the presence of **109** are shown in Figure 49. However, both complex **108** and **109** showed a much weaker stabilization for CA mismatch, and complex **110** and **98** almost did not present any binding effect on matched or mismatched DNA because of steric hindrance caused by bulky ligands.

Table 4. UV-melting points (°C) of 19mer matched (**CG**) and mismatched (**CC**, **CA**, **CT**) DNA duplexes in the absence and presence of one equivalent of silicon complexes **96~98** or ruthenium-silicon hybrids **108~110**.[a]

```
5'—G—C—T—C—G—T—C—A—T⎥ C ⎢G—C—T—A—G—A—G—C—A—3'
    |  |  |  |  |  |  |  |  | ⎥   ⎢ |  |  |  |  |  |  |  |  |
3'—C—G—A—G—C—A—G—T—A⎥ X ⎢C—G—A—T—C—T—C—G—T—5'
```

DNA	T_m (°C)	96	97	98	108	109	110
CG	61.8	63.8	64.8	62.9	61.9	61.9	61.8
		(+2.0)	(+3.0)	(+1.1)	(+0.1)	(+0.1)	(-)
CC	51.0	56.3	53.7	51.0	58.3	58.2	51.1
		(+5.3)	(+2.7)	(-)	(+7.3)	(+7.2)	(+0.1)
CA	53.3	55.4	56.2	53.4	56.3	53.4	53.7
		(+2.1)	(+2.9)	(+0.1)	(+3.0)	(+0.1)	(+0.4)
CT	50.5	52.1	51.2	50.6	57.3	57.7	50.9
		(+1.6)	(+0.7)	(+0.1)	(+6.8)	(+7.2)	(+0.4)

[a] Changes in UV absorbance upon heating as monitored at 260 nm. Conditions: 5 mM Tris-HCl, 50 mM NaCl, pH 7.4, and 2 μM of each strand. T_m were determined from three independent experiments and the mean values were taken.   G = guanine, A = adenine, C = cytosine, and T = thymine.

Looking back to the structure of the silicon-ruthenium complex **109**, we found that the distance from the pyrenediolate plane to the Cp* plane is around 3.5 Å, which is similar to the distance between stacked base pairs—3.4 Å. In addition, as the geometries shown in Figure 48, the whole ruthenium-coordinated fragment is 8.7 Å wide that is smaller than the width of minor groove (12 Å), and its length is close to the reported metallo-intercalators or metallo-insertors (6.3 Å).[10] Taken together, we proposed that these silicon-ruthenium complexes ejected the mismatch and a neighboring base pair *via* the minor groove, in a similar manner as metallo-insertors, and acted as a π-stacking replacement in the DNA base stack.

Figure 48. Geometries of silicon-ruthenium compound **109**.
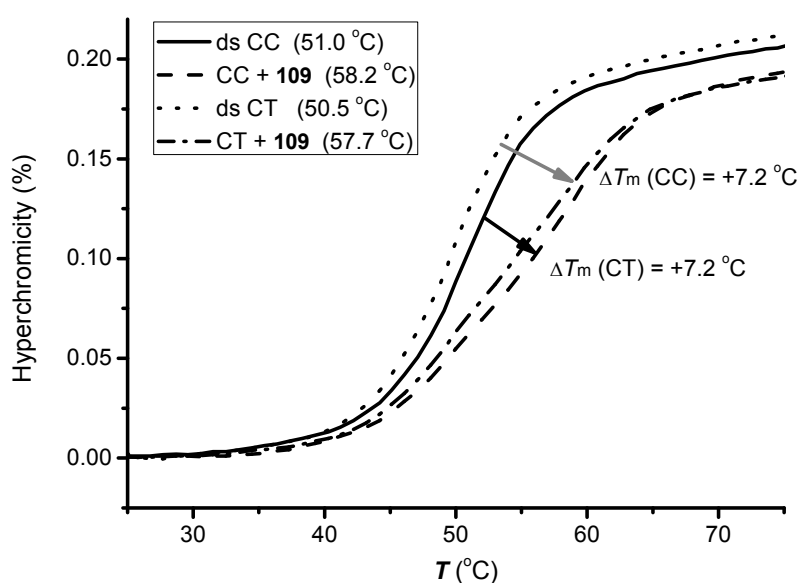
Figure 49. UV-melting curves of 2 μM 19mer oligonucleotides **CC** and **CT** in Tris-HCl (5 mM, pH 7.4) with NaCl (50 mM) and in the presence of 1.0 equiv **109**.

In a proof-of-principle study, the hydrolytically stable silicon-ruthenium sandwich complexes have shown that they could serve as DNA mismatch stabilizers. However, we faced the same problem as other nucleic acid research groups, which is the limited availability of characterization about the resulting assemblies and the attempted DNA crystallization efforts failed.

Chapter 4 Summary and Outlook

I. Asymmetric Synthesis of Octahedral Ruthenium Complexes

We found that natural amino acid L-proline can be used as an efficient auxiliary for the asymmetric synthesis of mononuclear polypyridyl ruthenium(II) complexes [Ru(pp)(pp')(pp'')]$(PF_6)_2$, as shown in Scheme 37. Since the synthesis of disclosed chiral auxiliaries is lengthy and expensive, and L-proline is readily available and cheap, L-proline is superior to these previous auxiliaries for certain reaction. Furthermore, it can be easily applied to a large-scale (gram level) synthesis of enantiopure mononuclear polypyridyl ruthenium(II) complexes.
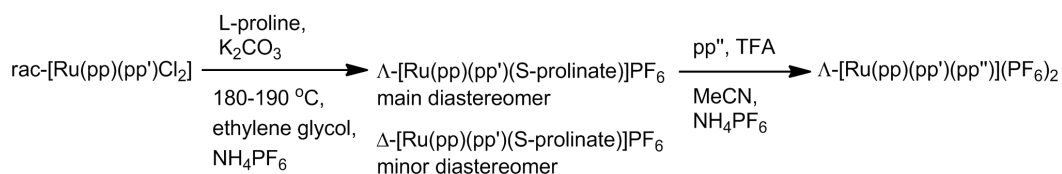
PP, PP' = bpy, dmb,dbb, phen, biq;

Scheme 37. Asymmetric synthesis of mononuclear polypyridyl ruthenium (II) complexes [Ru(pp)(pp')(pp'')]$(PF_6)_2$ mediated by L-proline.

We thereby proposed the mechanism of the diastereoselective reaction, from starting *rac*-[Ru(pp)(pp')Cl$_2$] to Λ-[Ru(pp)(pp')(*S*-prolinate)]PF$_6$, proceeding through a dynamic resolution under thermodynamic control: Both diastereomers Δ-(*S*) and Λ-(*S*) are initially formed, but under the optimized high temperature reaction conditions, the diastereomer Δ-(*S*) is unstable and reversibly releases the proline ligand to form related Δ-intermediate. Δ and Λ-intermediates are in an equilibrium with each other, thus the unstable and reversibly formed diastereomer Δ-(*S*) can convert to the thermodynamically more stable diastereomer Λ-(*S*) *via* the equilibrium (Scheme 38). This mechanism was further supported by an exemplified experiment, in which we heated the minor diastereomer Δ-(*S*)-**61** in ethylene glycol at 190 °C under argon for 10 min and found a conversion from Δ-(*S*)-**61** to the major diastereomer Λ-(*S*)-**61** with an isolated yield of 60%.
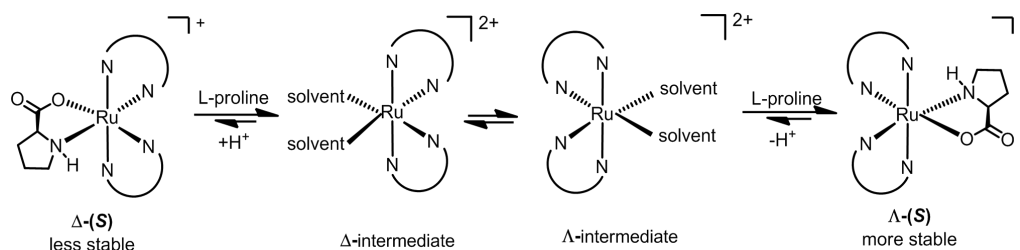
Scheme 38. Proposed mechanism of the diastereoselective synthesis of complex Λ-(*S*) *via* dynamic resolution under thermodynamic control.

Furthermore, we made a preliminary investigation about the asymmetric synthesis of dinuclear octahedral ruthenium(II) complexes, and obtained an enantiomerically enriched dinuclear complex **79** with a ratio of (Λ, Λ) to (Δ, Δ) around 3 : 1 (Scheme 39). On the basis of ^{1}H-NMR spectrum and X-ray crystallographic analysis, it can be concluded that only one diastereomer (two enantiomers) existed in the dinuclear complex **79**. We therefore assumed that the strategy we predesigned transferring chirality from one metal center to the other metal center through steric repulsion between the ligands on both metal centers was feasible. We were not able to get the dinuclear complex **79** with a higher ee might due to racemization of initially formed enantiopure complex **79**.
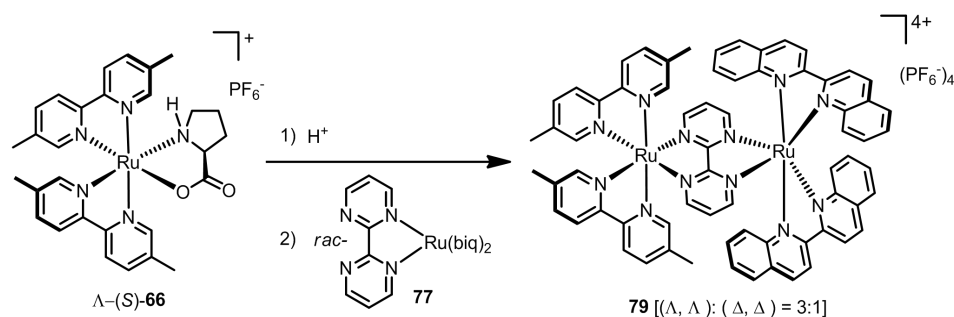
Scheme 39. Asymmetric synthesis of dinuclear octahedral ruthenium(II) complex **79**.

However, all the successful examples for asymmetric synthesis of [Ru(pp)(pp')(pp'')](PF$_6$)$_2$ to date are limited to the polypyridyl (pp) ligands in small size (such as bpy and phen), but for bulky ligands (such as biq), all the existing methods could not offer ideal results. Thus, we should continue to explore more auxiliaries to enrich the asymmetric synthesis toolbox in the future. Apparently, the sole steric repulsion is not enough to effciently control the stereochemistry. We expect

that the enantiopurity of the dinuclear ruthenium complex might be improved by introducing more controlling factors, such as a modification of the ligands with some electron withdrawing/donating groups or H-bonding et al.. If possible, we should develop a highly reactive auxiliary that can make the formation of dinuclear complexes be carried out at low temperature, resulting in less racemization.

II. Synthesis and Biological Activities of Octahedral Silicon Complexes

We have successfully synthesized silicon complexes with arenediolate ligands (**86~89**, **96~100**), silicon complexes with diaminate ligand (**102~104**), enantiopure silicon *R*-BINOLate complexes {Λ-(*R*)-**105**, Λ-(*R*)-**106**}, and silicon-ruthenium sandwich complexes (**108-110**) (Scheme 40). All these silicon complexes were proved be stable, and no signs of any decomposition from the complexes can be detected by ^{1}H-NMR in more than one week at room temperature.
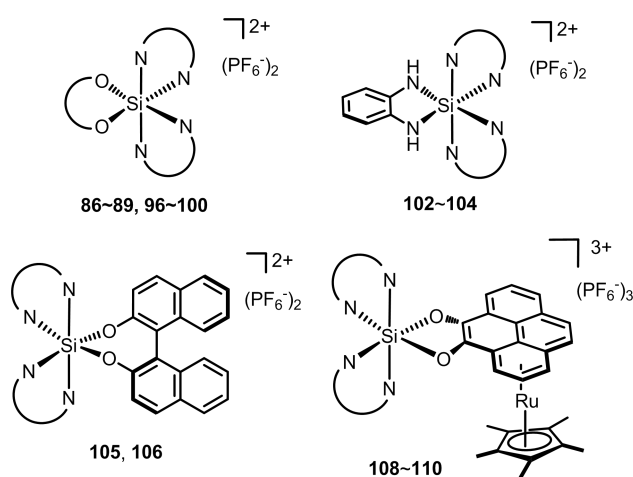
Scheme 40. Structures of the synthesized octahedral silicon complexes.

Firstly, we investigated the interaction between silicon arenediolate complexes and duplex DNA, and found that complexes (**87**, **89**, **97** and **100**) with different polyaromatic π-systems obviously altered the melting temperature of the DNA duplex on different levels {ΔT_m = +1.0 °C (**87**), ΔT_m = +19.3 °C (**97**), ΔT_m = +5.6 °C (**100**)}. Taking silicon complex **89** as an example, the strong thermal stabilization (ΔT_m = + 11.5 °C) of duplex DNA, together with the modulation of the secondary structure as observed by CD spectroscopy, all indicate an intercalative binding between the silicon

compound and DNA duplex.

We next studied the interaction between bulky silicon-ruthenium sandwich complexes (**108~110**) and mismatched DNA duplexes, and found that **108** and **109** can significantly stabilize mismatched DNA duplexes that contain CC {$\Delta T_m = +7.3$ ^oC (**108**), $\Delta T_m = +7.2$ ^oC (**109**)} and CT {$\Delta T_m = +6.8$ ^oC (**108**), $\Delta T_m = +7.2$ ^oC (**109**)} mismatch. We assumed that these silicon-ruthenium complexes ejected the mismatch and a neighboring base pair, in a similar manner as metallo-insertors, and acted as a π-stacking replacement in the DNA base stack.

In conclusion, we presented the first examples of designed biologically active complexes based on octahedral silicon. In a proof-of-principle study, using the example of classical metallo-intercalators, we demonstrated that structural transition metals can be replaced by inert octahedral silicon. For the sole purpose of providing a structural octahedral center, the metalloid silicon may possess several advantages over transition metals, such as low price, unlimited availability as the second most abundant element in the Earth's crust and lack of toxic concerns et al.. However, we faced the same problem as other nucleic acid research groups, the limited methods that can be used for characterization. In order to further understand the interaction between the silicon complexes and duplex DNA, we will try to grow a single crystal of duplex DNA with related silicon complex or modify the ligands by introducing an fluorescent group to the system, which may help us to confirm the results.

Chapter 5 Experimental part

5.1 Materials and Methods

Solvents and Reagents

All reactions were carried out under nitrogen or argon atmosphere and the reactions involving chiral ruthenium complexes were performed in the dark. Solvents were distilled under nitrogen from calcium hydride (CH_3CN, $CHCl_3$, CH_2Cl_2 and DMF) or sodium/benzophenone (Et_2O, THF). HPLC grade solvents, such as chlorobenzene, 1,2-dichloroethane, ethanol, acetone and toluene were used directly without further drying. All reagents were purchased from Acros, Aldrich, Alfa, Strem and Fluorochem and used without further purification. Metal precursors, the racemic *cis*-[Ru(bpy)$_2$Cl$_2$] (bpy = 2,2'-bipyridine), *cis*-[Ru(phen)$_2$Cl$_2$] (phen = 1,10-phenanthroline), *cis*-[Ru(biq)$_2$Cl$_2$] (biq = 2,2'-biquinoline), *cis*-[Ru(dmb)$_2$Cl$_2$](dmb = 5,5'-dimethyl-2,2'-bipyridine), and *cis*-[Ru(bpy)(dmb)Cl$_2$] were prepared according to the published procedures.[85]

Chromatographic Methods

The course of the reactions and the column chromatographic elutions were traced by thin layer chromatography [Macherey-Nagel (ALUGRAM®Xtra Sil G/UV254) or Merck (aluminum silica gel 60 F254)] with fluorescent indicator UV254 or color developing agent (cerium sulfate / ammonium molybdate solution). For column chromatography silica gel, Merck (particle size 0.040-0.063 mm) was used. The elution was performed at room temperature using a compressed air overpressure. The corresponding mobile phase was specified in the followed procedure. If substance showed poor solubility in eluent solvent, the crude product was firstly absorbed by proper amount of coarse silica gel, and then the adsorbed gel was subjected to the silica gel chromatographic column.

Nuclear Magnetic Resonance Spectroscopy (NMR)

Bruker Advance 300 MHz (^{1}H-NMR: 300 MHz, ^{13}C-NMR: 75 MHz)

Bruker DRX 400 MHz (^{1}H-NMR: 400 MHz, ^{13}C-NMR: 100 MHz)

Bruker AM 500 MHz (^{1}H-NMR: 500 MHz, ^{13}C-NMR: 125 MHz)

In the experiments, the spectroscopic NMR data are given as follows: "(MHz, deuterated solvent): δ (ppm)". According to the literature by Fulmer et al,[86] NMR standards used are as follows: (^{1}H-NMR) CD_3CN = 1.94 ppm, $CDCl_3$ = 7.26 ppm, CD_3COCD_3 = 2.05 ppm, CD_3SOCD_3 = 2.50 ppm; (^{13}C-NMR) CD_3CN = 1.32 ppm, $CDCl_3$ = 77.16 ppm, CD_3COCD_3 = 206.26, 29.84 ppm, CD_3SOCD_3 = 39.52 ppm. The characteristic signals were specified from the low field to high-field with the chemical shifts (δ in ppm). ^{1}H-NMR spectra peak multiplicities indicated as singlet (s), doublet (d), doublet of doublet (dd), doublet of doublet of doublet (ddd), triplet (t), doublet of triplet (dt), quartet (q), multiplet (m).The coupling constant J indicated in hertz (Hz). And ^{1}H-NMR spectra peak also show the number of protons.

High-Performance Liquid Chromatography (HPLC)

Chiral HPLC was performed with an Agilent 1200 Series HPLC System. All the compounds in the thesis were detected by UV at λ = 254 nm. The flow rate was 0.5 mL/min. The injection was 1~2 μL for 2 mM solutions. Y-axis range was adjusted to 100~300 mAu. The corresponding mobile phase and the type of the columns were specified in the individual procedures.

Infrared Spectroscopy (IR)

IR measurements were recorded on a Bruker Alpha-P FT-IR spectrometer. The absorption bands were indicated a wave numbers v (cm^{-1}). All substances were measured as films or solids. For films, the substances were dissolved in DCM or MeCN or suspended and the solution applied to the device. The samples were measured only after complete evaporation of the solvent.

Circular Dichroism Spectroscopy (CD)

CD spectra were recorded on a JASCO J-810 CD spectropolarimeter. The parameters we used as follows: from 600 nm to 200 nm; data pitch (0.5 nm); band with (1 nm); response (1 second); sensitivity (standard); scanning speed (50 nm/min); accumulation (5 times). The concentration of the compounds for the measurements was 0.1 mM (metal and silicon complexes) and 1 mM (organic compounds).The formula for converting θ to ε is shown in the Figure 50.[87]

$$\Delta\varepsilon = \frac{\theta\ [\text{mdeg}]}{32980 \times c(\text{mol/L}) \times L(\text{cm})}$$

c: concetration of the sample

L: thickness of the measurement vessel

Figure 50. Formula for converting θ to ε.

Crystal Structure Analysis

Crystal X-ray measurements and the crystal structure analysis were carried out by Dr. Klaus Harms (Chemistry Department, Philipps University of Marburg) on the devices IPDS-II (Mo-Kα-irradiation, bis $2\theta = 77°$, Oxford Cryosystem) or IPDS-IIT (Mo-Kα-irradiation, bis $2\theta = 135°$, Oxford Cryosystem). The solution and refinement of the structures were carried with the corresponding programs. Details of crystal structures can be found in the Appendix.

Thermal Denaturation

The melting studies were carried out in 1 cm path length quartz cells (total volume 325 μL; 200 μL sample solutions were covered by mineral oil) on a Beckman 800 UV/Vis-absorption spectrophotometer equipped with a thermo-programmer. Melting curves were monitored at 260 nm with a heating rate of 1 °C/min. Melting temperatures were calculated from the first derivatives of the heating curves. Experiments were performed in duplicate and mean values were taken.

80

5.2 Asymmetric Synthesis of Octahedral Ruthenium(II) Complexes

5.2.1 Synthesis of Mononuclear Ruthenium Complexes
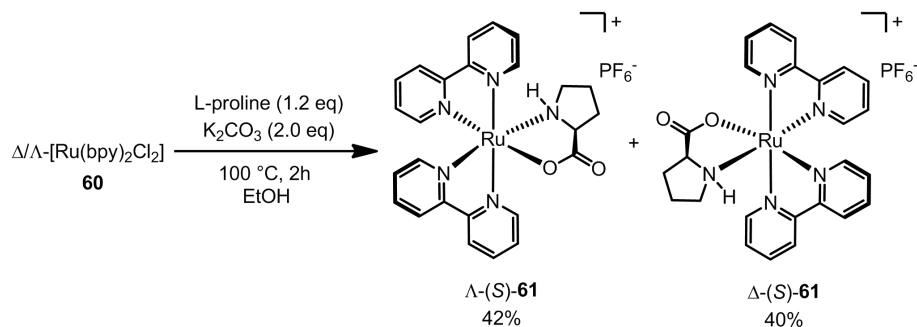
Mixture of diastereomers Λ-/Δ-(*S*)-61. In a closed brown vial (10 mL) fitted with a septum, a solution of *cis*-[Ru(bpy)$_2$Cl$_2$] (100 mg, 0.192 mmol), L-proline (27 mg, 0.230 mmol), and K$_2$CO$_3$ (53 mg, 0.384 mmol) in EtOH (3.8 mL) was degassed with argon for 5 min and then heated at 100 °C (oil bath temperature) for 2 h. The resulting mixture was cooled to room temperature, dried *in vacuo*, then the residue was dissolved in CH$_3$CN (2 mL) and subjected to silica gel chromatography (eluent : CH$_3$CN, CH$_3$CN : H$_2$O = 10 : 1, CH$_3$CN : H$_2$O : KNO$_3$ (sat) = 100 : 3 : 1, CH$_3$CN : H$_2$O : KNO$_3$ (sat) = 50 : 3 : 1). There were two separated purple-red bands can be seen in the column, the first (faster moving) one was assigned as Λ-(*S*)-61 while the second (slower moving) one was assigned as Δ-(*S*)-61. Assignment was based on the combination of X-ray crystallography and CD spectra of the resulting two compounds from the related bands (Figure 51). The first fraction was concentrated to dryness and then redissolved in nearly 15 mL water, the purple-red solution was subsequently precipitated by the addition of excess solid NH$_4$PF$_6$ until the solution turned colorless. The dark-red suspended solid was collected, dissolved in CH$_2$Cl$_2$ (15 mL), and the organic phase was washed with water twice (2 × 5 mL), dried under high vacuum to afford Λ-(*S*)-61 (deep-purple solid, 56 mg, 43%) as a single diastereomer. Analogously, Δ-(*S*)-61 (deep-purple solid, 45 mg, 35%) was obtained from the second

fraction through the same procedures.

Λ-(*S*)-**61:** ^{1}H-NMR (300 MHz, CD$_3$CN): δ (ppm) 9.16 (ddd, *J* = 5.7, 1.3, 0.8 Hz, 1H), 9.06 (ddd, *J* = 5.6, 1.5, 0.8 Hz, 1H), 8.49 (ddd, *J* = 8.2, 1.3, 0.7 Hz, 1H), 8.46 (d, *J* = 8.0 Hz, 1H), 8.33 (ddd, *J* = 3.2, 1.2, 0.8 Hz, 1H), 8.31 (ddd, *J* = 3.3, 1.2, 0.8 Hz, 1H), 8.14 (ddd, *J* = 8.8, 7.6, 1.7 Hz, 1H), 8.09 (ddd, *J* = 8.8, 7.5, 1.5 Hz, 1H), 7.97 (ddd, *J* = 5.8, 1.5, 0.9 Hz, 1H), 7.78 (ddd, *J* = 7.6, 5.6, 1.3 Hz, 1H), 7.75 (m, 3H), 7.36 (ddd, *J* = 5.9, 1.5, 0.7 Hz, 1H), 7.12 (m, 2H), 4.96 (dd, *J* = 14.5, 8.0 Hz, 1H), 3.90 (td, *J* = 13.4, 7.1 Hz, 1H), 2.21 (m, 1H), 2.08 (m, 1H), 1.80 (m, 1H), 1.43 (m, 3H). ^{13}C-NMR (75 MHz, CD$_3$CN): δ (ppm) 182.9, 160.3, 159.66, 159.65, 159.1, 155.0, 152.9, 152.8, 151.5, 137.14, 137.12, 136.0, 135.4, 128.3, 127.6, 126.7, 126.5, 124.6, 124.5, 124.4, 124.2, 64.3, 50.3, 30.6, 27.2. IR (neat): *v* (cm^{-1}) 3645, 2961, 2922, 1597, 1462, 1444, 1420, 1368, 1318, 1262, 1160, 1104, 1064, 1019, 929, 830, 759, 729, 657, 555, 423. CD (Δε/M^{-1}cm^{-1}, MeCN): 282.5 nm (-72), 297 nm (+203). HRMS calcd for C$_{25}$H$_{24}$N$_5$O$_2$Ru (M-PF$_6$)$^+$: 528.0975, found: 528.0963.
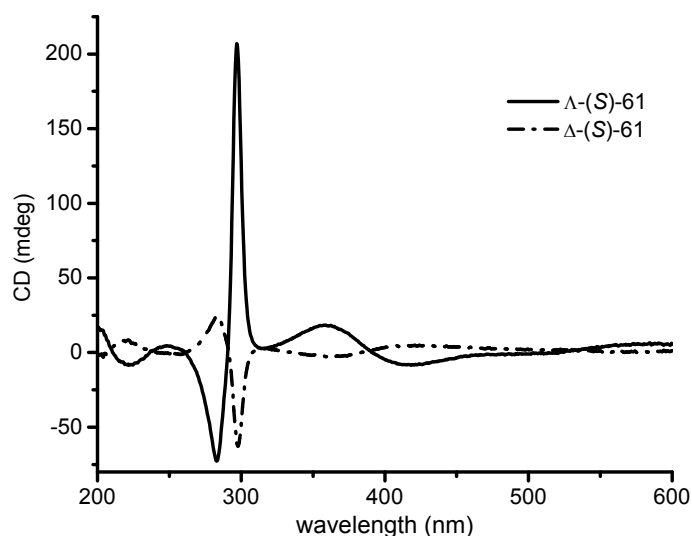
Figure 51. CD spectra of compounds Λ-(*S*)-**61** and Δ-(*S*)-**61** in CH$_3$CN (0.1 mM).

Δ-(*S*)-**61:** ^{1}H-NMR (300 MHz, CD$_3$CN): δ (ppm) 9.17 (d, *J* = 5.3 Hz, 1H), 8.97 (ddd, *J* = 5.6, 1.4, 0.7 Hz, 1H), 8.50 (dt, *J* = 8.1, 1.2 Hz, 1H), 8.45 (d, *J* = 7.7 Hz, 1H), 8.31 (m, 2H), 8.16 (ddd, *J* = 8.1, 7.6, 1.5 Hz, 1H), 8.09 (ddd, *J* = 8.1, 7.6, 1.4 Hz, 1H), 7.99 (ddd, *J* = 5.7, 1.3, 0.7 Hz, 1H), 7.75 (m, 4H), 7.37 (ddd, *J* = 5.7, 1.3, 0.7 Hz, 1H), 7.09

(m, 2H), 4.15 (dd, J = 16.4, 8.0 Hz, 1H), 3.56 (m, 1H), 3.00 (m, 1H), 2.78 (m, 1H), 2.05 (m, 1H), 1.69 (m, 3H). ^{13}C-NMR (75 MHz, CD$_3$CN): δ (ppm) 182.8, 160.7, 160.2, 159.8, 159.6, 154.9, 153.8, 153.0, 152.2, 137.8, 136.1, 135.5, 128.3, 127.5, 126.9, 126.4, 124.8, 124.4, 124.1, 65.1, 52.3, 31.0, 27.2. IR (neat): v (cm^{-1}) 3645, 3192, 1596, 1462, 1444, 1420, 1368, 1318, 1262, 1160, 1105, 1064, 1019, 929, 830, 759, 729, 657, 555, 423. CD ($\Delta\varepsilon$/M^{-1}cm^{-1}, MeCN): 282 nm (+54), 296.5 nm (-143). HRMS calcd for C$_{25}$H$_{24}$N$_5$O$_2$Ru (M-PF$_6$)$^+$: 528.0975, found: 528.0973.
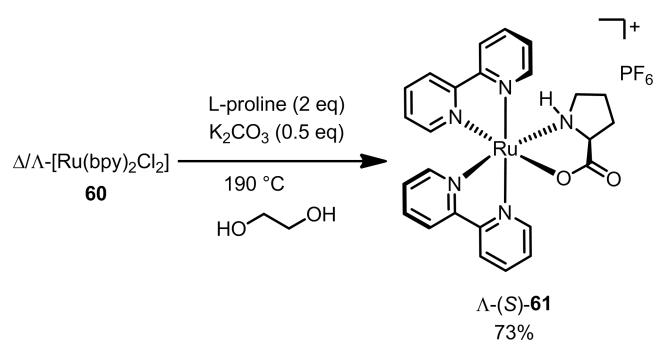
Single diastereomer Λ-(S)-61. In a closed brown vial (10 mL) fitted with a septum, a solution of *cis*-[Ru(bpy)$_2$Cl$_2$] (260 mg, 0.5 mmol), L-proline (115 mg, 1.0 mmol), and K$_2$CO$_3$ (34.5 mg, 0.25 mmol) in ethylene glycol (2.5 mL) was degassed with argon for 5 min and then heated at 190 °C (oil bath temperature) for 3.5 min. In order to get rid of the most ethylene glycol and make the subsequent purification easier, 25 mL water was added to the reaction mixture after it was cooled to room temperature, then the deep red solution was precipitated by the addition of excess solid NH$_4$PF$_6$. The dark suspended solid (crude product) was collected, dissolved in CH$_3$CN (5 mL) and subjected to silica gel chromatography (eluent : CH$_3$CN, CH$_3$CN : H$_2$O = 10 : 1, CH$_3$CN : H$_2$O : KNO$_3$ (sat) = 100 : 3 : 1, CH$_3$CN : H$_2$O : KNO$_3$ (sat) = 50 : 3 : 1). The product eluents were concentrated and redissolved in nearly 20 mL water, and the product was precipitated by the addition of excess solid NH$_4$PF$_6$ again. The suspension was extracted with CH$_2$Cl$_2$ twice (2 × 30 mL), and the combined organic extracts were dried (Na$_2$SO$_4$), filtered, concentrated and dried under high vacuum to afford Λ-(S)-61 (250 mg, 73%) as a single diastereomer.

Thermal conversion of Δ-(*S*)-61 into Λ-(*S*)-61. In a closed brown vial (1 mL) fitted with a septum, a solution of Δ-(*S*)-**61** (10 mg, 0.015 mmol), L-proline (17.3 mg, 0.150 mmol) in ethylene glycol (0.15 mL) was degassed with argon for 5 min and then heated at 190 °C (oil bath temperature) for 20 min. The reaction mixture was cooled to room temperature and subjected to silica gel chromatography (eluent : CH₃CN, CH₃CN : H₂O : KNO₃ (sat) = 40 : 3 : 1). The dark-purple eluents were concentrated and redissolved in nearly 10 mL water, and the product was precipitated by the addition of excess solid NH₄PF₆. The suspension was extracted with CH₂Cl₂ twice (2 × 10 mL), and the combined organic extracts were dried (Na₂SO₄), filtered, concentrated and dried under high vacuum to afford Λ-(*S*)-**61** as a single diastereomer (8.2 mg, 82%).
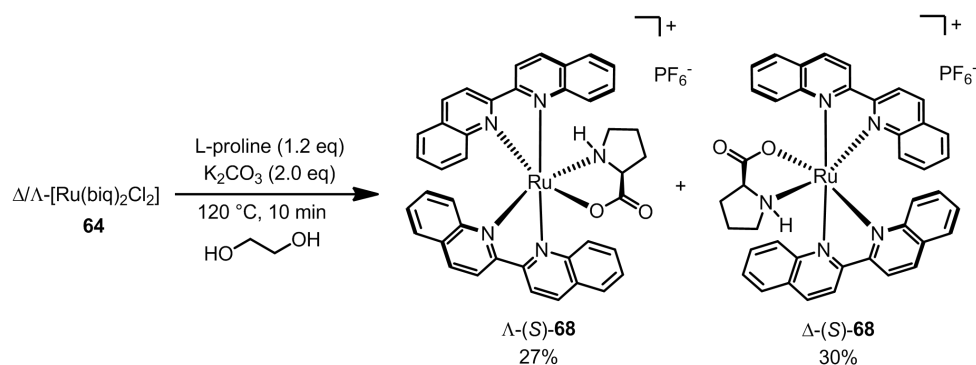
Mixture of diastereomers Λ-/Δ-(*S*)-68. In a closed brown vial (5 mL) fitted with a septum, a solution of *cis*-[Ru(biq)₂Cl₂] **64** (80 mg, 0.11 mmol), L-proline (25.6 mg, 0.22 mmol), and K₂CO₃ (7.6 mg, 0.056mmol) in ethylene glycol (2.2 mL) was degassed with argon for 5 min and then heated at 120 °C (oil bath temperature) for 10 min. In order to get rid of the most ethylene glycol and make the subsequent purification easier, 20 mL water was added to the reaction mixture after it was cooled to room temperature, then the deep-blue solution was precipitated by the addition of excess solid NH₄PF₆. The dark blue suspended solid (crude product) was collected, dissolved in CH₃CN (3 mL) and subjected to silica gel chromatography (eluent : CH₃CN, CH₃CN : H₂O : KNO₃ (sat) = 200 : 3 : 1, CH₃CN : H₂O : KNO₃ (sat) = 100 : 3 : 1). There were two separated deep-blue bands can be seen in the column, first deep-blue fraction was assigned as Δ-(*S*)-**68** and the second deep-blue fraction was assigned as Λ-(*S*)-**68**, based on a comparison of theirs CD spectra with the CD spectra

of Λ-/Δ-(*S*)-**61** (Figure 52). The first fraction was concentrated and dissolved in a mixture of H_2O/EtOH (10 mL/1 mL), and the product was precipitated by the addition of excess solid NH_4PF_6. The precipitate was collected, washed twice with water (2 × 5 mL) and dried under high vacuum to afford Δ-(*S*)-**68** (deep-blue solid, 29 mg, 30%) as a single diastereomer, while Λ-(*S*)-**68** (deep-blue solid, 23 mg, 27%) was obtained by the same procedures.

Λ-(*S*)-**68:** ^{1}H-NMR (300 MHz, CD$_3$CN): *δ* (ppm) 8.78 (m, 6H), 8.58 (d, *J* = 8.8 Hz, 1H), 8.53 (d, *J* = 8.8 Hz, 1H), 8.16 (d, *J* = 8.1 Hz, 1H), 8.03 (ddd, *J* = 7.0, 2.6, 1.2 Hz, 2H), 7.85 (dd, *J* = 8.1, 0.8 Hz, 1H), 7.64 (ddd, *J* = 8.1, 5.0, 3.0 Hz, 1H), 7.54 (m, 2H), 7.40 (ddd, *J* = 8.0, 7.0, 0.9 Hz, 1H), 7.32 (m, 2H), 7.20 (m, 2H), 7.04 (d, *J* = 8.8 Hz, 1H), 6.82 (ddd, *J* = 8.8, 7.0, 1.4 Hz, 1H), 6.66 (ddd, *J* = 8.8, 6.9, 1.4 Hz, 1H), 6.05 (d, *J* = 8.8 Hz, 1H), 4.13 (m, 1H), 2.32 (m, 2H), 1.34 (m, 1H), 1.17 (m, 2H), 1.00 (m, 1H), 0.43 (dq, *J* = 11.5, 5.3 Hz, 1H). ^{13}C-NMR (75 MHz, CD$_3$CN): *δ* (ppm) 180.7, 163.8, 163.2, 163.0, 161.7, 153.2, 153.0, 151.9, 151.5 139.0, 138.9, 137.1, 136.4, 133.2, 131.91, 131.85, 131.4, 131.2, 129.8, 129.73, 129.67, 129.63, 129.61, 129.4, 129.1, 128.7, 128.5, 128.2, 127.9, 126.1, 125.2, 122.4, 122.0, 121.84, 121.75, 64.2, 49.5, 28.4, 25.2. IR (neat): *v* (cm^{-1}) 3640, 3322, 1595, 1509, 1429, 1367, 1302, 1247, 1147, 1098, 964, 812, 748, 635, 555, 488, 431. CD (Δε/M^{-1}cm^{-1}, MeCN): 256 nm (-81), 270 nm (+104), 324 nm (-48), 349 nm (+127). HRMS calcd for $C_{41}H_{32}N_5O_2Ru$ (M-PF$_6$)$^+$: 728.1605, found: 728.1588.
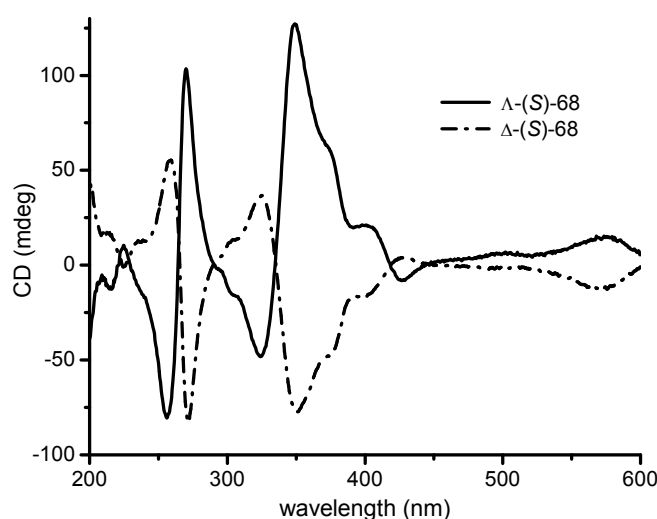
Figure 52. CD spectra of compounds Λ-(*S*)-**68** and Δ-(*S*)-**68** in CH$_3$CN (0.1 mM).

Δ-(*S*)-**68**: ^{1}H-NMR (300 MHz, CD$_3$CN): δ (ppm) 8.77 (m, 5H), 8.68 (d, *J* = 8.8 Hz, 1H), 8.57 (d, *J* = 5.4 Hz, 1H), 8.55 (d, *J* = 5.2 Hz, 1H), 8.08 (dd, *J* = 8.1, 1.2 Hz, 1H), 8.04 (dt, *J* = 7.4, 1.2 Hz, 2H), 7.83 (dd, *J* = 8.1, 1.2 Hz, 1H), 7.59 (ddd, *J* = 8.2, 6.9, 1.1 Hz, 1H), 7.52 (ddd, *J* = 8.2, 6.8, 1.2 Hz, 1H), 7.39 (ddd, *J* = 8.1, 6.9, 1.1 Hz, 1H), 7.28 (d, *J* = 8.2 Hz, 1H), 7.16 (m, 3H), 7.10 (ddd, *J* = 8.3, 6.9, 1.4 Hz, 1H), 6.97 (d, *J* = 8.9 Hz, 1H), 6.74 (ddd, *J* = 8.8, 7.2, 1.4 Hz, 1H), 6.58 (ddd, *J* = 8.9, 7.2, 1.4 Hz, 1H), 5.83 (d, *J* = 8.8 Hz, 1H), 2.71 (m, 1H), 2.52 (m, 1H), 2.10 (m, 1H), 1.39 (m, 1H), 1.29 (m, 1H), 1.21 (m, 3H). ^{13}C-NMR (75 MHz, CD$_3$CN): δ (ppm) 180.1, 163.4, 162.9, 162.4, 161.0, 153.2, 152.4, 151.4, 150.8, 139.4, 138.2, 137.6, 135.5, 132.0, 131.7, 131.5, 130.8, 130.01, 130.00, 129.9, 129.7, 129.7, 129.42, 129.35, 129.0, 128.81, 128.79, 128.5, 128.2, 126.3, 125.9, 123.3, 123.1, 121.7, 121.5, 68.4, 54.7, 27.8, 25.4. IR (neat): v (cm^{-1}) 3641, 3321, 2925, 1627, 1595, 1509, 1452, 1363, 1279, 1247, 1213, 1147, 1097, 963, 835, 811, 778, 748, 634, 556, 515, 488, 436. CD ($\Delta\varepsilon$/M^{-1}cm^{-1}, MeCN): 259 nm (+55), 271.5 nm (-83), 325 nm (+37), 350 nm (-77). HRMS calcd for C$_{41}$H$_{32}$N$_5$O$_2$Ru (M-PF$_6$)$^+$: 728.1605, found: 728.1599.
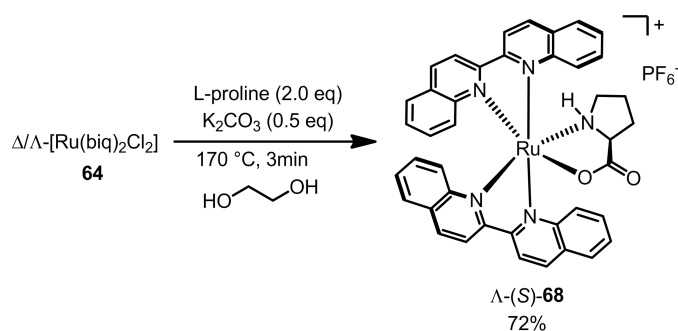
Single diastereomer Λ-(*S*)-68. In a closed brown vial (5 mL) fitted with a septum, a solution of *cis*-[Ru(biq)$_2$Cl$_2$] (200 mg, 0.278 mmol), (*L*)-proline (64 mg, 0.555 mmol), and K$_2$CO$_3$ (19.2 mg, 0.139 mmol) in ethylene glycol (1.4 mL) was degassed with argon for 5 min and then heated at 170 °C (oil bath temperature) for 3 min. 15 mL water was added to the reaction mixture after it was cooled to room temperature, then the deep-blue solution was precipitated by the addition of excess solid NH$_4$PF$_6$. The crude product was collected, dissolved in CH$_3$CN (2 mL) and subjected to silica gel chromatography (eluent : CH$_3$CN, CH$_3$CN : H$_2$O : KNO$_3$ (sat) = 200 : 3 : 1, CH$_3$CN :

H_2O : KNO_3 (sat) = 100 : 3 : 1). The dark-blue eluents was concentrated and dissolved in a mixture of H_2O/EtOH (10 mL/1 mL), and the product was precipitated by the addition of excess solid NH_4PF_6. The precipitate was collected, washed twice with water (2 × 15 mL) and dried under high vacuum to afford Λ-(*S*)-**68** as a single diastereomer (175 mg, 72%).

Λ-(*S*)-**66**
73%
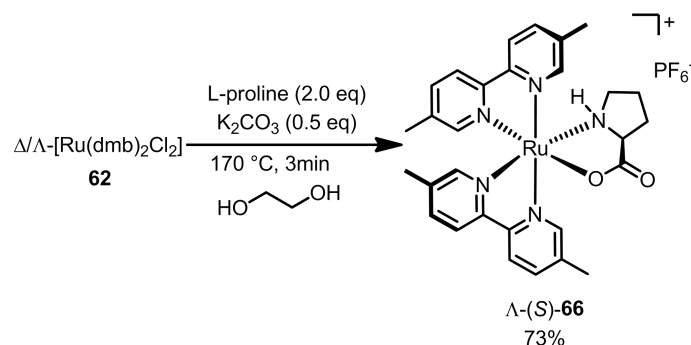
Single diastereomer Λ-(*S*)-66. In a closed brown vial (5 mL) fitted with a septum, a solution of *cis*-[Ru(dmb)$_2$Cl$_2$] (200 mg, 0.347 mmol), (*L*)-proline (80 mg, 0.694 mmol), and K_2CO_3 (24 mg, 0.173 mmol) in ethylene glycol (1.7 mL) was degassed with argon for 5 min and then heated at 190 °C (oil bath temperature) for 3 min. 20 mL water was added to the reaction mixture after it was cooled to room temperature, then the deep-red solution was precipitated by the addition of excess solid NH_4PF_6. The crude product was collected, dissolved in CH_3CN (3 mL) and subjected to silica gel chromatography (eluent : CH_3CN, CH_3CN : H_2O : KNO_3 (sat) = 200 : 3 : 1, CH_3CN : H_2O : KNO_3 (sat) = 80 : 3 : 1). The dark-blue eluents was concentrated and dissolved in a mixture of H_2O/EtOH (10 mL/1 mL), and the product was precipitated by the addition of excess solid NH_4PF_6. The precipitate was collected, washed twice with water (2 × 10 mL) and dried under high vacuum to afford Λ-(*S*)-**66** as a single diastereomer (177 mg, 70%). The configuration of Λ-(*S*)-**66** was determined by comparing its CD spectrum with the CD spectrum of Λ-(*S*)-**61** (Figure 53).

Λ-(*S*)-**66:** ^{1}H-NMR (300 MHz, CD$_3$CN): δ (ppm) 8.95 (t, *J* = 0.8 Hz, 1H), 8.82 (t, *J* = 0.8 Hz, 1H), 8.30 (dd, *J* = 10.4, 8.3 Hz, 2H), 8.14 (dd, *J* = 8.3, 3.1 Hz, 2H), 7.92 (dd, *J* = 8.3, 1.3 Hz, 1H), 7.87 (dd, *J* = 8.3, 1.0 Hz, 1H), 7.75 (t, *J* = 0.8 Hz, 1H), 7.55 (m, 2H), 7.11 (t, *J* = 0.8 Hz, 1H), 4.91 (dd, *J* = 14.5, 7.2 Hz, 1H), 3.93 (dt, *J* = 8.9, 7.2 Hz, 1H), 2.59 (s, 3H), 2.56 (s, 3H), 2.22 (m, 2H), 2.15 (s, 3H), 2.09 (s, 3H), 1.80 (m, 1H),

1.45 (m, 3H). ^{13}C-NMR (75 MHz, CD$_3$CN): δ (ppm) 183.1, 157.8, 157.3, 157.1, 156.7, 154.5, 152.7, 152.3, 151.1, 138.7, 138.3, 137.7, 137.6, 136.94, 136.90, 136.6, 136.0, 123.6, 123.5, 123.3, 123.1, 64.3, 50.3, 30.7, 27.3, 19.0, 18.8, 18.4, 18.2. IR (neat): v (cm^{-1}) 2962, 2924, 2852, 1603, 1475, 1452, 1388, 1259, 1087, 1014, 836, 794, 738, 697, 652, 557, 504, 436. CD ($\Delta\varepsilon$/M^{-1}cm^{-1}, MeCN): 290.5 nm (-90), 305 nm (+214). HRMS calcd for C$_{29}$H$_{32}$N$_5$O$_2$Ru (M-PF$_6$)$^+$: 584.1602, found: 584.1599.

Figure 53. CD spectra of compounds Λ-(*S*)-**66** in CH$_3$CN (0.1 mM).
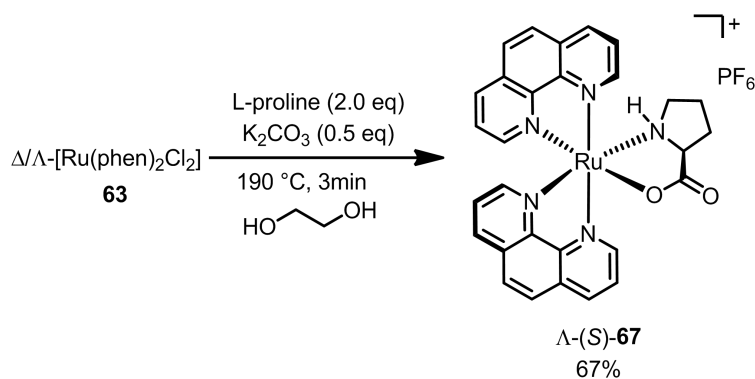
Single diastereomer Λ-(*S*)-67. In a closed brown vial (5 mL) fitted with a septum, a solution of *cis*-[Ru(phen)$_2$Cl$_2$] (200 mg, 0.352 mmol), L-proline (82 mg, 0.704 mmol), and K$_2$CO$_3$ (24 mg, 0.176 mmol) in ethylene glycol (1.7 mL) was degassed with argon for 5 min and then heated at 190 °C (oil bath temperature) for 3 min. 12 mL water was added to the reaction mixture after it was cooled to room temperature, then the deep-red solution was precipitated by the addition of excess solid NH$_4$PF$_6$. The crude product was collected, dissolved in CH$_3$CN (3 mL) and subjected to silica gel

chromatography (eluent : CH₃CN, CH₃CN : H₂O : KNO₃ (sat) = 200 : 3 : 1, CH₃CN : H₂O : KNO₃ (sat) = 100 : 3 : 1). The dark-red eluents was concentrated and dissolved in a mixture of $H_2O/EtOH$ (8 mL/1 mL), and the product was precipitated by the addition of excess solid NH_4PF_6. The precipitate was collected, washed twice with water (2 × 10 mL) and dried under high vacuum to afford Λ-(*S*)-**67** as a single diastereomer (170 mg, 67%). Similarly, the configuration of Λ-(*S*)-**67** was determined by comparing its CD spectrum with the CD spectrum of Λ-(*S*)-**61** (Figure 54).

Λ-(S)-**67:** ^{1}H-NMR (300 MHz, CD₃CN): δ (ppm) 9.62 (dd, *J* = 5.3, 1.1 Hz, 1H), 9.47 (dd, *J* = 5.3, 1.2 Hz, 1H), 8.72 (dd, *J* = 8.2, 1.2 Hz, 1H), 8.64 (dd, *J* = 8.2, 1.0 Hz, 1H), 8.14 (m, 9H), 7.57 (dd, *J* = 5.4, 1.3 Hz, 1H), 7.34 (dd, *J* = 8.1, 5.4 Hz, 1H), 7.30 (dd, *J* = 8.1, 5.4 Hz, 1H), 5.31 (dd, *J* = 13.7, 8.0 Hz, 1H), 4.07 (dt, *J* = 8.9, 7.1 Hz, 1H), 2.10 (m, 1H), 1.83 (m, 1H), 1.32 (m, 4H). ^{13}C-NMR (75 MHz, CD₃CN): δ (ppm) 183.2, 155.8, 153.91, 153.88, 152.7, 151.3, 150.6, 150.4, 149.8, 136.4, 136.1, 135.0, 134.4, 131.7, 131.6, 131.5, 131.4, 129.0, 128.6, 128.5, 127.1, 126.4, 125.5, 125.4, 64.6, 50.6, 30.8, 27.3. IR (neat): v (cm^{-1}) 1604, 1425, 1367, 1262, 1201, 1096, 1054, 1020, 930, 828, 768, 719, 555. CD ($\Delta\varepsilon$/M^{-1}cm^{-1}, MeCN): 260.5 nm (-120), 269.5 nm (+213). HRMS calcd for $C_{29}H_{24}N_5O_2Ru$ (M-PF₆)$^+$: 576.0976, found: 576.0960.
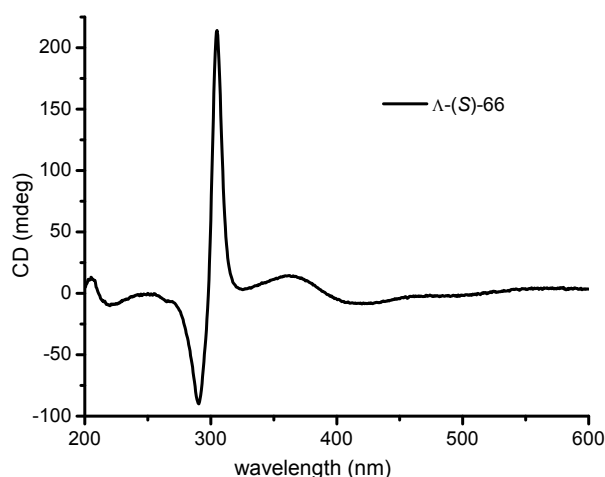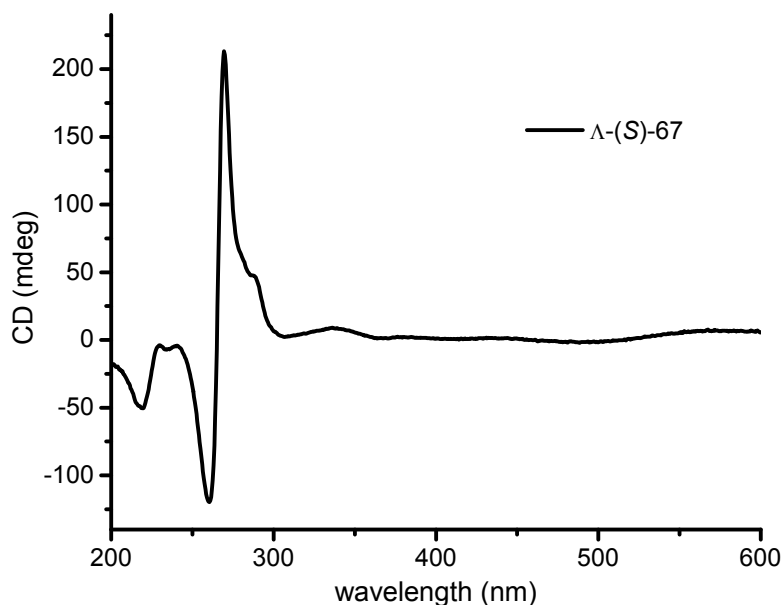

Figure 54. CD spectra of compounds Λ-(*S*)-**67** in CH₃CN (0.1 mM).
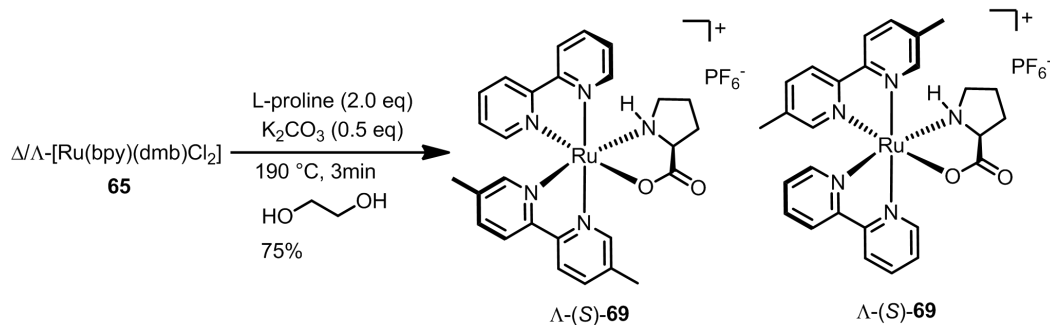
Two diastereomers of Λ-(*S*)-69. In a closed brown vial (10 mL) fitted with a septum, a solution of *cis*-[Ru(bpy)(dmb)Cl$_2$] (205 mg, 0.4 mmol), L-proline (92 mg, 0.8 mmol), and K$_2$CO$_3$ (27.6 mg, 0.2 mmol) in ethylene glycol (2.5 mL) was degassed with argon for 5 min and then heated at 190 °C (oil bath temperature) for 3 min. 15 mL water was added to the reaction mixture after it was cooled to room temperature, then the deep-red solution was precipitated by the addition of excess solid NH$_4$PF$_6$. The crude product was collected, dissolved in CH$_3$CN (3 mL) and subjected to silica gel chromatography (eluent : CH$_3$CN, CH$_3$CN : H$_2$O : KNO$_3$ (sat) = 200 : 3 : 1, CH$_3$CN : H$_2$O : KNO$_3$ (sat) = 100 : 3 : 1). The deep-red eluents were concentrated and dissolved in a mixture of H$_2$O/EtOH (10 mL/1 mL), and the product was precipitated by the addition of excess solid NH$_4$PF$_6$. The suspension was extracted with CH$_2$Cl$_2$ twice (2 × 15 mL), and the combined organic extracts were dried (Na$_2$SO$_4$), filtered, concentrated and dried under high vacuum to afford Λ-(*S*)-69 as a mixture of two diastereomers with the same metal-centered configuration (210 mg, 75%), which was determined by comparing its CD spectrum with the CD spectrum of Λ-(*S*)-61 (Figure 55).

Λ-(S)-**69:** The ratio of two diastereomers was assigned by characteristic signals from ^{1}H-NMR (the ratio of integration δ 2.60 ppm (-CH$_3$) : δ 2.56 ppm (-CH$_3$) = 2 : 5). IR (neat): v (cm^{-1}) 3629, 3185, 2924, 1596, 1476, 1420, 1374, 1318, 1262, 1098, 1026, 929, 831, 762, 729, 662, 555, 433. HRMS calcd for C$_{27}$H$_{28}$N$_5$O$_2$Ru (M-PF$_6$)$^+$: 556.1288, found: 556.1283. CD ($\Delta\varepsilon$/M^{-1}cm^{-1}, MeCN): 287 nm (-80), 300.5 nm (+166). Elemental analysis calcd for Λ-(S)-**69**·H$_2$O: C$_{27}$H$_{30}$F$_6$N$_5$O$_3$PRu: N 9.75, C 45.13, H 4.21; found: N 9.32, C 45.45, H 4.31.
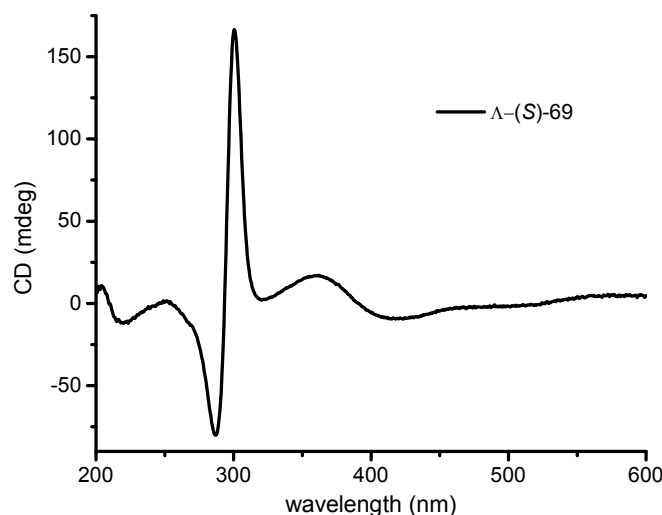
Figure 55. CD spectra of compounds Λ-(*S*)-**69** in CH$_3$CN (0.1 mM).
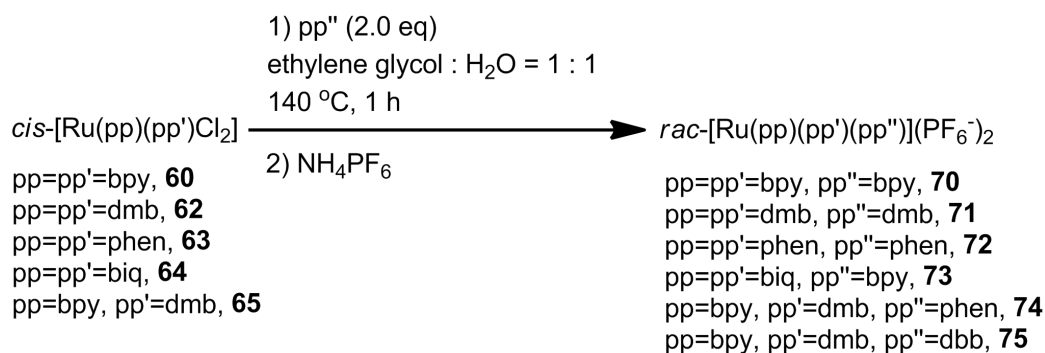
Synthesis of rac-complexes 70-75 as references. *General procedure.* In a closed brown vial fitted with a septum, a solution of *cis*-[Ru(pp)(pp')Cl$_2$] (1.0 eq), pp'' (2.0 eq) in ethylene glycol/water (1 : 1) (20 mM) was degassed with argon and then heated at 140 °C (oil bath temperature) for about 1 hour. In order to get rid of the most ethylene glycol and make the subsequent purification easier, the reaction mixture was precipitated by the addition of excess solid NH$_4$PF$_6$ after it was cooled to room temperature. The crude product was collected, dissolved in CH$_3$CN and subjected to silica gel chromatography (eluent : CH$_3$CN, CH$_3$CN : H$_2$O : KNO$_3$ (sat) = 100 : 3 : 1, CH$_3$CN : H$_2$O : KNO$_3$ (sat) = 50 : 3 : 1). The product eluents were concentrated and dissolved in minimal amounts of water or ethanol/water, subsequently, the product was precipitated by the addition of excess solid NH$_4$PF$_6$. The precipitate was collected, washed twice with water, and dried under high vacuum to afford racemic *cis*-[Ru(pp)(pp')(pp'')](PF$_6$)$_2$. NMR data of these *rac*-complexes were identical to the related enantiomers.

91
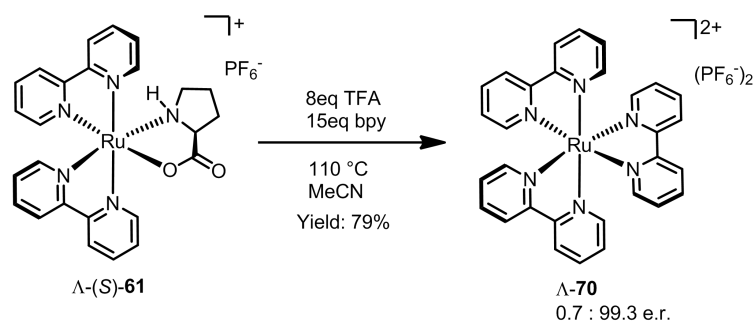
Λ-[Ru(bpy)₃](PF₆)₂ (Λ-70) In a closed 1.5 mL brown glass vial fitted with a septum, a solution of Λ-(S)-**61** (50 mg, 0.075 mmol), 2,2'-bipyridine (175 mg, 1.12 mmol), and TFA (0.044 mL, 0.595 mmol) in CH_3CN (0.8 mL) (freshly distilled) was heated at 110 °C (oil bath temperature) for 2.5 h under a nitrogen atmosphere. The reaction mixture was cooled to room temperature and then subjected to silica gel chromatography eluting with CH_3CN : H_2O : KNO_3(sat) = 50 : 6 : 2. The product eluents were concentrated and dissolved in a mixture of ethanol/water (10 mL/1 mL), and the product was precipitated by the addition of excess solid NH_4PF_6. The orange precipitate was centrifuged, washed twice with water (2 × 10 mL), diethyl ether (10 mL) and then dried under high vacuum to afford Λ-[Ru(bpy)₃](PF₆)₂ (Λ-**70**) (51 mg, 79%). The absolute configuration of Λ-[Ru(bpy)₃](PF₆)₂ was assigned by exciton analysis and compared with published reference complexes. Namely, the product **70** shows a similar CD spectrum to Λ-[Ru(dbb)(dmb)(bpy)]²⁺(PF₆)₂, the absolute configuration of which was confirmed by X-ray crystallography from our previous work, thus the comparison suggests that the absolute configuration of **70** is Λ.[39] The enantiopurity (0.7 : 99.3 e.r.) was determined by chiral HPLC analysis, as shown in Figure 57.

¹H-NMR (300.1 MHz, CD_3CN): δ (ppm) 8.53 (d, J = 8.1 Hz, 6H), 8.08 (td, J = 8.0, 1.4 Hz, 6H), 7.76 (d, J = 5.6 Hz, 6H), 7.42 (ddd, J = 7.4, 5.6, 1.0 Hz, 6H). ¹³C-NMR (100.6 MHz, CD_3CN): δ (ppm) 157.0, 151.7, 137.8, 127.5, 124.3. IR (neat): v (cm⁻¹) 1446, 833, 756, 555. CD ($\Delta\varepsilon$ /M⁻¹cm⁻¹, MeCN): 292 nm (+365), 278 nm (-155). HRMS (ESI) calcd for $RuF_6N_6C_{30}H_{24}P$ (M-PF₆) 715.0747, found: 715.0724.
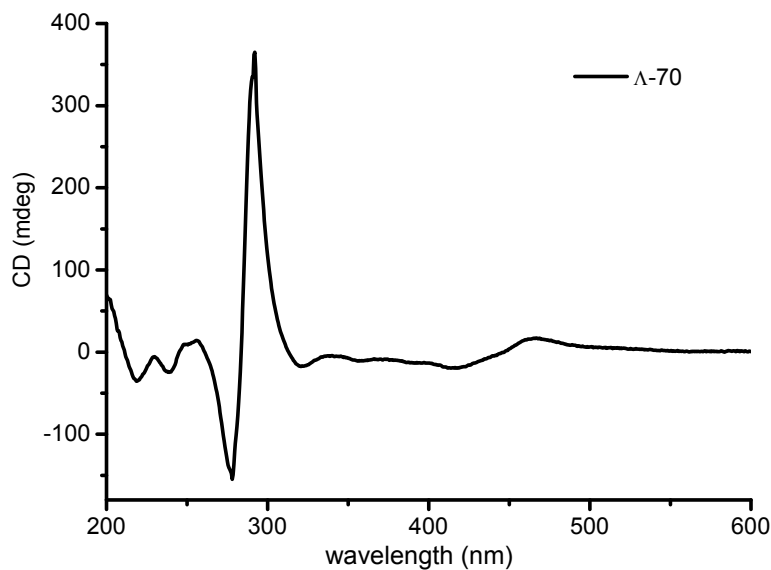
Figure 56. CD spectrum for Λ-[Ru(bpy)$_3$](PF$_6$)$_2$ (**Λ-70**) in CH$_3$CN (0.1 mM).

Determination of enantiomeric ratio of Λ-[Ru(bpy)$_3$](PF$_6$)$_2$ (Λ-70) by chiral HPLC using racemic [Ru(bpy)$_3$](PF$_6$)$_2$ as reference. The ruthenium complex was analyzed with a Chiralpak (250×4.6 mm) IA HPLC column on an Agilent 1200 Series HPLC System. The flow rate was 0.5 mL/min, the column temperature 40 °C, and UV-absorption was measured at 254 nm. Solvent A = 0.1% TFA (aq), solvent B = MeCN, with a linear gradient of 15% to 30% B in 20 min.
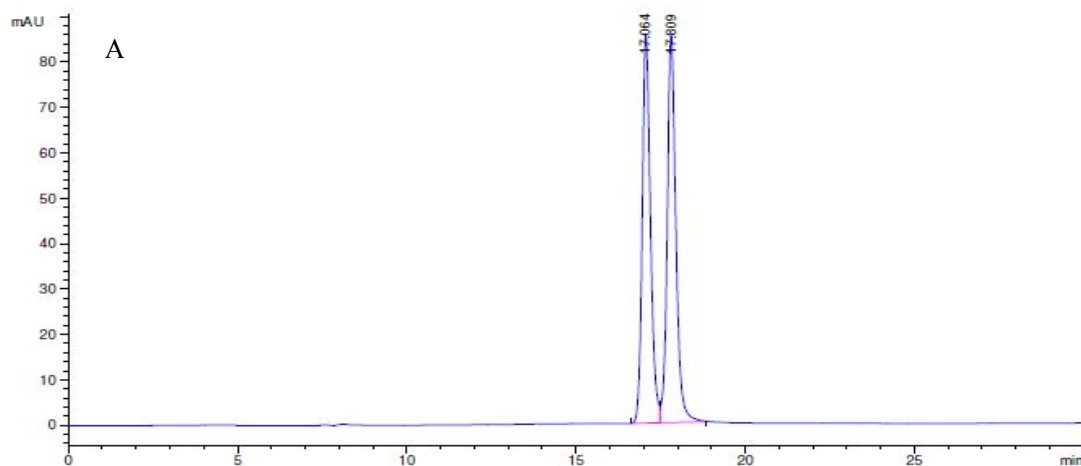
Figure 57. (A) HPLC trace for *rac*-[Ru(bpy)₃](PF₆)₂. (B) HPLC trace for enantiopure Λ-[Ru(bpy)₃](PF₆)₂ (Λ-**70**), integration of peak areas = 0.7 : 99.3 e.r.
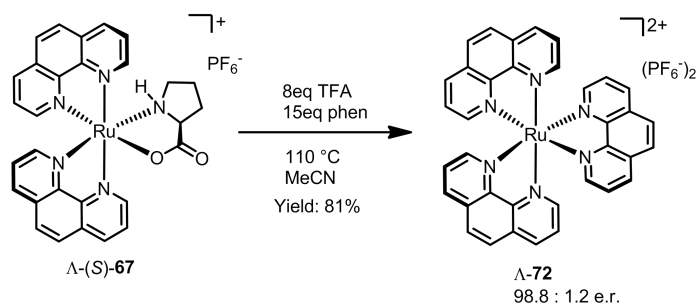
Λ-[Ru(phen)₃](PF₆)₂ (Λ-72) In a closed 1.5 mL brown glass vial fitted with a septum, a solution of Λ-(*S*)-**67** (50 mg, 0.070 mmol), 1,10-phenanthroline (188 mg, 1.04 mmol), and TFA (0.042 mL, 0.555 mmol) in CH₃CN (0.7 mL) (freshly distilled) was heated at 110 °C (oil bath temperature) for 2.5 h under a nitrogen atmosphere. The reaction mixture was cooled to room temperature and subjected to silica gel chromatography eluting with CH₃CN : H₂O : KNO₃(sat) = 50 : 6 : 2. The product eluents were concentrated and dissolved in a mixture of ethanol/water (12 mL/2 mL), and the product was precipitated by the addition of excess solid NH₄PF₆. The orange precipitate was centrifuged, washed twice with water (2 × 10 mL), diethyl ether (10 mL) and then dried under high vacuum to afford Λ-[Ru(phen)₃](PF₆)₂ (Λ-**72**) (53 mg, 81%). The configuration of Λ-**72** was assigned by comparing its CD spectrum (Figure 59) with the CD spectrum of Λ-[Ru(bpy)₃](PF₆)₂, and the enantiopurity (98.8 : 1.2 e.r.) was determined by chiral HPLC analysis (Figure 58).

^{1}H-NMR (500.1 MHz, CD$_3$CN): δ (ppm) 8.59 (dd, J = 8.3 Hz, J = 1.1 Hz, 6H), 8.25 (s, 6H), 8.01 (dd, J = 5.3 Hz, J = 1.1 Hz, 6H), 7.62 (dd, J = 8.2 Hz, J = 5.2 Hz, 6H). ^{13}C-NMR (100.6 MHz, CD$_3$CN): δ (ppm) 154.0, 149.0, 137.8, 132.0, 129.0, 126.9. IR (neat): ν (cm^{-1}) 1427, 831, 718,555. CD ($\Delta\varepsilon$/M^{-1}cm^{-1}, MeCN): 267 nm (+606), 257 nm (-496). HRMS (ESI) calcd for C$_{37}$H$_{27}$F$_6$N$_6$PRu (M-PF$_6$) 787.0752, found: 787.0735.

Determination of enantiomeric ratio of Λ-[Ru(phen)$_3$](PF$_6$)$_2$ (Λ-72) by chiral HPLC using racemic [Ru(phen)$_3$](PF$_6$)$_2$ as reference. The ruthenium complex was analyzed with a Chiralpak (250×4.6 mm) IB HPLC column on an Agilent 1200 Series HPLC System. The flow rate was 0.5 mL/min, the column temperature 40 °C, and UV-absorption was measured at 254 nm. Solvent A = 0.1% TFA (aq), solvent B = MeCN, with a linear gradient of 15% to 50% B in 20 min.
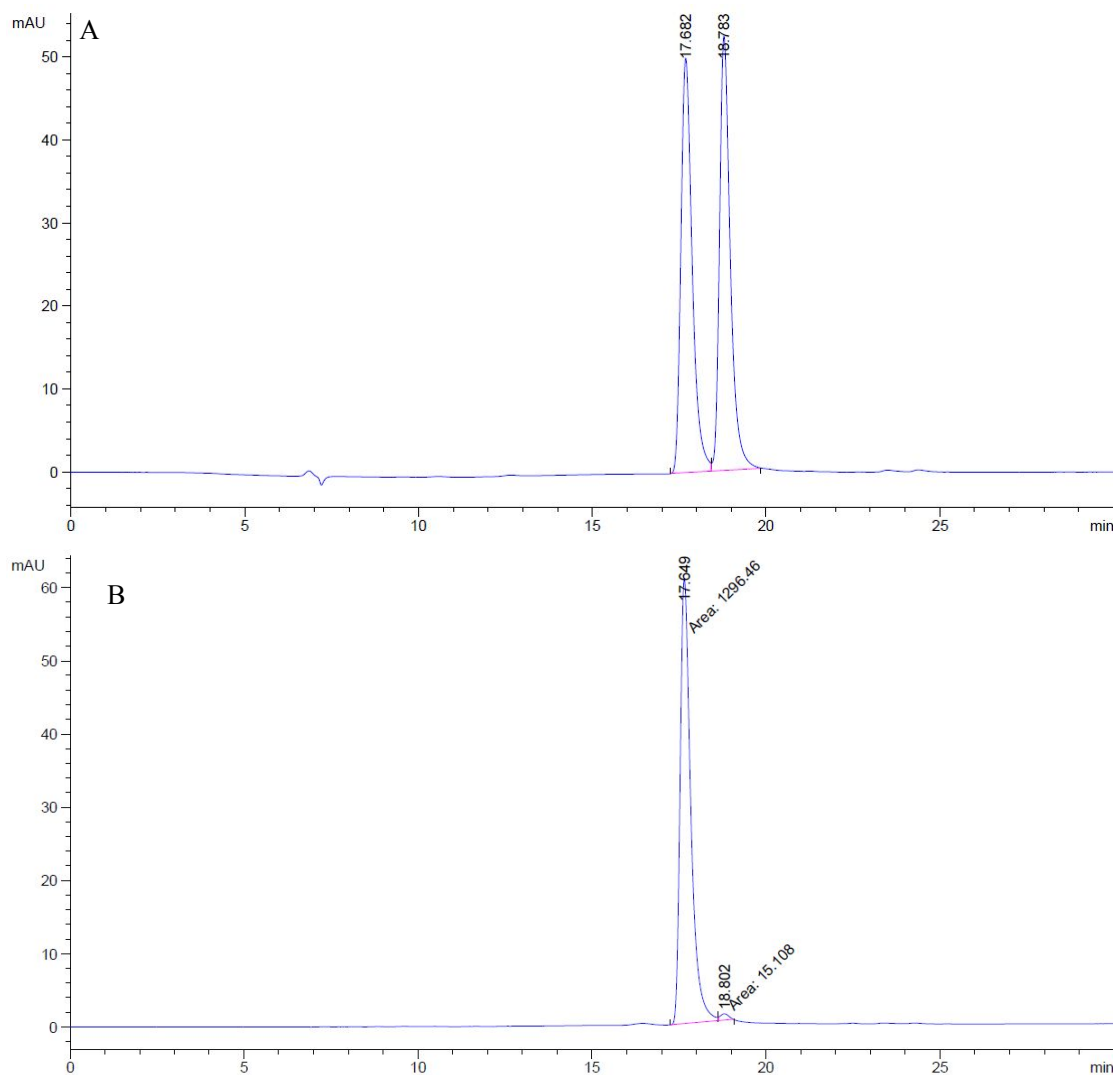
Figure 58. (A) HPLC trace for *rac*-[Ru(phen)$_3$](PF$_6$)$_2$. (B) HPLC trace for enantiopure Λ-[Ru(phen)$_3$](PF$_6$)$_2$ (Λ-**72**), integration of peak areas = 98.8 : 1.2 e.r.
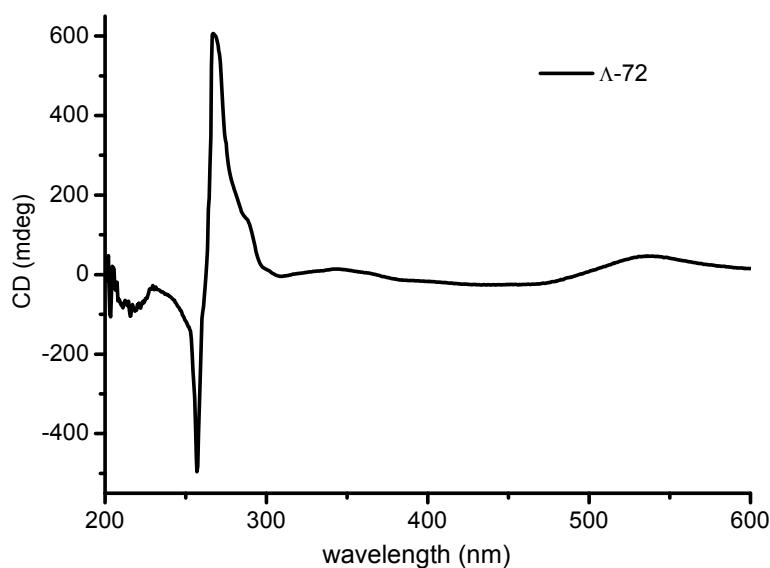
Figure 59. CD spectrum for Λ-[Ru(phen)₃](PF₆)₂ (**Λ-72**) in CH₃CN (0.1 mM).
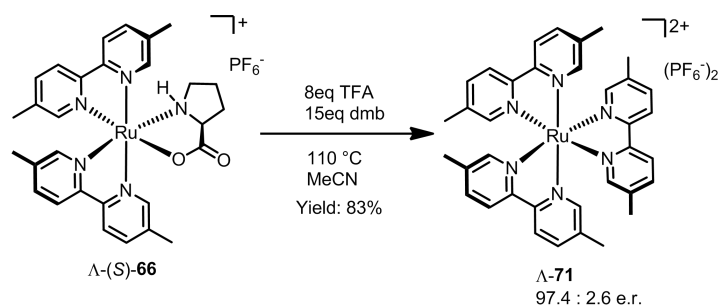
[Ru(dmb)₃](PF₆)₂ (Λ-71) In a closed 1.5 mL brown glass vial fitted with a septum, a solution of Λ-(*S*)-**66** (50 mg, 0.069 mmol), 5,5'-dimethyl-2,2'-bipyridine (dmb, 189 mg, 1.03 mmol), and TFA (0.041 mL, 0.552 mmol) in CH₃CN (0.7 mL) (freshly distilled) was heated at 110 °C (oil bath temperature) for 2.5 h under a nitrogen atmosphere. The reaction mixture was cooled to room temperature and subjected to silica gel chromatography eluting with CH₃CN : H₂O : KNO₃(sat) = 100 : 3 : 1. The product eluents were concentrated and dissolved in a mixture of ethanol/water (10 mL/2 mL), and the product was precipitated by the addition of excess solid NH₄PF₆. The red precipitate was centrifuged, washed twice with water (2 × 12 mL), diethyl ether (12 mL) and then dried under high vacuum to afford [Ru(dmb)₃](PF₆)₂ (Λ-**71**) (54 mg, 83%). The configuration of Λ-**71** was assigned by comparing its CD spectrum (Figure 60) with the CD spectrum of Λ-[Ru(bpy)₃](PF₆)₂, and the enantiopurity (97.4 : 2.6 e.r.) was determined by chiral HPLC analysis (Figure 61).

¹H-NMR (300 MHz, CD₃CN): *δ* (ppm) 8.31 (d, *J* = 8.4 Hz, 6H), 7.84 (ddd, *J* = 8.4,

1.8, 0.6 Hz, 6H), 7.44 (dd, J = 1.8, 1.0 Hz, 6H), 2.19 (s, 18H). ^{13}C-NMR (75 MHz, CD$_3$CN): δ (ppm) 155.6, 152.3, 139.06, 139.01, 124.2, 18.6. IR (neat): ν (cm^{-1}) 1606, 1475, 1241, 822, 727, 556, 520, 433. CD ($\Delta\varepsilon$/M^{-1}cm^{-1}, MeCN): 284 nm (-149), 298.5 nm (+324). HRMS calcd for C$_{36}$H$_{36}$F$_6$N$_6$PRu (M-PF$_6$)$^+$: 799.1691, found: 799.1666.
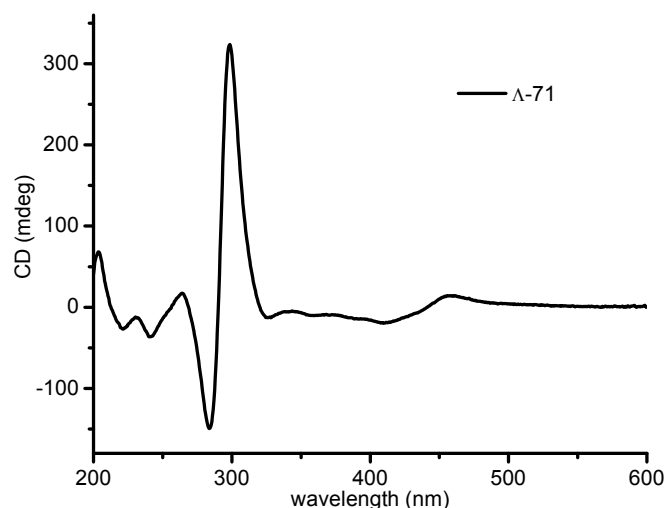
Figure 60. CD spectrum for [Ru(dmb)$_3$](PF$_6$)$_2$ (Λ-**71**) in CH$_3$CN (0.1 mM).

Determination of enantiomeric ratio of Λ-[Ru(dmb)$_3$](PF$_6$)$_2$ (Λ-71) by chiral HPLC using racemic [Ru(dmb)$_3$](PF$_6$)$_2$ as reference. The ruthenium complex was analyzed with a Chiralpak (250×4.6 mm) IB HPLC column on an Agilent 1200 Series HPLC System. The flow rate was 0.5 mL/min, the column temperature 40 °C, and UV-absorption was measured at 254 nm. Solvent A = 0.1% TFA (aq), solvent B = MeCN, with a linear gradient of 20% to 24% B in 25 min.
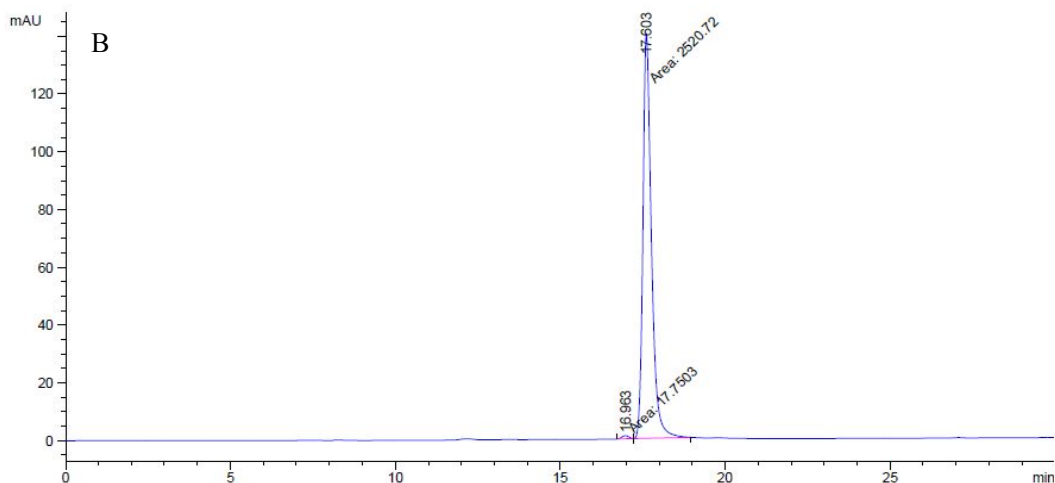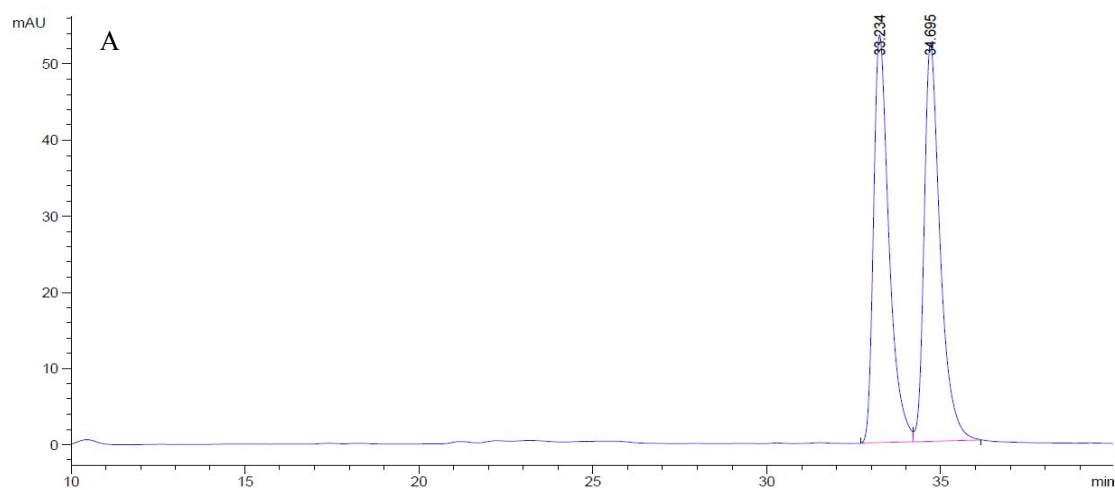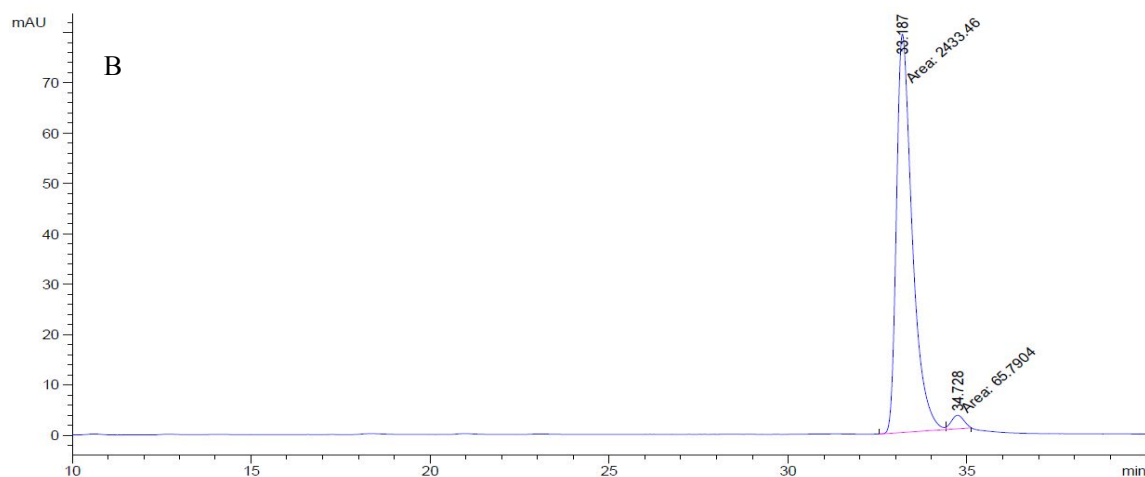
Figure 61. (A) HPLC trace for *rac*-[Ru(dmb)₃](PF₆)₂. (B) HPLC trace for enantiopure [Ru(dmb)₃](PF₆)₂ (Λ-**71**), integration of peak areas = 97.4 : 2.6 e.r.
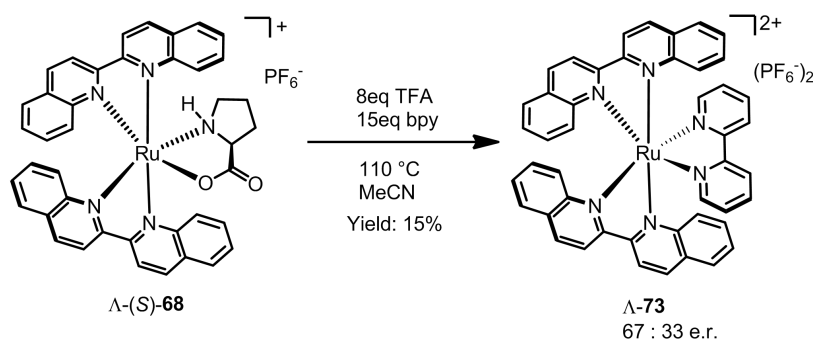
[Ru(biq)₂(bpy)](PF₆)₂ (Λ-73) In a closed 1.5 mL brown glass vial fitted with a septum, a solution of Λ-(*S*)-**68** (10.9 mg, 0.0125 mmol), 2,2'-bipyridine (29.3 mg, 0.1875 mmol), and TFA (0.0074 mL, 0.100 mmol) in CH₃CN (0.25 mL) (freshly distilled) was heated at 110 °C (oil bath temperature) for 12 h under a nitrogen atmosphere. The reaction mixture was cooled to room temperature and subjected to silica gel chromatography eluting with CH₃CN : H₂O : KNO₃(sat) = 200 : 3 : 1. The product eluents were concentrated and dissolved in a mixture of ethanol/water (12 mL/3 mL), and the product was precipitated by the addition of excess solid NH₄PF₆. The purple precipitate was centrifuged, washed twice with water (2 × 8 mL), diethyl ether (10 mL) and then dried under high vacuum to afford Λ-[Ru(biq)₂(bpy)](PF₆)₂ (2.0 mg, 15%). This compound is light-sensitive, not very stable and should be stored under argon at -20 °C. The configuration of Λ-**73** was assigned by comparing its CD

spectrum (Figure 62) with the CD spectrum of Λ-[Ru(bpy)$_3$](PF$_6$)$_2$, and the enantiopurity (67 : 33 e.r.) was determined by chiral HPLC analysis (Figure 63).

^{1}H-NMR (300 MHz, CD$_3$CN): δ (ppm) 9.01 (d, J = 8.9 Hz, 2H), 8.94 (d, J = 8.9 Hz, 2H), 8.82 (d, J = 8.9 Hz, 2H), 8.49 (d, J = 8.8 Hz, 2H), 8.12 (dd, J = 8.1, 1.2 Hz, 2H), 7.91 (d, J = 5.3 Hz, 2H), 7.86 (d, J = 8.1 Hz, 2H),7.73 (dt, J = 7.8, 1.4 Hz, 2H), 7.58 (d, J = 7.9 Hz, 2H), 7.51 (ddd, J = 8.2, 7.0, 0.9 Hz, 2H), 7.44 (ddd, J = 7.6, 6.0, 1.3 Hz, 2H), 7.40 (ddd, J = 8.6, 7.0, 0.9 Hz, 2H), 7.35 (d, J = 9.0 Hz, 2H), 7.10 (m, 4H), 6.93 (ddd, J = 8.9, 6.9, 1.3 Hz, 2H). ^{13}C-NMR (75 MHz, CD$_3$CN): δ (ppm) 162.3, 161.7, 157.4, 152.7, 152.6, 151.0, 141.2, 139.9, 139.6, 133.7, 131.6, 130.8, 130.5, 130.3,130.00, 129.97, 129.6, 128.5, 126.7, 126.2, 123.6, 123.5, 122.6. IR (neat): ν (cm^{-1}) 1595, 1509, 1432, 1369, 1246, 1213, 1146, 1098, 830, 812, 781, 767, 750, 632, 556, 516, 482, 431. CD ($\Delta\varepsilon$/M^{-1}cm^{-1}, MeCN): 262.5 nm (-35), 270.5 nm (+30). HRMS calcd for C$_{46}$H$_{32}$F$_6$N$_6$PRu (M-PF$_6$)$^+$: 915.1381, found: 915.1361.
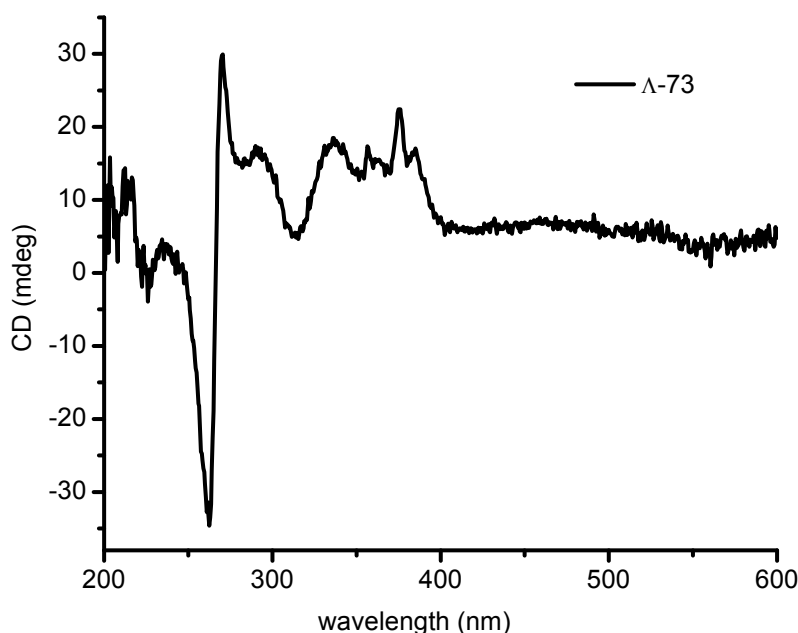
Figure 62. CD spectrum for Λ-[Ru(biq)$_2$(bpy)](PF$_6$)$_2$ (Λ-**73**) in CH$_3$CN (0.1 mM).

Determination of enantiomeric ratio of Λ-[Ru(biq)$_2$(bpy)](PF$_6$)$_2$ (Λ-73) by chiral HPLC using racemic [Ru(biq)$_2$(bpy)](PF$_6$)$_2$ as reference. The ruthenium complex was analyzed with a Chiralpak (250 × 4.6 mm) IA HPLC column on an Agilent 1200 Series HPLC System. The flow rate was 0.5 mL / min, the column temperature 40 °C,

and UV-absorption was measured at 254 nm. Solvent A = 0.1% TFA (aq), solvent B = MeCN, with a linear gradient of 22% to 30% B in 20 min.
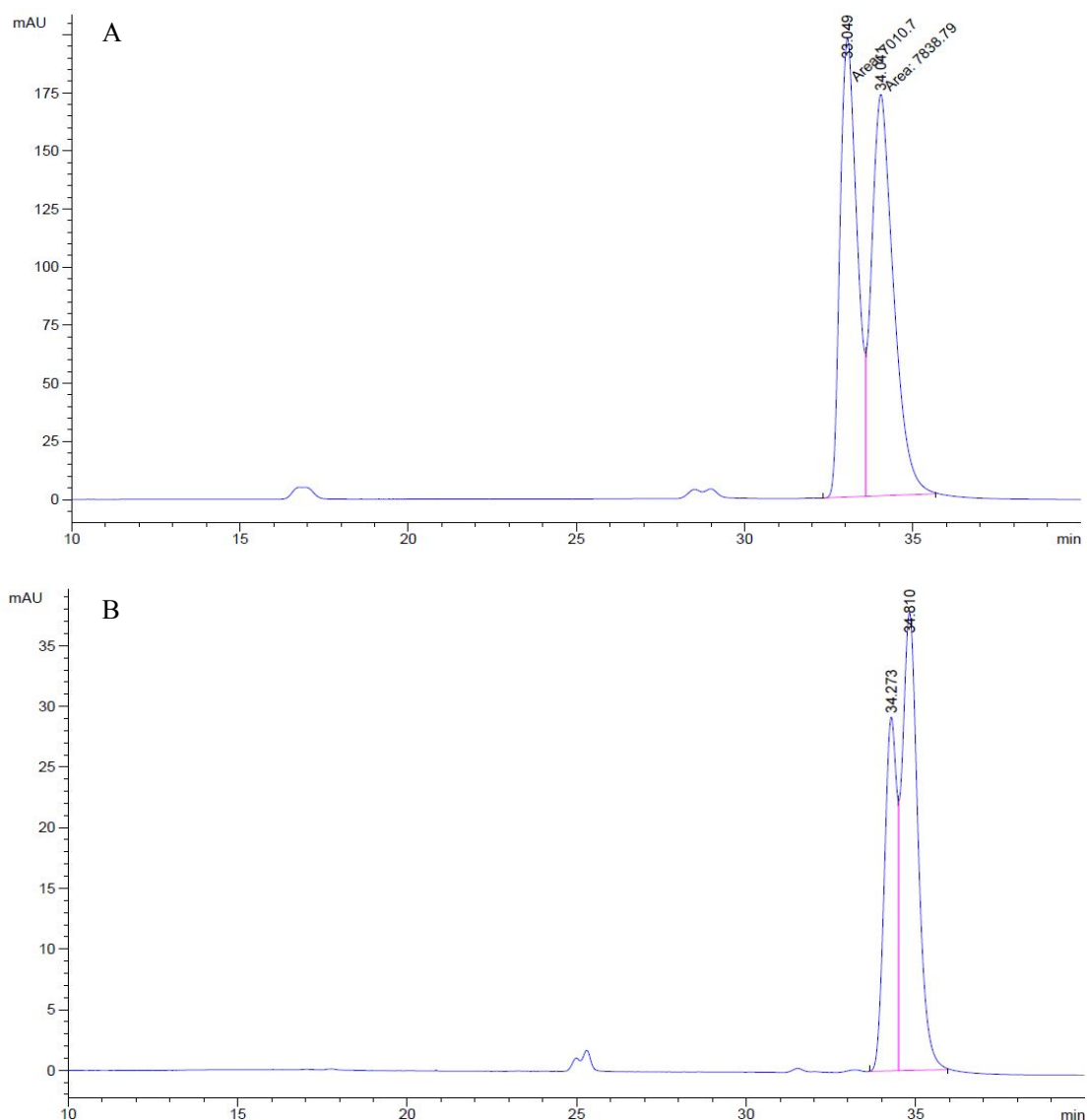

Figure 63. (A) HPLC trace for *rac*-[Ru(biq)$_2$(bpy)](PF$_6$)$_2$. (B) HPLC trace for enantiopure Λ-[Ru(biq)$_2$(bpy)](PF$_6$)$_2$ (Λ-**73**), integration of peak areas = 33 : 67 e.r.
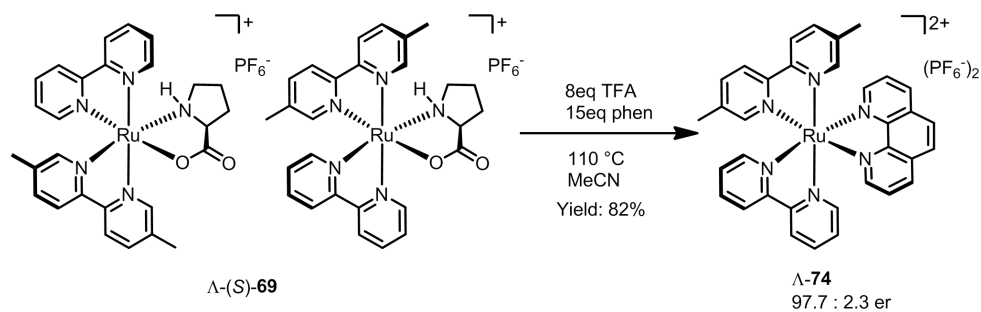
[Ru(bpy)(dmb)(phen)](PF$_6$)$_2$ (Λ-74) In a closed 1.5 mL brown glass vial fitted with a septum, a solution of Λ-(*S*)-**69** (45 mg, 0.064 mmol), 1,10-phenanthroline (174 mg,

100

0.968 mmol), and TFA (0.039 mL, 0.512 mmol) in CH_3CN (0.6 mL) (freshly distilled) was heated at 110 °C (oil bath temperature) for 2.5 h under a nitrogen atmosphere. The reaction mixture was cooled to room temperature and subjected to silica gel chromatography eluting with CH_3CN : H_2O : KNO_3(sat) = 80 : 3 : 1. The product eluents were concentrated and dissolved in a mixture of ethanol/water (12 mL/3 mL), and the product was precipitated by the addition of excess solid NH_4PF_6. The orange precipitate was centrifuged, washed twice with water (2 × 12 mL), diethyl ether (10 mL) and then dried under high vacuum to afford Λ-[Ru(bpy)(dmb)(phen)]$(PF_6)_2$ (Λ-**74**) (48 mg, 82%). The configuration of Λ-**74** was assigned by comparing its CD spectrum (Figure 65) with the CD spectrum of Λ-[Ru(bpy)$_3$]$(PF_6)_2$, and the enantiopurity (97.7 : 2.3 er) was determined by chiral HPLC analysis (Figure 64).

^{1}H-NMR (300 MHz, CD_3CN): δ (ppm) 8.62 (dt, J = 8.4, 1.1 Hz, 2H), 8.54 (d, J = 8.1 Hz, 1H), 8.49 (d, J = 8.2 Hz, 1H), 8.37 (d, J = 8.4 Hz, 1H), 8.33 (d, J = 8.4 Hz, 1H), 8.24 (s, 2H), 8.09 (m, 3H), 7.97 (dt, J = 7.6, 1.3 Hz, 1H), 7.90 (dd, J = 8.4, 1.0 Hz, 1H), 7.86 (dd, J = 5.5, 0.6 Hz, 1H), 7.80 (ddd, J = 8.3, 2.0, 1.0 Hz, 1H), 7.75 (ddd, J = 8.2, 7.5, 5.2 Hz, 2H), 7.61 (s, 1H), 7.47 (m, 2H),7.35 (s, 1H), 7.20 (ddd, J = 7.7, 5.6, 1.0 Hz, 1H), 2.23 (s, 3H), 2.04 (s, 3H). ^{13}C-NMR (75 MHz, CD_3CN): δ (ppm) 158.5, 158.1, 155.8, 155.5, 153.47, 153.44, 153.0, 152.8, 152.72, 152.66. 148.7, 148.6, 139.4, 139.32, 139.25, 139.21, 138.7, 138.5, 137.7, 132.1, 132.0, 129.12, 129.09, 128.4, 127.1, 127.0, 125.3, 125.2, 124.2, 124.1, 18.6, 18.4. IR (neat): v (cm^{-1}) 1596, 1510, 1428, 1211, 1126, 828, 762, 720, 555, 517. CD ($\Delta\varepsilon$/M^{-1}cm^{-1}, MeCN): 263.5 nm (-108), 292.5 nm (+277). HRMS calcd for $C_{34}H_{28}F_6N_6PRu$ (M-PF$_6$)$^+$: 767.1064, found: 767.1041.

Determination of enantiomeric ratio of Λ-[Ru(bpy)(dmb)(phen)]$(PF_6)_2$ (Λ-74) by chiral HPLC using racemic Λ-[Ru(bpy)(dmb)(phen)]$(PF_6)_2$ as reference. The ruthenium complex was analyzed with a Chiralpak (250×4.6 mm) IB HPLC column on an Agilent 1200 Series HPLC System. The flow rate was 0.5 mL/min, the column temperature 40 °C, and UV-absorption was measured at 254 nm. Solvent A = 0.1% TFA (aq), solvent B = MeCN, with a linear gradient of 10% to 25% B in 20 min.
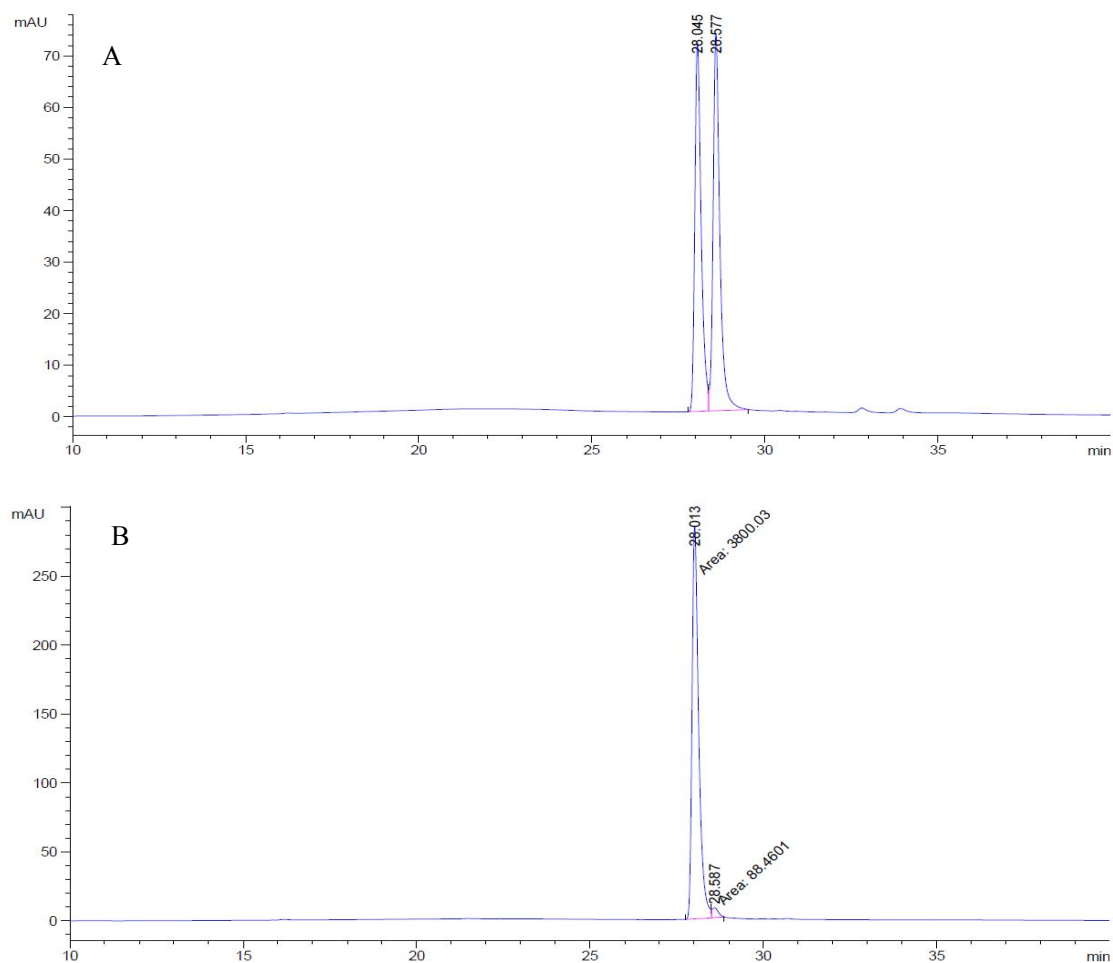
Figure 64. (A) HPLC trace for *rac*-Λ-[Ru(bpy)(dmb)(phen)](PF$_6$)$_2$. (B) HPLC trace for enantiopure Λ-[Ru(bpy)(dmb)(phen)](PF$_6$)$_2$ (Λ-**74**), integration of peak areas = 97.7 : 2.3 e.r.
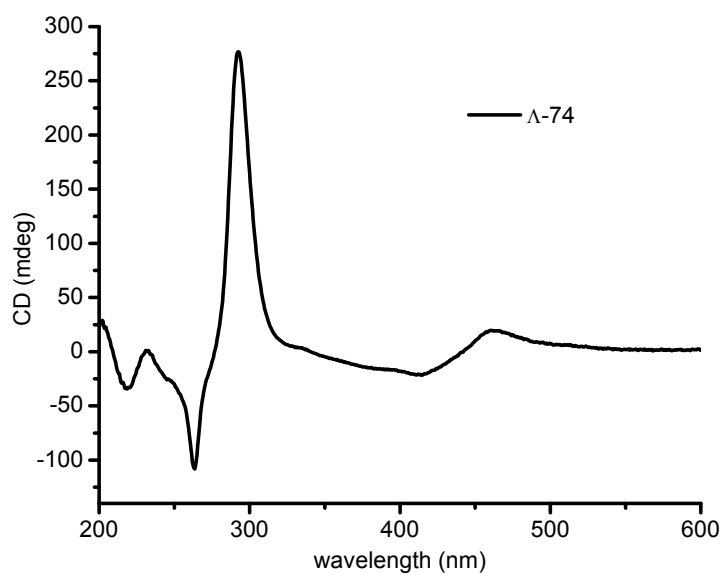
Figure 65. CD spectrum for Λ-[Ru(bpy)(dmb)(phen)](PF$_6$)$_2$ in CH$_3$CN (0.1 mM).
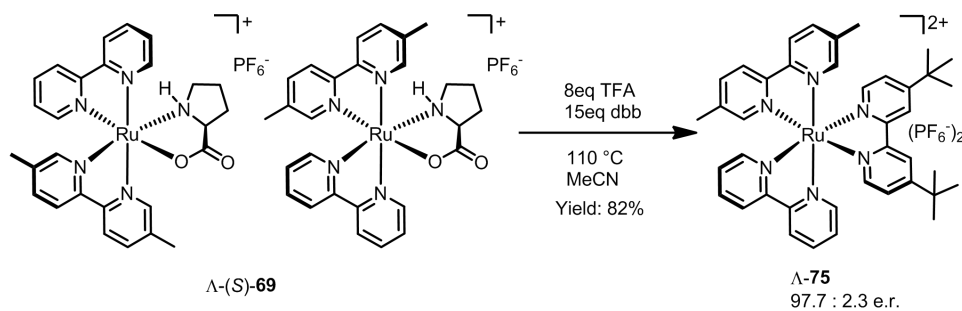
[Ru(bpy)(dmb)(dbb)](PF$_6$)$_2$ (Λ-75) In a closed 1.5 mL brown glass vial fitted with a septum, a solution of Λ-(*S*)-**69** (45 mg, 0.064 mmol), 4,4'-tert-butyl-2,2'-bipyridine (dbb, 260 mg, 0.968 mmol), and TFA (0.039 mL, 0.512 mmol) in CH$_3$CN (0.6 mL) (freshly distilled) was heated at 110 °C (oil bath temperature) for 2.5 h under a nitrogen atmosphere. The reaction mixture was cooled to room temperature and subjected to silica gel chromatography eluting with CH$_3$CN : H$_2$O : KNO$_3$(sat) = 80 : 3 : 1. The product eluents were concentrated and dissolved a mixture of ethanol/water (12 mL/4 mL), and the product was precipitated by the addition of excess solid NH$_4$PF$_6$. The orange precipitate was collected, washed twice with water (2 × 10 mL), diethyl ether (12 mL) and then dried under high vacuum to afford Λ-[Ru(bpy)(dmb)(dbb)](PF$_6$)$_2$ (Λ-**75**) (54 mg, 85%). The configuration of Λ-**75** was assigned by comparing its CD spectrum (Figure 66) with the CD spectrum of Λ-[Ru(bpy)$_3$](PF$_6$)$_2$, and the enantiomerically purity (97.9 : 2.1 e.r.) was determined by chiral HPLC analysis (Figure 67).
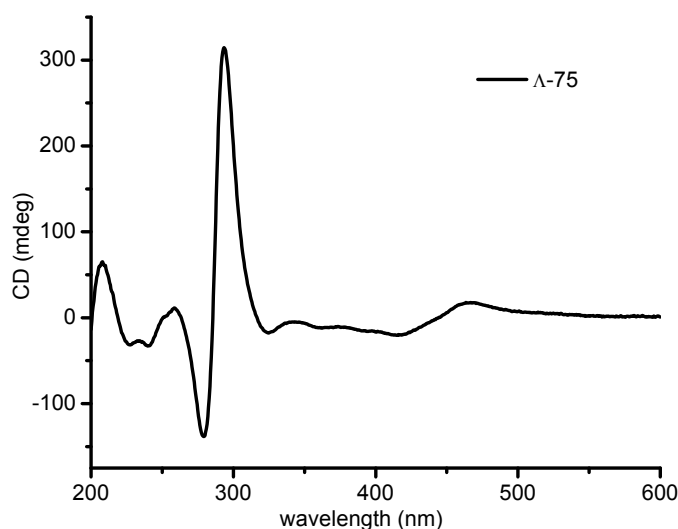
Figure 66. CD spectrum for Λ-[Ru(bpy)(dmb)(dbb)](PF$_6$)$_2$ in CH$_3$CN (0.1 mM).

Λ-**75:** ^{1}H-NMR (300 MHz, CD$_3$CN): δ (ppm) 8.52 (s, 1H), 8.50 (s, 1H), 8.485 (d, $J =$ 2.0 Hz, 1H), 8.475 (d, $J =$ 2.0 Hz, 1H), 8.345 (d, $J =$ 2.7 Hz, 1H), 8.328 (d, $J =$ 2.7 Hz, 1H), 8.05 (m, 2H), 7.86 (m, 2H), 7.73 (m, 2H), 7.61 (d, $J =$ 6.1 Hz, 1H), 7.59 (d, $J =$ 6.0 Hz, 1H), 7.48 (m, 1H), 7.44 (m, 1H), 7.41 (m, 4H), 2.207 (s, 3H), 2.198 (s, 3H), 1.426 (s, 9H), 1.412 (s, 9H). ^{13}C-NMR (75 MHz, CD$_3$CN): δ (ppm) 152.6, 152.52, 152.47, 152.4, 152.2, 151.96, 151.94, 139.28, 139.22, 139.1, 138.67, 138.64, 138.49, 138.46, 128.6, 128.5, 128.4, 125.7, 125.6, 125.5, 125.2, 124.2, 122.61, 122.57, 36.3, 30.52, 30.50, 18.62, 18.56. IR (neat): v (cm^{-1}) 2960, 2872, 1615, 1466, 1414, 1244, 828, 762, 606, 555, 419. CD ($\Delta\varepsilon$/M^{-1}cm^{-1}, MeCN): 279 nm (-138), 293.5 nm (+315). HRMS calcd for C$_{40}$H$_{44}$F$_6$N$_6$PRu (M-PF$_6$)$^+$: 855.2318, found: 855.2298.
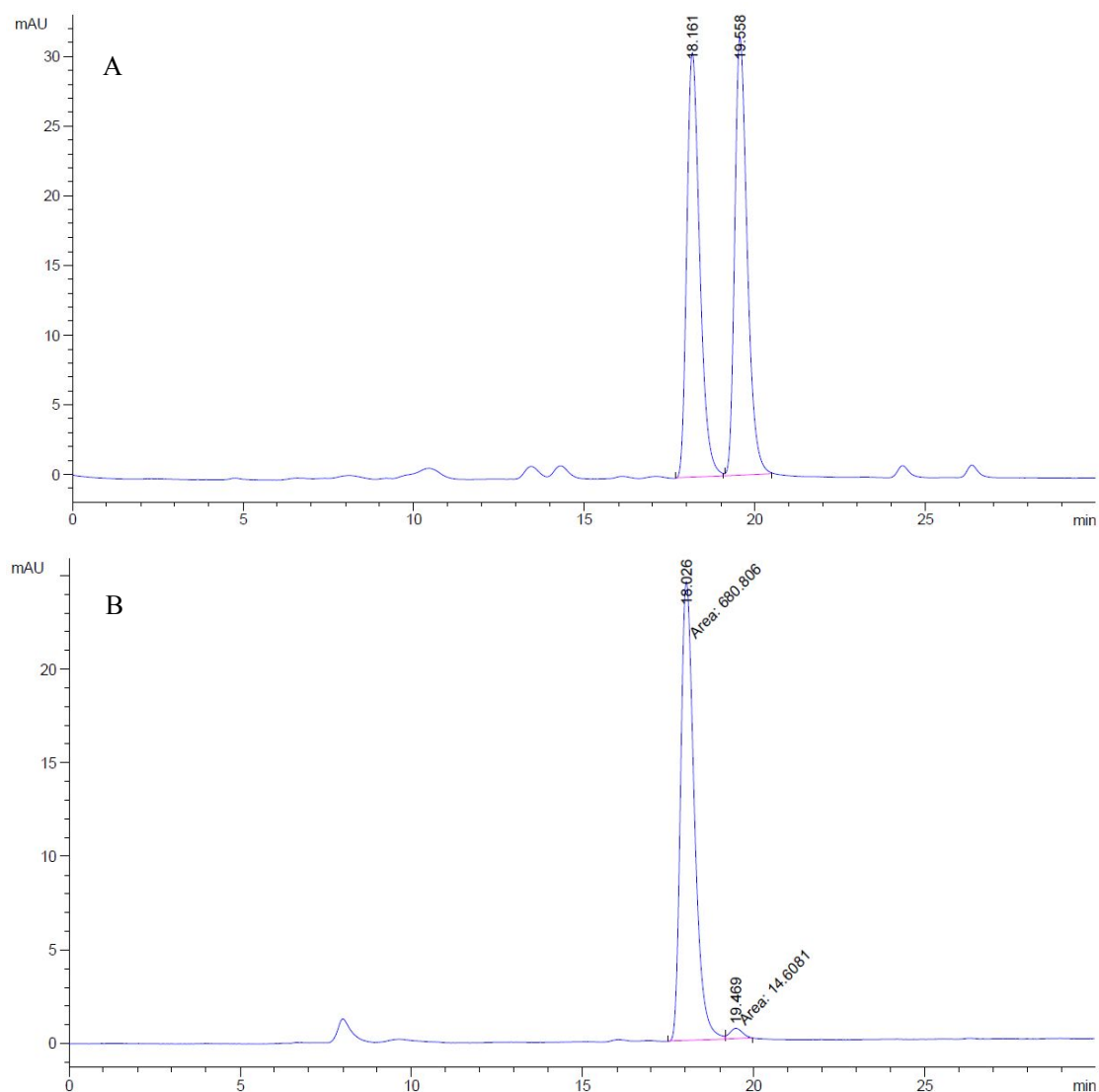
Figure 67. (A) HPLC trace for *rac*-[Ru(bpy)(dmb)(dbb)](PF$_6$)$_2$. (B) HPLC trace for enantiopure Λ-[Ru(bpy)(dmb)(dbb)](PF$_6$)$_2$ (Λ-**75**), integration of peak areas = 97.9 : 2.1 e.r.

Determination of enantiomeric ratio of Λ-[Ru(bpy)(dmb)(dbb)](PF$_6$)$_2$ (Λ-75) by chiral HPLC using racemic Λ-[Ru(bpy)(dmb)(dbb)](PF$_6$)$_2$ as reference. The ruthenium complex was analyzed with a Chiralpak (250 × 4.6 mm) IB HPLC column on an Agilent 1200 Series HPLC System. The flow rate was 0.5 mL / min, the column temperature 40 °C, and UV-absorption was measured at 254 nm. Solvent A = 0.1% TFA (aq), solvent B = MeCN, with a linear gradient of 30% to 35% B in 20 min.

5.2.2 Synthesis of Dinuclear Ruthenium Complexes
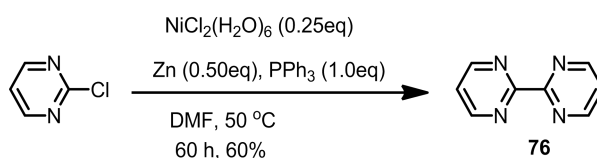
2,2'-Bipyrimidine (76) This compound was synthesized according to the reported procedures with some modification.[78] Triphenylphosphine (9.2 g, 35 mmol), NiCl$_2$(H$_2$O)$_6$ (2.1 g, 8.8 mmol), and zinc powder (1.14 g, 17.5 mmol) were mixed in a 250 mL Schlenk flask, and put under high vacuum for 1 h, and then freshly distilled DMF (150 mL) was added to the mixture under argon. Under vigorous stirring at room temperature, the heterogeneous solution turned first red after a few minutes and then gradually brownish. After 1 h, freshly sublimated 2-chloropyrimidine (4 g, 35 mmol) was added through a funnel under argon and the solution turned darker. The reaction mixture was stirred vigorously for 1 h at room temperature, then heated at 50 °C for 60 h. The resulting suspension was filtered through Celite and washed with chloroform (150 mL), the filtrate was collected and dried under reduced pressure. The resulting dark green residue was suspended in a solution of EDTA (15 g) in aqueous NH$_3$ (40 mL, 7%). The aqueous solution was extracted with diethyl ether (3×20 mL) and subsequently with chloroform (8×15 mL). The organic solvents were dried over Na$_2$SO$_4$ and evaporated under reduced pressure. The diethyl ether solution contained almost pure triphenylphosphine. The chloroform solution was concentrated and yielded **76** as a pale-yellow solid, which was recrystallized from ethanol as off-white plates: 2.25 g (82%).

^{1}H-NMR (CDCl$_3$, 400 MHz): δ (ppm) 8.93 (d, J = 4.8 Hz, 4H), 7.36 (t, J = 4.8 Hz, 2H). ^{13}C-NMR(CDCl$_3$, 100 MHz): δ (ppm) 162.0, 157.8, 121.4.
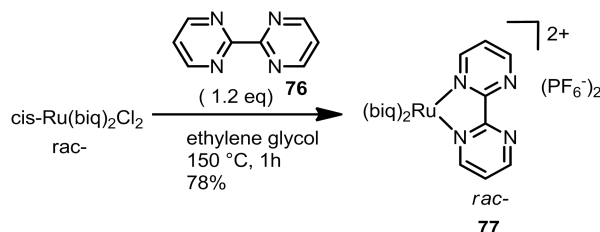
rac-Bis(2,2'-biquinoline)-(2,2'-bipyrimidine)ruthenium(II) bis(hexafluorophosphate) (77) In a closed brown vial (10 mL) fitted with a septum, a solution of *cis*-Ru(biq)$_2$Cl$_2$ (0.105 g, 0.153 mmol) and bipyrimidine **76** (37 mg, 0.170 mmol) in ethylene glycol (5 mL) was degassed with argon for 10 min and then heated at 150 °C (oil bath temperature) in the dark for 1 h. In order to get rid of the most ethylene glycol and make the subsequent purification easier, 25 mL water was added to the reaction mixture after it was cooled to room temperature, then the purple red solution was precipitated by the addition of excess solid NH$_4$PF$_6$. The deep purple suspended solid (crude product) was collected, dissolved in CH$_3$CN (5 mL) and subjected to silica gel chromatography (eluent : CH$_3$CN, CH$_3$CN: H$_2$O: KNO$_3$ (sat) = 200:3:1, CH$_3$CN: H$_2$O: KNO$_3$ (sat) = 100:3:1). The product eluents were concentrated and dissolved in a mixture of ethanol/water (12 mL/4 mL), and the product was precipitated by the addition of excess solid NH$_4$PF$_6$. The precipitate was centrifuged, washed twice with water (2 × 10 mL), and dried under high vacuum to afford the purple solid **77** (127 mg, 78%).

^{1}H-NMR (CD$_3$CN, 300 MHz): δ (ppm) 9.06 (d, J = 8.9 Hz, 2H), 8.99 (d, J = 8.9 Hz, 2H), 8.88 (d, J = 8.9 Hz, 2H), 8.73 (dd, J = 4.7, 1.8 Hz, 2H), 8.57 (d, J = 8.7 Hz, 2H), 8.26 (dd, J = 5.9, 1.9 Hz, 2H), 8.16 (d, J = 8.2 Hz, 2H), 7.93 (d, J = 7.7 Hz, 2H), 7.54 (m, 4H), 7.45 (t, J = 6.8 Hz, 2H), 7.33 (d, J = 8.9 Hz, 2H), 7.10 (dd, J = 9.0, 7.3 Hz, 2H), 7.02 (t, J = 7.7 Hz, 2H), 6.94 (d, J = 8.9 Hz, 2H). ^{13}C-NMR (75 MHz, CD$_3$CN): δ (ppm) 162.2, 161.6, 157.3, 152.6, 152.5, 151.0, 141.2, 139.9, 139.6, 133.7, 131.6, 130.8, 130.5, 130.3, 130.00, 129.6, 128.5, 126.7, 126.2, 123.6, 123.5, 122.6. IR (neat): ν (cm^{-1}) 1597, 1505, 1431, 1369, 1247, 1213, 1146, 1098, 830, 812, 782, 767, 750,

632, 556, 516, 482, 437. HRMS calcd for $C_{44}H_{30}F_6N_8PRu$ (M-PF$_6$)$^+$: 917.1279, found: 917.1292.

rac-Bis(2,2'-biquinoline)-(µ-2,2'-bipyrimidine)-bis(2,2'-bipyridine)ruthenium(II) tetra(hexafluorophosphate) (78) In a closed brown vial (10 mL) fitted with a septum, a solution of **77** (106 mg, 0.100 mmol) and *cis*-Ru(bpy)$_2$Cl$_2$ (121 mg, 0.250 mmol) in ethylene glycol (5 mL) was degassed with argon for 10 min and then heated at 150 ^{o}C (oil bath temperature) in the dark for 3 h. 20 mL water was added to the reaction mixture after it was cooled to room temperature, then the dark brown solution was precipitated by the addition of excess solid NH$_4$PF$_6$. The crude product was collected, dissolved in CH$_3$COCH$_3$ (3 mL) and subjected to silica gel chromatography (eluent : CH$_3$COCH$_3$: H$_2$O : KNO$_3$ (sat) = 20 : 3 : 1, CH$_3$COCH$_3$: H$_2$O : KNO$_3$ (sat) = 10 : 3 : 1). The product eluents were concentrated and dissolved in nearly 12 mL of water, subsequently, the product was precipitated by the addition of excess solid NH$_4$PF$_6$. The precipitate was centrifuged, washed twice with water (2 × 10 mL), and dried under high vacuum to afford the dark solid **78** (94 mg, 53%) as a mixture of two diastereomers.

^{1}H-NMR (CD$_3$COCD$_3$, 300 MHz): δ (ppm) 9.42 (d, J = 8.9 Hz, 1H), 9.34 (d, J = 4.7 Hz, 1H), 9.31 (d, J = 4.7 Hz, 1H), 9.17 (m, 3H), 8.99 (d, J = 8.8 Hz, 1H), 8.91 (ddd, J = 5.8, 3.9, 1.3 Hz, 2H), 8.76 (d, J = 8.7 Hz, 1H), 8.62 (m, 4H), 8.23 (m, 10H), 7.92 (t, J = 7.5 Hz, 1H), 7.81 (t, J = 5.8 Hz, 1H), 7.75 (t, J = 5.8 Hz, 1H), 7.52 (m, 11H), 7.21 (m, 5H), 6.99 (d, J = 4.9 Hz, 1H), 6.86 (ddd, J = 8.8, 7.0, 1.3 Hz, 1H), 6.65 (d, J = 4.9 Hz, 1H). IR (neat): v (cm^{-1}) 1595, 1504, 1429, 1367, 1249, 1215, 1145, 1097, 831, 817, 786, 769, 749, 631, 557, 517, 485, 439. HRMS calcd for $C_{64}H_{46}F_{18}N_{12}P_3Ru_2$

$(M-PF_6)^+$: 1621.0981, found:1621.1002.
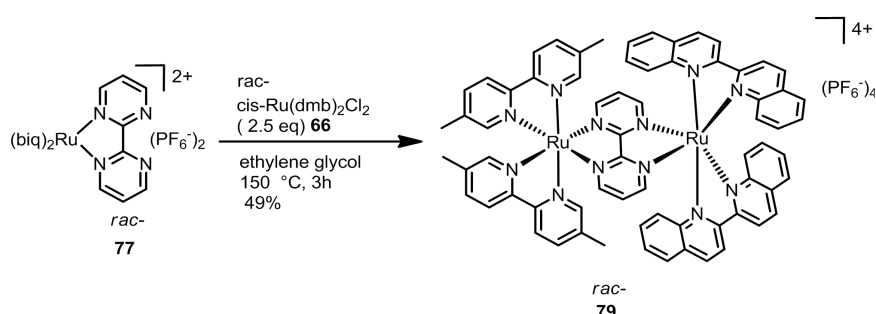
*rac-*Bis(2,2'-biquinoline)-(μ-2,2'-bipyrimidine)-bis(4,4'-dimethyl-2,2'-bipyridine) ruthenium(II) tetra(hexafluorophosphate) (79) In a closed brown vial (10 mL) fitted with a septum, a solution of 77 (106 mg, 0.100 mmol) and *cis*-Ru(dmb)$_2$Cl$_2$ (dmb : 4,4'-dimethyl-2,2'-bipyridine) (135 mg, 0.250 mmol) in ethylene glycol (5 mL) was degassed with argon for 10 min and then heated at 150 °C (oil bath temperature) in the dark for 3 h. 20 mL water was added to the reaction mixture after it was cooled to room temperature, then the dark brown solution was precipitated by the addition of excess solid NH$_4$PF$_6$. The crude product was collected, dissolved in CH$_3$COCH$_3$ (3 mL) and subjected to silica gel chromatography (eluent : CH$_3$COCH$_3$: H$_2$O : KNO$_3$ (sat) = 20 : 3 : 1, CH$_3$COCH$_3$: H$_2$O : KNO$_3$ (sat) = 10 : 3 : 1). The product eluents were concentrated and dissolved in nearly 15 mL of water, and the product was precipitated by the addition of excess solid NH$_4$PF$_6$. The precipitate was centrifuged, washed twice with water (2 × 10 mL), and dried under high vacuum to afford the dark solid racemic 79 (94 mg, 49%) as a single diastereomer.

^{1}H-NMR (CD$_3$COCD$_3$, 300 MHz): δ (ppm) 9.43 (d, J = 8.9 Hz, 2H), 9.38 (d, J = 8.9 Hz, 2H), 9.20 (d, J = 8.9 Hz, 2H), 9.08 (d, J = 8.9 Hz, 2H), 8.88 (dd, J = 6.0, 1.3 Hz, 2H), 8.47 (s, 2H), 8.44 (s, 2H), 8.27 (dd, J = 3.6, 1.2 Hz, 2H), 8.24 (dd, J = 3.6, 1.2 Hz, 2H), 8.19 (dd, J = 5.8, 1.4 Hz, 2H), 7.98 (dd, J = 8.5, 1.1 Hz, 2H), 7.93 (dd, J = 8.5, 1.1 Hz, 2H), 7.80 (t, J = 5.9 Hz, 2H), 7.56 (td, J = 7.6, 1.0 Hz, 2H), 7.50 (d, J = 9.0 Hz, 2H), 7.37 (td, J = 7.6, 1.2 Hz, 2H), 7.32 (m, 2H), 7.23 (d, J = 8.8 Hz, 2H), 7.11 (td, J = 8.1, 1.5 Hz, 2H), 6.90 (m, 4H), 2.17 (s, 6H), 2.07 (s, 6H). IR (neat): v (cm^{-1}) 1605, 1596, 1505, 1475, 1431, 1369, 1247, 1241, 1213, 1146, 1098, 830, 812,

782, 767, 750, 727, 632, 556, 520, 482, 434. HRMS calcd for $C_{68}H_{54}F_{24}N_{12}P_4Ru_2$ $(M-PF_6)^+$: 1822.1271, found: 1822.1297.
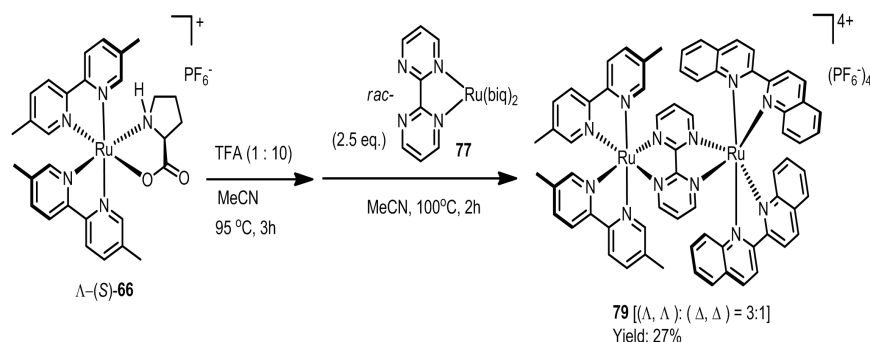
(Λ, Λ)-Bis(2,2'-biquinoline)-(μ-2,2'-bipyrimidine)-bis(4,4'-dimethyl-2,2'-bipyridine)ruthenium(II) tetra(hexafluorophosphate) (**79**) In a closed brown vial (5 mL) fitted with a septum, a solution of fresh diastereomerically pure compound Λ-(*S*)-**66** (100 mg, 0.137 mmol), and trifluoroacetic acid (TFA) (82 μL, 1.10mmol) in CH_3CN (1.37 mL) was heated at 95 °C (oil bath temperature) for 3 h under an argon atmosphere. The resulting brown solution was cooled to room temperature and **77** (18.6 mg, 0.10 mmol) was added. Then, the mixture was purged with argon for 10 min and heated at 100 °C in the dark for another 2 h. The reaction mixture was cooled to room temperature and subjected to silica gel chromatography (eluent : CH_3COCH_3 : H_2O : KNO_3 (sat) = 20 : 3 : 1, CH_3COCH_3 : H_2O : KNO_3 (sat) = 10 : 3 : 1). The product eluents were concentrated and dissolved in nearly 12 mL of water, and the product was precipitated by the addition of excess solid NH_4PF_6. The precipitate was centrifuged, washed twice with water (2 × 10 mL), and dried under high vacuum to afford the dark solid **79** (94 mg, 49%) with an enantiopurity of 50% {(Λ, Λ) : (Δ, Δ) = 3 : 1}. NMR data, IR and HR-MS of the enantiomerically enriched (Λ, Λ)-**79** were identical to *rac*-**79**.

5.3 Synthesis of Octahedral Silicon Complexes

5.3.1 Synthesis of Silicon Precursor Complexes and Ligands

81
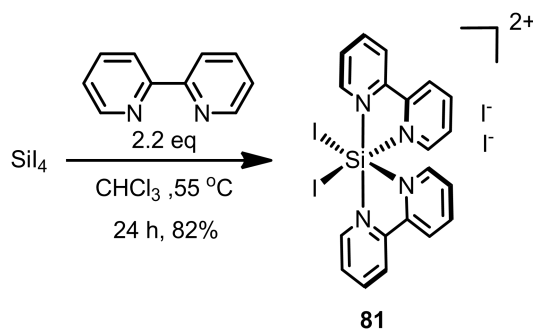
***cis*-Bis(2,2'-bipyridine)diiodosilicon(IV) diiodide** (**81**) A suspension of silicon(IV) iodide (1.0 g, 1.0 eq., 1.87 mmol) and 2,2′-bipyridine (0.65 g, 2.2 eq., 4.11 mmol) in dry $CHCl_3$ (30 mL) was purged with N_2 for 15 min and was then heated to 55 °C for 24 hours under N_2. The resulting brownish red suspension was cooled to room temperature and centrifuged to remove the solvent. The solid was washed with dry $CHCl_3$ (3 × 15 mL), and then it was dried under high vacuum to afford the brownish red solid **81** (1.35 g, 82%). The complex was stored under argon in -20 °C freezer and used directly for the next step without further purification.

82
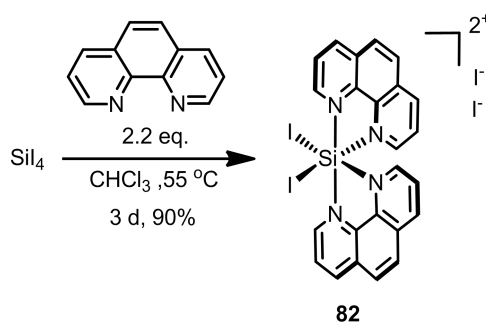
***cis*-Bis(1,10-phenanthroline)diiodosilicon(IV) diiodide** (**82**) A suspension of silicon(IV) iodide (1.0 g, 1.0 eq., 1.87 mmol) and 1,10-phenanthroline (0.74 g, 2.2 eq., 4.11 mmol) in dry $CHCl_3$ (30 mL) was purged with N_2 for 15 min and was then heated to 55 °C for 3 days under N_2. The resulting dark red suspension was cooled to room temperature and centrifuged to remove the solvent. The solid was washed with

dry CHCl$_3$ (3 × 15 mL), MeOH (15mL) and Et$_2$O (30 mL × 2) successively, and then it was dried under high vacuum to afford the dark red solid **82** (1.56 g, 90%). The complex was stored under argon in -20 °C freezer and used directly for the next step without further purification.

83
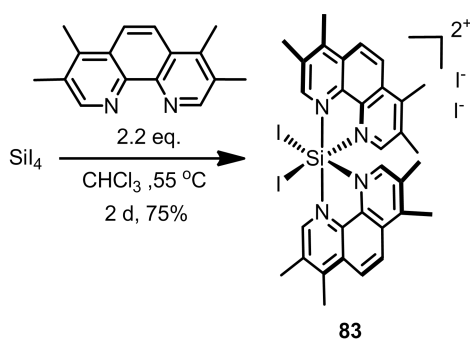
***cis*-Bis(3,4,7,8-tetramethyl-1,10-phenanthroline)diiodosilicon(IV)   diiodide   (83)**
A   suspension   of   silicon(IV)   iodide   **80**   (1.0   g,   1.0   eq.,   1.87   mmol)   and 3,4,7,8-tetramethyl-1,10-phenanthroline (0.97 g, 2.2 eq., 4.11 mmol) in dry CHCl$_3$ (30 mL) was purged with N$_2$ for 15 min and was then heated to 55 °C for 2 days under N$_2$. The resulting deep red suspension was cooled to room temperature and centrifuged to remove the solvent. The solid was washed with dry CHCl$_3$ (3 × 15 mL), and then it was dried under high vacuum to afford the deep red solid **83** (1.48 g, 75%). The complex was stored under argon in -20 °C freezer and used directly for the next step without further purification.

84
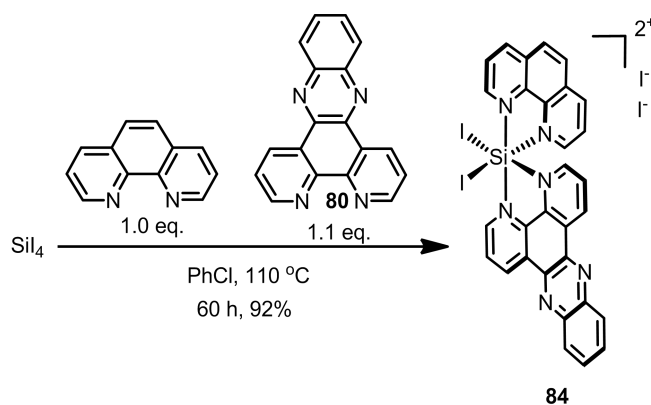
***cis*-(dipyrido[3,2-a:2',3'-c]phenazine)(1,10-phenanthroline)diiodosilicon(IV)**

diiodide (84) A suspension of silicon(IV) iodide (1.52 g, 1.0 eq., 2.83 mmol), 1,10-phenanthroline (0.51 g, 1.0 eq., 2.83 mmol) and dipyrido[3,2-a:2',3'-c]phenazine **80** (0.88 g, 1.1 eq., 3.12 mmol) in dry PhCl (40 mL) was purged with N_2 for 15 min and was then heated to 110 °C for 60 hours under N_2. The resulting pale red suspension was cooled to room temperature and centrifuged to remove the solvent. The solid was washed with dry $CHCl_3$ (3 × 15 mL), and then it was dried under high vacuum to afford the pale red solid **84** (2.6 g, 92%). The complex was stored under argon in -20 °C freezer and used directly for the next step without further purification.
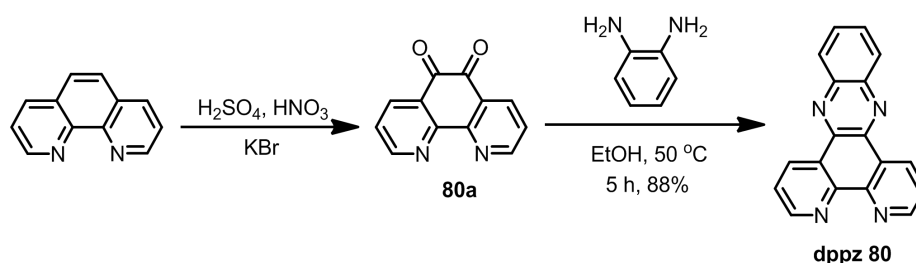
1,10-Phenanthroline-5,6-dione (80a) This compound was synthesized according to the reported procedures with some modification.[88] An ice cold mixture of concentrated H_2SO_4 (40 mL) and HNO_3 (20 mL) was added to 4.0 g of 1,10-phenanthroline and 4.0 g of KBr. The mixture was heated at reflux for 3 h. The hot yellow solution was poured over 500 g of ice and neutralized carefully with NaOH until it reached a pH of 5. Extraction with $CHCl_3$ (3 × 100 mL) followed by drying over Na_2SO_4 and removal of solvent gave 4.5 g (96%) of **80a**. This product could be further purified by recrystallization in ethanol.

^{1}H-NMR (400 MHz, $CDCl_3$) δ (ppm) 9.14 (d, J = 4.6 Hz, 2H), 8.53 (d, J = 7.8 Hz, 2H), 7.62−7.59 (m, 2H).

Dipyrido[3,2-a:2',3'-c]phenazine (80) This compound was synthesized according to the reported procedures.[89] A solution of 1,10-phenanthroline-5,6-dione **80a** (210.0 mg, 1.0 mmol) and 1,2-diaminobenzene (130.0 mg, 1.2 mmol) in ethanol (100.0 mL) was stirred for 5 h at 50 °C. The solvent was removed under vacuum and the residue was subjected to silicon column chromatography (dichloromethane / methanol, 10/1, V/V).

Compound **80** was obtained as a off-white solid (250.0 mg, 88%).

^{1}H-NMR (400 MHz, CDCl$_3$) δ (ppm) 9.65 (d, J = 8.0 Hz, 2H), 9.29 (d, J = 8.0 Hz, 2H), 8.34-8.36 (m, 2H), 7.92-7.94 (m, 2H), 7.79-7.82 (m, 2H).
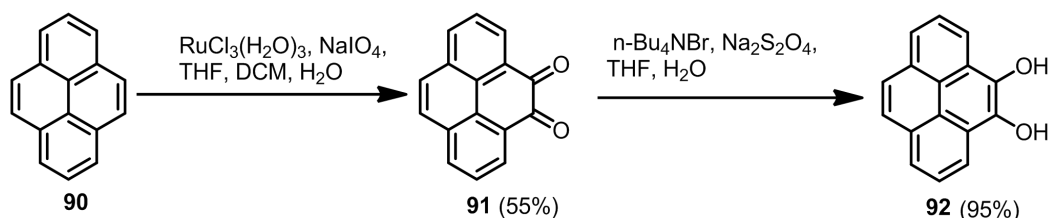
Pyrene-4,5-dione (**91**) This compound was synthesized according to the reported procedures.[80] To a solution of pyrene **90** (2.00 g. 10.0 mmol) in CH$_2$Cl$_2$ (40 mL) and THF (40 mL) were added NaIO$_4$ (9.53g, 44.5 mmol), H$_2$O (50 mL) and RuCl$_3$·3H$_2$O (0.25 g, 1.0 mmol). The dark brown suspension was stirred at room temperature for 3 h. The reaction mixture was then poured into H$_2$O (400 mL), and the aqueous phase was extracted with CH$_2$Cl$_2$ (3 × 50 mL). The CH$_2$Cl$_2$ extracts were combined and washed with H$_2$O (3 × 200 mL) to give a dark orange-red solution. The solvent was removed under reduced pressure to afford a dark residue, which was further purified by silica gel column chromatography (non-pressurized, eluent = CH$_2$Cl$_2$), and the product eluents were concentrated to dryness, dried under high vacuum to afford **91** as bright orange crystals (1.28 g, 55%).

^{1}H-NMR (300 MHz, CDCl$_3$): δ (ppm) 8.40 (dd, J = 7.3, 1.0 Hz, 2H), 8.10 (dd, J = 7.9, 1.0 Hz, 2H), 7.76 (s, 2H), 7.69 (t, J = 7.8 Hz, 2H). ^{13}C-NMR (75 MHz, CDCl$_3$): δ (ppm) 135.6, 131.9, 130.1, 130.0, 128.3, 127.9, 127.2.

Pyrene-4,5-diol (**92**) To a solution of the **91** (1.0 g, 4.28 mmol) in THF (20 mL) and H$_2$O (20 mL) were added tetra-*n*-butylammonium bromide (0.42 g, 1.3 mmol) and Na$_2$S$_2$O$_4$ (2.25 g, 13.0 mmol), the resulting suspension was stirred at room temperature under argon for 5 min. The reaction mixture was poured into H$_2$O (40 mL) and the aqueous phase was extracted with EtOAc (3 × 20 mL). The EtOAc extracts were combined and washed with H$_2$O (20 mL), and brine (20 mL) to give a colorless solution, which was concentrated to afford a dark solid **92** (95%). The crude product

was oxygen sensitive and used directly for the next step without further purification.

93   RuCl₃(H₂O)₃, NaIO₄, THF, DCM, H₂O   **94** (45%)   n-Bu₄NBr, Na₂S₂O₄, THF, H₂O   **95** (92%)
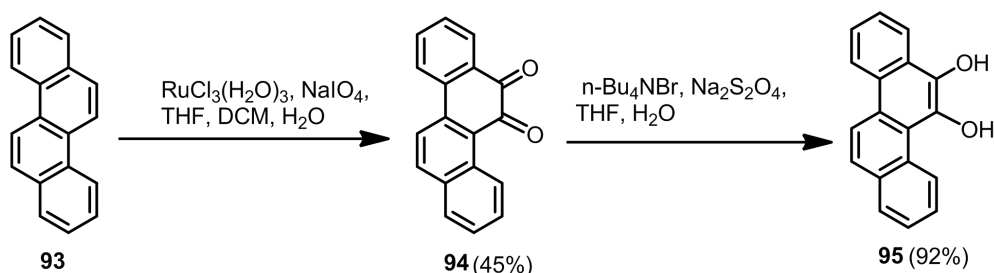
Chrysene-5,6-dione (94) This compound was prepared similarly as compound **91**. To a solution of chrysene **93** (2.28 g. 10.0 mmol) in CH_2Cl_2 (40 mL) and THF (40 mL) were added $NaIO_4$ (9.53g, 44.5 mmol), H_2O (50 mL) and $RuCl_3 \cdot 3H_2O$ (0.25 g, 1.0 mmol). The dark brown suspension was stirred at room temperature for 3 h, and then the reaction mixture was poured into H_2O (400 mL). The aqueous phase was extracted with CH_2Cl_2 (3 × 50 mL), and the CH_2Cl_2 extracts were combined, washed with H_2O (3 × 200 mL) to give a dark orange solution. The solution was concentrated to afford a dark residue, which was further purified by silica gel column chromatography (non-pressurized, eluent = CH_2Cl_2), and the product eluents were concentrated affording **94** as bright orange crystals (1.16 g, 45%).

^{1}H-NMR (500 MHz, CDCl₃): δ (ppm) 7.52 (t, J = 7.5 Hz, 1H), 7.60 (t, J = 7.7 Hz, 1H), 7.74 (t, J = 8.5 Hz, 1H), 7.77 (t, J = 8.1 Hz, 1H), 7.87 (d, J = 7.9 Hz, 1H), 8.12 (d, J = 8.6 Hz, 2H), 8.18 (d, J = 7.4 Hz, 1H), 8.20 (d, J = 8.6 Hz, 1H), 9.43 (d, J = 8.8 Hz, 1H). ^{13}C-NMR (125 MHz, CDCl₃): δ (ppm) 121.54, 125.64, 126.34, 127.62, 128.09, 129.09, 130.32, 130.45, 131.09, 131.28, 132.67, 134.23, 136.49, 137.06, 137.78, 138.29, 182.45, 184.63.

Chrysene-5,6-diol (95) To a solution of the **94** (1.0 g, 3.87 mmol) in THF (20 mL) and H_2O (20 mL) were added tetra-*n*-butylammonium bromide (0.38 g, 1.18 mmol) and $Na_2S_2O_4$ (2.04 g, 11.8 mmol), the resulting suspension was stirred at room temperature under argon for 5 min. Subsequently, the reaction mixture was poured into H_2O (40 mL) and the aqueous phase was extracted with EtOAc (3 × 20 mL). The EtOAc extracts were combined and washed with H_2O (20 mL), brine (20 mL) to give

a colorless solution. The solution was concentrated to afford the crude product, a dark solid **95** (92%), which was oxygen sensitive and used directly for the next step without further purification.

5.3.2 Synthesis of Octahedral Silicon Complexes
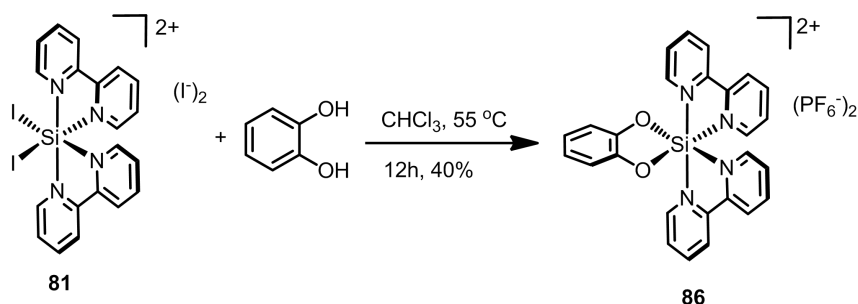
Bis(2,2'-bipyridine)catecholatosilicon(IV) bis(hexafluorophosphate) (86) A suspension of [Si(bpy)$_2$I$_2$]I$_2$ (**81**) (200 mg, 0.225 mmol) and 4 equivalents of catechol (100 mg, 0.90 mmol) in dry CHCl$_3$ (30 mL) was purged with N$_2$ for 15 min and then stirred at 55 °C (oil bath temperature) for 12 hours. The resulting dark-brown suspension was cooled to room temperature and the solvent was removed *in vacuo*. The residue was dissolved in 3 mL mixed solvent {CH$_3$CN : H$_2$O : KNO$_3$(sat) = 50 : 3 : 1} and subjected to silica gel chromatography with first CH$_3$CN, then switched to CH$_3$CN : H$_2$O : KNO$_3$(sat) = 100 : 3 : 1 and CH$_3$CN : H$_2$O : KNO$_3$(sat) = 50 : 3 : 1. The product eluents were concentrated and redissolved in 10 mL water, and the product was precipitated by the addition of excessive solid NH$_4$PF$_6$. The precipitate was centrifuged, washed twice with water (2 × 10 mL) and dried afford the pure diolate complex **86** as a pale-yellow solid (66 mg, 40%).

^{1}H-NMR (300 MHz, CD$_3$CN): δ (ppm) 9.07 (ddd, J = 5.8; 1.4, 0.7 Hz, 2H), 8.91 (m, 2H), 8.80 (m, 4H), 8.60 (dt, J = 7.9, 1.4 Hz, 2H), 8.16 (ddd, J = 7.7, 5.9, 1.2 Hz, 2H), 7.80 (ddd, J = 7.7, 6.0, 1.3 Hz, 2H), 7.58 (ddd, J = 5.9, 1.2, 0.7 Hz, 2H), 6.78 (m, 4H); ^{13}C-NMR (75 MHz, CD$_3$CN): δ (ppm) 148.63, 148.35, 148.02, 146.91, 146.16, 144.86, 144.13, 131.88, 131.36, 126.16, 125.92, 123.02, 114.66. IR (neat): v (cm^{-1}) 2934, 1674, 1592, 1482, 1454, 1443, 1387, 1335, 1283, 1242, 1179, 1140, 1104, 994,

979, 952, 927, 909, 838, 747, 730, 695, 675, 613, 588, 557, 534, 521, 502, 470, 455, 422, 410, 394, 384. HRMS calcd for $C_{26}H_{20}F_6N_4O_2PSi$ (M-PF$_6$)$^+$ 593.0992, found: 593.0982.
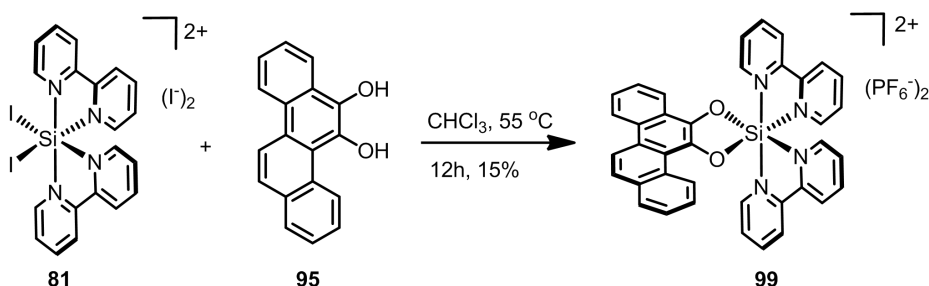
Bis(2,2'-bipyridine)-(5,6-chrysenediolato)silicon(IV)   bis(hexafluorophosphate) (99) A suspension of [Si(bpy)$_2$I$_2$]I$_2$ (**81**) (300 mg, 0.35 mmol) and 4 equivalents of chrysene-5,6-diol (**95**) (370 mg, 1.40 mmol) in dry CHCl$_3$ (40 mL) was purged with N$_2$ for 15 min and then stirred at 55 °C (oil bath temperature) for 12 hours. The resulting dark-brown suspension was cooled to room temperature and the solvent was removed *in vacuo*. The residue was dissolved in 3 mL mixed solvent {CH$_3$CN : H$_2$O : KNO$_3$(sat) = 50 : 3 : 1} and subjected to silica gel chromatography with first CH$_3$CN, then switched to CH$_3$CN : H$_2$O : KNO$_3$(sat) = 100 : 3 : 1 and CH$_3$CN : H$_2$O : KNO$_3$(sat) = 50 : 3 : 1. The product eluents were concentrated and redissolved in 10 mL water, and the product was precipitated by the addition of excessive solid NH$_4$PF$_6$. The precipitate was centrifuged, washed twice with water (2 × 10 mL) and dried under high vacuum to afford the pure diolate complex **99** as a pale-yellow solid (47 mg, 15%).

^{1}H-NMR (300 MHz, CD$_3$CN): δ (ppm) 9.20 (d, J = 8.6 Hz, 1H), 9.09 (dd, J = 5.9, 1.4 Hz, 1H), 9.07 (dd, J = 5.9, 1.4 Hz, 1H), 8.93 (m, 3H), 8.90 (d, J = 7.9 Hz, 1H), 8.81 (m, 1H), 8.76 (d, J = 8.6 Hz, 1H), 8.70 (m, 4H), 8.01 (ddd, J = 7.7, 5.9, 1.2 Hz, 1H), 7.95 (m, 5H), 7.89 (ddd, J = 7.8, 5.9, 1.3 Hz, 1H), 7.79 (dd, J = 5.9, 1.3 Hz, 1H), 7.72 (dd, J = 5.9, 1.2 Hz, 1H), 7.61 (m, 2H), 7.57 (ddd, J = 8.0, 6.9, 1.1 Hz, 1H), 7.37 (ddd, J = 8.0, 7.0, 1.6 Hz, 1H). ^{13}C-NMR (75 MHz, CD$_3$CN): δ (ppm) 148.8, 148.5, 148.10, 148.06, 146.42, 146.37, 145.1, 145.0, 144.1, 144.0, 139.7, 139.6, 133.7, 132.1, 132.0, 131.6, 131.4, 130.3, 128.9, 128.6, 127.8, 127.60. 127.57, 127.2, 126.8, 126.3, 126.15,

126.12, 126.0, 125.9, 124.6, 124.1, 122.6, 121.6, 120.9. IR (neat): v (cm^{-1}) 1619, 1579, 1509, 1480, 1450, 1392, 1321, 1249, 1173, 1126, 1070, 1036, 1006, 828, 767, 729, 684, 651, 587, 554, 515, 489, 461, 426. HRMS calcd for $C_{38}H_{26}F_6N_4O_2PSi$ (M-PF$_6$)$^+$ 743.1467, found: 743.1487.
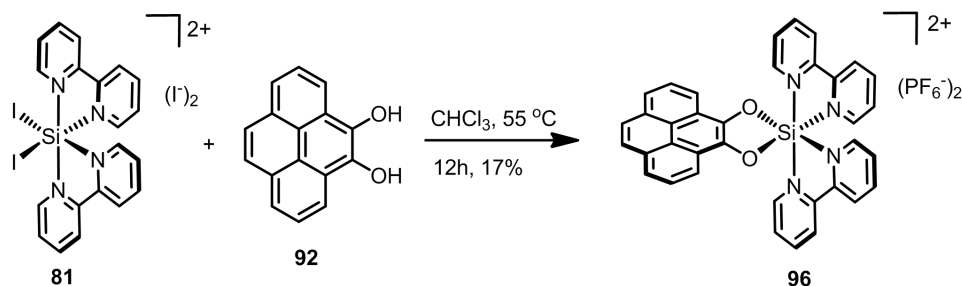
Bis(2,2'-bipyridine)-(4,5-pyrenediolato)silicon(IV) bis(hexafluorophosphate) (**96**)
A suspension of [Si(bpy)$_2$I$_2$]I$_2$ (**81**) (300 mg, 0.35 mmol) and 4 equivalents of pyrene-4,5-diol (**92**) (328 mg, 1.40 mmol) in dry CHCl$_3$ (40 mL) was purged with N$_2$ for 15 min and then stirred at 55 °C (oil bath temperature) for 12 hours. The resulting dark-brown suspension was cooled to room temperature and the solvent was removed *in vacuo*. The residue was dissolved in 3 mL mixed solvent {CH$_3$CN : H$_2$O : KNO$_3$(sat) = 50 : 3 : 1} and subjected to silica gel chromatography with first CH$_3$CN, then switched to CH$_3$CN : H$_2$O : KNO$_3$(sat) = 150 : 3 : 1 and CH$_3$CN : H$_2$O : KNO$_3$(sat) = 80 : 3 : 1. The product eluents were concentrated and redissolved in 12 mL water, and the product was precipitated by the addition of excessive solid NH$_4$PF$_6$. The precipitate was centrifuged, washed twice with water (2 × 12 mL) and dried to afford the pure diolate complex **96** as a pale-brown solid (50 mg, 17%).
^{1}H-NMR (300 MHz, CD$_3$CN): δ (ppm) 9.12 (d, J = 5.8 Hz, 2H), 8.95 (d, J = 8.1 Hz, 2H), 8.91 (d, J = 8.1 Hz, 2H), 8.68 (m, 4H), 8.14 (dd, J = 7.6, 1.2 Hz, 2H), 8.10 (m, 4H), 7.97 (m, 4H), 7.90 (ddd, J = 7.6, 6.0, 1.2 Hz, 2H), 7.75 (d, J = 5.9 Hz, 2H).
^{13}C-NMR (75 MHz, CD$_3$CN): δ (ppm) 148.9, 148.4, 148.0, 146.3, 145.1, 144.1, 138.0, 132.3, 132.0, 131.4, 128.6, 127.1, 126.1, 126.0, 124.8, 125.3, 122.0, 118.7. IR (neat): v (cm^{-1}) 1617, 1601, 1574, 1508, 1477, 1454, 1399, 1368, 1324, 1315, 1249, 1216, 1174, 1103, 1072, 1057, 1042, 906, 830, 798, 772, 740, 717, 685, 664, 643, 596, 583, 556, 517, 506, 486, 465, 444, 432, 420, 395. HRMS calcd for $C_{36}H_{24}F_6N_4O_2PSi$

(M-PF$_6$)$^+$ 717.1310, found: 717.1317.
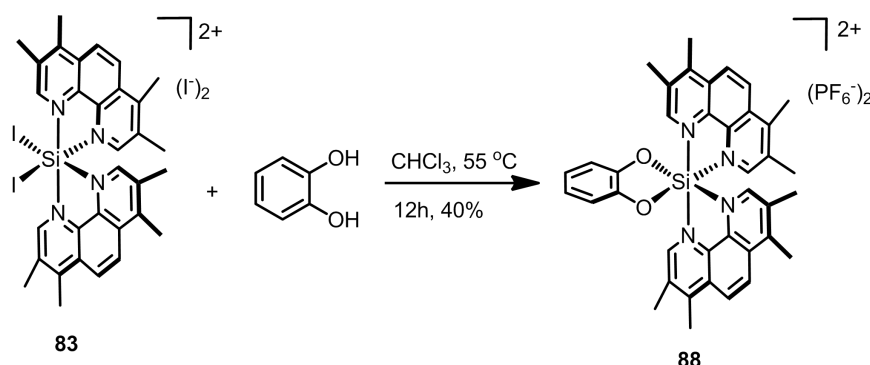
83   **88**

Bis(3,4,7,8-tetramethyl-1,10-phenanthroline)catecholatosilicon(IV) bis(hexafluorophosphate) (88) A suspension of [Si(phen*)$_2$I$_2$]I$_2$ (**83**) (300 mg, 0.30 mmol) and 4 equivalents of catechol (132 mg, 1.2 mmol) in dry CHCl$_3$ (30 mL) was purged with N$_2$ for 15 min and then stirred at 55 °C (oil bath temperature) for 12 hours. The resulting dark-brown suspension was cooled to room temperature and the solvent was removed *in vacuo*. The residue was dissolved in 4 mL mixed solvent {CH$_3$CN : H$_2$O : KNO$_3$(sat) = 80 : 3 : 1} and subjected to silica gel chromatography with first CH$_3$CN, then switched to CH$_3$CN : H$_2$O : KNO$_3$(sat) = 200 : 3 : 1 and CH$_3$CN : H$_2$O : KNO$_3$(sat) = 80 : 3 : 1. The product eluents were concentrated and redissolved in a mixture of water/ethanol (10 mL/2 mL), and the product was precipitated by the addition of excessive solid NH$_4$PF$_6$. The precipitate was centrifuged, washed twice with water (2 × 10 mL) and dried to afford the pure diolate complex **88** as a yellow solid (108 mg, 40%).

^{1}H-NMR (300 MHz, CD$_3$CN): δ (ppm) 9.09 (s, 2H), 8.64 (d, *J* = 9.6 Hz, 2H), 8.56 (d, *J* = 9.6 Hz, 2H), 7.36 (s, 2H), 6.80 (m, 2H), 6.72 (m, 2H), 3.03 (s, 6H), 2.84 (s, 6H), 2.68 (s, 6H), 2.30 (s, 6H). ^{13}C-NMR (75 MHz, CD$_3$CN): δ (ppm) 157.7, 156.6, 148.4, 147.5, 146.2, 138.7, 138.1, 134.5, 133.6, 129.6, 129.2, 125.9, 125.8, 122.7, 114.4, 18.8, 18.3, 16.7, 16.3. IR (neat): *v* (cm^{-1}) 1625, 1524, 1482, 1439, 1390, 1328, 1246, 1018, 912, 828, 765, 742, 641, 556, 521, 464, 429. HRMS calcd for C$_{38}$H$_{36}$F$_6$N$_4$O$_2$PSi (M-PF$_6$)$^+$ 753.2249, found: 753.2257.
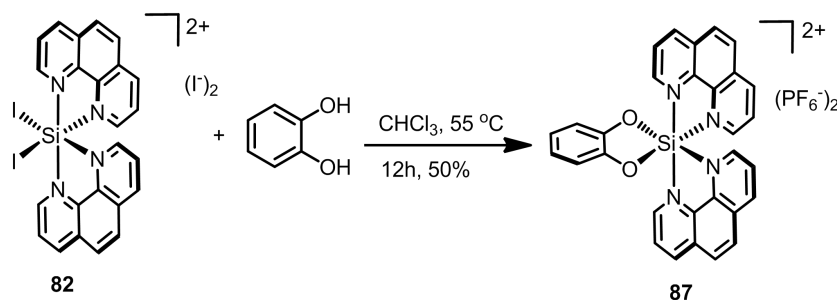
Bis(1,10-phenanthroline)catecholatosilicon(IV) bis(hexafluorophosphate) (**87**) A suspension of [Si(phen)$_2$I$_2$]I$_2$ (**82**) (200 mg, 0.22 mmol) and 4 equivalents of catechol (100 mg, 0.89 mmol) in dry CHCl$_3$ (20 mL) was purged with N$_2$ for 15 min and then stirred at 55 °C (oil bath temperature) for 12 hours. The resulting dark-brown suspension was cooled to room temperature and the solvent was removed *in vacuo*. The residue was dissolved in 4 mL mixed solvent {CH$_3$CN : H$_2$O : KNO$_3$(sat) = 50 : 3 : 1} and subjected to silica gel chromatography with first CH$_3$CN, then switched to CH$_3$CN : H$_2$O : KNO$_3$(sat) = 80 : 3 : 1 and CH$_3$CN : H$_2$O : KNO$_3$(sat) = 50 : 3 : 1. The product eluents were concentrated and redissolved in a mixture of water/ethanol (10 mL/1 mL), and the product was precipitated by the addition of excessive solid NH$_4$PF$_6$. The precipitate was centrifuged, washed twice with water (2 × 10 mL) and dried affording the pure diolate complex **87** as a pale-yellow solid (87 mg, 50%).

^{1}H-NMR (300 MHz, CD$_3$CN): δ (ppm) 9.47 (dd, J = 5.4, 1.1 Hz, 2H), 9.37 (dd, J = 8.3, 1.1 Hz, 2H), 9.10 (dd, J = 8.3, 1.0 Hz, 2H), 8.60 (d, J = 9.1 Hz, 2H), 8.51 (d, J = 9.1 Hz, 2H), 8.49 (dd, J = 8.3, 5.5 Hz, 2H), 7.92 (dd, J = 8.3, 5.5 Hz, 2H), 7.73 (dd, J = 5.5, 1.0 Hz, 2H), 6.81 (m, 4H). ^{13}C-NMR (75 MHz, CD$_3$CN): δ (ppm) 149.7, 147.5, 147.3, 147.0, 146.4, 135.8, 134.8, 131.4, 131.0, 129.7, 129.6, 129.3, 128.9, 123.0, 114.6. IR (neat): v (cm^{-1}) 3075, 1629, 1585, 1528, 1482, 1437, 1335, 1244, 1154, 1115, 1019, 884, 826, 759, 738, 714, 666, 620, 582, 554, 521, 484, 456, 416. HRMS calcd for C$_{30}$H$_{20}$F$_6$N$_4$O$_2$PSi (M-PF$_6$)$^+$ 641.1003, found: 641.0978.
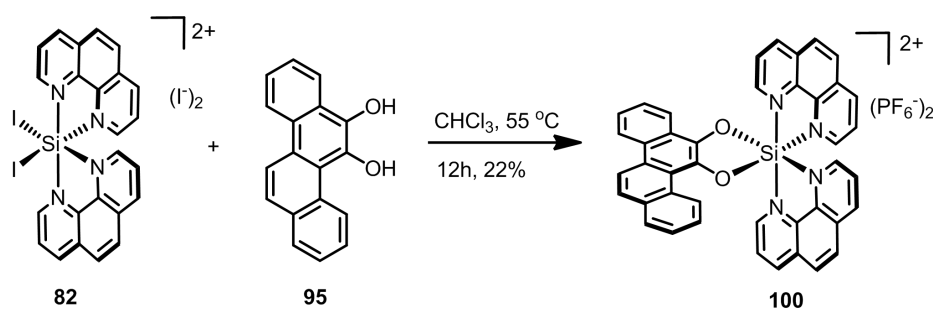
Bis(1,10-phenanthroline)-(5,6-chrysenediolato)silicon(IV)   bis(hexafluorophosphate) (100)   A suspension of [Si(phen)$_2$I$_2$]I$_2$ (**82**) (200 mg, 0.22 mmol) and 4 equivalents of chrysene-5,6-diol (**95**) (235 mg, 0.89 mmol) in dry CHCl$_3$ (20 mL) was purged with N$_2$ for 15 min and then stirred at 55 °C (oil bath temperature) for 12 hours. The resulting dark-brown suspension was cooled to room temperature and the solvent was removed *in vacuo*. The residue was dissolved in 3 mL mixed solvent {CH$_3$CN : H$_2$O : KNO$_3$(sat) = 50 : 3 : 1} and subjected to silica gel chromatography with first CH$_3$CN, then switched to CH$_3$CN : H$_2$O : KNO$_3$(sat) = 100 : 3 : 1 and CH$_3$CN : H$_2$O : KNO$_3$(sat) = 50 : 3 : 1. The product eluents were concentrated and redissolved in a mixture of water/ethanol (10 mL/2 mL), and the product was precipitated by the addition of excessive solid NH$_4$PF$_6$. The precipitate was centrifuged, washed twice with water (2 × 12 mL) and dried affording the pure diolate complex **100** as a dark-brown solid (45 mg, 22%).

^{1}H-NMR (300 MHz, CD$_3$CN): δ (ppm) 9.48 (dd, J = 5.4, 1.2 Hz, 1H), 9.44 (dd, J = 5.4, 1.2 Hz, 1H), 9.29 (dd, J = 4.5, 1.2 Hz, 1H), 9.28 (dd, J = 4.4, 1.2 Hz, 1H), 9.20 (m, 2H), 9.14 (dd, J = 8.4, 1.0 Hz, 1H), 8.79 (dd, J = 7.6, 1.4 Hz, 1H), 8.75 (d, J = 9.3 Hz, 1H), 8.56 (m, 4H), 8.34 (dd, J = 8.4, 5.4 Hz, 1H), 8.29 (dd, J = 8.4, 5.4 Hz, 1H), 8.05 (dd, J = 8.3, 5.5 Hz, 1H), 8.00 (dd, J = 8.3, 5.6 Hz, 1H), 7.93 (m, 4H), 7.82 (dd, J = 5.6, 1.1 Hz, 1H), 7.58 (m, 2H), 7.51 (ddd, J = 8.0, 7.0, 1.1 Hz, 1H), 7.26 (ddd, J = 8.6, 7.0, 1.5 Hz, 1H). ^{13}C-NMR (75 MHz, CD$_3$CN): δ (ppm) 149.9, 149.6, 147.9, 147.7, 146.8, 146.7, 146.4, 146.2, 134.0, 139.8, 135.8, 135.7, 134.6, 133.6, 131.3, 131.2, 131.1, 131.0, 130.2, 129.7, 129.6, 129.5, 129.2, 129.0, 128.92, 128.86, 128.80, 128.7, 128.6, 127.7, 127.4, 127.09, 127.06, 126.6, 126.1, 125.7, 124.5, 124.1, 122.5, 121.6, 120.9. IR (neat): v (cm^{-1}) 1625, 1584, 1528, 1501, 1436, 1357, 1220, 1153,

1109, 1044, 983, 882, 828, 760, 712, 664, 598, 551, 515, 477, 416. HRMS calcd for $C_{42}H_{26}F_6N_4O_2PSi$ $(M-PF_6)^+$ 791.1467, found: 791.1480.
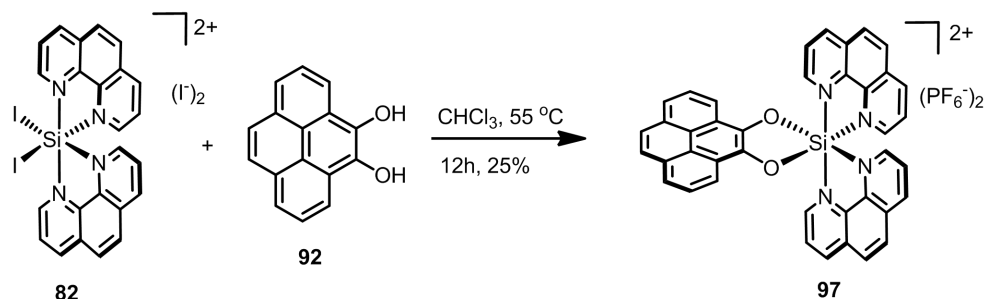
Bis(1,10-phenanthroline)-(4,5-pyrenediolato)silicon(IV) bis(hexafluorophosphate)
(97) A suspension of $[Si(phen)_2I_2]I_2$ (**82**) (200 mg, 0.22 mmol) and 4 equivalents of pyrene-5,6-diol (**92**) (208 mg, 0.89 mmol) in dry $CHCl_3$ (20 mL) was purged with N_2 for 15 min and then stirred at 55 °C (oil bath temperature) for 12 hours. The resulting dark-brown suspension was cooled to room temperature and the solvent was removed *in vacuo*. The residue was dissolved in 4 mL mixed solvent {CH_3CN : H_2O : KNO_3(sat) = 50 : 3 : 1} and subjected to silica gel chromatography with first CH_3CN, then switched to CH_3CN : H_2O : KNO_3(sat) = 100 : 3 : 1 and CH_3CN : H_2O : KNO_3(sat) = 50 : 3 : 1. The product eluents were concentrated and redissolved in a mixture of water/ethanol (12 mL/2 mL), and the product was precipitated by the addition of excessive solid NH_4PF_6. The precipitate was centrifuged, washed twice with water (2 × 10 mL) and dried affording the pure diolate complex **97** as a brown-red solid (48 mg, 25%).

^{1}H-NMR (300 MHz, CD_3CN): δ (ppm) 9.49 (dd, J = 5.4, 1.1 Hz, 2H), 9.29 (dd, J = 8.4, 1.1 Hz, 2H), 9.16 (dd, J = 8.3, 1.0 Hz, 2H), 8.59 (d, J = 9.1 Hz, 2H), 8.54 (d, J = 9.1 Hz, 2H), 8.31 (dd, J = 8.4, 5.4 Hz, 2H), 8.15-7.93 (m, 10H), 7.87 (dd, J = 5.5, 1.0 Hz, 2H). ^{13}C-NMR (75 MHz, CD_3CN): δ (ppm) 150.0, 147.7, 146.8, 146.4, 138.3, 135.9, 134.8, 132.3, 131.4, 131.1, 129.8, 129.7, 129.3, 129.0, 128.6, 127.1, 124.7, 124.4, 122.0, 118.8. IR (neat): v (cm^{-1}) 3110, 1625, 1600, 1585, 1529, 1435, 1399, 1363, 1312, 1215, 1154, 1117, 1097, 1037, 903, 886, 827, 797, 757, 738, 715, 668, 622, 587, 555, 524, 508, 481, 449, 429, 386. HRMS calcd for $C_{40}H_{24}F_6N_4O_2PSi$

(M-PF$_6$)$^+$ 765.1305, found: 765.1296.
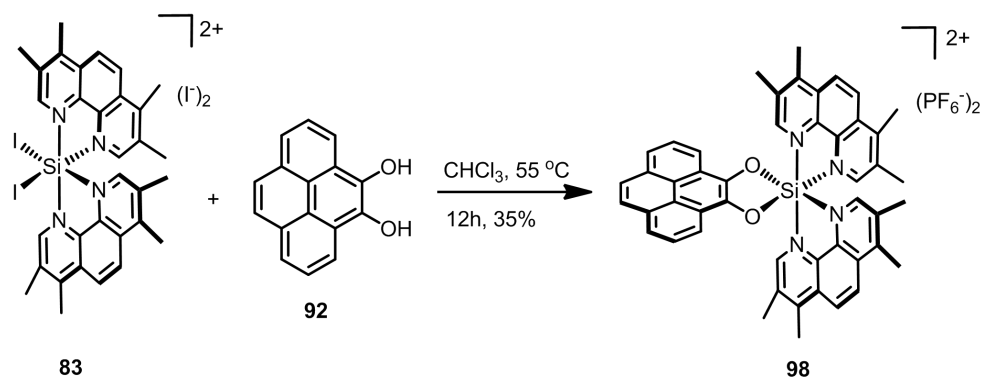
Bis(3,4,7,8-tetramethyl-1,10-phenanthroline)-(4,5-pyrenediolato)silicon(IV) bis(hexafluorophosphate) (98) A suspension of [Si(phen*)$_2$I$_2$]I$_2$ **(83)** (300 mg, 0.30 mmol) and 4 equivalents of pyrene-5,6-diol **(92)** (280 mg, 1.20 mmol) in dry CHCl$_3$ (30 mL) was purged with N$_2$ for 15 min and then stirred at 55 °C (oil bath temperature) for 12 hours. The resulting dark-brown suspension was cooled to room temperature and the solvent was removed *in vacuo*. The residue was dissolved in 3 mL mixed solvent {CH$_3$CN : H$_2$O : KNO$_3$(sat) = 50 : 3 : 1} and subjected to silica gel chromatography with first CH$_3$CN, then switched to CH$_3$CN : H$_2$O : KNO$_3$(sat) = 100 : 3 : 1 and CH$_3$CN : H$_2$O : KNO$_3$(sat) = 50 : 3 : 1. The product eluents were concentrated and redissolved in a mixture of water/ethanol (8 mL/2 mL), and the product was precipitated by the addition of excessive solid NH$_4$PF$_6$. The precipitate was centrifuged, washed twice with water (2 × 12 mL) and dried to afford the pure diolate complex **98** as a brown-yellow solid (107 mg, 35%).

^{1}H-NMR (300 MHz, CD$_3$CN): δ (ppm) 9.12 (s, 2H), 8.61 (dd, J = 14.0, 9.6 Hz, 4H), 8.12 (m, 4H), 8.01 (d, J = 7.9 Hz, 2H), 7.95 (dd, J = 7.8, 7.7 Hz, 2H), 7.48 (s, 2H), 2.94 (s, 6H), 2.90 (s, 6H), 2.42 (s, 6H), 2.36 (s, 6H). ^{13}C-NMR (75 MHz, CD$_3$CN): δ (ppm) 156.4, 155.4, 148.1, 145.6, 137.7, 137.6, 137.3, 137.1, 133.7, 132.6, 131.4, 128.6, 128.3, 127.6, 126.1, 124.85, 124.84, 123.52, 123.49, 120.9, 17.8, 17.3, 15.6, 15.3. IR (neat): ν (cm^{-1}) 1619, 1598, 1543, 1439, 1398, 1366, 1313, 1253, 1177, 1104, 1042, 903, 875, 829, 796, 767, 731, 717, 648, 633, 601, 593, 583, 556, 517, 490, 454, 442, 395. HRMS calcd for C$_{48}$H$_{40}$F$_6$N$_4$O$_2$PSi (M-PF$_6$)$^+$ 877.2562, found: 877.2581.
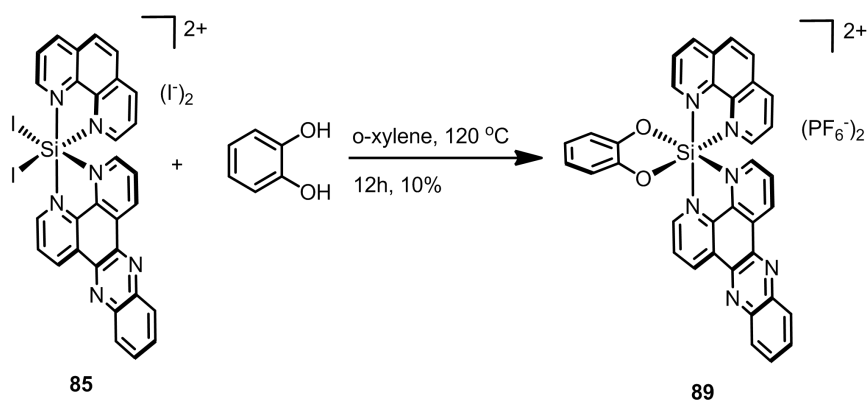
cis-(1,10-Phenanthroline)(dipyrido[3,2-a:2',3'-c]phenazine)catecholatosilicon(IV)
bis(hexafluorophosphate) (89) A suspension of [Si(dppz)(phen)I$_2$]I$_2$ **(85)** (200 mg,
0.20 mmol) and 4 equivalents of catechol (89 mg, 0.80 mmol) in dry _o_-xylene (20 mL)
was purged with N$_2$ for 15 min and then stirred at 120 °C (oil bath temperature) for 12
hours. The resulting dark-brown suspension was cooled to room temperature and the
solvent was removed _in vacuo_. The residue was dissolved in 3 mL mixed solvent
{CH$_3$CN : H$_2$O : KNO$_3$(sat) = 80 : 3 : 1} and subjected to silica gel chromatography
with first CH$_3$CN, then switched to CH$_3$CN : H$_2$O : KNO$_3$(sat) = 150 : 3 : 1 and
CH$_3$CN : H$_2$O : KNO$_3$(sat) = 80 : 3 : 1. The product eluents were concentrated and
redissolved in a mixture of water/ethanol (10 mL/1 mL), and the product was
precipitated by the addition of excessive solid NH$_4$PF$_6$. The precipitate was
centrifuged, washed twice with water (2 × 5 mL) and dried to afford the pure diolate
complex **89** as a pale-yellow solid (18 mg, 10%).

^{1}H-NMR (300 MHz, CD$_3$CN): δ (ppm) 10.30 (dd, _J_ = 8.3, 1.3 Hz, 1H), 10.02 (dd, _J_ =
8.3, 1.1 Hz, 1H), 9.54 (dd, _J_ = 5.5, 1.3 Hz, 1H), 9.50 (dd, _J_ = 5.3, 1.1 Hz, 1H), 9.41
(dd, _J_ = 8.5, 1.1 Hz, 1H), 9.12 (dd, _J_ = 8.3, 1.3 Hz, 1H), 8.68 (dd, _J_ = 8.4, 5.4 Hz, 1H),
8.62 (d, _J_ = 9.2 Hz, 1H), 8.59 (m, 1H), 8.53 (m, 3H), 8.24 (m, 2H), 8.09 (dd, _J_ = 8.3,
5.7 Hz, 1H), 7.96 (dd, _J_ = 8.3, 5.7 Hz, 1H), 7.91 (d, _J_ = 5.5 Hz, 1H), 7.80 (dd, _J_ = 5.5,
1.2 Hz, 1H), 6.87 (m, 2H), 6.82 (m, 2H). ^{13}C-NMR (75 MHz, CD$_3$CN): δ (ppm) 150.1,
149.6, 148.3, 147.6, 147.3, 147.2, 147.1, 146.6, 144.18, 144.16, 143.7, 143.0, 139.9,
139.8, 138.4, 137.6, 135.8, 134.8, 134.7, 132.2, 131.5, 131.4, 131.1, 130.90, 130.86,
130.7, 129.8, 129.4, 128.9, 123.1, 114.8, 114.7. IR (neat): ν (cm^{-1}) 1614, 1594, 1487,
1454, 1443, 1387, 1337, 1283, 1241, 1179, 1140, 1104, 994, 979, 953, 927, 909, 838,

745, 730, 695, 675, 613, 589, 557, 534, 521, 502, 471, 455, 422, 410, 401, 387. HRMS calcd for $C_{36}H_{22}F_6N_6O_2PSi$ (M-PF$_6$)$^+$ 743.1215, found: 743.1208.
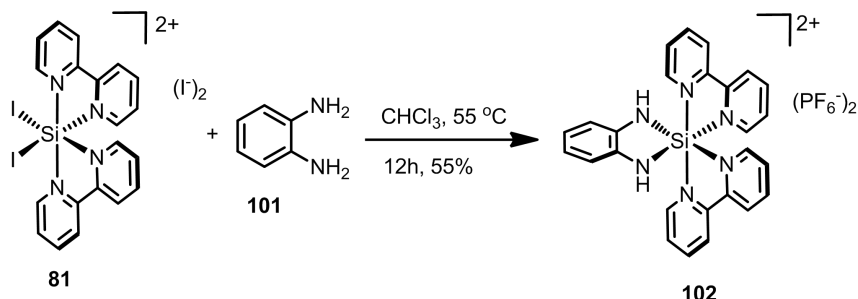
Bis(2,2'-bipyridine)(o-phenylenediaminato)silicon(IV) bis(hexafluorophosphate) (102) A suspension of [Si(bpy)$_2$I$_2$]I$_2$ (**81**) (200 mg, 0.225 mmol) and 4 equivalents of 1,2-phenylenediamine (**101**) (97 mg, 0.90 mmol) in dry CHCl$_3$ (25 mL) was purged with N$_2$ for 15 min and then stirred at 55 °C (oil bath temperature) for 12 hours. The resulting dark-brown suspension was cooled to room temperature and the solvent was removed *in vacuo*. The residue was dissolved in 4 mL mixed solvent {CH$_3$CN : H$_2$O : KNO$_3$(sat) = 50 : 3 : 1} and subjected to silica gel chromatography with first CH$_3$CN, then switched to CH$_3$CN : H$_2$O : KNO$_3$(sat) = 80 : 3 : 1 and CH$_3$CN : H$_2$O : KNO$_3$(sat) = 50 : 3 : 1. The product eluents were concentrated and redissolved in a mixture of water/ethanol (10 mL/1 mL), and the product was precipitated by the addition of excessive solid NH$_4$PF$_6$. The precipitate was centrifuged, washed twice with water (2 × 8 mL) and dried affording the pure diaminate complex **102** as a brown solid (91 mg, 55%).

^{1}H-NMR (300 MHz, CD$_3$CN): δ (ppm) 9.26 (d, J = 5.6 Hz, 2H), 8.82 (d, J = 8.0 Hz, 2H), 8.74 (d, J = 8.0 Hz, 2H), 8.64 (dd, J = 7.9, 7.8 Hz, 2H), 8.48 (dd, J = 7.9, 7.8 Hz, 2H), 8.13 (dd, J = 7.3, 6.1 Hz, 2H), 7.72 (dd, J = 7.0, 6.6 Hz, 2H), 7.48 (d, J = 5.9 Hz, 2H), 6.47 (m, 2H) 6.37 (m, 2H) 4.63 (s, 2H). ^{13}C-NMR (75 MHz, CD$_3$CN): δ (ppm) 148.9, 146.9, 146.5, 145.9, 145.4, 142.6, 136.4, 131.2, 130.9, 125.5, 119.5, 111.7. IR (neat): v (cm^{-1}) 1619, 1497, 1448, 1387, 1319, 1256, 1172, 1074, 1032, 832, 770, 738, 672, 606, 557, 522, 483, 434. HRMS calcd for $C_{26}H_{22}F_6N_6PSi$ (M-PF$_6$)$^+$ 591.1317, found: 591.1338.
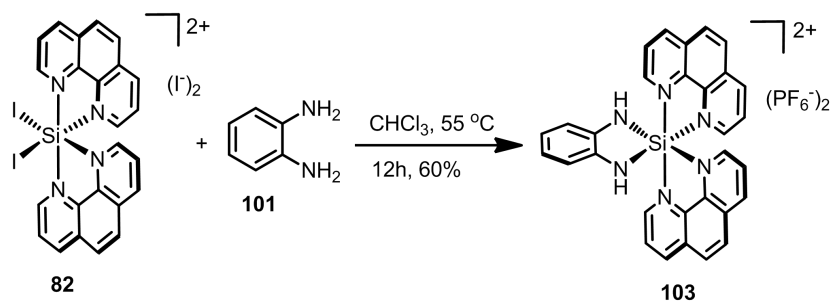
Bis(1,10-phenanthroline)(*o*-phenylenediaminato)silicon(IV) bis(hexafluorophosphate) (**103**) A suspension of [Si(phen)$_2$I$_2$]I$_2$ (**82**) (200 mg, 0.22 mmol) and 4 equivalents of 1,2-phenylenediamine (**101**) (96 mg, 0.89 mmol) in dry CHCl$_3$ (20 mL) was purged with N$_2$ for 15 min and then stirred at 55 °C (oil bath temperature) for 12 hours. The resulting dark-brown suspension was cooled to room temperature and the solvent was removed *in vacuo*. The residue was dissolved in 4 mL mixed solvent {CH$_3$CN : H$_2$O : KNO$_3$(sat) = 50 : 3 : 1} and subjected to silica gel chromatography with first CH$_3$CN, then switched to CH$_3$CN : H$_2$O : KNO$_3$(sat) = 100 : 3 : 1 and CH$_3$CN : H$_2$O : KNO$_3$(sat) = 50 : 3 : 1. The product eluents were concentrated and redissolved in a mixture of water/ethanol (10 mL/1 mL), and the product was precipitated by the addition of excessive solid NH$_4$PF$_6$. The precipitate was centrifuged, washed twice with water (2 × 10 mL) and dried to afford the diaminate complex **103** as a deep brown solid (104 mg, 60%).

^{1}H-NMR (300 MHz, CD$_3$CN): δ (ppm) 9.61 (dd, J = 5.3, 1.2 Hz, 2H), 9.28 (dd, J = 8.3, 1.2 Hz, 2H), 9.00 (dd, J = 8.3, 1.0 Hz, 2H), 8.57 (d, J = 9.1 Hz, 2H), 8.51 (dd, J = 8.3, 5.4 Hz, 2H), 8.46 (d, J = 9.1 Hz, 2H), 7.85 (dd, J = 8.3, 5.6 Hz, 2H), 7.66 (dd, J = 5.6, 1.1 Hz, 2H), 6.51 (dd, J = 5.6, 3.4 Hz, 2H), 6.38 (dd, J = 5.4, 3.4 Hz, 2H), 4.78 (s, 2H). ^{13}C-NMR (75 MHz, CD$_3$CN): δ (ppm) 149.7, 147.5, 147.3, 147.0, 146.4, 135.8, 134.8, 131.4, 131.0, 129.7, 129.6, 129.3, 128.9, 123.0, 114.6. IR (neat): ν (cm^{-1}) 1629, 1585, 1528, 1482, 1437, 1335, 1244, 1154, 1115, 1019, 884, 826, 759, 738, 714, 666, 620, 582, 554, 521, 484, 456, 416. HRMS calcd for C$_{30}$H$_{22}$F$_6$N$_6$PSi (M-PF$_6$)$^+$ 639.1317, found: 639.1357.
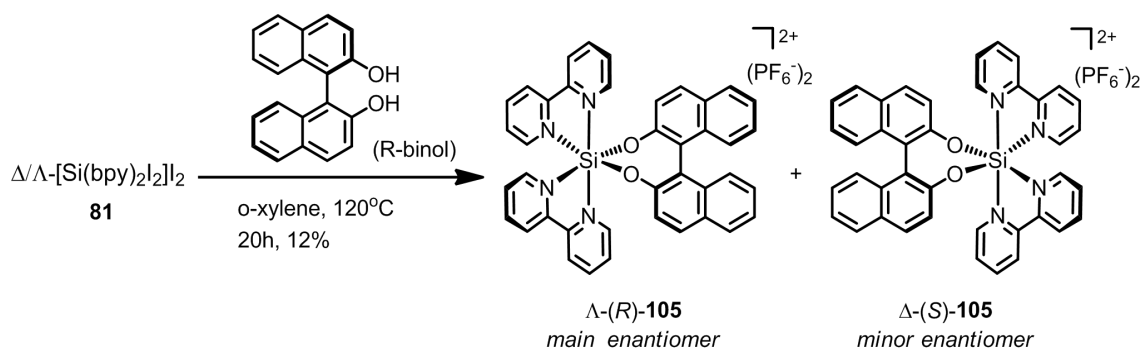
Λ-Bis(2,2'-bipyridine)(*R*-BINOLato)silicon(IV) bis(hexafluorophosphate) (**105**) A suspension of [Si(bpy)₂I₂]I₂ (**81**) (400 mg, 0.47 mmol) and 4 equivalents of (R)-(+)-1,1′-Bi(2-naphthol) (R-BINOL) (540 mg, 1.89 mmol) in dry *o*-xylene (30 mL) was purged with N₂ for 15 min and then heated to 120 °C (oil bath temperature) for 20 hours. The resulting dark-brown suspension was cooled to room temperature and the solvent was removed *in vacuo*. The residue was dissolved in 5 mL mixed solvent {CH₃CN : H₂O : KNO₃(sat) = 50 : 3 : 1} and subjected to silica gel chromatography with first CH₃CN, then switched to CH₃CN : H₂O : KNO₃(sat) = 100 : 3 : 1 and CH₃CN : H₂O : KNO₃(sat) = 50 : 3 : 1. The product eluents were concentrated and redissolved in a mixture of water/ethanol (12 mL/2 mL), and the product was precipitated by the addition of excessive solid NH₄PF₆. The pale-yellow precipitate was centrifuged, washed twice with water (2 × 8 mL) and dried under high vacuum. Λ-(*R*)-**105** appeared as the major enantiomer (e.r. ≈ 95 : 5) in an overall yield of 12%. The absolute configuration of Λ-(*R*)-**105** was determined by X-ray crystallography. The predominant minor isomer was identified as Δ-(*S*)-**105** by chiral HPLC analysis, and the racemic mixture of **105** was prepared analogously with the racemic (*R/S*)-1,1′-Bi(2-naphthol) as the starting material.

¹H-NMR (300 MHz, CD₃CN): δ (ppm) 8.97 (d, *J* = 8.0 Hz, 2H), 8.88 (d, *J* = 8.0 Hz, 2H), 8.80 (ddd, *J* = 5.9, 1.5, 0.7 Hz, 2H), 8.64 (dt, *J* = 7.9, 1.5 Hz, 2H), 8.55 (dt, *J* = 7.9, 1.3 Hz, 2H), 7.83 (d, *J* = 8.1 Hz, 2H), 7.71 (ddd, *J* = 7.6, 6.0, 1.3 Hz, 2H), 7.49 (m, 4H), 7.41 (m, 4H), 7.24 (m, 2H), 7.13 (d, *J* = 8.2 Hz, 2H), 6.24 (d, *J* = 8.8 Hz, 2H). ¹³C-NMR (CD₃CN, 75 MHz): δ (ppm) 152.6, 149.1, 148.4, 146.6, 145.2, 144.6, 143.3, 133.8, 131.33, 131.30, 130.8, 130.3, 129.2, 127.6, 127.3, 126.4, 125.9, 125.5,

122.5, 121.2. IR (neat): v (cm^{-1}) 3132, 3035, 2364, 2050, 1585, 1528, 1482, 1437, 1335, 1244, 1154, 1115, 1019, 884, 826, 759, 738, 714, 666, 620, 582, 554, 521, 484, 456, 416. CD ($\Delta\varepsilon$/M^{-1}cm^{-1}, MeCN): 218 nm (+234), 229 nm (-432). HRMS calcd for C$_{40}$H$_{28}$F$_6$N$_4$O$_2$PSi (M-PF$_6$)$^+$ 769.1618, found: 769.1612.

Λ-(R)-**106**
main enantiomer

Δ-(S)-**106**
minor enantiomer
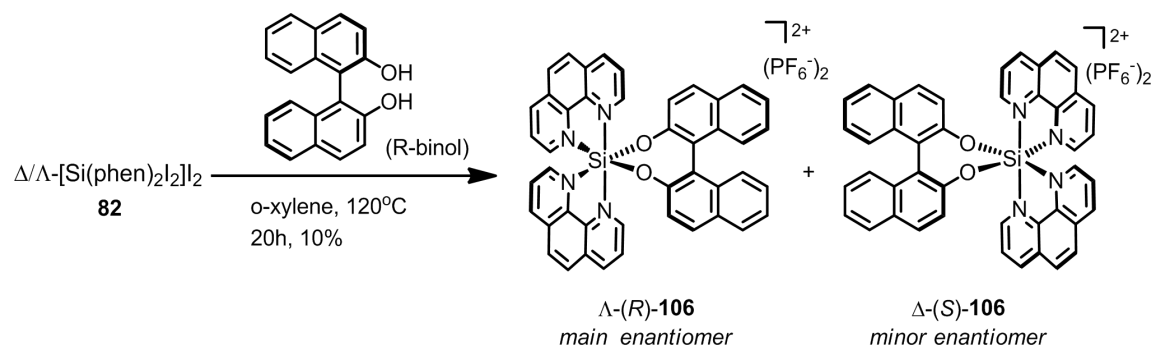
Λ-Bis(1,10-phenanthroline)(R-BINOLato)silicon(IV) bis(hexafluorophosphate) (**106**) A suspension of [Si(phen)$_2$I$_2$]I$_2$ (200 mg, 0.44 mmol) and 4 equivalents of (R)-(+)-1,1′-Bi(2-naphthol) (R-BINOL) (503 mg, 1.76 mmol) in dry o-xylene (30 mL) was purged with N$_2$ for 15 min and then heated to 120 °C (oil bath temperature) for 20 hours. The resulting dark-brown suspension was cooled to room temperature and the solvent was removed *in vacuo*. The residue was dissolved in 4 mL mixed solvent {CH$_3$CN : H$_2$O : KNO$_3$(sat) = 50 : 3 : 1} and subjected to silica gel chromatography with first CH$_3$CN, then switched to CH$_3$CN : H$_2$O : KNO$_3$(sat) = 100 : 3 : 1 and CH$_3$CN : H$_2$O : KNO$_3$(sat) = 50 : 3 : 1. The product eluents were concentrated and redissolved in a mixture of water/ethanol (10 mL/2 mL), and the product was precipitated by the addition of excessive solid NH$_4$PF$_6$. The yellow precipitate was centrifuged, washed twice with water (2 × 8 mL) and dried under high vacuum to afford Λ-(R)-**106** as the major enantiomer (e.r. ≈ 94 : 6) in an overall yield of 10% (Figure 68). The predominant minor isomer was identified as Δ-(S)-**106** by chiral HPLC analysis, and the racemic mixture of **106** was prepared analogously with the racemic (R/S)-1,1′-Bi(2-naphthol) as the starting material.

^{1}H-NMR (300 MHz, CD$_3$CN): δ (ppm) 9.28 (dd, J = 8.3 , 1.2 Hz, 2H), 9.06 (dd, J = 3.3, 1.2 Hz, 2H), 9.04 (d, J = 1.1 Hz, 2H), 8.66 (d, J = 9.1 Hz, 2H), 8.58 (d, J = 9.1 Hz, 2H), 7.82 (m, 6H), 7.63 (dd, J = 5.4, 1.0 Hz, 2H), 7.41 (ddd, J = 8.1, 6.7, 1.3 Hz, 2H),

7.29 (m, 4H), 7.18 (d, J = 8.5 Hz, 2H), 5.64 (d, J = 8.9 Hz, 2H). ^{13}C-NMR (CD$_3$CN, 75 MHz): δ (ppm) 152.5, 150.3, 147.1, 146.0, 145.0, 135.6, 134.6, 133.8, 131.6, 131.2, 130.9, 130.8, 129.9, 129.23, 129.21, 128.9, 128.5, 128.0, 127.6, 127.3, 125.6, 120.8. IR (neat): v (cm^{-1}) 1623, 1590, 1542, .1503, 1436, 1389, 1329, 1249, 1075, 1000, 960, 911, 836, 753, 719, 679, 646, 554. CD ($\Delta\varepsilon$/M^{-1}cm^{-1}, MeCN): 219 nm (+208), 230.5 nm (-384). HRMS calcd for C$_{44}$H$_{28}$N$_4$O$_2$Si (M-PF$_6$)$^+$ 672.1982, found: 672.1997.

The enantiomers of **106** were resolved with a CHIRALPAK IB HPLC column (250 × 4.6 mm) on an Agilent 1200 Series HPLC System. The flow rate was 0.5 mL/min, the column temperature 40°C, and UV-absorption was measured at 254 nm. Solvent A = 0.1% TFA, solvent B = MeCN, with a linear gradient of 20% to 27% B in 30 min.
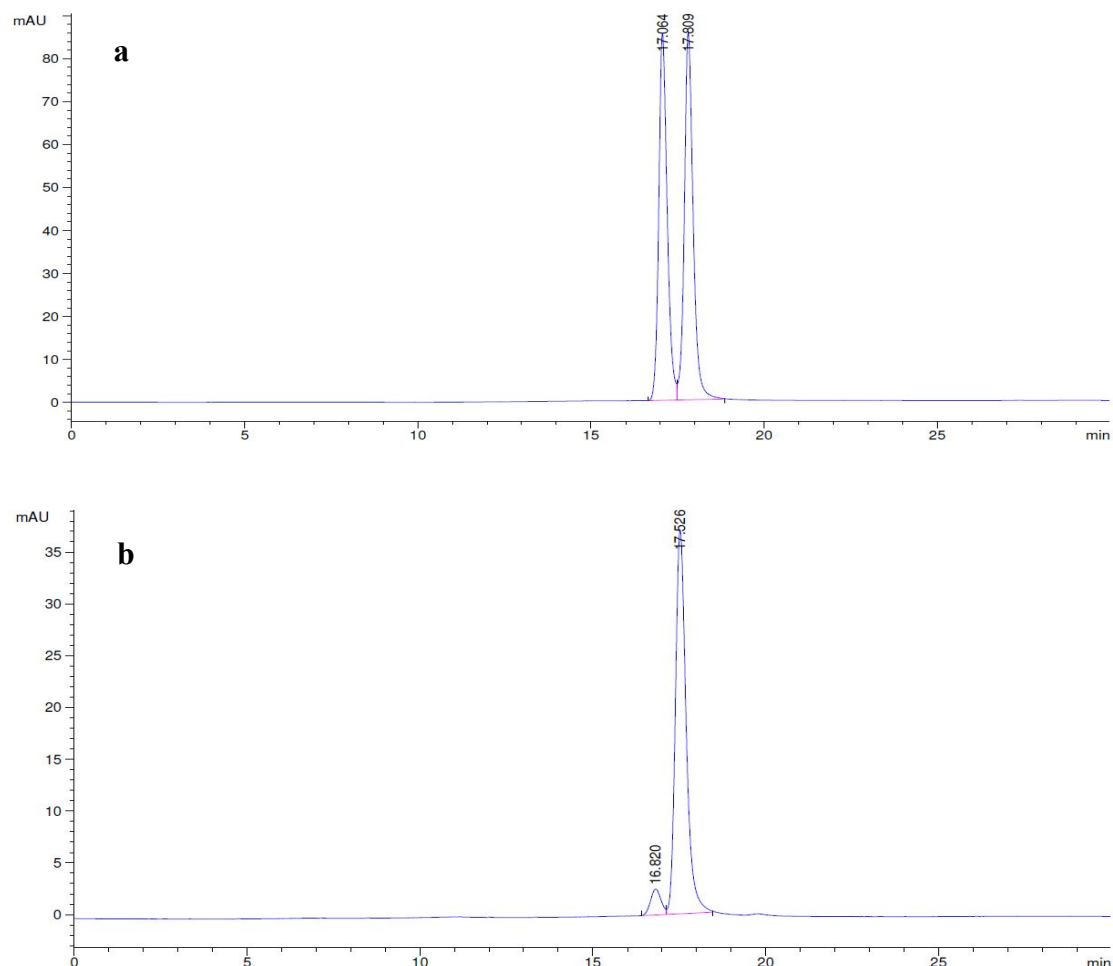
Figure 68. (a) HPLC trace for the racemic mixture of **106**. (b) HPLC trace for enantiopure Λ-(*R*)-**106**, integration of peak areas = 6 : 94 e.r.
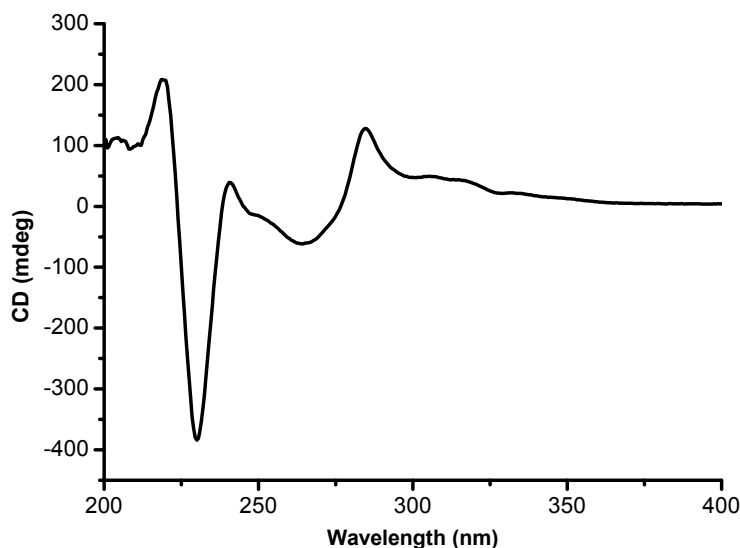
Figure 69. CD spectrum for compound Λ-(*R*)-**106** in CH₃CN (0.1 mM).
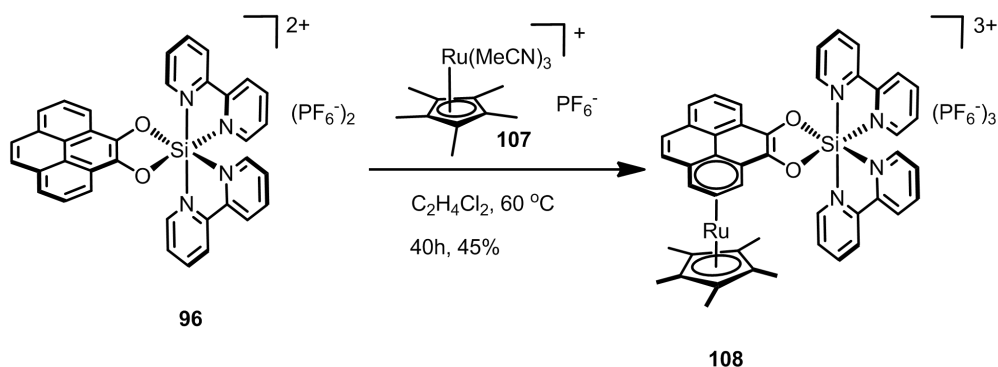
{Cp*Ru(η⁶-pyrene)}-bis(2,2'-bipyridine)-(4,5-pyrenediolato)silicon(IV)

tris(hexafluorophosphate) (**108**) A suspension of [Si(bpy)₂(pyrenediolate)](PF₆)₂ (**96**)

(100 mg, 0.116 mmol) and 0.9 equivalents of pentamethylcyclopentadienyl tris-

(acetonitrile)ruthenium(II) hexafluorophosphate (**107**) (53 mg, 0.104 mmol) in dry

1,2-dichloroethane (20 mL) was purged with N₂ for 15 min and then stirred at 60 °C

(oil bath temperature) for 40 hours. The resulting dark-brown solution was cooled to

room temperature and the solvent was removed *in vacuo*. The residue was dissolved

in 2 mL CH₃COCH₃ and subjected to silica gel chromatography with first CH₃COCH₃,

then switched to CH₃COCH₃ : H₂O : KNO₃(sat) = 50 : 3 : 1 and CH₃COCH₃ : H₂O :

KNO₃(sat) = 10 : 3 : 1. The collected eluents were concentrated and redissolved in

nearly 10 mL water, and the solid was precipitated by the addition of excessive solid

NH₄PF₆. The precipitate was centrifuged, washed twice with water (2 × 8 mL) and

dried to afford the complex **108** as a pale-yellow solid (58 mg, 45%).

^{1}H-NMR (300 MHz, CD$_3$COCD$_3$): δ (ppm) 9.83 (d, J = 5.7 Hz, 1H), 9.51 (d, J = 7.6 Hz, 1H), 9.35 (m, 4H), 9.16 (m, 1H), 8.90 (m, 3H), 8.65 (t, J = 6.7 Hz, 1H), 8.36 (m, 2H), 8.28 (d, J = 5.0 Hz, 1H), 8.20 (d, J = 7.6 Hz, 1H), 8.10 (m, 5H), 7.81 (d, J = 9.3 Hz, 1H), 6.78 (d, J = 5.9 Hz, 1H), 6.70 (d, J = 5.9 Hz, 1H), 6.39 (t, J = 6.0 Hz, 1H), 1.19 (s, 15H). ^{13}C-NMR (75 MHz, CD$_3$COCD$_3$): δ (ppm) 149.7, 149.5, 148.8, 148.7, 148.6, 148.4, 146.8, 145.5, 145.0, 144.9, 144.5, 141.7, 134.3, 133.1, 132.9, 132.8, 132.0, 131.7, 131.5, 130.2, 128.2, 126.8, 126.4, 126.30, 126.27, 126.2, 126.0, 122.3, 121.4, 94.2, 93.5, 91.8, 88.3, 88.2, 85.8, 79.9, 9.2. IR (neat): ν (cm^{-1}) 1618, 1575, 1509, 1477, 1454, 1367, 1325, 1276, 1249, 1217, 1174, 1102, 1072, 1045, 896, 829, 793, 773, 734, 685, 664, 641, 595, 580, 555, 517, 485, 461, 420. HRMS calcd for C$_{46}$H$_{39}$F$_{12}$N$_4$O$_2$P$_2$RuSi (M-PF$_6$)$^+$ 1099.1169, found: 1099.1147.
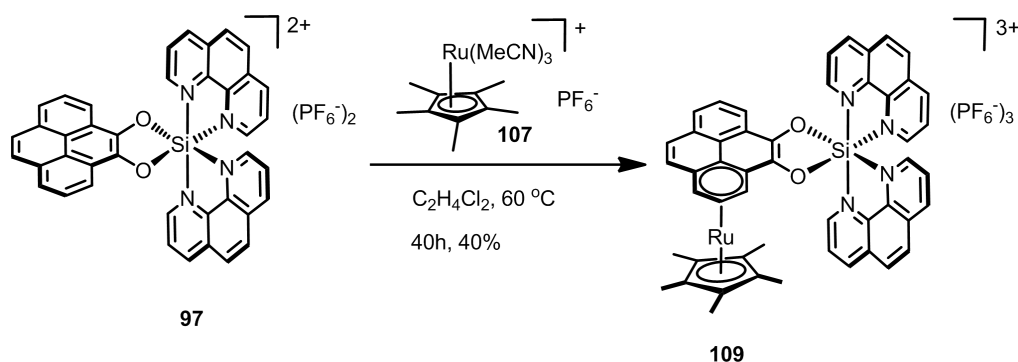
{Cp*Ru(η^6-pyrene)}-bis(1,10-phenanthroline)-(4,5-pyrenediolato)silicon(IV) tris(hexafluorophosphate) (**109**) A suspension of [Si(phen)$_2$(pyrenediolate)](PF$_6$)$_2$ (**97**) (100 mg, 0.110 mmol) and 0.9 equivalents of pentamethylcyclopentadienyl tris (acetonitrile)ruthenium(II) hexafluorophosphate (**107**) (50 mg, 0.100mmol) in dry 1,2-dichloroethane (20 mL) was purged with N$_2$ for 15 min and then stirred at 60 ^{o}C (oil bath temperature) for 40 hours. The resulting dark-brown solution was cooled to room temperature and the solvent was removed *in vacuo*. The residue was dissolved in 2 mL CH$_3$COCH$_3$ and subjected to silica gel chromatography with first CH$_3$COCH$_3$, then switched to CH$_3$COCH$_3$: H$_2$O : KNO$_3$(sat) = 40 : 3 : 1 and CH$_3$COCH$_3$: H$_2$O : KNO$_3$(sat) = 10 : 3 : 1. The collected eluents were concentrated and redissolved in nearly 12 mL water, and the solid was precipitated by the addition of excessive solid NH$_4$PF$_6$. The precipitate was centrifuged, washed twice with water (2 × 8 mL) and

dried under high vacuum to afford the complex **109** as a yellow solid (52 mg, 40%).

^{1}H-NMR (300 MHz, CD$_3$COCD$_3$): δ (ppm) 10.2 (d, J = 4.9 Hz, 1H), 9.80 (m, 2H), 9.53 (d, J = 8.2 Hz, 1H), 9.45 (m, 2H), 8.96 (dd, J = 8.6, 6.1 Hz, 1H), 8.89 (d, J = 9.2 Hz, 1H), 8.83 (d, J = 9.2 Hz, 1H), 8.77 (m, 2H), 8.47 (m, 3H), 8.33 (d, J = 9.0 Hz, 1H), 8.20 (m, 3H), 8.09 (d, J = 7.7 Hz, 1H), 8.03 (m, 1H), 7.81 (d, J = 9.4 Hz, 1H), 6.75 (d, J = 5.7 Hz, 1H), 6.69 (d, J = 6.3 Hz, 1H), 6.35 (t, J = 6.2 Hz, 1H), 1.13 (s, 15H). ^{13}C-NMR (75 MHz, CD$_3$COCD$_3$): δ (ppm) 150.6, 150.4, 148.5, 148.4, 148.1, 147.2, 146.88, 146.86, 141.9, 136.1, 135.9, 135.1, 134.9, 134.7, 133.2, 133.0, 131.6, 131.5, 131.3, 131.1, 130.5, 130.3, 130.1, 130.0, 129.8, 129.5, 129.4, 129.2, 128.2, 126.6, 126.2, 122.4, 121.5, 94.3, 93.5, 91.8, 88.4, 88.2, 85.8, 79.9, 9.2. IR (neat): v (cm^{-1}) 1628, 1529, 1440, 1366, 1326, 1219, 1159, 1098, 1033, 832, 762, 724, 588, 555, 519, 482, 453. HRMS calcd for C$_{50}$H$_{39}$F$_{12}$N$_4$O$_2$P$_2$RuSi (M-PF$_6$)$^+$ 1147.1169, found: 1147.1187.
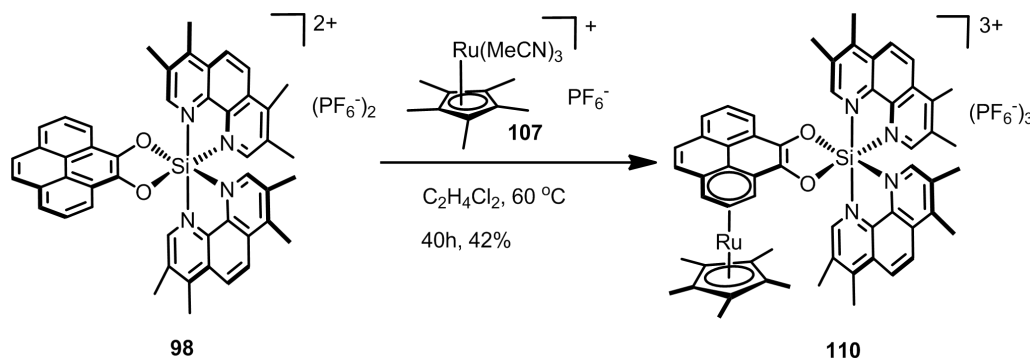
{Cp*Ru(η^6-pyrene)}-bis(3,4,7,8-tetramethyl-1,10-phenanthroline)-(4,5-pyrenedio lato)silicon(IV) tris(hexafluorophosphate) (110) A suspension of [Si(phen*)$_2$(pyrenediolate)](PF$_6$)$_2$ (**100**) (100 mg, 0.098 mmol) and 0.9 equivalents of pentamethylcyclopentadienyl tris (acetonitrile)ruthenium(II) hexafluorophosphate (**111**) (44 mg, 0.088 mmol) in dry 1,2-dichloroethane (20 mL) was purged with N$_2$ for 15 min and then stirred at 60 °C (oil bath temperature) for 40 hours. The resulting dark-brown solution was cooled to room temperature and the solvent was removed *in vacuo*. The residue was dissolved in 2 mL CH$_3$COCH$_3$ and subjected to silica gel chromatography with first CH$_3$COCH$_3$, then switched to CH$_3$COCH$_3$: H$_2$O : KNO$_3$(sat) = 80 : 3 : 1 and CH$_3$COCH$_3$: H$_2$O : KNO$_3$(sat) = 20 : 3 : 1. The collected

eluents were concentrated and redissolved in nearly 12 mL water, and the solid was precipitated by the addition of excessive solid NH_4PF_6. The precipitate was centrifuged, washed twice with water (2×10 mL) and dried under high vacuum to afford the complex **110** as a dark-yellow solid (52 mg, 42%).

^{1}H-NMR (300 MHz, CD_3COCD_3): δ (ppm) 9.78 (s, 1H), 9.41 (s, 1H), 8.89 (d, $J = 9.7$ Hz, 1H), 8.84 (d, $J = 9.7$ Hz, 1H), 8.78 (s, 1H), 8.77 (s, 1H), 8.33 (d, $J = 9.7$ Hz, 1H), 8.17 (d, $J = 7.2$ Hz, 1H), 8.10 (m, 3H), 8.03 (t, $J = 7.6$ Hz, 1H), 7.79 (d, $J = 9.4$ Hz, 1H), 6.78 (d, $J = 5.8$ Hz, 1H), 6.66 (d, $J = 5.8$ Hz, 1H), 6.33 (t, $J = 6.1$ Hz, 1H), 3.21 (s, 3H), 3.01 (s, 3H), 2.99 (s, 3H), 2.98 (s, 3H), 2.82 (s, 3H), 2.46 (s, 3H), 2.35 (s, 3H), 2.34 (s, 3H), 1.09 (s, 15H). ^{13}C-NMR (75 MHz, CD_3COCD_3): δ (ppm) 159.5, 158.6, 157.5, 156.7, 149.2, 149.1, 147.3, 147.2, 141.8, 139.1, 138.8, 138.7, 138.3, 134.8, 134.7, 134.6, 134.1, 133.7, 133.1, 132.9, 130.2, 129.7, 129.6, 129.4, 129.1, 128.0, 126.8, 126.5, 126.2, 125.9, 125.8, 125.6, 124.4, 122.1, 121.3, 94.4, 93.2, 91.7, 88.4, 88.3, 85.9, 79.8, 18.8, 18.5, 18.2, 16.6, 16.3, 16.1, 8.9. IR (neat): v (cm^{-1}) 1626, 1545, 1443, 1368, 1322, 1269, 1219, 1178, 1100, 1031, 833, 722, 641, 592, 554, 520, 444, 410. HRMS calcd for $C_{58}H_{55}F_{12}N_4O_2P_2RuSi$ (M-PF$_6$)$^+$ 1259.2421, found: 1259.2439.

Chapter 6 References

6.1 Literature

1   Abell, J. P. & Yamamoto, H. Development and applications of tethered bis(8-quinolinolato) metal complexes (TBOxM). *Chemical Society reviews* **39**, 61-69, doi:Doi 10.1039/B907303p (2010).

2   Bauer, E. B. Chiral-at-metal complexes and their catalytic applications in organic synthesis. *Chemical Society reviews* **41**, 3153-3167, doi:Doi 10.1039/C2cs15234g (2012).

3   Campagna, S., Puntoriero, F., Nastasi, F., Bergamini, G. & Balzani, V. Photochemistry and photophysics of coordination compounds: Ruthenium. *Photochemistry and Photophysics of Coordination Compounds I* **280**, 117-214, doi:Doi 10.1007/128_2007_133 (2007).

4   Kumar, P., Gupta, R. K. & Pandey, D. S. Half-sandwich arene ruthenium complexes: synthetic strategies and relevance in catalysis. *Chemical Society reviews* **43**, 707-733, doi:Doi 10.1039/C3cs60189g (2014).

5   Werner, A. Beitrag zur Konstitution anorganischer Verbindungen. XVII. Mitteilung. Über Oxalatodiäthylendiaminkobaltisalze. *Zeitschrift für anorganische Chemie* **21**, 145-158 (1899).

6   Werner, A. Information on asymmetric cobalt atoms XII. Optic activity with carbon compounds. *Berichte Der Deutschen Chemischen Gesellschaft* **47**, 3087-3094, doi:DOI 10.1002/cber.191404703108 (1914).

7   Bailar Jr., J. C. The numbers and structures of isomers of hexacovalent complexes. *J. Chem. Educ.* **34**, 334-338, doi:10.1021/ed034p334 (1957).

8   Chavarot, M. *et al.* "Chiral-at-metal" octahedral ruthenium(II) complexes with achiral ligands: A new type of enantioselective catalyst. *Inorganic chemistry* **42**, 4810-4816, doi:Doi 10.1021/Ic0341338 (2003).

9   Lasa, M., Lopez, P., Cativiela, C., Carmona, D. & Oro, L. A. Chiral-at-metal ruthenium(II) complexes as catalysts in the asymmetric cyclopropanation reaction. *J Mol Catal a-Chem* **234**, 129-135, doi:DOI 10.1016/j.molcata.2005.02.030 (2005).

10   Liu, H. K. & Sadler, P. J. Metal Complexes as DNA Intercalators. *Accounts Chem Res* **44**, 349-359, doi:Doi 10.1021/Ar100140e (2011).

11   Jonassen, H. B., Bailar, J. C. & Huffman, E. H. The Sterochemistry of Complex Inorganic Compounds .9. The Diastereoisomers of Dextro-Tartrato-Bis-Ethylenediamine Cobaltic Ion. *Journal of the American Chemical Society* **70**, 756-758, doi:Doi 10.1021/Ja01182a095 (1948).

12   Feng, L. *et al.* Structurally Sophisticated Octahedral Metal Complexes as Highly Selective Protein Kinase Inhibitors. *Journal of the American Chemical Society* **133**, 5976-5986, doi:Doi 10.1021/Ja1112996 (2011).

13   Chen, L. A. *et al.* Asymmetric Catalysis with an Inert Chiral-at-Metal Iridium Complex. *Journal of the American Chemical Society* **135**, 10598-10601, doi:Doi 10.1021/Ja403777k (2013).

14   Lacour, J., Torche-Haldimann, S., Jodry, J. J., Ginglinger, C. & Favarger, F. Ion pair chromatographic resolution of tris(diimine)ruthenium(II) complexes using TRISPHAT anions as resolving agents. *Chemical communications*, 1733-1734, doi:Doi 10.1039/A803904f (1998).

15   Lacour, J. & Hebbe-Viton, V. Recent developments in chiral anion mediated asymmetric chemistry. *Chemical Society reviews* **32**, 373-382, doi:Doi 10.1039/B205251m (2003).

16   Lacour, J. & Moraleda, D. Chiral anion-mediated asymmetric ion pairing chemistry. *Chemical communications*, 7073-7089, doi:Doi 10.1039/B912530b (2009).

17   Keene, F. R., Smith, J. A. & Collins, J. G. Metal complexes as structure-selective binding agents for nucleic acids. *Coordination Chemistry Reviews* **253**, 2021-2035, doi:DOI 10.1016/j.ccr.2009.01.004 (2009).

18   Jodry, J. J. & Lacour, J. Efficient resolution of a dinuclear triple helicate by asymmetric extraction/precipitation with TRISPHAT anions as resolving agents. *Chemistry-a European Journal* **6**, 4297-4304, doi:Doi 10.1002/1521-3765(20001201)6:23<4297::Aid-Chem4297>3.0.Co;2-# (2000).

19   Lacour, J., Jodry, J. J., Ginglinger, C. & Torche-Haldimann, S. Diastereoselective ion pairing of TRISPHAT anions and tris(4,4 '-dimethyl-2,2 '-bipyridine)iron(II). *Angew Chem Int Edit* **37**, 2379-2380, doi:Doi 10.1002/(Sici)1521-3773(19980918)37:17<2379::Aid-Anie2379>3.0.Co;2-C (1998).

20   Monchaud, D., Lacour, J., Coudret, C. & Fraysse, S. TRISPHAT salts. Efficient NMR chiral shift and resolving agents for substituted cyclometallated ruthenium bis(diimine) complexes. *J Organomet Chem* **624**, 388-391, doi:Doi 10.1016/S0022-328x(01)00685-4 (2001).

21   Crassous, J. Transfer of chirality from ligands to metal centers: recent examples. *Chemical communications* **48**, 9684-9692, doi:Doi 10.1039/C2cc31542d (2012).

22   Caspar, R. *et al.* Efficient asymmetric synthesis of Delta- and alpha-enantiomers of (bipyridyl)ruthenium complexes and crystallographic analysis of Delta-bis(2,2 '-bipyridine)(2,2 '-bipyridine-4,4 '-dicarboxylato)ruthenium: Diastereoselective homo- and heterochiral ion pairing revisited. *European Journal of Inorganic Chemistry*, 499-505 (2003).

23   Drahonovsky, D. & von Zelewsky, A. Asymmetric synthesis of coordination compounds: Back to the roots. Diastereoselective synthesis of simple platinum(IV) complexes. *Helv Chim Acta* **88**, 496-506, doi:DOI 10.1002/hlca.200590034 (2005).

24   Crassous, J. Chiral transfer in coordination complexes: towards molecular materials. *Chemical Society reviews* **38**, 830-845, doi:Doi 10.1039/B806203j (2009).

25   Smirnoff, A. P. On the stereochemistry of plantium atoms : On the relatively assymetric with anorganic complexes. *Helv Chim Acta* **3**, 177-224, doi:DOI 10.1002/hlca.19200030117

(1920).

26   Constable, E. C. Stereogenic metal centres - from Werner to supramolecular chemistry. *Chemical Society reviews* **42**, 1637-1651, doi:Doi 10.1039/C2cs35270b (2013).

27   Gnas, Y. & Glorius, F. Chiral auxiliaries - Principles and recent applications. *Synthesis-Stuttgart*, 1899-1930, doi:DOI 10.1055/s-2006-942399 (2006).

28   Hayoz, P., Vonzelewsky, A. & Stoecklievans, H. Stereoselective Synthesis of Octahedral Complexes with Predetermined Helical Chirality. *Journal of the American Chemical Society* **115**, 5111-5114, doi:Doi 10.1021/Ja00065a023 (1993).

29   Howson, S. E. *et al.* Self-assembling optically pure Fe(A-B)(3) chelates. *Chemical communications*, 1727-1729, doi:Doi 10.1039/B821573a (2009).

30   Damas, A., Moussa, J., Rager, M. N. & Amouri, H. Chiral Octahedral Bimetallic Assemblies with Delta-TRISPHAT as Counter Anion: Design, Anion Metathesis, and (CpIr)-Ir-star as a Probe for Chiral Recognition. *Chirality* **22**, 889-895, doi:Doi 10.1002/Chir.20882 (2010).

31   Knof, U. & von Zelewsky, A. Predetermined chirality at metal centers. *Angew Chem Int Edit* **38**, 302-322, doi:Doi 10.1002/(Sici)1521-3773(19990201)38:3<302::Aid-Anie302>3.0.Co;2-G (1999).

32   Jarvo, E. R. & Miller, S. J. Amino acids and peptides as asymmetric organocatalysts. *Tetrahedron* **58**, 2481-2495, doi:Pii S0040-4020(02)00122-9 Doi 10.1016/S0040-4020(02)00122-9 (2002).

33   Cordova, A. *et al.* Acyclic amino acid-catalyzed direct asymmetric aldol reactions: alanine, the simplest stereoselective organocatalyst. *Chemical communications*, 3586-3588, doi:Doi 10.1039/B507968n (2005).

34   Liu, C. F., Liu, N. C. & Bailar, J. C. Stereochemistry of Complex Inorganic Compounds .27. Asymmetric Syntheses of Tris(Bipyridine) Complexes of Ruthenium)2) + Osmium)2). *Inorganic chemistry* **3**, 1085-1087, doi:Doi 10.1021/Ic50018a004 (1964).

35   Constable, E. C., Zhang, G. Q., Housecroft, C. E., Neuburger, M. & Zampese, J. A. Diastereoselective Assembly of Helicates Incorporating a Hexadentate Chiral Scaffold. *European Journal of Inorganic Chemistry*, 2000-2011, doi:DOI 10.1002/ejic.201000206 (2010).

36   Sato, I., Kadowaki, K., Ohgo, Y., Soai, K. & Ogino, H. Highly enantioselective asymmetric autocatalysis induced by chiral cobalt complexes due to the topology of the coordination of achiral ligands. *Chemical communications*, 1022-1023, doi:Doi 10.1039/B102143p (2001).

37   Meggers, E. Asymmetric Synthesis of Octahedral Coordination Complexes. *European Journal of Inorganic Chemistry*, 2911-2926, doi:DOI 10.1002/ejic.201100327 (2011).

38   Lacour, J. & Linder, D. Hexacoordinated phosphates: How to teach old chiral anions new asymmetric tricks. *Chem Rec* **7**, 275-285, doi:Doi 10.1002/Tcr.20124 (2007).

39   Gong, L., Mulcahy, S. P., Harms, K. & Meggers, E. Chiral-Auxiliary-Mediated Asymmetric Synthesis of Tris-Heteroleptic Ruthenium Polypyridyl Complexes. *Journal of the American*

Chemical Society **131**, 9602-9603, doi:Doi 10.1021/Ja9031665 (2009).

40   Gong, L., Muller, C., Celik, M. A., Frenking, G. & Meggers, E. 2-Diphenylphosphino-2 '-hydroxy-1,1 '-binaphthyl as a chiral auxiliary for asymmetric coordination chemistry. *New J Chem* **35**, 788-793, doi:Doi 10.1039/C0nj00787k (2011).

41   Gong, L., Lin, Z., Harms, K. & Meggers, E. Isomerization-induced asymmetric coordination chemistry: from auxiliary control to asymmetric catalysis. *Angewandte Chemie* **49**, 7955-7957, doi:10.1002/anie.201003139 (2010).

42   Lin, Z. *et al.* Asymmetric coordination chemistry by chiral-auxiliary-mediated dynamic resolution under thermodynamic control. *Chemistry, an Asian journal* **6**, 474-481, doi:10.1002/asia.201000555 (2011).

43   Armitage, B. A. Cyanine dye-DNA interactions: Intercalation, groove binding, and aggregation. *Top Curr Chem* **253**, 55-76, doi:Doi 10.1007/B100442 (2005).

44   Komor, A. C. & Barton, J. K. The path for metal complexes to a DNA target. *Chemical communications* **49**, 3617-3630, doi:Doi 10.1039/C3cc00177f (2013).

45   Zeglis, B. M., Pierre, V. C. & Barton, J. K. Metallo-intercalators and metallo-insertors. *Chemical communications*, 4565-4579, doi:Doi 10.1039/B710949k (2007).

46   Wing, R. *et al.* Crystal-Structure Analysis of a Complete Turn of B-DNA. *Nature* **287**, 755-758, doi:Doi 10.1038/287755a0 (1980).

47   Bailly, C. & Henichart, J. P. DNA Recognition by Intercalator Minor-Groove Binder Hybrid Molecules. *Bioconjugate Chem* **2**, 379-393, doi:Doi 10.1021/Bc00012a001 (1991).

48   Erkkila, K. E., Odom, D. T. & Barton, J. K. Recognition and reaction of metallointercalators with DNA. *Chemical reviews* **99**, 2777-2795, doi:Doi 10.1021/Cr9804341 (1999).

49   Dupureur, C. M. & Barton, J. K. Structural studies of Lambda- and Delta-[Ru(phen)(2)dppz](2+) bound to d(GTCGAC)(2): Characterization of enantioselective intercalation. *Inorganic chemistry* **36**, 33-43, doi:Doi 10.1021/Ic960738a (1997).

50   Foxon, S. P. *et al.* Synthesis, Characterization, and DNA Binding Properties of Ruthenium(II) Complexes Containing the Redox Active Ligand Benzo[i]dipyrido[3,2-a:2 ',3 '-c]phenazine-11,16-quinone. *Inorganic chemistry* **51**, 463-471, doi:Doi 10.1021/Ic201914h (2012).

51   Friedman, A. E., Chambron, J. C., Sauvage, J. P., Turro, N. J. & Barton, J. K. Molecular Light Switch for DNA - Ru(Bpy)2(Dppz)2+. *Journal of the American Chemical Society* **112**, 4960-4962, doi:Doi 10.1021/Ja00168a052 (1990).

52   Song, H., Kaiser, J. T. & Barton, J. K. Crystal structure of Delta-[Ru(bpy)(2)dppz](2+) bound to mismatched DNA reveals side-by-side metalloinsertion and intercalation. *Nat Chem* **4**, 615-620, doi:Doi 10.1038/Nchem.1375 (2012).

53   Niyazi, H. *et al.* Crystal structures of Lambda-[Ru(phen)(2)dppz](2+) with oligonucleotides containing TA/TA and AT/AT steps show two intercalation modes. *Nat Chem* **4**, 621-628, doi:Doi 10.1038/Nchem.1397 (2012).

54   Wang, A. H. J., Nathans, J., Vandermarel, G., Vanboom, J. H. & Rich, A. Molecular-Structure of a Double Helical DNA Fragment Intercalator Complex between Deoxy Cpg and a Terpyridine Platinum Compound. *Nature* **276**, 471-474, doi:Doi 10.1038/276471a0 (1978).

55   Kelley, S. O., Boon, E. M., Barton, J. K., Jackson, N. M. & Hill, M. G. Single-base mismatch detection based on charge transduction through DNA. *Nucleic Acids Res* **27**, 4830-4837, doi:DOI 10.1093/nar/27.24.4830 (1999).

56   Jackson, B. A. & Barton, J. K. Recognition of base mismatches in DNA by 5,6-chrysenequinone diimine complexes of rhodium(III): A proposed mechanism for preferential binding in destabilized regions of the double helix. *Biochemistry-Us* **39**, 6176-6182, doi:Doi 10.1021/Bi9927033 (2000).

57   Zeglis, B. M. & Barton, J. K. DNA base mismatch detection with bulky rhodium intercalators: synthesis and applications. *Nature protocols* **2**, 357-371, doi:DOI 10.1038/nprot.2007.22 (2007).

58   Ohmori, Y., Kojima, M., Kashino, S. & Yoshikawa, Y. Silicon review2. *Journal of Coordination Chemistry* **39**, 219-230, doi:10.1080/00958979608024330 (1996).

59   Chuit, C., Corriu, R. J. P., Reye, C. & Young, J. C. Reactivity of Pentacoordinate and Hexacoordinate Silicon-Compounds and Their Role as Reaction Intermediates. *Chemical reviews* **93**, 1371-1448, doi:Doi 10.1021/Cr00020a003 (1993).

60   Holmes, R. R. Comparison of phosphorus and silicon: Hypervalency, stereochemistry, and reactivity. *Chemical reviews* **96**, 927-950, doi:Doi 10.1021/Cr950243n (1996).

61   Muller, R. & Dathe, C. Uber Silikone .67. Uber Organofluorsilane Und Organopentafluorosilikate. *J Prakt Chem* **22**, 232-240, doi:DOI 10.1002/prac.19630220504 (1963).

62   Tamao, K. *et al.* Organofluorosilicates in Organic-Synthesis .12. Preparation of Organopentafluorosilicates and Their Cleavage Reactions by Halogens and N-Bromosuccinimide - Synthetic and Mechanistic Aspects. *Organometallics* **1**, 355-368, doi:Doi 10.1021/Om00062a022 (1982).

63   Kummer, D., Gaisser, K. E. & Seshadri, T. Contributions to Chemistry of Halosilane Adducts .10. Bis(2,2'-Bipyridine) Complexes of Silicon, Direct Synthesis, Structure, and Properties. *Chem Ber-Recl* **110**, 1950-1962, doi:DOI 10.1002/cber.19771100539 (1977).

64   Kummer, D. & Seshadri, T. Preparation of [Sicl2bipy2](Clo4)2 by Oxidation of Sicl2bipy2. *Angewandte Chemie* **14**, 699-670, doi:DOI 10.1002/anie.197506991 (1975).

65   Kummer, D. & Koster, H. Contributions to Chemistry of Halogenosilane Adducts .4. [Si(Och3)2bipy2]Cl2 and [Si(Oh)2bipy2]Cl2. Bis-2,2'-Bipyridine Complexes of Silicon with Unexpected Properties. *Z Anorg Allg Chem* **398**, 279-292, doi:DOI 10.1002/zaac.19733980308 (1973).

66   Liu, H. L., Ohmori, Y., Kojima, M. & Yoshikawa, Y. Stereochemistry of six-coordinate octahedral silicon(IV) complexes containing 2,2 '-bipyridine. *Journal of Coordination*

Chemistry **44**, 257-268, doi:Doi 10.1080/00958979808023078 (1998).

67   Ohmori, Y., Namba, M., Kuroda, Y., Kojima, M. & Yoshikawa, Y. Stereochemistry of 6-Coordinated Silicon Complexes .2. Optical Resolution of [Si(Alpha-Diimine)3]4+ (Alpha-Diimine = Bpy, Phen). *Inorganic chemistry* **31**, 2299-2300, doi:Doi 10.1021/Ic00038a003 (1992).

68   Voronkov, M. G., Trofimova, O. M., Bolgova, Y. I. & Chernov, N. F. Hypervalent silicon-containing organosilicon derivatives of nitrogen heterocycles. *Usp Khim+* **76**, 885-906 (2007).

69   Kummer, D. & Koster, H. Contributions to Chemistry of Halosilane Adducts .5. [Si Bipy3]Br4 a Novel Ionic Tris-2,2'-Bipyridine Complex of Silicon. *Z Anorg Allg Chem* **402**, 297-304, doi:DOI 10.1002/zaac.19734020307 (1973).

70   Kummer, D. & Seshadri, T. Contributions to Chemistry of Halogenosilane Adducts .8. Preparation and Properties of Cationic Bis-2,2'-Bipyridinesilicon Complexes, [Sicl2bipy2]2+ and [Sif2bipy2]2+. *Z Anorg Allg Chem* **428**, 129-144, doi:DOI 10.1002/zaac.19774280118 (1977).

71   Gill, M. R. *et al.* A ruthenium(II) polypyridyl complex for direct imaging of DNA structure in living cells. *Nat Chem* **1**, 662-667, doi:Doi 10.1038/Nchem.406 (2009).

72   Kazmaier, U. Amino acids - Valuable organocatalysts in carbohydrate synthesis. *Angew Chem Int Edit* **44**, 2186-2188, doi:DOI 10.1002/anie.200462873 (2005).

73   MacMillan, D. W. C. The advent and development of organocatalysis. *Nature* **455**, 304-308, doi:Doi 10.1038/Nature07367 (2008).

74   Vagg, R. S. & Williams, P. A. Chiral Metal-Complexes .1. Photochemical Inversion in Ternary Ru(Ii) Complexes of Diimines and L-Tryptophane. *Inorg Chim a-Article* **51**, 61-65, doi:Doi 10.1016/S0020-1693(00)88318-8 (1981).

75   Vagg, R. S. & Williams, P. A. Chiral Metal-Complexes .2. Light-Catalyzed Diastereoisomeric Equilibration in Aqueous-Solutions of Cis-[Ru(Phen)2(L-Serine)]+ and Its 2,2'-Bipyridyl Analog. *Inorg Chim a-Article* **52**, 69-72, doi:Doi 10.1016/S0020-1693(00)88574-6 (1981).

76   Andersson, J. & Lincoln, P. Stereoselectivity for DNA Threading Intercalation of Short Binuclear Ruthenium Complexes. *Journal of Physical Chemistry B* **115**, 14768-14775, doi:Doi 10.1021/Jp2062767 (2011).

77   Gill, M. R. & Thomas, J. A. Ruthenium(II) polypyridyl complexes and DNA-from structural probes to cellular imaging and therapeutics. *Chemical Society reviews* **41**, 3179-3192, doi:Doi 10.1039/C2cs15299a (2012).

78   Schwab, P. F. H., Fleischer, F. & Michl, J. Preparation of 5-brominated and 5,5 '-dibrominated 2,2 '-bipyridines and 2,2 '-bipyrimidines. *Journal of Organic Chemistry* **67**, 443-449, doi:Doi 10.1021/Jo010707j (2002).

79   Kummer, D. & Seshadri, T. Contributions to Chemistry of Halosilane Adducts .11. Bis(1,10-Phenanthroline) Complexes of Silicon, Synthesis, Structure, and Properties. *Chem*

Ber-Recl **110**, 2355-2367, doi:DOI 10.1002/cber.19771100631 (1977).

80   Venkataramana, G. *et al.* 1,8-Pyrenylene-Ethynylene Macrocycles. *Organic Letters* **13**, 2240-2243, doi:Doi 10.1021/Ol200485x (2011).

81   Allen, F. H. *et al.* Tables of Bond Lengths Determined by X-Ray and Neutron-Diffraction .1. Bond Lengths in Organic-Compounds. *J Chem Soc Perk T 2*, S1-S19, doi:Doi 10.1039/P298700000s1 (1987).

82   Shibasaki, M. & Matsunaga, S. Design and application of linked-BINOL chiral ligands in bifunctional asymmetric catalysis. *Chemical Society reviews* **35**, 269-279, doi:Doi 10.1039/B506346a (2006).

83   Brunel, J. M. BINOL: A versatile chiral reagent. *Chemical reviews* **105**, 857-897, doi:Doi 10.1021/Cr040079g (2005).

84   Mcnair, A. M. & Mann, K. R. Synthesis and Reactivity of [(Eta-5-C5h5)Ruleta-6-Arene)]Pf6, [(Eta-5-C5[Ch3]5)Ru(Eta-6-Arene)]Pf6 Complexes of Naphthalene, Anthracene, Pyrene, Chrysene, and Azulene - Kinetic-Studies of Arene Displacement-Reactions in Acetonitrile Solutions. *Inorganic chemistry* **25**, 2519-2527, doi:Doi 10.1021/Ic00235a008 (1986).

85   Sullivan, B. P., Salmon, D. J. & Meyer, T. J. Mixed Phosphine 2,2'-Bipyridine Complexes of Ruthenium. *Inorganic chemistry* **17**, 3334-3341, doi:Doi 10.1021/Ic50190a006 (1978).

86   Fulmer, G. R. *et al.* NMR Chemical Shifts of Trace Impurities: Common Laboratory Solvents, Organics, and Gases in Deuterated Solvents Relevant to the Organometallic Chemist. *Organometallics* **29**, 2176-2179, doi:Doi 10.1021/Om100106e (2010).

87   Drake, A. F. Polarization Modulation - the Measurement of Linear and Circular-Dichroism. *J Phys E Sci Instrum* **19**, 170-181, doi:Doi 10.1088/0022-3735/19/3/002 (1986).

88   Paw, W. & Eisenberg, R. Synthesis, characterization, and spectroscopy of dipyridocatecholate complexes of platinum. *Inorganic chemistry* **36**, 2287-2293, doi:Doi 10.1021/Ic9610851 (1997).

89   Ji, S. M., Guo, H. M., Wu, W. T., Wu, W. H. & Zhao, J. Z. Ruthenium(II) Polyimine-Coumarin Dyad with Non-emissive (IL)-I-3 Excited State as Sensitizer for Triplet-Triplet Annihilation Based Upconversion. *Angew Chem Int Edit* **50**, 8283-8286, doi:DOI 10.1002/anie.201008134 (2011).

6.2 List of Synthesized Compounds

1) Octahedral ruthenium(II) complexes

Λ-(*S*)-**61**

Δ-(*S*)-**61**

Λ-(*S*)-**68**

Δ-(*S*)-**68**

Λ-(*S*)-**66**

Λ-(*S*)-**67**

Λ-(*S*)-**69**

Λ-(*S*)-**69**

Λ-**70**

Λ-**72**

Λ-**71**

Λ-**73**
67 : 33 er

Λ-**74**

Λ-**75**

rac- **77**

rac- **78**

rac- / 50% e.e. **79**

2) Related ligands

76

80a

dppz 80

91

92

94

95

3) Octahedral silicon(IV) complexes

141

81

82

83

85

96

97

99

98

100

102

103

104

Λ-(*R*)-**105**
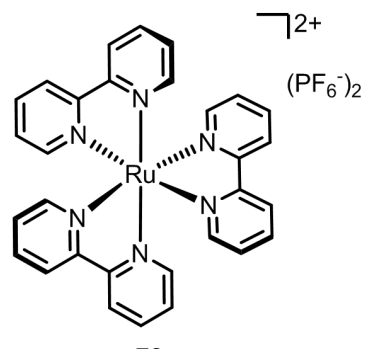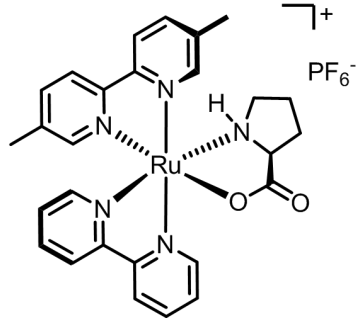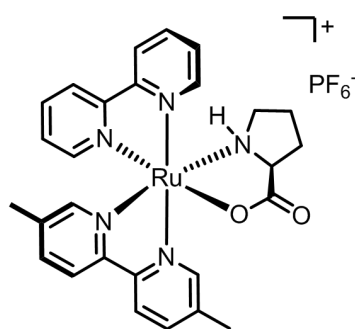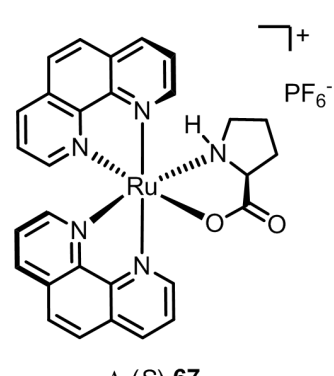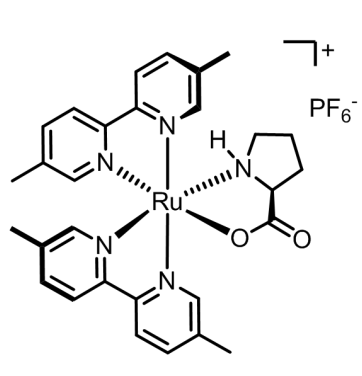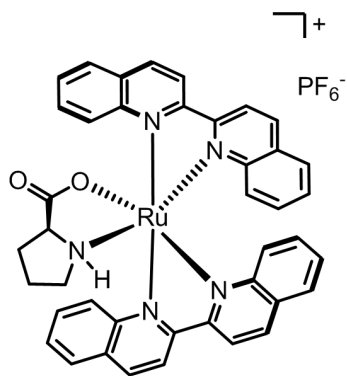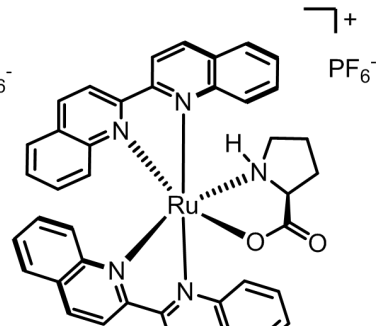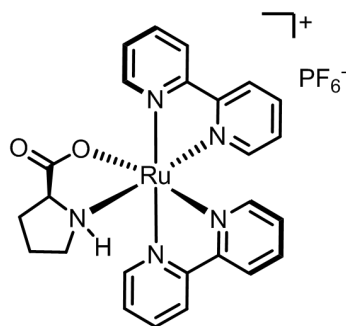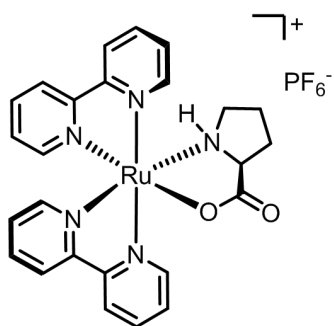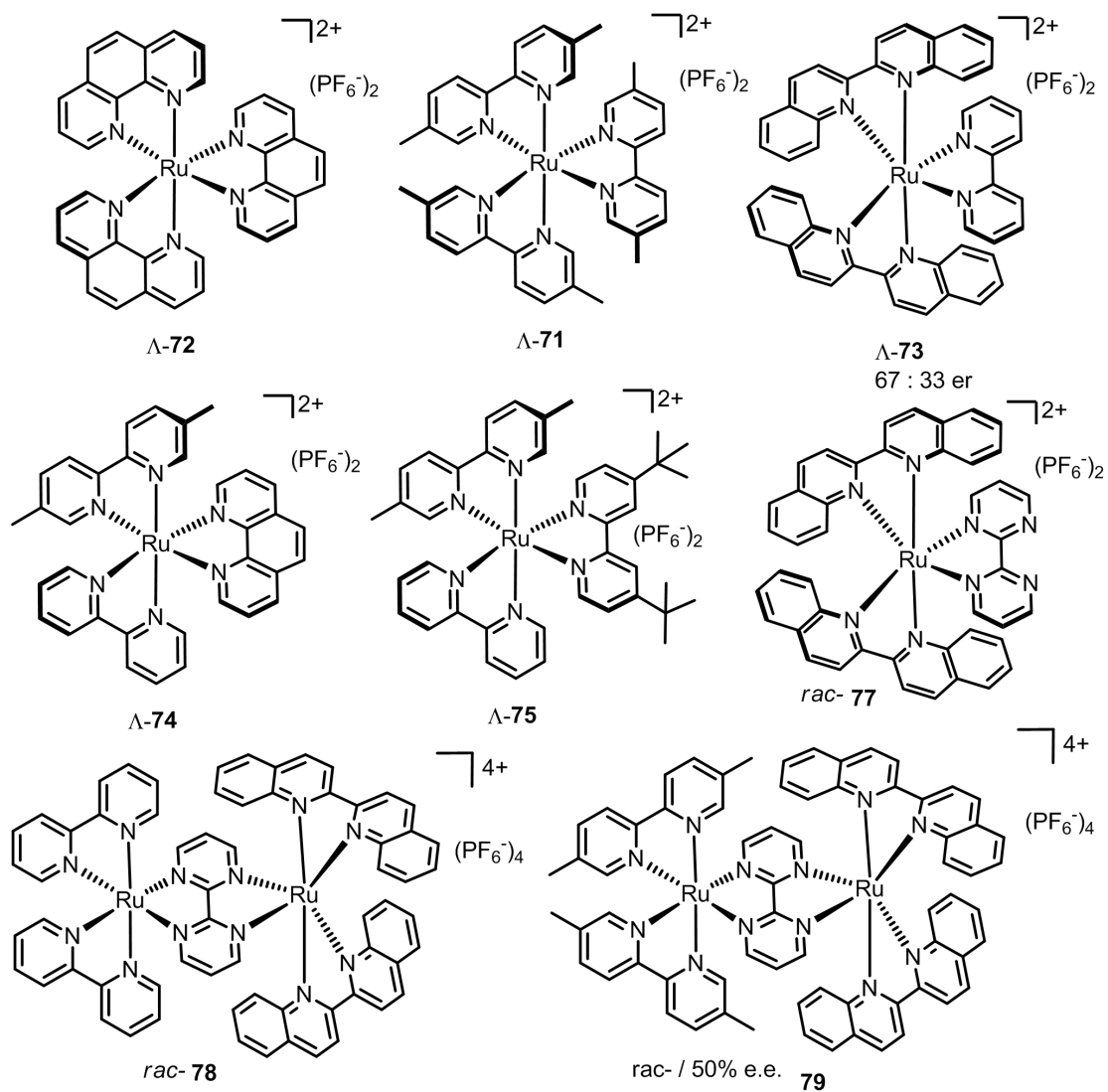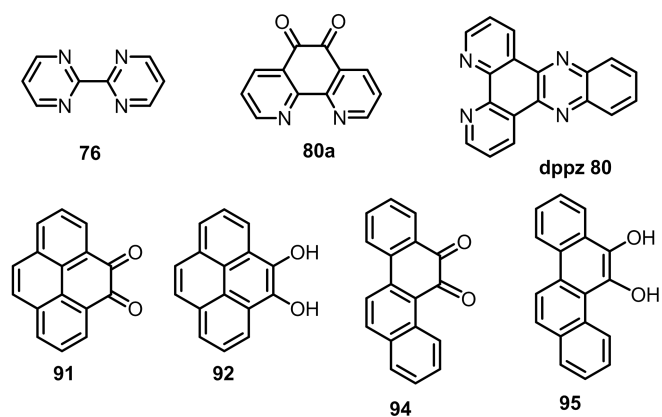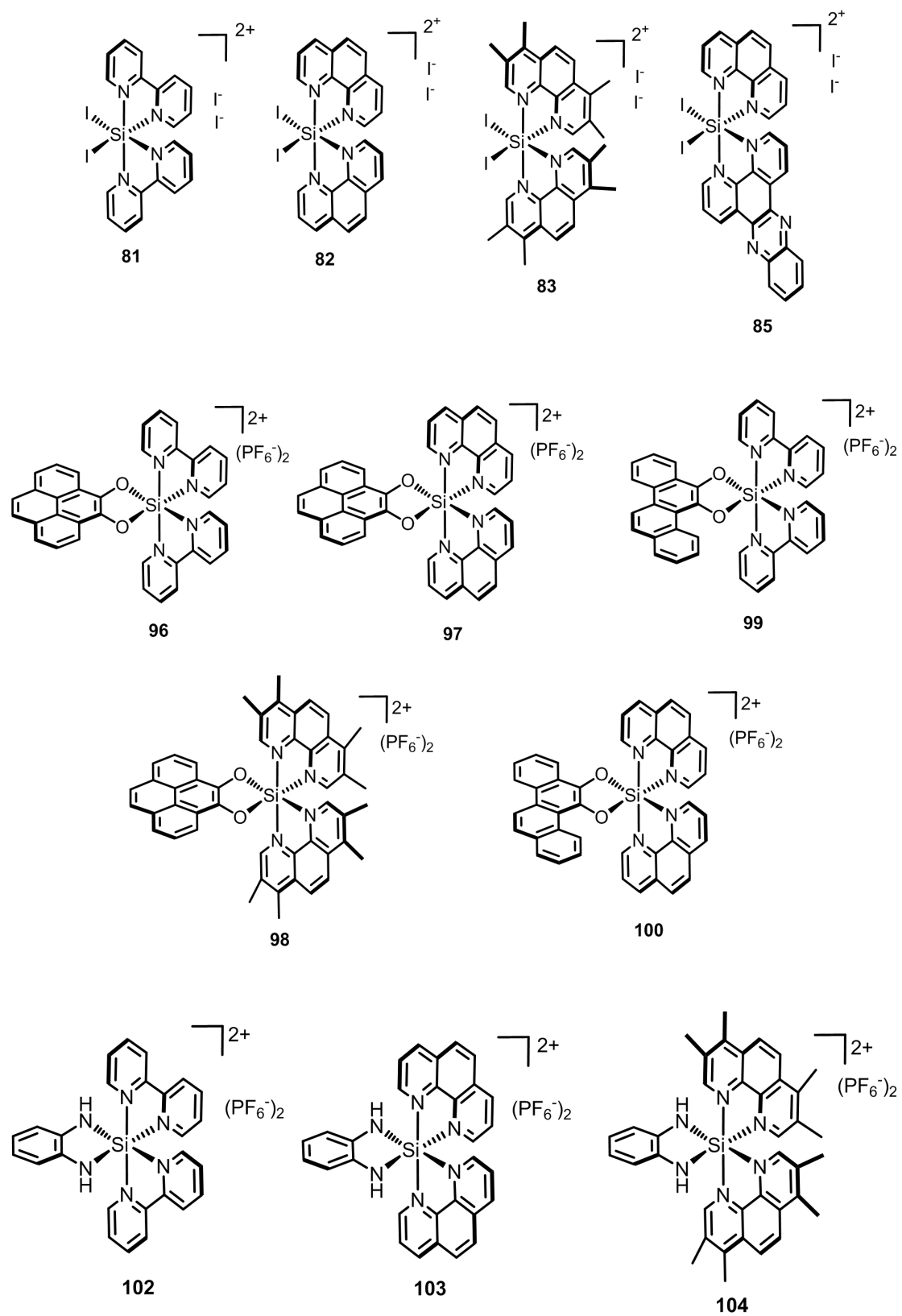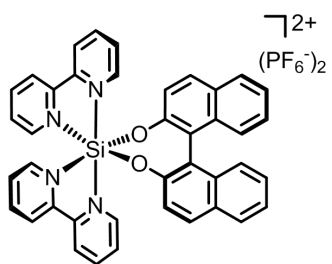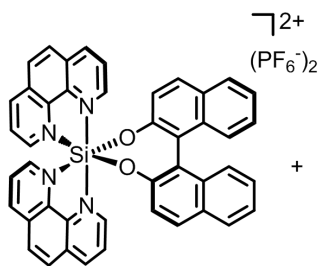
Λ-(*R*)-**106**   +
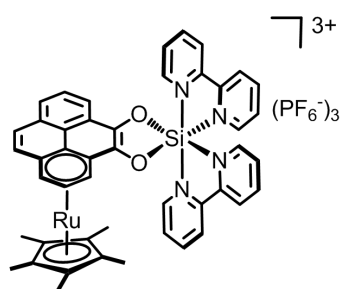
108
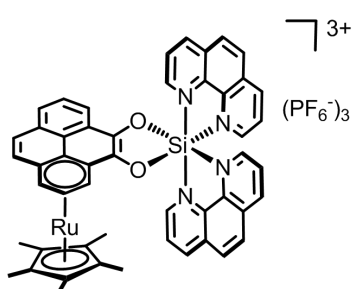
109
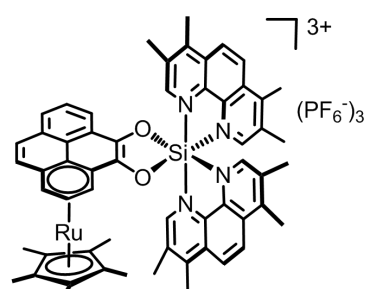
110

6.3 Abbreviations and Symbols

CD	circular dichroism
^{1}H-NMR	proton nuclear magnetic resonance spectroscopy
^{13}C-NMR	carbon-13 nuclear magnetic resonance spectroscopy
HPLC	high-performanc liquid chromatography
TLC	thin layer chromatography
UV	ultraviolet
IR spectra	infrared spectra
CH_2Cl_2 / DCM	dichloromethane
DMF	dimethylformamide
CH_3OH / MeOH	methanol
DMSO	dimethyl sulfoxide
DIPEA	*N,N*-diisopropylethylamine
CH_3CN / MeCN	acetonitrile
EtOH	ethanol
DNA	deoxyribonucleic acid
dmb	5,5'-dimethyl-2,2'-bipyridine
dppz	dipyrido[3,2-a:2',3'-c]phenazine
dbb	4,4'-di-tert-butyl-2,2'-bipyridine
biq	2,2'-biquinoline
phen	1,10-phenanthroline
dr	diastereomeric ratio
er	enantiomeric ratio
ee	enantiomeric excesses
Et_2O	diethyl ether
Et_2NH	diethyl amine
Et_3N	triethyl amine
EtOAc	ethyl acetate

144

en	ethylene diamine
THF	tetrahydrofuran
TFA	trifluoroacetic acid
NBS	*N*-bromosuccinimide
AcOH	acetic acid
aq	aqueous
Ar	argon
bpy	2,2′-bipyridine
cpd	compound
br	broad
N_2	nitrogen
Calcd	calculated
conc	concentrated
chrysi	5,6-chrysene quinone diimine
br	broad
d	doublet
DCE	1,2-dichloroethane
eq	equivalent(s)
DIPEA	*N,N*-diisopropylethylamine
DMAP	4-dimethylaminopyridine
EDTA	ethylenediaminetetraacetate acid
ESI	electrospray ionization
G	guanosine
C	cytosine
T	thymine
A	adenine
h	hour(s)
bpym	2,2′-bipyrimidine
PPh_3	triphenylphosphine

HRMS	high resolution mass spectrometry
L	Liter(s)
m	multiplet
M	mol/L
min	Minute(s)
mL	Milliliter(s)
MLCT	metal-to-ligand charge transfer
mmol	millimole
rac	racemate
Ph	phenyl
ppm	parts per million

6.4 Appendix
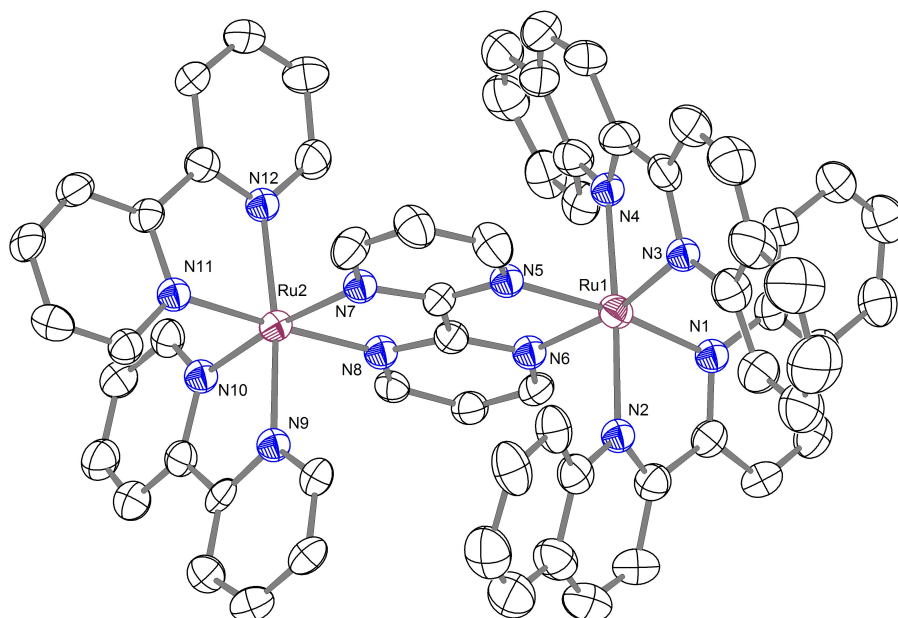
Crystal data

Identification code	platon-sr	
Habitus, colour	block, red	
Crystal size	0.25 x 0.17 x 0.10 mm^3	
Crystal system	Monoclinic	
Space group	P 2$_1$/c	Z = 12
Unit cell dimensions	a = 23.6864(9) Å	α= 90°.
	b = 20.8304(5) Å	β= 91.021(3)°.
	c = 46.2928(18) Å	γ = 90°.
Volume	22837.1(14) Å^3	
Cell determination	25415 peaks with Theta 1 to 25°.	
Empirical formula	C$_{64}$ H$_{46}$ F$_{24}$ N$_{12}$ P$_4$ Ru$_2$	
Formula weight	1765.15	
Density (calculated)	1.540 Mg/m^3	
Absorption coefficient	0.586 mm^{-1}	
F(000)	10536	

147

Data collection:

Diffractometer type	STOE IPDS 2T
Wavelength	0.71073 Å
Temperature	100(2) K
Theta range for data collection	1.30 to 25.12°.
Index ranges	-28<=h<=28, 0<=k<=24, 0<=l<=55
Data collection software	STOE X-AREA
Cell refinement software	STOE X-AREA
Data reduction software	STOE X-AREA

Solution and refinement:

Reflections collected	35859
Independent reflections	35859 [R(int) = 0.0000] ("squeezed" data)
Completeness to theta = 25.12°	87.9 % (due to overlap)
Observed reflections	13431[I>2sigma(I)]
Reflections used for refinement	35859
Absorption correction	Integration
Max. and min. transmission	0.9423 and 0.8903
Largest diff. peak and hole	1.047 and -0.799 e.Å^{-3}
Solution	Direct methods
Refinement	Full-matrix least-squares on F^2
Treatment of hydrogen atoms	Calculated positions, constr. Ref.
Programs used	SIR2008
	SHELXL-97 (Sheldrick, 1997)
	DIAMOND 3.2g
	STOE IPDS2 software
Data / restraints / parameters	35859 / 5362 / 2988
Goodness-of-fit on F^2	0.695
R index (all data)	wR2 = 0.1456
R index conventional [I>2sigma(I)]	R1 = 0.0628
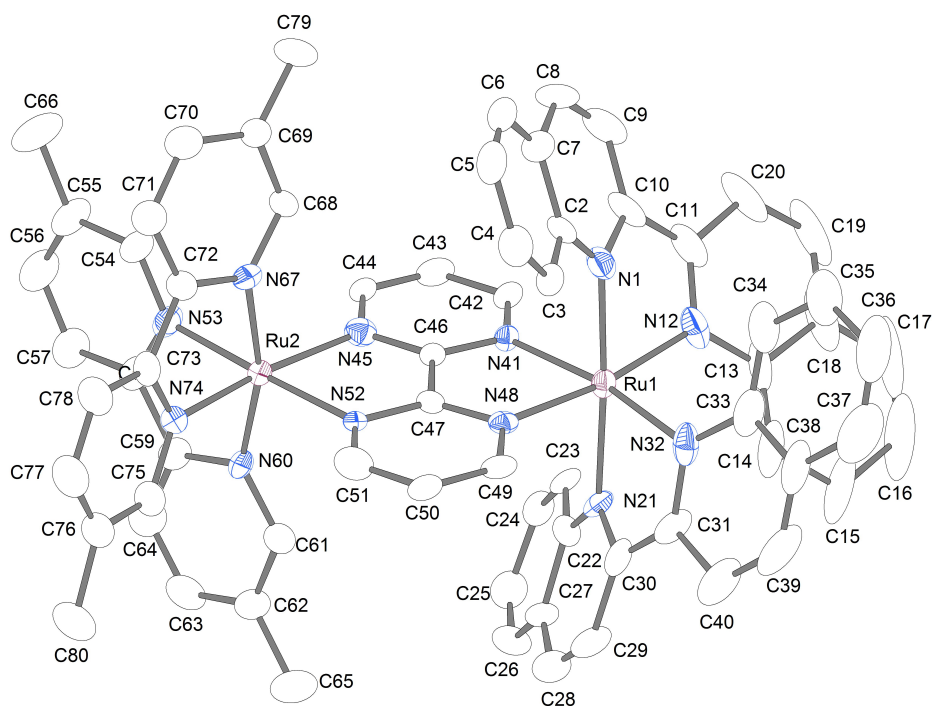
Crystal data

Identification code	fc110908	
Habitus, colour	needle, green	
Crystal size	0.30 x 0.09 x 0.08 mm^3	
Crystal system	Monoclinic	
Space group	C c	Z = 4
Unit cell dimensions	a = 19.9238(7) Å	α= 90°.
	b = 19.3309(4) Å	β= 99.682(3)°.
	c = 22.7672(8) Å	γ = 90°.
Volume	8643.8(5) Å^3	
Cell determination	36436 peaks with Theta 1.5 to 27°.	
Empirical formula	$C_{80} H_{78} F_{24} N_{12} O_4 P_4 Ru_2$	
Formula weight	2053.56	
Density (calculated)	1.578 Mg/m^3	
Absorption coefficient	0.532 mm^{-1}	
F(000)	4152	

Data collection:

Diffractometer type	STOE IPDS 2T
Wavelength	0.71073 Å
Temperature	100(2) K
Theta range for data collection	1.48 to 25.25°.

149

Index ranges	-23<=h<=23, -21<=k<=23, -27<=l<=27
Data collection software	STOE X-AREA
Cell refinement software	STOE X-AREA
Data reduction software	STOE X-AREA

Solution and refinement:

Reflections collected	39286
Independent reflections	14852 [R(int) = 0.0461]
Completeness to theta = 25.25°	100.0 %
Observed reflections	11689[I>2(I)]
Reflections used for refinement	14852
Absorption correction	Semi-empirical from equivalents
Max. and min. transmission	0.9551 and 0.9070
Flack parameter (absolute struct.)	0.47(2)
Largest diff. peak and hole	1.073 and -0.595 e.Å^{-3}
Solution	Direct methods
Refinement	Full-matrix least-squares on F^2
Treatment of hydrogen atoms	Calculated positions, constr. Ref.
Programs used	SIR92 (Giacovazzo et al, 1993)
	SHELXL-97 (Sheldrick, 2008)
	DIAMOND 3.2g
	STOE IPDS2 software
Data / restraints / parameters	14852 / 385 / 1148
Goodness-of-fit on F^2	0.890
R index (all data)	wR2 = 0.0717
R index conventional [I>2sigma(I)]	R1 = 0.0378

Identification code	fc562	
Habitus, colour	plate, red	
Crystal size	$0.20 \times 0.17 \times 0.04$ mm^3	
Crystal system	Orthorhombic	
Space group	P 2_1 2_1 2_1	Z = 4
Unit cell dimensions	a = 13.8864(7) Å	$\alpha = 90°$.
	b = 18.8230(9) Å	$\beta = 90°$.
	c = 23.6930(16) Å	$\gamma = 90°$.
Volume	6193.0(6) Å^3	
Cell determination	19235 peaks with Theta 1.7 to 24.5°.	
Empirical formula	$C_{50} H_{72} N_{12} O_{23} Ru_2$	
	$2(C_{25} H_{24} N_5 O_2 Ru)$, $2(N O_3)$, $13(H_2O)$	
Formula weight	1411.34	
Density (calculated)	1.514 Mg/m^3	
Absorption coefficient	0.574 mm^{-1}	
F(000)	2912	

Data collection:

Diffractometer type   STOE IPDS 2

Wavelength   0.71073 Å

Temperature   100(2) K

Theta range for data collection   1.38 to 25.50°.

Index ranges   -16<=h<=16, -22<=k<=22, -28<=l<=28

Data collection software   STOE X-AREA

Cell refinement software   STOE X-AREA

Data reduction software   STOE X-RED

Solution and refinement:

Reflections collected   42032

Independent reflections   11537 [R(int) = 0.1432]

Completeness to theta = 25.50°   100.0 %

Observed reflections   5048[I>2sigma(I)]

Reflections used for refinement   11537

Absorption correction   Semi-empirical from equivalents

Max. and min. transmission   1.0896 and 0.7850

Flack parameter (absolute struct.)   -0.02(4)

Largest diff. peak and hole   0.488 and -0.730 e.Å^{-3}

Solution   Direct methods

Refinement   Full-matrix least-squares on F^2

Treatment of hydrogen atoms   Calculated positions, riding model

Programs used   SIR-2011

                                                       SHELXL-97 (Sheldrick, 1997)

                                                       DIAMOND 3.2h

                                                       STOE IPDS2 software

Data / restraints / parameters   11537 / 102 / 802

Goodness-of-fit on F^2 0.780

R index (all data)   wR2 = 0.1173

R index conventional   [I>2sigma(I)]   R1 = 0.0555

Crystal data

Identification code	fc201202	
Habitus, colour	block, black	
Crystal size	0.23 x 0.23 x 0.21 mm^3	
Crystal system	Monoclinic	
Space group	P 2$_1$	Z = 4
Unit cell dimensions	a = 14.0011(5) Å	α= 90°.
	b = 18.2927(6) Å	β= 106.071(3)°.
	c = 14.4932(5) Å	γ = 90°.
Volume	3566.9(2) Å^3	
Cell determination	23958 peaks with Theta 1.8 to 27.1°.	
Empirical formula	C$_{41}$ H$_{32}$ F$_6$ N$_5$ O$_2$ P Ru	
Formula weight	872.76	
Density (calculated)	1.625 Mg/m^3	
Absorption coefficient	0.562 mm^{-1}	
F(000)	1768	

Data collection:

Diffractometer type	STOE IPDS 2
Wavelength	0.71073 Å
Temperature	100(2) K
Theta range for data collection	1.46 to 25.50°.
Index ranges	-16<=h<=16, -22<=k<=22, -17<=l<=17
Data collection software	STOE X-AREA
Cell refinement software	STOE X-AREA
Data reduction software	STOE X-RED

Solution and refinement:

Reflections collected	34262
Independent reflections	13276 [R(int) = 0.0590]
Completeness to theta = 25.50°	100.0 %
Observed reflections	9196[I>2sigma(I)]
Reflections used for refinement	13276
Absorption correction	Empirical
Max. and min. transmission	0.7094 and 0.5301
Flack parameter (absolute struct.)	-0.03(2)
Largest diff. peak and hole	0.626 and -0.420 e.Å^{-3}
Solution	Direct methods
Refinement	Full-matrix least-squares on F^2

Treatment of hydrogen atoms	Calculated positions, riding model
Programs used	SHELXS-97 (Sheldrick, 1990)
	SHELXL-97 (Sheldrick, 1997)
	DIAMOND 3.2g
	STOE IPDS2 software
Data / restraints / parameters	13276 / 1 / 1009
Goodness-of-fit on F^2	0.688
R index (all data)	wR2 = 0.0506
R index conventional [I>2sigma(I)]	R1 = 0.0304
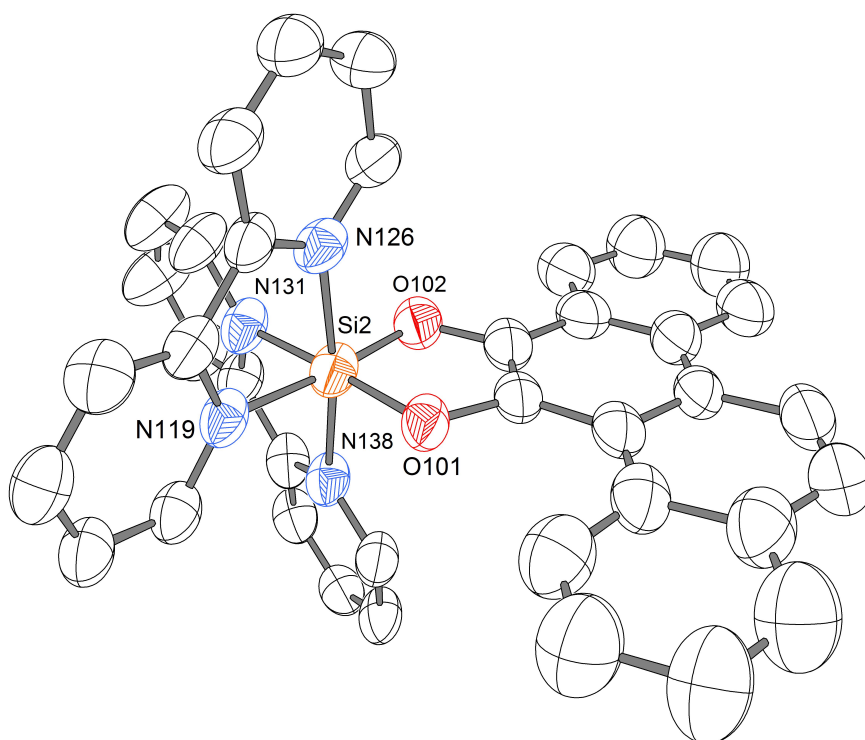
Crystal data

Identification code	fc489-2	
Habitus, colour	plate, red	
Crystal size	0.30 x 0.15 x 0.08 mm^3	
Crystal system	Triclinic	
Space group	P -1	Z = 6
Unit cell dimensions	a = 11.9871(6) Å	α= 60.574(3)°.
	b = 25.6899(12) Å	β= 80.511(4)°.
	c = 25.7102(11) Å	γ = 79.019(4)°.
Volume	6746.2(5) Å^3	
Cell determination	18995 peaks with Theta 1.6 to 24.8°.	
Empirical formula	C$_{44}$ H$_{39}$ F$_{12}$ N$_5$ O$_3$ P$_2$ Si	
	C$_{38}$ H$_{26}$ N$_4$ O$_2$ Si, 2PF$_6$, MeCN, Et$_2$O	
Formula weight	1003.83	
Density (calculated)	1.483 Mg/m^3	
Absorption coefficient	0.220 mm^{-1}	
F(000)	3084	

Data collection:

Diffractometer type	STOE IPDS 2T
Wavelength	0.71073 Å
Temperature	100(2) K

Theta range for data collection	1.57 to 25.25°.
Index ranges	-14<=h<=14, -26<=k<=30, 0<=l<=30
Data collection software	STOE X-AREA
Cell refinement software	STOE X-AREA
Data reduction software	STOE X-RED

Solution and refinement:

Reflections collected	24301
Independent reflections	24301 [R(int) = 0.0745]
Completeness to theta = 25.25°	99.4 %
Observed reflections	8460[I>2sigma(I)]
Reflections used for refinement	24301
Absorption correction	Integration
Max. and min. transmission	0.9845 and 0.9458
Largest diff. peak and hole	0.384 and -0.246 e.Å^{-3}
Solution	Direct methods
Refinement	Full-matrix least-squares on F^2
Treatment of hydrogen atoms	Calculated positions, riding model
Programs used	SIR2011
	SHELXL-97 (Sheldrick, 2008)
	DIAMOND 3.2h
	STOE IPDS2 software
Data / restraints / parameters	24301 / 2188 / 2035
Goodness-of-fit on F^2	0.739
R index (all data)	wR2 = 0.1640
R index conventional [I>2sigma(I)]	R1 = 0.0667
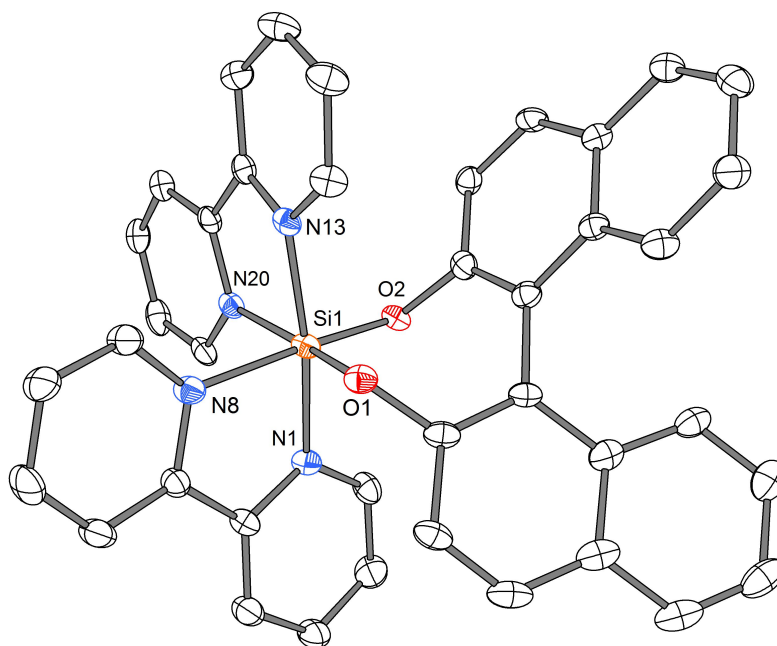
Crystal data

Identification code	fc499	
Habitus, colour	prism, red	
Crystal size	0.12 x 0.11 x 0.06 mm^3	
Crystal system	Monoclinic	
Space group	P 2$_1$	Z = 2
Unit cell dimensions	a = 10.8645(5) Å	α= 90°.
	b = 13.3145(5) Å	β= 110.703(3)°.
	c = 13.5307(6) Å	γ = 90°.
Volume	1830.90(14) Å^3	
Cell determination	1422 peaks with Theta 2.0 to 26.9°.	
Empirical formula	C$_{40}$ H$_{28}$ F$_{12}$ N$_4$ O$_2$ P$_2$ Si	
Formula weight	914.69	
Density (calculated)	1.659 Mg/m^3	
Absorption coefficient	0.259 mm^{-1}	
F(000)	928	

Data collection:

Diffractometer type	STOE IPDS 2T
Wavelength	0.71073 Å
Temperature	100(2) K
Theta range for data collection	1.61 to 26.73°.

158

Index ranges	-13<=h<=13, -16<=k<=16, -17<=l<=17
Data collection software	STOE X-AREA
Cell refinement software	STOE X-AREA
Data reduction software	STOE X-RED

Solution and refinement:

Reflections collected	14542
Independent reflections	7653 [R(int) = 0.0390]
Completeness to theta = 26.73°	99.5 %
Observed reflections	6005[I>2sigma(I)]
Reflections used for refinement	7653
Absorption correction	Integration
Max. and min. transmission	0.9908 and 0.9671
Flack parameter (absolute struct.)	0.00(7)
Largest diff. peak and hole	0.304 and -0.321 e.Å^{-3}
Solution	Direct methods
Refinement	Full-matrix least-squares on F^2
Treatment of hydrogen atoms	Calculated positions, constr. ref.
Programs used	SIR2011
	SHELXL-97 (Sheldrick, 1997)
	DIAMOND
	STOE IPDS2 software
Data / restraints / parameters	7653 / 1 / 587
Goodness-of-fit on F^2	0.889
R index (all data)	wR2 = 0.0603
R index conventional [I>2sigma(I)]	R1 = 0.0364
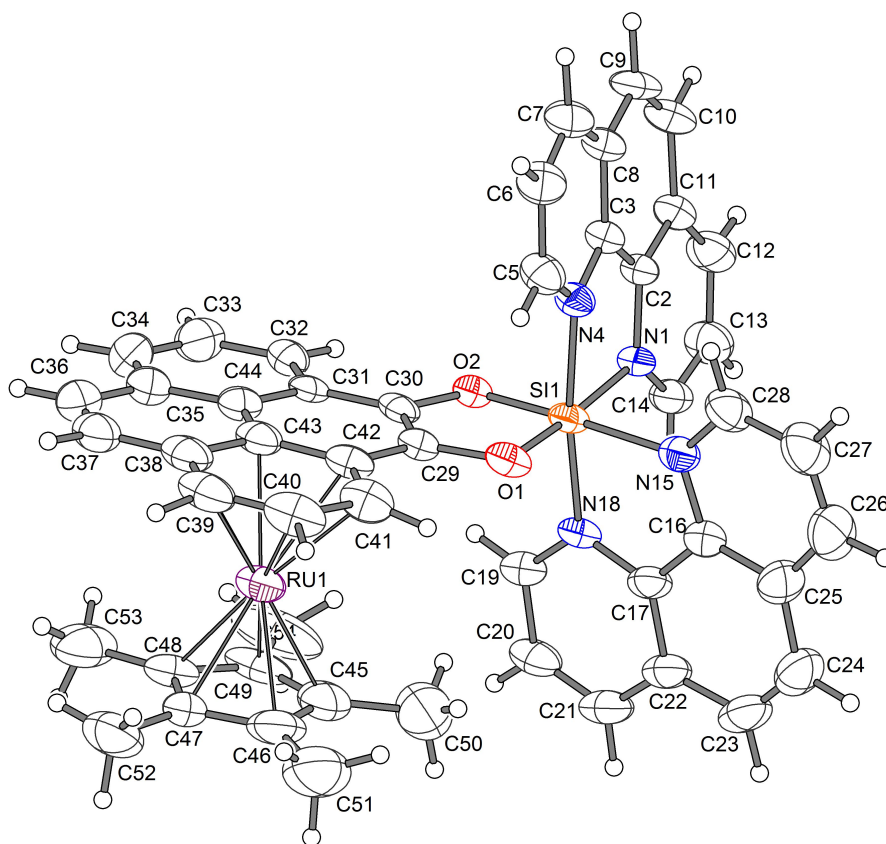
Crystal data

Identification code	fc933b_0m
Habitus, colour	prism, colourless
Crystal size	0.264 x 0.157 x 0.106 mm^3
Crystal system	Monoclinic
Space group	P 2$_1$/c Z = 4
Unit cell dimensions	a = 13.2610(5) Å α= 90°.
	b = 13.0303(6) Å β= 92.1125(16)°.
	c = 30.4909(13) Å γ = 90°.
Volume	5265.1(4) Å^3
Cell determination	9852 peaks with Theta 2.3 to 27.5°.
Empirical formula	C$_{53}$ H$_{45}$ F$_{18}$ N$_4$ O$_3$ P$_3$ Ru Si
Formula weight	1350.00
Density (calculated)	1.703 Mg/m^3
Absorption coefficient	0.526 mm^{-1}
F(000)	2720

Data collection:

Diffractometer type	Bruker D8 QUEST area detector
Wavelength	0.71073 Å
Temperature	100(2) K
Theta range for data collection	2.275 to 25.500°.
Index ranges	-15<=h<=16, -15<=k<=12, -24<=l<=36
Data collection software	BRUKER APEX II
Cell refinement software	SAINT V8.34A (Bruker AXS Inc., 2013)
Data reduction software	SAINT V8.34A (Bruker AXS Inc., 2013)

Solution and refinement:

Reflections collected	25495
Independent reflections	9798 [R(int) = 0.0378]
Completeness to theta = 25.242°	99.9 %
Observed reflections	7298[II > 2(I)]
Reflections used for refinement	9798
Absorption correction	Semi-empirical from equivalents
Max. and min. transmission	0.95 and 0.85
Largest diff. peak and hole	1.162 and -1.027 e.Å^{-3}
Solution	Direct methods
Refinement	Full-matrix least-squares on F^2
Treatment of hydrogen atoms	Calculated positions, constr. ref.
Programs used	SHELXS-97 (Sheldrick, 2008)
	SHELXL-2013 (Sheldrick, 2013)
	DIAMOND (Crystal Impact)
	SAINT, SADABS (BRUKER AXS)
Data / restraints / parameters	9798 / 441 / 947
Goodness-of-fit on F^2	1.079
R index (all data)	wR2 = 0.1806
R index conventional [I>2sigma(I)]	R1 = 0.0671
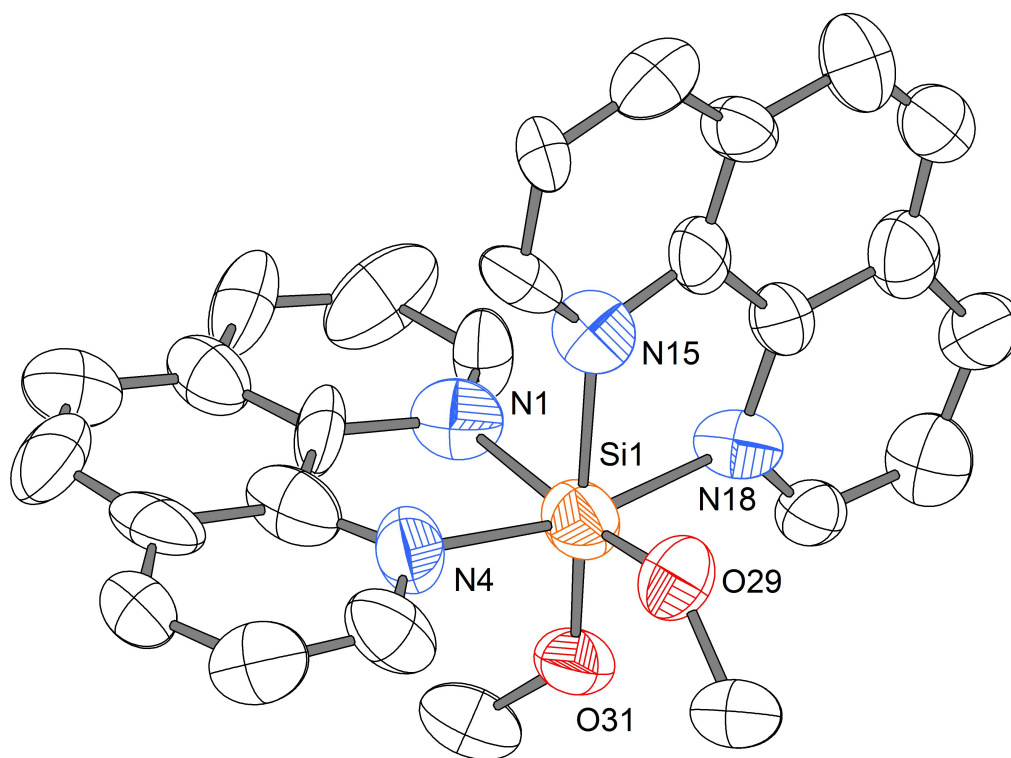
Crystal data

Identification code	fc2013	
Habitus, colour	needle, orange	
Crystal size	0.27 x 0.03 x 0.03 mm^3	
Crystal system	Orthorhombic	
Space group	P b c a	Z = 8
Unit cell dimensions	a = 17.996(2) Å	α= 90°.
	b = 11.3694(16) Å	β= 90°.
	c = 27.034(4) Å	γ = 90°.
Volume	5531.2(12) Å^3	
Cell determination	4225 peaks with Theta 1.9 to 20.0°.	
Empirical formula	C$_{26}$ H$_{22}$ I$_2$ N$_4$ O$_2$ Si	
Formula weight	704.49	
Density (calculated)	1.692 Mg/m^3	
Absorption coefficient	2.348 mm^{-1}	
F(000)	2736	

Data collection:

Diffractometer type	STOE IPDS 2

162

Wavelength	0.71073 Å
Temperature	100(2) K
Theta range for data collection	1.51 to 25.25°.
Index ranges	-21<=h<=21, -11<=k<=13, -32<=l<=29
Data collection software	STOE X-AREA
Cell refinement software	STOE X-AREA
Data reduction software	STOE X-RED

Solution and refinement:

Reflections collected	19311
Independent reflections	5016 [R(int) = 0.2137]
Completeness to theta = 25.25°	100.0 %
Observed reflections	1256[I>2sigma(I)]
Reflections used for refinement	5016
Absorption correction	Semi-empirical from equivalents
Max. and min. transmission	0.8523 and 0.7843
Largest diff. peak and hole	0.822 and -0.607 e.Å^{-3}
Solution	Direct methods
Refinement	Full-matrix least-squares on F^2
Treatment of hydrogen atoms	Calculated positions, constr. ref.
Programs used	Superflip
	SHELXL-97 (Sheldrick, 1997)
	DIAMOND 3.2h
	STOE IPDS2 software
Data / restraints / parameters	5016 / 19 / 340
Goodness-of-fit on F^2	0.735
R index (all data)	wR2 = 0.1289
R index conventional [I>2sigma(I)]	R1 = 0.0540

Curriculum Vitae

Name: Fu, Chen
Gender: Male
Date of the birth: 30. 05. 1985
Email: fuchen0794@gmail.com

EDUCATION BACKGROUND

02. 2011~Present   Ph.D. in Chemical Biology, Philipps-Universität Marburg
Ph.D. thesis with Prof. Eric Meggers

Research: Asymmetric synthesis of bioactive octahedral ruthenium complexes;
Synthsis of octahedral silicon complexes as DNA binders and insertors.

Publications: 1) Huo, H.; **Fu, C.**; Harms, K.; Meggers, E. *J. Am. Chem. Soc.*, **2014**, *136* (8), 2990–2993.
2) **Fu, C.**; Wenzel, M.; Treutlein, E.; Harms, K.; Meggers E. *Inorg. Chem.* **2012**, *51*, 10004−10011.
3) Xiang, Y. ; **Fu, C.**; Breiding, T.; Sasmal, P.; Liu, H.; Shen, Q.; Harms, K.; Zhang, L.; Meggers, E. *Chem. Commun.* **2012**, *48*, 7131.
4) Lin, Z.; Celik, M.; **Fu, C.**; Harms, K.; Frenking, G.; Meggers, E. *Chem. Eur. J.* **2011**, *17*, 12602-12605.

09. 2007~12. 2010   M.S. in Organic Chemistry, Xiamen University
M.S. thesis with Prof. Tingbin Wen

Courses: Advanced Organic Synthesis; Asymmetric Organic Chemistry; Organometallics Organic spectroscopy; Advanced Inorganic Chemistry.

Research: Organometallic chemistry of late transition metal complexes with boron analogs of cyclopentadienyl ligands

Publications: *Dalton Trans.*, **2013**, *42*, 11976–11980.

09. 2003~07. 2007   B.S. in Chemistry, Southwest University
B.S. thesis with Prof. Xuebing Ma

Awards: Outstanding Graduate in Session 2007 of Southwest University; Triple-A student, First-class Scholarship.

Research: Synthesis and characterization of a chiral amino alcohol

---